Title

The microbiome responds to environmental perturbations during critical periods to shape neurodevelopmental outcomes

Author

Coley-O'Rourke, Elena Julia

Publication Date

2024

Peer reviewed|Thesis/dissertation

UNIVERSITY OF CALIFORNIA

Los Angeles

The microbiome responds to environmental perturbations during critical periods to shape neurodevelopmental outcomes

A dissertation submitted in partial satisfaction of the requirements

for the degree of Doctor of Philosophy in Neuroscience

by

Elena Julia Coley-O'Rourke

2024

ABSTRACT OF THE DISSERTATION

The microbiome responds to environmental perturbations during critical periods to shape neurodevelopmental outcomes

by

Elena Julia Coley-O'Rourke

Doctor of Philosophy in Neuroscience

University of California, Los Angeles, 2024

Professor Elaine Yih-Nien Hsiao, Chair

The gut microbiome interacts with host physiology to influence neurodevelopment during critical periods of life. Brain-gut interactions during these critical periods can occur through direct communication, such as via gut-derived metabolites or vagal activity, or by indirect or secondary body systems, such as immune or endocrine signaling. Regardless of mechanism, these brain-gut interactions shape neurological trajectories for later-life function. The compilation of work making up this dissertation aims to profile mechanisms of developmental brain-gut interactions in response to environmental perturbations, and explore avenues of microbiota-targeted methods for amelioration of subsequent neurological impairment. **Chapters 2** and **3** and **Appendix 1** investigate how the microbiome responds to, and moderates effects of, perinatal malnutrition on the developing brain. Here, we report that the maternal microbiome modifies effects of protein undernutrition on fetal neurodevelopment and offspring behavior, and that gut-modulated

metabolites ameliorate select phenotypes. **Chapter 4** investigates signatures of gestational fluoxetine use on transcriptomic disruptions in the developing fetal brain, and reports a mediating role of the maternal microbiome. **Chapter 5** is a translational study investigating correlations between metabolomic changes, functional brain connectivity, and psychiatric symptoms in adults following exposure to early life adversity. We find that four gut-modulated metabolites and connectivity of brain networks including sensorimotor, salience, and central executive, are associated both with early life adversity and with current stress, anxiety, and depression symptoms. Together, this body of work supports the notion of sensitivity of not only the brain, but also the gut, and interactions between the two, to environmental perturbations. Results indicates a causal role of the microbiome during critical windows of prenatal or postnatal development in shaping neurodevelopment and influencing persistent trajectories of behavior, and demonstrate that these interactions occur in response to outside influences including diet, medications, and stress. Finally, this work highlights the gut microbiome as a target of potential intervention for critical period neurodevelopmental disruptions.

The dissertation of Elena Julia Coley-O'Rourke is approved.

Carlos Portera-Cailliau

Bridget Callaghan

Sherin U. Devaskar

Bennett G. Novitch

Elaine Yih-Nien Hsiao, Committee Chair

University of California, Los Angeles

2024

For my family – the originals, and the ones added along the way.

PREFACE

This work was supported in part by a Graduate Research Fellowship from the National Science Foundation and a UCLA Dissertation Year Fellowship. All previously published work is included in a manner consistent with Elsevier copyrights, and when applicable, with the permission of the lead/senior author.

A version of **Chapter 2** has been published as:

> **Coley, E.J.L.,** Hsiao, E.Y. (2021). Microbiome and nutritional contributions to early neurodevelopment. *Trends in Neurosciences, 44*(9), 753-764. 10.1016/j.tins.2021.06.004

Author contributions: E.J.L.C. and E.Y.H.: Conceptualization, review of literature, drafting of the manuscript, critical revision of the manuscript, visualization. E.Y.H.: Supervision, funding acquisition.

A version of **Chapter 3** is currently under review and is available as a pre-print on Biorxiv as:

> **Coley-O'Rourke, E.J.,** Lum G.R., Pronovost, G.N., Özcan. E., Yu, K.B., McDermott, J., Chakhoyan, A., Goldman, E., Vuong. H.E., Paramo, J., Chu, A., Calkins, K.L., Hsiao, E.Y. (2024). The maternal microbiome modifies adverse effects of protein undernutrition on offspring neurobehavioral impairment in mice. 10.1101/2024.02.22.581439

Author contributions: E.J.C.O. led the study, performed the experiments, and analyzed the data. G.R.L assisted with analyzing datasets from 16S rRNA gene sequencing, transcriptomics, and metabolomics. G.N.P. assisted with timed matings and provided key technical guidance on establishing the PR model.E.O. and K.B.Y. assisted with 16S analysis and gnotobiotic interpretations. J.M., A.C., and E.G. assisted with behavioral and ELISA assays. H.E.V. assisted with timed matings and provided key technical guidance. J.P. assisted with mouse experiments

and provided technical guidance on gnotobiotic work. A.C. and K.L.C led the human FGR study. E.J.C.O. and E.Y.H. designed the study and wrote the manuscript. All authors discussed the results and commented on the manuscript.

A version of **Chapter 4** has been published as:

> Vuong, H.E., **Coley, E.J.L.,** Kazantsev, M., Cooke, M.E., Rendon, T., Paramo, J., Hsiao, E.Y. (2021). Interactions between maternal fluoxetine exposure, the maternal gut microbiome and fetal neurodevelopment in mice. *Behavioral Brain Research, 410,* 113353. 10.1016/j.bbr.2021.113353

Author contributions: H.E.V.: Conceptualization, Methodology, Validation, Formal analysis, Investigation, Writing – Original Draft, Visualization, Supervision. Project administration. E.J.L.C.: Validation, Formal Analysis, Investigation, Writing – Review & Editing, Visualization. M.K.: Validation, Formal Analysis, Investigation, Writing – Review & Editing, Visualization. M.E.C.: Validation, Formal Analysis, Investigation, Writing – Review & Editing. T.K.R.: Resources. J.P.: Resources. E.Y.H.: Conceptualization, Methodology, Validation, Writing – Original Draft, Supervision. Project administration, Funding acquisition.

A version of **Chapter 5** has been published as:

> **Coley, E.J.L.**, Mayer, E.A., Osadchiy, V., Chen, Z., Subramanyam, V., Zhang, Y., Hsiao, E.Y., Gao, K., Bhatt, R., Dong, T., Vora, P., Naliboff, B., Jacobs, J.P., Gupta, A. (2021). Early life adversity predicts brain-gut alterations associated with increased stress and anxiety. *Neurobiology of Stress, 15,* 100348. 10.1016/j.ynstr.2021.100348

Author contributions: EC: analysis, drafting of the manuscript, critical revision of the manuscript for important intellectual content. AG: funding, study concept and design, analysis and interpretation of data, drafting of the manuscript, critical revision of the manuscript for important intellectual content, statistical analysis, technical support, study supervision. EAM: funding, study

concept and design, critical revision of the manuscript for important intellectual content, study supervision. ZC, PV, RB, YZ, KG: statistical analysis. VO, BN, TD, JPJ, EYH: data interpretation, critical revision of the manuscript for important intellectual content.

The supplementary data displayed in the **Appendix** are unpublished. Work in this section was contributed to by Anna Chakhoyan, Dr. Geoff Pronovost, Dr. Ezgi Özcan, and Dr. Kristie Yu.

TABLE OF CONTENTS

LIST OF FIGURES

LIST OF TABLES

ACKNOWLEDGEMENTS

I am endlessly thankful to my PhD advisor, Dr. Elaine Hsiao. You are such an inspiration to me – both an incredible scientist, and a wonderful mentor. You have challenged and encouraged me to grow more as a scientist than I thought possible. I am so appreciative for all the guidance and opportunities (and of course, the science gossip!) you have offered me over the last five years. I would also like to thank my undergraduate research advisor, Dr. Heather Brenhouse. You introduced me to neuroscience research, and provided both the opportunity and the support to first pursue an independent research project, for which I am so grateful.

I am also appreciative of the generous guidance and feedback from my committee members: Dr. Carlos Portera-Cailliau, Dr. Bridget Callaghan, Dr. Sherin Devaskar , and Dr. Bennet Novitch. Your insights have greatly strengthened my work. I would also like to thank collaborators over my time at UCLA, including Dr. Emeran Mayer and Dr. Annie Gupta at the Goodman Luskin Microbiome Center, and Dr. Alison Chu and Dr. Kara Calkins at UCLA Neonatology.

I would like to acknowledge my colleagues in the Hsiao Lab, both past and present: Julissa Alvarado, Dr. Gulistan Agirman, Hannah Espey, Dr. Ping Fang, Dr. Thomas Fung, Dr. Kelly Jameson, Alonso Iñiguez, Jie Ji, Maria Kazantsev, Sabeen Kazmi, Noah Liberty, Arlene Lopez-Romero, Dr. Greg Lum, Dr. Jon Lynch, Dr. Taka Ohara, Dr. Christine Olson, Dr. Ezgi Özcan, Jorge Paramo, Dr. Geoff Pronovost, Dr. Cheng Qian, Michael Quicho, Tomiko Rendon, Celine Son, Dr. Helen Vuong, Dr. Kristie Yu, and Lewis Yu. Without your support, both scientifically and otherwise, the last five years would have been much less enjoyable. You all have made lab such a fun place to be!

I would like to acknowledge the mice who were sacrificed to advance this work.

Finally, I have to thank my incredible family. To my parents, John and Rebekah, thank you for always being willing to read through a draft or listen to me practice a talk, for always helping me to pick out outfits that look professional, and for always, always believing in me. To my sister Maya, thank you for being the best partner in crime. I'm so glad that all our practice "publishing the papers" as preschoolers is finally paying off! To my extended family, thank you for all the love and support. To my husband Matt, I could not have done this without you. I cannot express enough appreciation for all your wisdom and absurd humor (even when I don't laugh), and of course for talking me off a ledge every other day. And to my dog Mango, thanks for always bringing a smile to my face! Don't you dare repeat the stunt you pulled at the last family defense.

VITA

EDUCATION

Doctor of Philosophy, Neuroscience (in progress) Sep 2018-present
Neuroscience Interdepartmental Program, University of California, Los Angeles
Bachelor of Science, Behavioral Neuroscience with Honors Sep 2014-May 2018
Northeastern University, Boston, MA
M*agna cum laude,* University Honors Program, Dean's List

RESEARCH EXPERIENCE

Graduate Student Researcher Apr 2019- present
Dr. Elaine Hsiao Lab, University of California, Los Angeles, Los Angeles, CA

- *Doctoral Thesis: The maternal microbiome modifies effects of protein undernutrition on offspring neurobehavioral development*

Graduate Rotation Student Jan-Mar 2019
Dr. Pamela Kennedy Lab, University of California, Los Angeles, Los Angeles, CA
Graduate Rotation Student Sep-Dec 2018
Dr. Emeran Mayer Center, University of California, Los Angeles, Los Angeles, CA
Undergraduate Student Researcher Jul-Aug 2013, May 2015-Jul 2018
Dr. Heather Brenhouse**,** Northeastern University, Boston, MA

- *Honors Thesis: Transgenerational effects of early life stress: Epigenetics, expression, and behavior*

Research Assistant Jul-Dec 2016
Dr. Michael MacKenzie Research Unit, Rutgers University, New Brunswick, NJ

HONORS & AWARDS

1st Place Poster Award, Goodman-Luskin Microbiome Center Symposium, $500	2024
UCLA Dissertation Year Fellowship, $20,000	2023-2024
National Science Foundation Graduate Research Fellowship, $138,000	2020-2023
American Psychosomatic Society Scholar Award, $500	2019
UC Riverside Provost Research Fellowship, $50,000 (declined)	2018
Northeastern University Advanced Research/Creative Endeavor Award, $3,000	2017-2018
Best Undergraduate Poster Award, Boston Area Neuroscience Group	2017
Faculty for Undergraduate Neuroscience Student Travel Award, $750	2017
Northeastern University Honors Early Research Assistantship, $500	2015
Nu Rho Psi National Honors Society for Neuroscience	2015-2018

PUBLICATIONS

Coley-O'Rourke, E.J., Lum G.R., Pronovost, G.N., Ozcan. E., Yu, K.B., McDermott, J., Chakhoyan, A., Goldman, E., Vuong. H.E., Paramo, J., Chu, A., Calkins, K.L., Hsiao, E.Y. (2024). The maternal microbiome modifies adverse effects of protein undernutrition on offspring neurobehavioral impairment in mice. Manuscript under review.

Coley-O'Rourke, E.J. & Hsiao, E.Y. (2023). Microbiome alterations in autism spectrum disorder. *Nature Microbiology, 8,* 1615-1616. (Preview Article)

Pronovost, G.N., Yu, K.B., **Coley-O'Rourke, E.J.L.,** Telang, S.S., Chen, A.S., Vuong, H.E., Williams, D.W., Chandra, A., Rendon, T.K., Paramo, J., Kim, R.H., Hsiao, E.Y. (2023). The maternal microbiome promotes placental development in mice. *Science Advances, 9*(40), eadk1887.

Coley, E.J.L., Hsiao, E.Y. (2021). Microbiome and nutritional contributions to early neurodevelopment. *Trends in Neurosciences, 44*(9), 753-764.

Vuong, H.E., **Coley, E.J.L.,** Kazantsev, M., Cooke, M.E., Rendon, T., Paramo, J., Hsiao, E.Y. (2021). Interactions between maternal fluoxetine exposure, the maternal gut microbiome and fetal neurodevelopment in mice. *Behavioral Brain Research, 410,* 113353.

Coley, E.J.L., Mayer, E.A., Osadchiy, V., Chen, Z., Subramanyam, V., Zhang, Y., Hsiao, E.Y., Gao, K., Bhatt, R., Dong, T., Vora, P., Naliboff, B., Jacobs, J.P., Gupta, A. (2021). Early life adversity predicts brain-gut alterations associated with increased stress and anxiety. *Neurobiology of Stress, 15,* 100348.

Vuong, H.E., Pronovost, G.N., Williams, D.W., **Coley, E.J.L.**, Siegler, E.L., Qui, A., Kazantsev, M., Wilson, C.J., Rendon, T., Hsiao, E.Y. (2020). The maternal microbiome modulates fetal neurodevelopment in mice. *Nature, 568*(7828)*,* 281-286*.*

Coley, E.J.L., Demaestri, C., Ganguly, P., Honeycutt, J.A., Peterzell, S., Rose, N., Ahmed, N., Holschbach, M., Trivedi, M., Brenhouse, H. (2019). Cross-generational transmission of early life stress effects on HPA regulators and Bdnf are mediated by sex, lineage, and upbringing. *Frontiers in Behavioral Neuroscience, 13*(101).

PRESENTATIONS

2024 Goodman-Luskin Microbiome Center Symposium. UCLA. Oral presentation.
2024 Goodman-Luskin Microbiome Center Symposium. UCLA. Poster.
2023 Maternal Fetal Medicine Group. University of California, Los Angeles. Oral presentation.
2023 Society of Biological Psychiatry. San Diego, CA. Oral presentation.
2023 UCLA Joint SCORE Symposium. University of California, Los Angeles. Oral presentation.
2022 Department of Psychology, Northeastern University. Boston, MA. Oral presentation.
2022 Developmental Origins of Health and Disease World Congress. Vancouver, BC. Poster.
2021 Maternal Fetal Medicine Group. University of California, Los Angeles. Oral presentation.
2019 Digestive Disease Week American Gastroenterological Association. San Diego, CA. Poster.
2019 American Psychosomatic Society. Vancouver, BC. Poster.
2018 UCLA Brain Research Institute 30th Annual Neuroscience Session. Los Angeles,CA. Poster.
2018 Northeastern University Research, Innovation, and Scholarship Expo. Boston, MA. Poster.
2017 Society for Neuroscience. Washington, DC. Poster.
2017 Boston Area Neuroscience Group. Boston, MA. Poster.

SELECT TEACHING & MENTORSHIP EXPERIENCE

Teaching Assistant, *The Microbiome in Health & Disease*, UCLA	Apr-Jun 2024
Guest Lecturer, *The Microbiome in Health & Disease*, UCLA	Apr 2024
Mentorship of Sarah Hong, PhD rotation student	Jan-Mar 2024
Mentorship of Francis Chandra, PhD rotation student	Jan-Mar 2024
Mentorship of Janet McDermott, undergraduate research assistant	Oct 2021-Aug 2023
Mentorship of Eliza Goldman, high school research assistant	Feb 2020-Nov 2021
Mentorship of Anna Chakhoyan, undergraduate research assistant	Oct 2019-Aug 2022
Center for the Improvement of Mentored Experiences in Research (CIMER) Entering Mentoring Research Training	Apr-Jun 2021

SELECT LEADERSHIP & VOLUNTEER EXPERIENCE

Neuroscience Communication Affinity Group (Director), UCLA	2020-2023
CZI Neurodegenerative Disease Network (UCLA Symposium Organizing Committee)	2019-2021
Neuroscience Interdepartmental Program (Mentor), UCLA	2019-2021
Brain Bee (Outreach Volunteer), UCLA	2019
Bioscience Women's Circle (Organizer), UCLA	2018-present
Neuroscience Graduate Program Social Committee (Organizer), UCLA	2018-2022
SACNAS (Outreach Volunteer), UCLA	2018-2019

Chapter 1: Overview

The gut microbiome plays an essential role in host neurodevelopment and neurobehavioral functioning throughout the lifespan[1]. Furthermore, the gut microbiome is sensitive to prenatal and early-postnatal environmental inputs including birth method[2], early nutrition[3], exposure to antibiotics[2], and maternal stress[4,5] or immune activation[6]. These time periods are also critical for gut-brain interactions to shape lifelong neurobehavioral trajectories[7–9]. Further work is needed to understand neural-microbial interactions during these developmental windows and how they influence host brain and behavior in a persistent manner, particularly in the context of environmental stressors. To this end, my dissertation research is focused on elucidating i) how the microbiome is altered in response to environmental perturbations during critical periods; ii) how interactions in the gut-brain axis inform neurological and behavioral responses to environmental perturbations during critical periods; and iii) whether the gut microbiome presents a viable therapeutic target for intervening in neurological and behavioral impairments following environmental perturbations during critical periods. I will investigate these questions in the contexts of malnutrition (**Chapters 2 and 3; Appendix 1**), maternal selective serotonin reuptake inhibitor (SSRI) exposure (**Chapter 4**), and early life adversity (**Chapter 5**).

In **Chapter 2**, I present a review of literature relating to malnutrition, gut microbiome, and host neurodevelopment. Malnutrition remains a pressing global health concern, and further understanding of the nuanced and persistent physiological impacts is needed. I cover the spectrum of malnutrition, including undernutrition, overnutrition, and micronutrient deficiencies, and explore findings in diverse human populations and animal models. I first present evidence for the influence of perinatal malnutrition on brain development, including structural changes and behavioral dysregulation. I then present evidence for the influence of perinatal malnutrition on the microbiome, including reduced diversity and altered functional output. Finally, I present emerging evidence for the microbiome as a mediator of malnutrition-driven neurological changes, and discuss potential mechanisms by which this may occur, including direct metabolite-mediated signaling, and indirect immune, endocrine, or epigenetic regulation. A version of this work has

been published as: **Coley, E.J.L.,** Hsiao, E.Y. (2021). Microbiome and nutritional contributions to early neurodevelopment. *Trends in Neurosciences, 44*(9), 753-764. 10.1016/j.tins.2021.06.004

In **Chapter 3**, I present original research investigating the role of the maternal microbiome in gestational protein restriction. Protein restriction (PR) is a common form of undernutrition globally, and is particularly known to lead to impaired growth[10], persistent neurodevelopmental impairments[11,12], and microbial shifts[13]. Critically, current nutritional interventions are not adequate to prevent these long-lasting microbial and behavioral effects, despite their benefit to gross physiological recovery[14–16]. Therefore an urgent need remains for a deeper understanding of mechanisms by which brain and behavior are influenced by malnutrition, and what types of interventions may be able to target these mechanisms. In this study, I highlight a moderating influence of the maternal microbiome during gestational protein restriction on neurodevelopment and behavioral trajectories of offspring. I found that in a mouse model, PR during gestation induces fetal growth restriction, and in combination with PR-associated rearing in the early postnatal period, reduces pup survival and induces anxiety-like behavior and cognitive impairment in adult offspring. Using genomic, transcriptomic, and metabolomic techniques, I identified shifts in the maternal microbiota and serum metabolome, as well as in the fetal brain transcriptome and metabolome in late gestation. Using broad-spectrum antibiotics to deplete the maternal microbiota during gestation, I found that a subset of these behavioral, transcriptomic, and metabolomic changes in response to diet are ameliorated or exacerbated by the microbiota, suggesting a modulating role. Finally, I observed that a cocktail of 10 microbially-modulated metabolites supplemented throughout gestation to PR dams was sufficient to ameliorate pup survival and adult offspring behavioral impairment in a sexually-dimorphic manner, where females display reduced anxiety-like behaviors, and males display restored memory. These experiments highlight the gestational period as a critical window for malnutrition, suggest that dietary perturbations act on both maternal and fetal systems to induce subsequent impairment, and implicate the maternal microbiome as both a moderating influence, and as a potential therapeutic target. In addition to

using a mouse model, I utilized data from a cohort of preterm infants with or without growth restriction, provided by Dr. Kara Calkins and Dr. Alison Chu, to ascertain if growth restriction relates to gut-brain alterations in humans. I found that growth-restricted infants had reduced microbial diversity and increased *Staphylococcus* in the early postnatal period, as well as impaired cognitive development scores in the first two years of life. Critically, the microbial findings in the first few weeks of life correlated with the later neurodevelopmental scores in cognitive, language, and motor domains, further suggesting translational potential for gut-brain signaling to set developmental trajectories following growth restriction. A version of this work is currently under review and is available as a pre-print on Biorxiv as: **Coley-O'Rourke, E.J.,** Lum G.R., Pronovost, G.N., Ozcan. E., Yu, K.B., McDermott, J., Chakhoyan, A., Goldman, E., Vuong. H.E., Paramo, J., Chu, A., Calkins, K.L., Hsiao, E.Y. (2024). The maternal microbiome modifies adverse effects of protein undernutrition on offspring neurobehavioral impairment in mice. 10.1101/2024.02.22.581439

In **Appendix 1**, I describe additional original research supplementary to **Chapter 3**. I first explored the effects of PR at mid-gestation, and show that placental and maternal disruptions precede fetal growth restriction. I then discuss results of an extensive behavioral battery performed on cross-fostered offspring of PR or CD dams. Although there were mild and sexually-dimorphic effects of PR gestation and associated rearing in exploratory behavior, sociability, and tactile sensitivity, the overall absence of clear behavioral signatures in these domains led me to conclude that the strongest behavioral phenotypes fall into anxiety-like and cognitive domains, as explored in **Chapter 3**. I next present a deeper investigation of fetal brain changes following gestational PR and maternal microbiota depletion. Multi-'omics findings in **Chapter 3** raised potential avenues by which PR manipulates fetal brain, including hypothalamic-pituitary-adrenal (HPA) axis dysregulation and serotonergic signaling. Using immunostaining and confocal imaging, I found that serotonin transporter-positive axons were depleted in subregions of the fetal hippocampus and frontal cortex following gestational PR, and that this reduction was exacerbated

by maternal microbial depletion. Conversely, I saw no effect of gestational PR on proliferation or microglia in the developing hippocampus and frontal cortex, and quantitative polymerase chain reaction (qPCR) revealed no significant differences in HPA axis-related genes in the fetal brain. I also discuss effects of PR on short chain fatty acids (SCFA) in fetal brain. I find that maternal serum is unaffected, and that microbial depletion has no discernable impact. I then present findings on maternal splenic and placental insufficiency induced by gestational PR. These phenotypes were unchanged by maternal microbial depletion or any microbial-informed interventions including supplementation of short-chain fatty acids, gut-modulated metabolites, or bacterial cocktail. These spleen and placental phenotypes may present further avenues by which fetal brain changes occur in response to diet, as they may suggest potential maternal immune dysregulation, or impaired nutrient, oxygen, and waste transport between maternal and fetal compartments. Finally, I share the results of a bacterial supplementation experiment, which aimed to replenish microbes depleted by the PR diet with the goal of ameliorating offspring phenotypes. To this end, 7 microbes were identified, cultured, and supplemented throughout gestation to PR dams by oral gavage. However, this supplementation was largely unsuccessful, as there were no significant effects of supplementation on prenatal maternal or fetal phenotypes. There were select domain- and sex-specific behavioral changes, including anxiety-like behavior that was less severe in male offspring, but more severe in females. In conclusion, these supplementary findings suggest myriad physiological consequences of gestational PR, both on the maternal and fetal side, only some of which seem to be microbiome-dependent.

In **Chapter 4**, I describe original research led by Dr. Helen Vuong investigating how exposure to SSRIs during pregnancy affects maternal microbiome and fetal brain. Peripartum depression is a serious psychiatric condition with negative health consequence for individuals and their infants[17]. However, treatments specific to pregnancy and the postpartum period are lacking. SSRIs are the most common medication used to treat depression in pregnancy[18], but they have been associated with adverse outcomes in offspring[19,20]. Additionally, SSRIs are known to interact

with the microbiome[21,22], and microbial heterogeneity may explain individual differences in response to SSRI treatment. Using a mouse model, we found that daily treatment with fluoxetine during mid-gestation induced myriad transcriptional changes in the fetal brain by RNA sequencing, including in genes relating to neuronal signaling and synaptic organization. Using 16S sequencing, we observed that fluoxetine treatment did not alter maternal microbial composition, however treatment with broad-spectrum antibiotics to deplete the maternal microbiota was sufficient to alter fetal transcriptomic responses to fluoxetine. RNAscope,in situ hybridization revealed that maternal fluoxetine treatment increased region-specific *opioid binding protein/cell adhesion molecule like (Opcml)* staining in the fetal brain, but maternal microbial depletion prevented this increase. We concluded that maternal fluoxetine treatment during mid-gestation alters fetal brain transcriptomic signatures in a microbiome-dependent manner. A version of this work has been published as: Vuong, H.E., **Coley, E.J.L.,** Kazantsev, M., Cooke, M.E., Rendon, T., Paramo, J., Hsiao, E.Y. (2021). Interactions between maternal fluoxetine exposure, the maternal gut microbiome and fetal neurodevelopment in mice. *Behavioral Brain Research, 410,* 113353. 10.1016/j.bbr.2021.113353

In **Chapter 5**, I describe original research overseen by Dr. Arpana Gupta and Dr. Emeran Mayer investigating gut-brain signatures of early adversity in a human adult cohort. Stress and adversity during critical periods is a well-appreciated neurodevelopmental disruptor that increases vulnerability to a variety of health conditions throughout the lifespan[23]. Early adversity has been correlated with various structural and functional brain changes[24,25]. Furthermore, the gut microbiome is sensitive to stressors[26,27]. There is evidence that behavioral responses to early adversity are microbiome-dependent[28], and microbially-derived metabolites such as short chain fatty acids have been shown to temper host responses to stress[29,30]. In a sample of 128 healthy participants, we assessed incidence of early adversity before 18 years of age and current perceived stress, anxiety, and depression using validated questionnaires. We first observed that participants with high early adversity scores also had significantly higher current anxiety scores.

16S rRNA sequencing showed no differences in microbial composition based on early adversity, but untargeted metabolomics on stool samples revealed four gut-related metabolites – 5-oxoproline, malate, urate, and glutamate gamma methyl ester – that were significantly decreased in participants with high early adversity exposure. Using magnetic resonance imaging, we found that early adversity correlated with various alterations in brain functional connectivity, primarily within sensorimotor, salience, and central executive networks. Integrated analysis revealed significant associations between the identified metabolites, functional brain connectivity, and current stress, anxiety, and depression, leading us to hypothesize that critical period stressors may increase vulnerability to negative mood and stress later in life via alterations in brain-gut signaling. A version of this work has been published as: **Coley, E.J.L.**, Mayer, E.A., Osadchiy, V., Chen, Z., Subramanyam, V., Zhang, Y., Hsiao, E.Y., Gao, K., Bhatt, R., Dong, T., Vora, P., Naliboff, B., Jacobs, J.P., Gupta, A. (2021). Early life adversity predicts brain-gut alterations associated with increased stress and anxiety. *Neurobiology of Stress, 15,* 100348. 10.1016/j.ynstr.2021.100348

Overall, this dissertation aims to contribute to the existing understanding of how the gut microbiome interacts with the developing brain to respond to environmental perturbations and set life-long trajectories of neurological and neurobehavioral function. There is still much work to be done in this area, including narrowing down critical periods for discrete neurological or behavioral impairments, clearly elucidating specific mechanisms by which developmental gut-brain interactions occur and determining whether these mechanisms are conserved across contexts, and translating these findings to well-controlled and highly powered longitudinal human cohorts.

References

1. Lynch, C.M.K., et al. Critical windows of early-life microbiota disruption on behaviour, neuroimmune function, and neurodevelopment. *Brain. Behav. Immun.* **108**, 309–327 (2023).

2. Yassour, M., et al. Natural history of the infant gut microbiome and impact of antibiotic treatment on bacterial strain diversity and stability. *Sci. Transl. Med.* **8**, 343ra381 (2016).

3. Bergstrom, A., et al. Establishment of intestinal microbiota during early life: a longitudinal, explorative study of a large cohort of Danish infants. *Appl. Environ. Microbiol.* **80**, 2889–2990 (2014).

4. Zijlmans, M.A., et al. Maternal prenatal stress is associated with the infant intestinal microbiota. *Psychoneuroendocrinology* **53**, 233–245 (2015).

5. Jasarevic, E. *et al.* Stress during pregnancy alters temporal and spatial dynamics of the maternal and offspring microbiome in a sex-specific manner. *Sci. Rep.* **7**, 44182 (2017).

6. Kim, et al., S. Maternal gut bacteria promote neurodevelopmental abnormalities in mouse offspring. *Nature* **549**, 528–532 (2017).

7. Jasarevic, T. L., E. &. Bale. Prenatal and postnatal contributions of the maternal microbiome on offspring programming. *Front. Neuroendocrinol.* **55**, (2019).

8. Vuong, H. E. *et al.* The maternal microbiome modulates fetal neurodevelopment in mice. *Nature* **586**, 281–286 (2020).

9. Clarke, G., et al. The microbiome-gut-brain axis during early life regulates the hippocampal serotonergic system in a sex-dependent manner. *Mol. Psychiatry* **18**, 666–673 (2013).

10. Ghosh, et al., S. Assessment of protein adequacy in developing countries: quality matters. *Br. J. Nutr.* **108**, S77–S87 (2012).

11. Walker, et al., S. P. Early Childhood Stunting Is Associated with Poor Psychological Functioning in Late Adolescence and Effects Are Reduced by Psychosocial Stimulation. *J. Nutr.* **137**, 2464–2469 (2007).

12. Walker, et al., S. P. Effects of early childhood psychosocial stimulation and nutritional supplementation on cognition and education in growth-stunted Jamaican children: prospective cohort study. *The Lancet* **366**, 1804–1807 (2005).

13. Smith, et al., M. I. Gut microbiomes of Malawian twin pairs discordant for kwashiorkor. *Science* **339**, 548–554 (2013).

14. Waber, et al., D. P. Neuropsychological outcomes at midlife following moderate to severe malnutrition in infancy. *Neuropsychology* **28**, 530–540 (2014).

15. Subramanian, et al., S. Persistent gut microbiota immaturity in malnourished Bangladeshi children. *Nature* **510**, 417–421 (2014).

16. Galler, et al., J. R. Infant malnutrition is associated with persisting attention deficits in middle adulthood. *J. Nutr.* **142**, 788–794 (2012).

17. O'Donnell, K.J., et al. The persisting effect of maternal mood in pregnancy on childhood psychopathology. *Dev. Psychopathol.* **26**, 393–403 (2014).

18. Jimenez-Solem, E., et al. Prevalence of antidepressant use during pregnancy in Denmark, a nation-wide cohort study. *PLoS One* **8**, e63034 (2013).

19. Videman, M., et al. Newborn brain function is affected by fetal exposure to maternal serotonin reuptake inhibitors. *Cereb. Cortex* **27**, 3208–3216 (2017).

20. Hayes, R.M., et al. Maternal antidepressant use and adverse outcomes: a cohort study of 228,876 pregnancies. *Am. J. Obstet. Gynecol.* **207**, e41-49 (2012).

21. Fung, T.C., et al. Intestinal serotonin and fluoxetine exposure modulate bacterial colonization in the gut. *Nat. Microbiol.* **4**, 2064–2073 (2019).

22. Vich Villa, A., et al. Impact of commonly used drugs on the composition and metabolic function of the gut microbiota. *Nat. Commun.* **11**, (2020).

23. Shonkoff, J.P., et al. The lifelong effects of early childhood adversity and toxic stress. *Pediatrics* **129**, e232-246 (2012).

24. Gupta, A., et al. Early adverse life events are associated with altered brain network architecture in a sex- dependent manner. *Neurobiol. Stress* **7**, 16–26 (2017).

25. Miskovic, V., et al. Adolescent females exposed to child maltreatment exhibit atypical EEG coherence and psychiatric impairment: linking early adversity, the brain, and psychopathology. *Dev. Psychopathol.* **22**, 419–432 (2010).

26. Callaghan, B.L., et al. Mind and gut: Associations between mood and gastrointestinal distress in children exposed to adversity. *Dev. Psychopathol.* **32**, 309–328 (2020).

27. Hantsoo, L., et al. Childhood adversity impact on gut microbiota and inflammatory response to stress during pregnancy. *Brain. Behav. Immun.* **75**, 240–250 (2019).

28. De Palma, G., et al. Microbiota and host determinants of behavioural phenotype in maternally separated mice. *Nat. Commun.* **6**, 7735 (2015).

29. Dalile, B., et al. Colon-delivered short-chain fatty acids attenuate the cortisol response to psychosocial stress in healthy men: a randomized, placebo-controlled trial. *Neuropsychopharmacology* **0**, 1–10 (2020).

30. Van de Wouw, M., et al. Short-chain fatty acids: microbial metabolites that alleviate stress-induced brain-gut axis alterations. *J. Physiol.* **596**, 4923–4944 (2018).

Chapter 2: Malnutrition and the microbiome as modifiers of early neurodevelopment

Abstract: Malnutrition refers to a dearth, excess, or altered differential ratios of calories, macronutrients, or micronutrients. Malnutrition, particularly during early life, is a pressing global health and socioeconomic burden that is increasingly associated with neurodevelopmental impairments. Understanding how perinatal malnutrition influences brain development is crucial to uncovering fundamental mechanisms for establishing behavioral neurocircuits, with the potential to inform public policy and clinical interventions for neurodevelopmental conditions. Recent studies reveal that the gut microbiome can mediate dietary effects on host physiology and that the microbiome modulates the development and function of the nervous system. This review discusses evidence that perinatal malnutrition alters brain development, and examines the maternal and neonatal microbiome as a potential contributing factor.

The Persistent Burden of Malnutrition

Perinatal nutrition is an early determinant of healthy growth and long-term developmental trajectories [1]. Malnutrition during critical developmental periods, whether characterized by overabundance, lack, or altered relative abundances of energy or nutrients, can drastically and persistently alter the course of development across many body systems, including the nervous system. With early-life malnutrition remaining a foremost global health burden and an indicator of systemic inequities, alongside a rising prevalence of neurodevelopmental disorders, it is critical to understand the roles that malnutrition may play in disrupting brain development, the underlying mechanisms involved, and how this process may be thwarted. The microbiome is increasingly implicated in these processes, as it interacts directly with diet to inform nutrition, and has myriad influences on host physiology, including brain function and behavior. Previous work has explored links between malnutrition and neurodevelopment [2, 3], between malnutrition and the gut microbiome [4, 5], and between neurodevelopment and the gut microbiome [6, 7] during early developmental periods. Very recently, ties between nutrition and the developmental brain-gut-microbiome axis have been presented [8], as well as maternal diet and offspring

neurodevelopment through a lens of inflammation, in which the gut microbiome may play a role [9]. The current review aims to evaluate evidence linking malnutrition, the gut microbiome, and neurodevelopment by highlighting associations between perinatal malnutrition and neurodevelopmental outcomes of the offspring and drawing attention to emerging evidence suggesting that the maternal microbiome may mediate this relationship. It further explores molecular mechanisms by which the maternal microbiome and diet may impact core neurodevelopmental processes and potential implications of microbiome-dietary interactions for human neurological health and disease. Wherever possible, this review will isolate the prenatal period as a critical window for neural effects of malnutrition and contributions of maternal microbiome, but where evidence is lacking or models are nonspecific, and particularly when humans are the subject, findings will be presented from the perinatal period. Unless otherwise stated, malnutrition models described here are characterized by alterations in ratios of nutrients, rather than in absolute values.

Perinatal Malnutrition and Neurodevelopment

Undernutrition is a staggering problem around the world: about 50% of deaths of children under five are due to undernutrition and associated conditions [10]. The most commonly reported neurobehavioral effects of early macronutrient undernutrition are in cognitive and social domains (**Table 2.S1**). In a cohort of 3913 children from Brazil, female offspring of previously undernourished mothers, characterized by low BMI and gestational weight gain, had higher likelihood of exhibiting a global, language, or motor delay at two years of age [11]. Young children subjected to poor nutrition had deficits in social behavior [12]. Early postnatal protein intake in particular was positively correlated with motor and cognitive scores as well as total brain volume in preterm infants [13] and negatively correlated with myelination-related deficits [14], cerebral atrophy and ventricular dilation [15, 16], cortical dendritic dysplasia [17], and enlarged cisterna magna and periventricular white matter abnormalities [16]. Youth exposed to low protein during

the first year of life displayed reduced cognitive function including IQ and attention in childhood [18], and increased depressive symptoms in adolescence [18, 19]. Other macronutrients are similarly crucial: in preterm infants, early postnatal fat intake was associated with larger cerebellum [13], basal ganglia [13, 20], thalamus [13], and total brain [20], in addition to increased fractional anisotropy in the internal capsule [13], corona radiata [20], thalamic radiations [20], posterior longitudinal fasciculus [20], and corticospinal tract [20]. Critically, brain growth was associated with later psychomotor function [20]. Some neural deficits may persist into adulthood: in 118 members of the Dutch Famine birth cohort, exposure to prenatal undernutrition was associated with reduced white matter perfusion in later adulthood, as well as reduced blood flow in cingulate cortex in men [21] and brain features linked to aging in men [22]. In addition, adults from Barbados subjected to protein restriction during the first year of life had persistent attention deficits [23] and reduced executive functions, including cognitive flexibility, working memory, and visuospatial integration [24].

Such links are not restricted to macronutrient undernutrition, as early postnatal deficiencies in micronutrients such as vitamin B12, folate and vitamin K have also been associated with brain atrophy and corpus callosum thinning [25], psychiatric disorders [26], and increased risk for intracranial hemorrhage [27]. Moreover, while not as well-studied as undernutrition, perinatal overnutrition is a growing global health concern, as an estimated 38 million children under five are obese or overweight [28]. Maternal overnutrition, measured by high BMI before and/or during pregnancy, is associated with reduced infant scores in cognitive and language development domains [11], impaired visual-motor skills [29], decreased sociability and learning, particularly in boys [30], and altered fetal thalamic and cortical connectivity [31, 32]. Altogether, the increasing number of studies linking perinatal malnutrition to neurodevelopmental abnormalities highlight a need to understand their underlying neurobiological bases.

Complementary investigations using animal models provide causal evidence that prenatal malnutrition can impair neurodevelopment and later-life behavior. In rats and guinea pigs,

absolute food restriction during gestation led to reduced brain size [33, 34], increased corticosterone and corticotropin-releasing hormone [33], and altered hippocampal physiology [34]. In baboons, overall food restriction during gestation led to reduction of subventricular zone size, glial markers, neuronal processes, and neurotrophic factors, increased apoptosis ratio, and dysregulated gene expression, including downregulation of signaling pathways relevant for neurogenesis and axon guidance [35]. Prenatal protein restriction in rats reproducibly impaired operant conditioning learning [36-38], recognition memory and hippocampal morphology [39], oligodendrocyte development [40], cortical physiology [38], and anxiety-like behaviors [37, 41]. Notably, even a very limited period of protein restriction during the pre-conception period alone was sufficient to disrupt fetal cortical development and impair hippocampal-dependent recognition memory in rats [42]. Similar effects were reported in rats fed a micronutrient-deficient diet – lacking vitamin D, zinc, or folate – during gestation, where offspring had alterations in levels of neurochemicals across various brain regions [43], impaired memory [44, 45], and increased hippocampal apoptosis [45, 46]. Analogous to observations of overnutrition in humans, prenatal high-fat diet in rodents also induced neural alterations, including fetal microglial reactivity [47], changes in neurochemical levels [48], and increased addiction-like behaviors [48]. While these results illustrate the vital role that nutrition during the prenatal period plays in early neurodevelopment and long-term trajectories, it is critical to mention that many of these diet models are simplified and reductionist, lacking for example soluble fiber in addition to having low protein or high fat. Dietary fiber has been shown to alleviate obesity and metabolic effects of high-fat diet, and is metabolized by the gut microbiome [49, 50]. It may indeed be the case that nutritional requirements, and consequences of those not being met, are more complex and interdependent than what previous models may suggest, and may constitute a spectrum rather than a binary phenomenon of undernutrition versus overnutrition. To further understand malnutrition as a continuum, it is critical to investigate fundamental mechanisms by which specific subtypes of prenatal malnutrition disrupts brain and behavioral development.

Perinatal Malnutrition and the Microbiome

The gut microbiome, comprising trillions of microorganisms indigenous to the gastrointestinal tract, is increasingly implicated as a key determinant of dietary effects on host physiology, with the capacity to modulate brain development and behavior. Alterations in diet and nutrition shift the structure and function of the gut microbiome, especially during critical periods of development (**Table 2.S1**). Postnatal severe acute malnutrition (SAM) in children from Bangladesh up to two years of age was associated with reduced microbial alpha diversity – species richness and evenness – suggesting community immaturity, which persisted even after dietary intervention [51]. In a similar cohort, reduced alpha diversity was explained by the discrimination of bacteriophages – bacterial viruses – between stunted and non-stunted children [52]. In young children from Senegal and Niger, microbial differences between subtypes of postnatal malnutrition were apparent, with those with kwashiorkor – a form of protein deficiency characterized by edema – showing a severe reduction in diversity [53, 54], and increased pathogenic species [54], and those with marasmus – a form of calorie deficiency characterized by weight loss and dehydration – showing an intermediate reduction in diversity [53]. Additionally, taxonomic abundances were differentially altered between subtypes, with increased *Proteobacteria* and *Fusobacteria* in kwashiorkor and decreased *Bacteroidetes* in marasmus [53]. Children with postnatal SAM harbored microbiomes with reduced bacterial load [55], decreased functional pathways relating to metabolism and nutrient uptake [56], and increased virulence-related genes [56]. They also displayed increased intestinal redox potential [55], a possible functional consequence of altered microbial community composition. In contrast, children from Uganda under two years of age with postnatal kwashiorkor displayed increased alpha diversity [57, 58], a modest difference in beta diversity [57], and alterations in relative taxonomic abundances, both compared to controls and across subtypes of malnutrition [58]. In regard to overnutrition, maternal high-fat diet during gestation in humans correlated with alterations in the

infant microbiota, such as increased *Enterococcus* and decreased *Bacteroides* [59]. A similar prenatal diet in nonhuman primates resulted in not only altered taxonomic abundances in the dams, but also reduced *Proteobacteria* and increased *Firmicutes* in the offspring [60]. Altogether, these findings highlight key context-specific effects of malnutrition on the gut microbiome and further emphasize the need for equally context-specific approaches to considering interventions.

Interestingly, altered dietary composition alone does not determine malnutrition; rather, how the host and microbiota respond to the diet are critical factors for the manifestation of malnourished phenotypes. Indeed, twins from Malawi discordant for postnatal kwashiorkor had altered microbiota compared to their unaffected twin on the same diet [61]. Transplantation of the kwashiorkor-associated microbiota into mice yielded altered microbial taxonomic profiles and metabolite levels, in addition to marked weight loss – a feature analogous to the growth restriction characteristic of human undernutrition – when compared to transplantation of the microbiota from the unaffected twin [61]. These findings provide strong proof-of-concept that the gut microbiome is altered by malnutrition and can contribute to the detrimental effects of early malnutrition on growth and development.

Additional studies highlight the potential to develop microbiome-based treatments for core symptoms of early malnutrition. In a study examining effects of the maternal microbiota on offspring malnutrition, mouse dams were reared as wildtype, germ-free, or monocolonized with *Lactobacillus plantarum*, and offspring were placed on a protein-, fat-, and vitamin-depleted diet on postnatal day 21 [62]. Offspring of germ-free and monocolonized dams exhibited impaired growth, increased growth hormone, and decreased insulin-like growth factor-1 and its binding protein-3, in response to the depleted diet [62]. Notably, maternal colonization with the bacterium *L. plantarum* mitigated the compounding effects of microbiome depletion and malnutrition, with the *L. plantarum* monocolonized mice showing comparable growth and growth-related biomarkers to wildtype controls [62]. In a human study examining postnatally malnourished children under five years of age, characterized by low weight and height, supplementation of a sufficient diet with

L. rhamnosus GG reduced infections, increased body mass index, and elevated protein levels, compared to children given a sufficient diet alone [63]. Additionally, “microbiota-directed foods”, formulated to support healthy maturation and development of the gut microbiota, were shown to alter the gut microbiota and improve bone and immune development in children with postnatal moderate acute malnutrition [64]. Notably, interventions may not be universally effective. In a comparison of infants from Nicaragua and Mali who were provided a rice bran supplement, infants from different geographical areas exhibited divergent outcomes: Nicaraguan infants had improved length scores but Malian infants did not, and each had differential microbial taxonomic profiles and metabolite levels [65]. These studies highlight varying effects of malnutrition on the gut microbiome, and present it as a potential target, both for mechanistic investigations and therapeutic interventions.

Emerging Roles for the Microbiome in Perinatal Malnutrition and Neurodevelopment

Mounting evidence that the microbiome contributes to the ability of malnutrition to impair offspring growth raises the important question of whether the microbiome also contributes to the neurodevelopmental abnormalities associated with malnutrition. Up until this point of the review, neurodevelopmental and microbial alterations in response to malnutrition have been discussed as separate; going forward, evidence will be presented for their interdependence. In postnatally undernourished children from Mumbai – many of whom displayed stunting, wasting, anemia, and iron deficiency – microbial alpha diversity and relative abundance of *Actinobacteria* correlated positively with head circumference [66]. In a cohort of children from Bangladesh with postnatal SAM, treatment with microbiota-targeted diets not only ameliorated growth restriction and microbial immaturity, but also altered levels of plasma hormones, metabolites, and expression of key proteins related to neurodevelopment, such as axonal guidance cues and neurotrophin receptors [64]. These changes were further associated with alterations in short-chain fatty acids (SCFAs), select amino acids, hydroxyanthranillic acid and indole-3-lactic acid [64], suggesting a

microbiome-dependent and neurodevelopmental response to dietary intervention. Similarly, children from Bangladesh with postnatal MAM treated with the same dietary intervention displayed increased weight-for-age and weight-for-length, the latter of which also positively correlated with plasma proteins related to axonal guidance and neurotrophins, as well as 23 gut taxa including *P. copri* and *F. prausnitzii* [67]. Low-weight preterm infants displayed reduced head circumference and microbial alpha-diversity, greater relative abundances of *Staphylococcaceae* and *Enterobacteriaceae*, and increased metabolites relating to fatty acid oxidation and lipolysis [68]. And low-weight preterm infants who received a pro/prebiotic supplement during the first week of life had better weight gain, larger head circumference, and a shorter time to solely enteric feeding [69].

Analogous links between malnutrition, the microbiome, and brain development exist for early overnutrition in animal models. Offspring born from mice fed a high-fat diet during gestation and lactation displayed cognitive deficits and disparate microbiota which clustered based on maternal diet [70]. Critically, the researchers identified specific taxa in the offspring, including *Clostridium, Parabacteroides* and *Proteobacteria*, which correlated with both maternal obesity and offspring cognitive deficits [70]. In an independent mouse study, maternal consumption of a high-fat diet during gestation and lactation altered the composition of the maternal and offspring microbiota, and yielded offspring with reduced oxytocin-positive neurons in the paraventricular nuclei, disrupted dopaminergic long-term potentiation in the ventral tegmental area, and impaired social behavior [71]. Critically, the microbiome changes were shown to be causal: co-housing offspring of dams fed a high-fat diet with control offspring corrected the microbiome and social deficits [71]. Moreover, supplementation with *L. reuteri*, which was significantly reduced in the high-fat diet-associated microbiota, was sufficient to rescue deficits in social behavior, central oxytocin expression, and long-term potentiation in the offspring of dams fed the high-fat diet [71]. Overall, these studies provide evidence that the gut microbiome may contribute to effects of nutrition on neurodevelopment and behavior.

Proposed Mechanisms for Microbial Effects on Malnutrition and Neurodevelopment

Direct signaling mechanisms: Microbiome-dependent metabolites implicated in neuronal development

Metabolites produced or modulated by the gut microbiota have garnered interest for their roles in regulating the function of various physiological systems, including the central nervous system. In cases of prenatal malnutrition, subsets of metabolites regulated by the maternal microbiome are capable of crossing the placenta and interacting with the fetus before birth [72] (**Fig. 2.1**). SCFAs, such as butyrate, propionate, and acetate, are of particular interest, as they are direct end-products of microbial fermentation of complex carbohydrates, and are thought to be critical players in neurodevelopmental processes such as the early maturation of microglia [30, 73]. Indeed, human undernutrition has been associated with alterations in SCFAs, amino acids, and various microbiota-dependent metabolites across body compartments [64], suggesting that microbiome impacts metabolic responses to dietary malnutrition. In a human cohort, levels of propionate and butyrate in the maternal serum correlated with levels of the same molecules seen in cord blood, highlighting the potential for maternal bioavailability of SCFAs to impact levels seen in developing offspring [74]. Supporting a role for SCFAs in modifying neurodevelopment, offspring of mice fed a low-fiber diet during gestation exhibited impaired motor and learning/memory behavior, increased anxiety-like behavior, and decreased hippocampal glutamate receptor subunit expression and excitatory postsynaptic potentials [74]. Furthermore, dams on the low-fiber diet had distinct microbiomes, including higher *Firmicutes* and lower *Bacteroidetes*, as well as lower levels of butyrate and propionate in maternal serum and offspring serum and brain [74]. Critically, butyrate supplementation during gestation attenuated abnormalities in offspring, seemingly by decreasing histone deacetylase (HDAC) 4 expression in the hippocampus [74]. Moreover, in a model of overnutrition (using a diet high in fructose, fat, and energy) during gestation and lactation in Yucatan minipigs, dams on a high-fat diet had reduced

fecal SCFAs and increased plasma free fatty acids during gestation, and offspring showed similar phenotypes one to three months postnatally [75]. This phenotype in piglets coincided with reduced hippocampal neurogenesis, particularly in the granule cell layer, and yet a contradictory increase in working and reference memory, which could potentially be explained by a difference in motivation for sugary food rewards [75]. Similarly, offspring of mice fed a high-fat diet during gestation and lactation displayed impaired long-term and working memory, less sociability and social novelty preference, reduced levels of acetate, butyrate, and propionate, and decreased expression of the SCFA receptor *Olfr78* as well as genes relating to microglial maturation, glutamatergic signaling, neural development, and synaptic plasticity in the prefrontal cortex and hippocampus [30]. Furthermore, the microbiome was altered by maternal diet, including specific taxa such as S24-7, *Bifidobacterium animalis*, *Prevotella*, Clostridiales, and *Ruminococcus* [30], and was shown to be causal to neurological outcomes, as co-housing, fecal-microbial transplants, and cross-fostering across diets were effective at ameliorating deficits in the offspring [30]. Interestingly, the behavioral, neurophysiological, and bacterial perturbations were rescued by a high-fiber diet delivered either maternally or to the offspring post-weaning, and also by acetate and propionate supplementation to offspring post-weaning [30]. This suggests a mechanistic role for SCFAs in mediating the effect of diet on gut microbiome and brain, as well as an exciting override of traditionally understood critical periods with these interventions. These studies suggest a role for microbial carbohydrate metabolism in brain development.

In addition to products from carbohydrate metabolism, microbiome-dependent metabolites generated largely from protein metabolism have also been implicated in linking early malnutrition to alterations in the nervous system. In cohorts of postnatally acutely malnourished children under two and a half years of age from Zambia and Brazil, various gut microbe-related metabolites measured in urine – such as 3-indoxyl sulfate [76, 77] and trimethylamine [76], which are produced in response to microbial metabolism of L-tryptophan and dietary carnitine, respectively – were negatively correlated with measures of enteropathy [76] and growth [77]. 3-indoxyl sulfate

is of particular interest, as it has also been shown to promote the development of fetal thalamocortical circuits underlying sensory behavior in mice [78]. Children from Uganda with postnatal SAM displayed high levels of even-chain acylcarnitines before treatment [79]. In a mid-gestational choline deficiency model in pigs, brains of prenatally deficient piglets were smaller than controls, and offspring displayed postnatal alterations in microbiota-dependent metabolites, such as increased deoxycarnitine [80]. Moreover, a prospective study of 35 mother-infant pairs reported that breast milk from obese mothers had differential levels of metabolites compared to lean mothers, including various acylcarnitines as well as human milk oligosaccharides (HMOs) which are critical for development of an infant's microbiome [81]. Studies such as these present the potential for microbial protein metabolism to be relevant to neurodevelopment.

Lipid-associated metabolites have also been linked to the infant microbiome and brain development [82], and may similarly be altered by maternal malnutrition. In a cohort from Malawi, sialylated HMOs were observed to be significantly decreased in mothers of severely stunted infants [83]. When sialylated oligosaccharides were supplemented to gnotobiotic mice and piglets colonized with a stunted infant's microbiota and fed a Malawian diet, the animals exhibited increased growth and altered metabolites in serum, liver, muscle, and brain, as compared to vehicle-treated controls [83]. Particularly affected were N-acetylneuraminic acid, a component of gangliosides that is important for synaptic development and function [84], adenosine, which plays a role in the neuroimmune system [85], and inosine, a purine nucleoside with neuroprotective properties [86]. These changes were shown to be microbiome-dependent, as germ-free animals lacked the same positive effects [83]. In a longitudinal study, prenatally overweight/obese mothers examined during mid-gestation and their offspring examined at a four-year follow-up had significantly reduced plasma ceramides [87], a class of sphingolipids widely modulated by the gut microbiome [88]. Notably, sphingolipids play a critical role in neurodevelopment: they form a major component of myelin, their expression supports key developmental processes including neuronal differentiation, and their depletion results in inappropriate axonal outgrowth and synaptogenesis

[89]. These results suggest that microbiome-dependent changes in lipid-based metabolites may interact with the developing brain. Altogether, these studies support the potential for microbially-modulated metabolites from nutrient catabolism to impact neurodevelopmental processes.

Indirect Signaling Mechanisms: Potential influences of the microbiome on secondary systems that impact neurodevelopment

Aside from regulating dietary metabolites with direct roles in neurodevelopment, the microbiome can also interact with host physiology in ways that indirectly alter neurodevelopmental trajectories (**Fig. 2.1**). For example, the microbiome regulates immune development and function, and early neuroimmune interactions are integral to healthy perinatal neurodevelopment [7]. Models of malnutrition have been linked to both impaired immunity and increased inflammation, in relation to alterations in the maternal or developing microbiome [90, 91]. Additionally, activation of the maternal immune system during pregnancy, through infection or antigen exposure, has been studied in rodents and commonly shown to induce neurodevelopmental and behavioral abnormalities. These abnormalities are associated with widespread alterations in the composition of the gut microbiome, mediated by maternal colonization with segmented filamentous bacterium, an inflammation-promoting member of the gut microbiome [92]. Treatment with *Bacteroides fragilis*, a commensal bacterium that promotes immunosuppression, was shown to ameliorate abnormalities resulting from maternal inflammation [93]. Furthermore, interleukin-17a produced by gut bacteria-induced Th17 cells was necessary to impart neural and behavioral consequences of maternal inflammation [92]. Overall, these studies provide a proof-of-concept that changes in the maternal microbiome can alter neurodevelopment by promoting inflammatory responses, and further raise the question of whether maternal malnutrition can similarly shape the microbiome in ways that influence neurodevelopment through immune-mediated pathways.

Another potential pathway by which malnutrition-induced alterations in the microbiome may impact neurodevelopment is through regulation of stress systems. Numerous studies linking

the microbiome to the nervous system have focused on anxiety systems and behaviors, which established reproducible roles of the microbiome in regulating hypothalamic-pituitary-adrenal axis function [94]. Furthermore, malnutrition can induce a stress response in both humans [79] and rodents [33, 37, 41], and stress is a known developmental disruptor: maternal corticosterone treatment (at levels analogous to endogenous stressors) reduced placental perfusion and amino acid transfer to fetuses [95]. Microbial regulation of responses to environmental stressors can indirectly affect neurodevelopment, as in mouse models of prenatal stress, where reduction of *Lactobacillus* species in the maternal vaginal and infant gut microbiomes correlated with altered infant metabolites and brain amino acids [96]. In addition, transplants of maternal vaginal microbiome contributed to the influence of prenatal stress on gene expression in the hypothalamus [97]. Given that the microbiome has been implicated in stress signaling and stress-based disorders [94], it may be the case that malnutrition-induced stress interacts with the microbiome to induce neurodevelopmental changes in offspring.

Finally, a burgeoning area of study is the potential for the microbiome to influence early epigenetic programming. Indeed, the microbiome has been implicated as a key mediator of nutrient metabolism and epigenetic regulation [98]. Microbiome-dependent SCFAs such as butyrate play a critical role as HDAC inhibitors [73], and in germ-free mice, long non-coding RNAs are differentially expressed in a tissue-specific manner [99]. There is also evidence for epigenetic modulation in malnutrition: in a multi-generational study of postnatal protein-energy malnutrition during the first year of life in 168 human subjects, 134 regions were differentially methylated based on nutritional status, including specific neuropsychiatric risk genes such as *COMT*, *ABCF1*, *SYNGAP1*, and *IFNG*, which were associated with measures of attention and/or IQ [100]. Consistent with these phenotypes, rats exposed to protein restriction during gestation showed attention deficits, reduced glucose metabolism in the cerebral cortex, and decreased interferon gamma expression in the prefrontal cortex [100]. Furthermore, during gestation the nutrient choline, along with others such as vitamin B12 and folic acid, modified DNA and histone

methylation by providing methyl groups and acting as cofactors [101]. Based on the studies within these three domains, it is likely that the microbiome could mediate the impact of maternal malnutrition on fetal neurodevelopment through direct or indirect signaling pathways (Figure 1).

Concluding Remarks & Future Perspectives

The broadening of perspectives on malnutrition to include the microbiome as a contributing factor has begun to illuminate novel biological insights and potential clinical interventions. Probiotics, microbiome-targeted foods, and therapeutic microbiome-dependent biomolecules are under active investigation as treatments for immediate symptoms and long-term repercussions of malnutrition. While perinatal malnutrition and its relationship with the gut microbiome and neurodevelopment is increasingly a focus of research, further epidemiological and mechanistic investigation is needed (see Outstanding Questions). Large epidemiological studies are crucial for investigating the prevalence of not only different types of malnutrition across human populations, but associated neurological conditions as well. These would serve to establish more rigorous and reproducible associations between particular forms of malnutrition and subsets of neurological abnormalities. Furthermore, a critical examination of the current paradigms of malnutrition research is required: is it indeed the case that subtypes of malnutrition – macronutrient over- versus undernutrition, micronutrient deficiencies, etc. – should be viewed as distinct conditions with specific mechanisms and phenotypes? Or should malnutrition instead be viewed as a continuum, where the dearth of one nutrient may inherently alter the relative abundances of others, and where there may exist common underlying pathways and/or phenotypes? Due to the commonly interactive effects of different nutrients, it is rarely possible to tease apart the impact of a single aspect of malnutrition independently from others. Subsequently, while often not captured in reductionist experimental designs, real-life situations may constitute a spectrum of nutritional needs and consequences.

Another need is to understand precisely how the gut microbiome informs neurodevelopment during malnutrition. The effects may occur via direct mechanisms such as metabolite signaling to the developing brain, or indirectly, via mechanisms such as epigenetic regulation of genes critical for developmental trajectories. A related question is how these relationships interact with other bodily systems, such as the immune and stress responses. Well-controlled animal experiments and interventional studies in humans that can capture a systems or molecular level understanding are necessary to probe these questions further. Advances in these areas will also require close cooperation between various societal sectors, including basic-research scientists, medical professionals, and public health officials.

Malnutrition often goes hand-in-hand with other socioeconomic, sociocultural, and sociopolitical factors that have the potential to disrupt developmental processes. Therefore, diversity of experience and opportunity must be taken into consideration when conceptualizing the issue of malnutrition and establishing potential solutions. Across a multitude of countries and cultures, common risk factors for maternal and child malnutrition and associated conditions are apparent, including low income [102], lack of prenatal care [103], and caregiver illness [102] or lack of formal education [103]. Based on these clear correlations with social determinants, it is of great importance to conduct culture-informed investigations into malnutrition and associated conditions. Furthermore, these contextual factors must be taken into account when developing and applying public health initiatives and interventions, with the goals of designing equitable health policies.

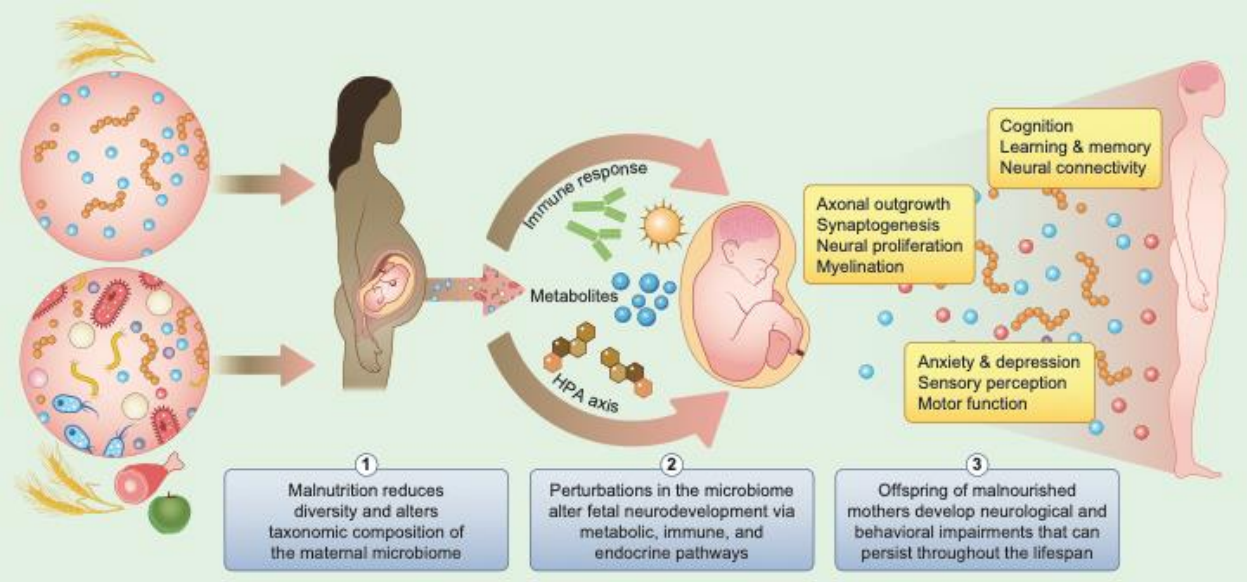

Figure 2.1: Conceptual model describing how the maternal gut microbiome may mediate effects of malnutrition on early neurodevelopment. Panel 1: Both over- and undernutrition, and alterations in ratios of macro- or micronutrients, lead to perturbations in the maternal microbiome during gestation. These perturbations include alterations in diversity and relative abundances of specific taxa. Panel 2: Changes in maternal nutrition effects circulating biomolecules, immune homeostasis and endocrine function. These changes may be mediated by observed shifts in the maternal microbiome. Panel 3: These changes in maternal biology can in turn directly or indirectly impact the fetus, including the developing fetal brain. Offspring malnourished during the prenatal or early postnatal period display impairments in key neurodevelopmental processes that can result in persistent abnormalities in brain function and behavior, and that may be mediated by microbial processes, either by direct or secondary mechanisms. Please see Table 2.S1 for supporting literature.

Sample	Country of Origin	Diet Perturbation	Microbiome Findings	Brain or Behavior Findings	Source
Humans Findings – Macronutrient Deficiency					
3776 2 year olds	Brazil	↓ maternal BMI pre-conception or ↑ gestational weight gain		↑ language, motor, & global delays in girls or ↑ language, cognitive, & global delays in boys	[S1]
118 children 12-18 months old	Bangladesh	↓ protein & calories (MAM); diet intervention → microbiome-targeted vs standard	23 taxa correlated with weight-for-length (21 ↑, 2 ↓) including ↑ *P. copri* ↑ *F. prausnitzii* ↓ Bifidobacterium species, 21 ↑ taxa also correlated with 70 plasma proteins ↑ with weight-for-length	↑ weight-for-length & weight-for-age, significant correlations between weight-for-length & 75 plasma proteins including ↑ axon guidance proteins ↑ axon guidance receptors ↑ neurotrophic receptors	[S2]
77 adults (+59 healthy controls)	Barbados	↓ protein within first year of life (kwashiorkor or marasmus) then adequate nutrition; ↓ birth weight then catch-up growth		↓ cognitive flexibility, concept formation, initiation, verbal fluency, working memory, processing speed, visuospatial integration	[S3]
1553 3 year olds	Mauritius	↓ protein, ↓ vitamin B2, ↓ niacin, ↓ iron measured by angular stomatitis, hair growth/ pigment, anemia		↓ social behavior, mediated by cognitive function	[S4]
57 youths (+60 healthy controls)	Barbados	↓ protein (kwashiorkor or marasmus) during first year		↓ cognitive function in childhood (IQ, attention, exam scores), ↑ depressive symptoms in adolescence	[S5]
131 preterm infants	The Netherlands	Measures of weight gain and fat, calorie, and protein intake		↓ fat, protein, calories → ↓ volume of cerebellum, basal ganglia/thalamus; ↓	[S6]

				protein → ↓ total brain volume; ↓ fat, protein, calories → ↓ fractional anisotropy of posterior internal capsule; ↓ protein → ↓ cognitive & motor scores at 2 years	
31 Turkish children 3-36 months (+25 healthy controls 3-48 months)	Turkey	↓ protein (moderate to severe), ↓ iron, ↓ albumin		↑ interval of auditory brainstem potentials (suggest myelination deficits)	[S7]
20 children 3-36 months	Turkey	↓ protein (moderate to severe), ↓ iron, ↓ albumin		↑ cerebral atrophy (75%), ↑ ventricular dilation (50%), ↑ cerebral sulci (25%), ↓ myelination (6.6%)	[S8]
5 children 7-52 months	Nigeria	↓ protein, ↓ weight, ↑ edema (kwashiorkor)		↑ cerebral atrophy, ↑ ventricular dilation, ↑ Sylvian fissures & basal cisterns, changes in paraventricular white matter (40%), ↑ cisterna magna (20%)	[S9]
13 infants 8-24 months (+7 healthy controls), all postmortem	Mexico	Death by severe ↓ protein-calories, ↓ weight		↓ apical dendrite length, ↓ spines per dendrite (in motor, somatosensory, occipital cortices), abnormal spine morphology	[S10]
49 preterm infants	Switzerland	Measures of weight gain and fat, calorie, and protein intake		↓ lipids, calories → ↓ volume of total brain, basal nuclei, cerebellum; ↓ protein, carbohydrates → ↓ total brain volume; ↓ energy, lipids → ↓ maturation of posterior corona radiata, posterior thalamic radiations, superior longitudinal fasciculus; ↓ lipids → ↓ maturation of superior corona radiata, corticospinal tract; ↓ total brain, basal nuclei, cerebellum growth → ↓ psychomotor outcomes at 18 months	[S11]

118 adults from the Dutch Famine birth cohort (30% born before famine, 35% exposed, 35% conceived after famine)	The Netherlands	Prenatal exposure to Dutch Famine during early gestation		↓ white matter signal, ↑ grey/white matter ratio, ↓ cerebral blood flow in cingulate cortex (men), ↑ spatial coefficient of variation (men)	[S12]
118 adults from the Dutch Famine birth cohort (30% born before famine, 35% exposed, 35% conceived after famine)	The Netherlands	Prenatal exposure to Dutch Famine during early gestation		↓ intracranial volume (men), ↑ brain aging (men), ↓ cognitive flexibility (men)	[S13]
145 adults (of which 65 health controls)	Barbados	↓ protein-calories, (moderate to severe kwashiorkor or marasmus) as children, then recovery		↓ attention, ↑ ADHD symptoms, correlations between attention deficits in childhood and adulthood	[S14]
168 youths 11-17 (52 kwashiorkor, 56 marasmus, 60 healthy controls)	Barbados	↓ protein-calories, (kwashiorkor or marasmus) during first year of life		↑ depressive symptoms regardless of malnutrition type	[S15]
64 children up to 2 years old (+50 healthy children, and additional twins/triplets & family)	Bangladesh	↓ protein-calories (SAM & MAM)	↓ microbial maturity, various taxa altered, only transiently ameliorated by nutritional intervention		[S16]
60 children 14-38 months	Bangladesh	↓ growth (stunting - ↓ height for age)	↓ microbial diversity, ↑ pathogenic *Escherichia coli*, ↓		[S17]

			phage diversity, *in vitro* introduction of phages of one group to bacteria of other group alters diversity & relative abundances		
17 children (+5 healthy controls)	Nigeria & Senegal	↓ protein (kwashiorkor or marasmus)	↓ microbial diversity, ↑ *Proteobacteria* (kwashiorkor), ↑ potentially pathogenic species (kwashiorkor), ↓ *Actinobacteria* & *Bacteroidetes* (marasmus), ↑ *Firmicutes* (marasmus)		[S18]
10 children (+5 healthy controls)	Nigeria & Senegal	↓ protein (kwashiorkor)	↓ microbial diversity, ↑ *Proteobacteria*, ↓ *Firmicutes* & *Euryarchaeota*, ↓ anaerobic species		[S19]
69 children	Nigeria & Senegal	↓ protein-calories (SAM)	↓ anaerobic species, ↑ aerobic species, ↓ bacterial load, ↑ gut redox potential		[S20]
20 children	India	↓ protein-calories (SAM)	↓ *Roseburia, Faecalibacterium*, *Butyrivibrio,* ↑ Proteobacteria, ↓ Synergistetes, ↓ nutrient uptake- and metabolism-related pathways, ↑ virulence- & pathological-related pathways & genes		[S21]
87 children 6-24 months	Uganda	↓ protein-calories (SAM), 62% with kwashiorkor	↑ microbial alpha & beta diversity (in kwashiorkor compared to non-)		[S22]
400 children 8-25 months (+22 healthy controls 6-59 months)	Uganda	↓ protein-calories (SAM), 66% with kwashiorkor	↑ *Prevotellaceae*, *Lachnospiraceae*, *Ruminoccaceae*, *Clostridiaceae*, *Veillonelaceae*, *Comamonadaceae*, *Pasteurellaceae* (in kwashiorkor compared to non-), ↓ *Enterococcus (*in kwashiorkor compared to non-), ↑ alpha diversity (in		[S23]

			kwashiorkor compared to non-)		
317 sets of twins up to 3 years old & adult male gnotobiotic mice transplanted with human fecal samples	Malawi	↓ protein (kwashiorkor)	↓ maturity in humans, altered taxa in mice (↑ *Bilophila wadsworthia* & *Clostridium innocuum*), transient changes with nutrient intervention in mice (↑ *Bifidobacteria*, *Lactobacilli*, *Ruminococcus*, ↓ *Bacteroidales*), alterations in fecal & cecal metabolites in mice (↓ SCFAs, products of carbohydrate, amino acid, nucleotide, lipid metabolism), most ↑ (only transiently) with nutrient intervention		[S24]
71 malnourished children 6 months-5 years old	Turkey	↑ protein-calories + *Lactobacillus rhamnosus* intervention	↓ infections, hospitalizations, ↑ weight & prealbumin in children who got the microbe intervention		[S25]
343 children 6-59 months & gnotobiotic C57Bl/6 mice & piglets transplanted with human or representative microbiota	Bangladesh	↓ protein-calories & nutritional intervention (SAM → MAM)	Metabolites altered before vs after treatment (humans), microbiota-targeted food altered microbial taxa & metabolites such as ↑ butyrate (mice), transplants + microbiota-targeted nutrients altered microbial taxa & metabolic pathways (mice), colonization + microbiota-targeted nutrients altered growth, taxa & serum proteins (piglets)	microbiota-targeted nutrients altered brain-related metabolites such as ↑ tryptophan & indole-3-lactic acid (mice), microbiota-targeted nutrients altered brain development-related plasma proteins such as ↓ axon inhibitors & ↑ neurotrophin receptors & axon guidance cues (humans)	[S26]
47 & 48 infants at 6, 8, and 12 months	Mali & Nicaragua	Rice brain-based nutritional intervention	↑ body length (Nicaraguan), differential taxonomic changes such as ↑ *Lactobacilli* species (Malian) vs ↑ *Bacteroides* species (Nicaraguan) & differential metabolite changes		[S27]

53 children 10-18 months	India	↓ nutrition – 30% stunted, 25% underweight, 12% wasted, 74% iron deficient	↑ *Proteobacteria*, ↓ *Actinobacteria*, suggests ↓ maturity of microbiome and/or ↑ inflammation; ↓ fat & iron → ↓ diversity	↓ alpha diversity → ↓ head circumference (females)	[S28]
58 extremely preterm infants	United States	↓ postnatal growth (60%)	↓ microbial diversity, ↓ microbial & metabolome maturity, ↑ *Staphylococcaceae* & *Enterobacteriaceae*, ↓ anaerobic species, ↑ pathways related to fatty acid & lipid metabolism	↓ head circumference	[S29]
110 preterm infants	Turkey	↓ birth weight + ↑ probiotic intervention		↓ risk of <10th percentile head circumference, ↑ probability 50th-90th percentile head circumference	[S30]
20 children 6-23 months	Zambia	↓ protein-calories (SAM)	↓ growth → ↑ enteropathy biomarkers, measures of gut physiology → ↓ urinary energy- & muscle-related metabolites (such as 3-indoxyl sulfate & choline metabolites), ↑ sucrose excretion		[S31]
326 children 6-26 months old	Brazil	↓ weight-for-age (wasting)	Urinary metabolites in choline, tryptophan, microbe-host co-metabolism pathways, ↑ microbial proteolysis, ↓ energy expenditure (↑ N-methylnicotinamide) → ↑ catch-up growth		[S32]
77 children 6 months-5 years old	Uganda	↓ protein, calories (SAM)	↑ acetylcarnitines & triglycerides	↑ cortisol	[S33]
59 & 215 mothers of stunted infants (+29 & 70 mothers of healthy infants) at 6 months postpartum, male	Malawi	Humans: ↓ height-for-age (stunting) Mice & piglets: colonized with stunted human microbiota & Malawian diet + sialylated milk	↓ breastmilk HMOs → ↓ infant growth (humans), ↑ oligosaccharides → ↑ growth (mice), alterations in transcription of microbes such as *Escherichia coli* & *Bacteroides fragilis* (↑ central energy	Alterations in brain metabolites such as ↑ N-acetylneuraminic acid, adenosine, & inosine (mice)	[S34]

C57Bl/6J GF 5 week-old mice, gnotobiotic piglets (3 per group)		oligosaccharides	metabolism) (mice), ↓ serum acylcarnitines (mice), ↑ serum non-esterified fatty acids (mice), ↑ cecal & fecal N-acetylneuraminic acid (piglets)		
Human Findings – Micronutrient Deficiency					
14 infants 2-25 months	Turkey	↓ vitamin B_{12}		↓ corpus callosum (50%), ↑ atrophy (42.8%), ↓ myelination (14.3%), ↑ Sylvian fissures (14.3%)	[S35]
30 infants 30-150 days	Turkey	↓ vitamin K (late onset)		↑ bulging or full fontanel (63%), ↑ collapsed fontanel (3%), ↑ intracranial hemorrhage (100%), ↑ extracranial hemorrhage (20%), ↑ intraparenchymal hemorrhage (50%), ↑ subdural hemorrhage (13%), ↑ subarachnoid hemorrhage (10%)	[S36]
168 adults from two generations & Long Evans hooded pregnant rats & adult offspring (8 per group)	Barbados	Humans: ↓ protein-calories during first year of life (gen 1 only) Rats: ↓ protein - 6% casein (vs 25% casein control diet) during gestation then fostered to well-nourished dams		134 differentially methylated regions (humans - most gen 1), methylation of psychiatric risk genes correlate with measures of attention & IQ (humans), ↓ prefrontal cortex interferon gamma (rats), ↓ attention (rats)	[S37]
Human Findings – Macronutrient Surplus					
1361 pregnant women (1246 mother-child pairs at median 3.2 years, 1070 at median 7.7 years)	United States	↑ maternal BMI		↓ visual-motor skills (partially mediated by maternal inflammation)	[S38]

109 pregnant women 26-39 gestational weeks	United States	↑ maternal BMI		↑ (47%) & ↓ (53%) functional connectivity between prefrontal cortex & left anterior insula/inferior frontal gyrus, ↑ intra-hemisphere connectivity, ↓ inter-hemisphere connectivity	[S39]
129 pregnant women 14-19 years old & 72 newborns)	United States	↑ maternal BMI		↑ thalamic connectivity, ↓ frontothalamic connectivity	[S40]
81 mothers-infant pairs & infants sampled at birth & 6 weeks	United States	↑ fat – 43.1% (vs 24.4% fat control) during gestation	Neonatal microbiome clustered based on maternal diet, ↑ *Enterococcus* (birth only), ↓ *Bacteroides* (birth & 6 weeks)		[S41]
35 mother-infant pairs at 1 & 6 months postpartum	United States	↑ maternal pregnancy BMI (overweight or obese)	Altered metabolites such as HMOs (↓ 2-fucosyllactose & Lacto-N-pentaose I ↑ Lacto-N-fucopentaose II/III) (1 month) & ↑ acylcarnitines (6 months)		[S42]
47 mother-infant pairs	Mexico	↑ maternal pregnancy BMI (overweight or obese)		↓ plasma ceramides (mothers at birth & 4 year olds), ↓ sphingomyelin (mothers) ↑ sphingomyelin (infants)	[S43]
778 children & C57BL/6J pregnant mice & adult offspring	China	Humans: ↑ maternal pre-pregnancy weight (overweight or obese) Mice: ↑ fat and/or fiber during gestation & lactation, fecal-microbial transplants and cross-fostering across dietary groups, ↑ fiber in offspring	Mice: maternal ↑ fat → ↓ S24-7 ↓ *Bifidobacterium animalis* ↓ *Prevotella* ↓ Clostridiales, altered microbial B-diversity, ↓ acetate ↓ butyrate ↓ propionate, ↓ SCFA receptor *Olfr78* in prefrontal cortex & hippocampus, maternal ↑ fiber → ↑ S24-7 ↑ *Bifidobacterium animalis* ↑ *Prevotella* ↑ Clostridiales, 5 taxa ↑ correlated with sociability & cognition,	Humans: ↓ social competency (worse in boys), ↓ learning (associated) Mice: maternal ↑ fat → ↓ working & long-term memory ↓ sociability & social novelty, ↓ genes related to synaptic plasticity, neural development, glutamatergic signaling, microglial maturation in prefrontal cortex & hippocampus, maternal ↑ fiber → ↑ working & long-term memory ↑ sociability & social	[S44]

		after weaning, ↑ SCFA in offspring after weaning	↑ acetate ↑ propionate, ↑ SCFA *Olfr78* in prefrontal cortex & hippocampus, offspring ↑ fiber → ↑ S24-7 (correlated with ↑ long-term memory) ↑ *Bacteroides* (correlated with ↑ long-term memory & ↑ sociability) ↓ *Ruminococcus* (correlated with ↓ memory & ↓ sociability), ↑ SCFA, acetate & propionate correlated with taxa, offspring ↑ acetate & proprionate → ↑ serum acetate, ↑ working & long-term memory ↑ sociability & social novelty, ↑ *Olfr78* in prefrontal cortex & hippocampus, ↑ post-synaptic densities ↑ microglial interaction & maturation ↑ synaptic function in prefrontal cortex & hippocampus	novelty, ↑ postsynaptic densities, ↑ genes related to synaptic plasticity, neural development, glutamatergic signaling, microglial maturation in prefrontal cortex & hippocampus, maternal FMT from ↑ fat → ↓ working & long-term memory ↓ sociability & social novelty, cross-fostering or co-housing → ↑ working & long-term memory ↑ sociability & social novelty, offspring ↑ fiber → ↑ working & long-term memory ↑ sociability & social novelty, ↓ RNA & protein synthesis genes in hippocampus	
Animal Findings – Macronutrient Deficiency					
Wistar pregnant rats & adult male offspring (8 per group, each from different litters)	N/A	↓ protein - 10% isocaloric casein diet (vs 20% casein control diet) during gestation		↑ increased learning time in operant conditioning, ↓ responses in progressive ratio	[S45]
Wistar pregnant rats & adult female offspring (8 per group, each from different litters)	N/A	↓ protein - 10% casein isocaloric diet (vs 20% casein control diet) during gestation		↓ time & distance in open arm of elevated plus maze, ↓ entries & distance in center of open field, ↑ increased learning time in operant conditioning, ↑ baseline corticosterone	[S46]

Sprague Dawley pregnant rats & adult male offspring (8 per group, all cross-fostered by control dams)	N/A	↓ protein - 8% casein isocaloric diet (vs 25% casein control diet) during gestation		↓ density of B-adrenoceptors in frontal & occipital cortices, ↓ BDNF protein expression in frontal & occipital cortices, ↓ *in vivo* LTP in frontal & occipital cortices, ↑ errors in radial arm maze, ↓ successes in operant conditioning	[S47]
Wistar pregnant rats & adult male offspring (10 per group, each from different litters)	N/A	↓ protein - 10% casein isocaloric diet (vs 20% casein control diet) during gestation		↑ latency to escape in Morris Water Maze, ↓ entries & time & distance in target quadrant, ↑ serum corticosterone, ↓ hippocampal CA3 *stratum* area, ↓ total, thin, mushroom spines & ↑ stubby spines of basal dendrites	[S48]
Sprague Dawley pregnant rats & E16, E18, P2 offspring (8 per group)	N/A	↓ protein - 8% protein diet (vs 20% protein control diet) during gestation		↑ PDGFRa expression (oligodendrocyte precursors) in thalamus at E18, ↓ PDGFRa fluorescence in thalamus at P2	[S49]
Wistar pregnant rats & adult male offspring (8 per group, each from different litters)	N/A	↓ protein - 10% casein isocaloric diet (vs 20% casein control diet) during gestation		↑ entries, time, distance in open arm of elevated plus maze	[S50]
Wistar pregnant rats & adult male offspring (16 per group, all cross-fostered by control dams)	N/A	↓ calories - ~40% of control diet during gestation		P2: ↑ brain/body weight, ↑ plasma corticosterone & CRH, ↑ hypothalamic CRH mRNA & protein; P40: ↓ brain/body weight, ↑ plasma corticosterone & CRH, ↑ hypothalamic CRH mRNA & protein	[S51]
Pregnant guinea pig sows & fetal offspring (delivered	N/A	↓ calories - 70% of control diet (switch to 90% mid-pregnancy)		↓ brain weight, ↑ brain sparing, ↑ apoptosis in paraventricular white matter, hippocampus, ↑ BAX-positive cells in CA4, ↓ Bcl-2-positive	[S52]

by c-section in late gestation, 18 per group, split by sex)				cells in dentate gyrus, ↑ Grp78 (females)	
Pregnant baboons (6-8 per group) & E90 fetal offspring	N/A	↓ calories - 70% of control diet		↓ SVZ thickness, ↑ SVZ cell proliferation & apoptosis, ↓ S-100B protein expression in SVZ, ↓ O4 protein expression in subplate/cortical plate, ↓ Golgi protein expression in subplate, ↓ BDNF gene expression, ↓ BDNF & IGF-1 protein expression, ↓ B-actin protein expression in cortical plate, ↓ EphB2 protein expression in cortical plate, ↓ MHC-B protein expression in SVZ, ↓ PSA-NCAM protein expression in intermediate zone, ↑ Bcl-2 protein expression in SVZ, intermediate zone, cortical plate, ↓ other key cerebral development-related genes	[S53]
MF-1 pregnant mice & fetal & adult offspring (3-5 litters per group)	N/A	↓ protein - 9% casein isocaloric diet (vs 18% casein control diet) for duration of gestation or for pre-implantation period only (E0-E3.5)		↓ neurosphere formation in ganglionic eminences & cortex (E12.5, 14.5, 17.5), ↓ neural stem cells/progenitors in ganglionic eminence cells (E12.5, 14.5, 17.5), ↑ differentiated neurons in ganglionic eminence cells (E12.5, 14.5, 17.5), ↓ proliferation in ganglionic eminences, ↑ apoptosis in ganglionic eminences, ↓ memory performance on novel object recognition task (pre-implantation), ↑ cortical	[S54]

				thickness (pre-implantation), ↓ Fragile-X-related genes	
GF, wildtype, or monocolonized BALB/c mice P7, P14, P56 (12-20 per group)	N/A	↓ protein, fat, vitamins beginning at P21	↓ weight, IGF-1, IGFBP-3 in GF compared to WT, ↑ growth hormone in GF compared to wildtype, *L. plantarum*^{WJL} strain rescued weight & hormone phenotypes from low nutrients + GF		[S55]
Animal Findings – Micronutrient Deficiency					
Sprague Dawley pregnant rats & P0 pups (14-22 per group)	N/A	↓ vitamin D during gestation		↑ dopamine, DOPAC, 3-MT in basal ganglia, ↑ noradrenaline in hippocampus, hypothalamus, thalamus, midbrain, ↓ serotonin in caudate putamen & basal ganglia, ↓ 5-HIAA in prefrontal cortex, ↓ glutamine in prefrontal cortex, caudate putamen, hippocampus, basal ganglia, hypothalamus, thalamus, cerebellum, ↓ glutamate, GABA, aspartate in hippocampus, ↑ serine in prefrontal cortex, basal ganglia, midbrain, cerebellum, ↑ glycine & taurine in midbrain	[S56]
Sprague Dawley pregnant rats & adult offspring (25-42 per group)	N/A	↓ vitamin D during gestation		↓ preference for novel object in novel object recognition paradigm	[S57]
Sprague Dawley pregnant rats & male offspring (12 per group)	N/A	↓ zinc – 2ug/g diet (vs 25ug/g control diet) during gestation & lactation		↑ latency & path length to escape in Morris water maze, abnormal hippocampal neuronal ultrastructure (suggesting ↑ apoptosis)	[S58]

C57Bl/6J pregnant mice & male E17 fetuses (8-11 per group)	N/A	↓ folate – 0.0mg/kg folic acid diet (vs 2mg/kg folic acid control diet) during late gestation (E11-E17)		↓ mitotic cells in septum, striatum, neocortex, hippocampus, periventricular zone, ↑ apoptosis in septum & hippocampus	[S59]
C57Bl/6J pregnant mice & female E18.5 or 6-8 week offspring (3-18 per group, depending on assay) & 31 Chinese pregnant females	N/A	↓ fiber – 2.3% cellulose diet (vs 5.5% inulin & 2.3% cellulose control diet) during gestation	↓ *Bacteroidetes* & ↑ *Firmicutes* (dams), altered microbial diversity (dams), ↓ serum butyrate & propionate (dams & offspring), human maternal SCFA correlate with fetal SCFA	↓ locomotion, ↓ time in center of open field & in open arm of elevated plus maze, ↑ latency to target & errors in Barnes maze, ↓ hippocampal glutamate receptor subunits, ↓ hippocampal postsynaptic potentials, gestational butyrate → ↓ anxiety-like behavior ↑ memory ↑ hippocampal synaptic proteins & physiology	[S60]
Yorkshire sows & 4 week old piglets (8 per group)	N/A	↓ choline – 625mg/kg (vs 1306 mg/kg control diet) starting in mid-gestation	altered metabolites such as ↑ deoxycarnitine	↓ relative brain size	[S61]
Animal Findings – Macronutrient Surplus					
C57Bl/6J pregnant mice & E17.5 fetuses (4-5 litters/group, 1-2 fetus/sex/)	N/A	↑ fat – 60% high-fat diet (vs 10% fat control diet) during gestation		↑ CD11b+ cells isolated from brain, ↑ microglial TNF-a production in response to LPS stimulation (males)	[S62]
C57Bl/6N pregnant mice & adult offspring (10 males & 10 females per group)	N/A	↑ fat – 60% high-fat diet (vs 10% fat control diet) during early (E0-E11) or late (E12-E21) gestation		↑ alcohol preference (late gestation), ↑ locomotion in response to amphetamine, ↓ dopamine in dorsal striatum (males), NAc (both late gestation), hypothalamus, ↑ dopamine in VTA, ↑ DOPAC in NAc (early gestation), VTA (late gestation), dorsal striatum, ↓ DOPAC in hypothalamus, ↓ HVA in NAc & hypothalamus	[S63]

				(both males), ↑ HVA in ventral tegmental area (females)	
Japanese macaque (*Macaca fuscata*)	N/A	↑ fat – 36% high fat diet (vs 13% fat control diet) during gestation & lactation	↑ *Bacteroides* & *Prevotella* (dams), ↓ *Spirochetes* & *Treponema* (dams), ↑ *Firmicutes (Ruminococcus* & *Dialister)* (offspring) ↓ *Proteobacteria (Campylobacter* & *Heliobacter)* (offspring), *Campylobacter* correlates with predictive metagenomics for nutrient metabolism pathways		[S64]
B6129SF2/J pregnant mice & offspring at 1 & 6 months (45 total)	N/A	↑ fat – 58% high-fat diet (vs 11% fat control diet) during gestation & lactation	↑ Tenericutes in colon (1 month), ↑ Actinobacteria & Proteobacteria in colon & cecum (6 months), ↓ Firmicutes in colon & cecum (6 months), ↑ predictive microbial function within metabolism pathways including glutamatergic (6 months), correlations between taxa and both maternal diet & offspring cognitive behaviors, particularly *Bacteroidetes* (6 months)	↓ exploratory & memory/cognition behavior (6 months), ↓ cerebral density, ↑ (1 month) & ↓ (6 months) cerebral response to insulin	[S65]
C57Bl6/J pregnant mice & male offspring 7-12 weeks (3-23 per group depending on assay)	N/A	↑ fat – 60% high-fat diet (vs 13.4% fat control diet) during gestation & lactation	↓ microbial diversity, altered taxa, microbiome-dependent neurological impairments & social behavior → prevented by co-housing & by colonizing GF	↓ social behavior, ↓ oxytocin neurons in hypothalamus, ↓ synaptic plasticity in dopamine neurons in VTA, ↑ marble burying, *Lactobacillus reuteri* treatment → rescue neurological impairments & social behavior	[S66]
Yucatan minipig sows & piglets (17-	N/A	↑ calorie, fat, fructose - Western diet (125% energy of control diet	↓ fecal SCFA, ↑ lipids in milk (sows), ↑ plasma free fatty acids,	↑ working & reference memory in cognitive holeboard test, ↓ granule cell layer ↓ neurogenesis ↑	[S67]

65 based on assay)		during gestation & 167% energy of control diet during lactation)		proliferation in hippocampus	
C57Bl/6 pregnant mice at E18.5 (5 per group)	N/A	↑ fat – 37.1% saturated fat (vs 23.4% control diet) throughout gestation OR ↓ calories (30% restriction) E5.5-E17.5	Maternal weight associated with microbial taxa abundances, ↑ *Pseudomonadaceae* (high-fat), ↓ *Catabacteriaceae* (high-fat), ↓ *Proteobacteria* (calorie-restriction), ↓ *Porphyromonadaceae*		[S68]

Table 2.S1: Microbiome and brain changes in perinatal malnutrition.
IQ: intelligence quotient; ADHD: attention deficit hyperactivity disorder; SAM: severe acute malnutrition; MAM: moderate acute malnutrition; GF: germ-free; SCFA: short-chain fatty acids; HMO: human milk oligosaccharides; SCFA: short-chain fatty acids; BDNF: brain-derived neurotrophic factor; LTP: long-term potentiation; P: postnatal day; PDGFRa: platelet-derived growth factor receptor alpha; CRH: corticotropin-releasing hormone; mRNA: messenger ribonucleic acid; BAX: bcl-2-like protein 4; Bcl-2: B-cell lymphoma 2; Grp78: immunoglobulin heavy chain-binding protein; E: embryonic day; SVZ: subventricular zone; IGF-1: insulin-like growth factor 1; EphB2: ephrin type-B receptor 2; MHC-B: major histocompatibility complex class B; PSA-NCAM: polysialylated-neural cell adhesion molecule; IGFBP-3: insulin-like growth factor binding protein 3; VTA: ventral tegmental area; NAc: nucleus accumbens; DOPAC: 3,4-Dihydroxyphenylacetic acid; 3-MT: 3-methoxytyramine; 5-HIAA: 5-Hydroxyindoleacetic acid; GABA: gamma-aminobutyric acid; TNF-a: tumor necrosis factor-alpha; LPS: lipopolysaccharide; HVA: homovanillic acid.

Table References

S1 Neves, P.A.R., Gatica-Dominguez, G., Santos, I.A., Bertoldi, A.D., Domingues, M., Murray, J., Silveira, M.F. (2020) Poor maternal nutritional status before and during pregnancy is associated with suspected child developmental delay in 2-year old Brazilian children. *Scientific Reports* 10, 1851

S2 Chen, R.Y., Mostafa, I., Hibberd, M.C., Das, S., Mahfuz, M., Naila, N.N., Islam, M.M., Huq, S., Alam, M.A., Zaman, M.U., Raman, A.S., Webber, D., Zhou, C., Sundaresan, V., Ahsan, K., Meier, M.F., Barratt, M.J., Ahmed, T., Gordon, J.I. (2021) A microbiota-directed food intervention for undernourished children. *The New England Journal of Medicine* 384, 1517-1528

S3 Waber, D.P., Bryce, C.P., Fitzmaurice, G.M., Zichlin, M.L., McGaughy, J., Girard, J.M., Galler, J.R. (2014) Neuropsychological outcomes at midlife following moderate to severe malnutrition in infancy. *Neuropsychology* 28, 530-540

S4 Liu, J.R., A. (2017) Nutritional status and social behavior in preschool children: the mediating effects of neurocognitive functioning. *Maternal & Child Nutrition* 13, e12321

S5 Waber, D.P., Eaglesfield, D., Fitzmaurice, G.M., Bryce, C.P., Harrison, R.H., Galler, J.R. (2011) Cognitive impairment as a mediator in the developmental pathway from infant malnutrition to adolescent depressive symptoms in Barbadian youth. *Journal of Developmental and Behavioral Pediatrics* 32, 225-232

S6 Coviello, C., Kuenen, K., Kersbergen, K.J., Groenendaal, F., Leemans, A., Peels, B., Isgum, I., Viergever, M.A., de Vries, L.S., Buonocore, G., Carnielli, V.P., Benders, M.J.N.L. (2018) Effects of early nutrition and growth on brain volumes, white matter microstructure, and neurodevelopmental outcome in preterm newborns. *Pediatric Research* 83, 102-110

S7 Odabas, D., Caksen, H., Sar, S., Tombul, T., Kisli, M., Tuncer, O., Yuca, K., Yilmaz, C. (2005) Auditory brainstem potentials in children with protein energy malnutrition. *International Journal of Pediatric Otorhinolaryngology* 69, 923-928

S8 Odabas, D., Caksen, H., Sar, S., Unal, O., Tuncer, O., Atas, B., Yilmaz, C. (2005) Cranial MRI findings in children with protein energy malnutrition. *International Journal of Neuroscience* 115, 829-837

S9 Atalabi, O.M., Lagunju, I.A., Tongo, O.O., Akinyinka, O.O. (2010) Cranial Magnetic Resonance Imaging Findings in Kwashiorkor. *International Journal of Neuroscience* 120, 23-27

S10 Benitez-Bribiesca, L., De la Rosa-Alvarez, I., Mansilla-Olivares, A. (1999) Dendritic spine pathology in infants with severe protein-calorie malnutrition. *Pediatrics* 104, e21

S11 Schneider, J., Fumeaux, C.J.F., Duerden, E.G., Guo, T., Foong, J., Graz, M.B., Hagmann, P., Chakravarty, M.M., Huppi, P.S., Beauport, L., Truttmann, A.C., Miller, S.P. (2018) Nutrient Intake in the First Two Weeks of Life and Brain Growth in Preterm Neonates. *Pediatrics* 141, e20172169

S12 de Rooij, S.R., Mutsaerts, H.J.M.M., Petr, J., Asllani, I., Caan, M.W.A., Groot, P., Nederveen, A.J., Schwab, M., Roseboom, T.J. (2019) Late-life brain perfusion after prenatal famine exposure. *Neurobiology of Aging* 82, 1-9

S13 Franke, K., Gaser, C., Roseboom, T.J., Schwab, M., de Rooij, S.R. (2018) Premature brain aging in humans exposed to maternal nutrient restriction during early gestation. *Neuroimage* 173, 460-471

S14 Galler, J.R., Bryce, C.P., Zichlin, M.L., Fitzmaurice, G., Eaglesfield, G.D., Waber, D.P. (2012) Infant malnutrition is associated with persisting attention deficits in middle adulthood. . *Journal of Nutrition* 142, 788-794

S15 Galler, J.R., Bryce, C.P., Waber, D., Hock, R.S., Exner, N., Eaglesfield, D., Fitzmaurice, G., Harrison, R. (2010) Early childhood malnutrition predicts depressive symptoms at ages 11-17. *Journal of Child Psychology and Psychiatry* 51, 789-798

S16 Subramanian, S., Huq, S., Yatsunenko, T., Haque, R., Mahfuz, M., Alam, M.A., Benezra, A., DeStefano, J., Meier, M.F., Muegge, B.D., Barratt, M.J., VanArendonk, L.G., Zhang, Q., Province, M.A., Petri, W.A., Ahmed, T., Gordon, J.I. (2014) Persistent Gut Microbiota Immaturity in Malnourished Bangladeshi Children. *Nature* 510, 417-421

S17 Mirzaei, M.K., Khan, M.A.A., Ghosh, P., Taranu, Z.E., Taguer, M., Ru, J., Chowdhury, R., Kabir, M.M., Deng, L., Mondal, D., Maurice, C.F. (2020) Bacteriophages Isolated from Stunted Children Can Regulate Gut Bacterial Communities in an Age-Specific Manner. *Cell Host & Microbe* 27, 199-212

S18 Pham, T.P.T., Alou, M.T., Bachar, D., Levasseur, A., Brah, S., Alhousseini, D., Sokhna, C., Diallo, A., Wieringa, F., Million, M., Raoult, D., (2019) Gut Microbiota Alteration is Characterized by a Proteobacteria and Fusobacteria Bloom in Kwashiorkor and a Bacteroidetes Paucity in Marasmus. *Scientific Reports* 9, 9084

S19 Alou, M.T., Million, M., Traore, S.I., Mouelhi, D., Khelaifia, S., Bachar, D., Caputo, A., Delerce, J., Brah, S., Alhousseini, D., Sokhna, C., Robert, C., Diallo, B.A., Diallo, A., Parola, P., Golden, M., Lagier, J., Raoult, D.` (2017) Gut Bacteria Missing in Severe Acute Malnutrition, Can We Identify Potential Probiotics by Culturomics? *Frontiers in Microbiology* 8, 899

S20 Million, M., Alou, M.T., Khelaifia, S., Bachar, D., Lagier, J., Dione, N., Brah, S., Hugon, P., Lombard, V., Armougom, F., Fromonot, J., Robert, C., Michelle, C., Diallo, A., Fabre, A., Guieu, R., Sokhna, C., Henrissat, B., Parola, P., Raoult, D. (2016) Increased Gut Redox and Depletion of Anaerobic and Methanogenic Prokaryotes in Severe Acute Malnutrition. *Scientific Reports* 6, 26051

S21 Ghosh, T.S., Gupta, S.S., Bhattacharya, T., Yadav, D., Barik, A., Chowdhury, A., Das, B., Mande, S.S., Nair, G.B., (2014) Gut Microbiomes of Indian Children of Varying Nutritional Status. *PLOS ONE* 9, e95547

S22 Kristensen, K.H.S., Wiese, M., Rytter, M.J.H., Ozcam, M., Hansen, L.H., Namusoke, H., Friis, H., Nielsen, D.S. (2016) Gut Microbiota in Children Hospitalized with Oedematous and Non-

Oedematous Severe Acute Malnutrition in Uganda. *PLoS Neglected Tropical Diseases* 10, e0004369

S23 Castro-Mejia, J.L., O'Ferrall, S., Krych, L., O'Mahoney, E., Namusoke, H., Lanyero, B., Kot, W., Nabukeera-Barungi, N., Michaelsen, K.F., Molgaard, C., Friis, H., Grenov, B., Nielsen, D.S. (2020) Restitution of gut microbiota in Ugandan children administered with probiotics (Lactobacillus rhamnosus GG and Bifidobacterium animalis subsp. lactis BB-12) during treatment for severe acute malnutrition. *Gut Microbes* 11, 855-867

S24 Smith, M.I., Yatsunenko, T., Manary, M.J., Trehan, I., Mkakosya, R., Cheng, J., Kau, A.L., Rich, S.S., Concannon, P., Mychaleckyj, J.C., Liu, J., Houpt, E., Li, J.V., Holmes, E., Nicholson, J., Knights, D., Ursell, L.K., Knight, R., Gordon, J.I. (2013) Gut microbiomes of Malawian twin pairs discordant for kwashiorkor. *Science* 339, 548-554

S25 Kara, S.S., Volkan, B., Erten, I. (2019) Lactobacillus rhamnosus GG can protect malnourished children. *Beneficial Microbes* 10, 237-244

S26 Gehrig, J.L., Venkatesh, S., Chang, H.W., Hibberd, M.C., Kung, V.L., Cheng, J., Chen, R.Y., Subramanian, S., Cowardin, C.A., Meier, M.F., O'Donnell, D., Talcott, M., Spears, L.D., Semenkovich, C.F., Henrissat, B., Giannone, R.J., Hettich, R.L., Ilkayeva, O., Muehlbauer, M., Newgard, C.B., Sawyer, C., Head, R.D., Rodionov, D.A., Arzamasov, A.A., Leyn, S.A., Osterman, A.L., Hossain, M.I., Islam, M., Choudhury, N., Sarker, S.A., Huq, S., Mahmud, I., Mostafa, I., Mahfuz, M., Barratt, M.J., Ahmen, T., Gordon, J.I. (2019) Effects of microbiota-directed foods in gnotobiotic animals and undernourished children. *Science* 365, 139

S27 Zambrana, L.E., McKeen, S., Ibrahim, H., Zarei, I., Borresen, E.C., Doumbia, L., Bore, A., issoko, A., Douyon, S., Kone, K., Perez, J., Perez, C., Hess, A., Abdo, Z., Sangare, L., Maiga, A., Becker-Dreps, S., Yuan, L., Koita, O., Vilchez, S., Ryan, E.P. (2019) Rice bran supplementation modulates growth, microbiota and metabolome in weaning infants: a clinical trial in Nicaragua and Mali. *Scientific Reports* 9, 13919

S28 Huey, S.L., Jiang, L., Fedarko, M.W., McDonald, D., Martino, C., Ali, F., Russel, D.G., Udipi, S.A., Thorat, A., Thakker, V., Ghugre, P., Potdar, R.D., Chopra, H., Rajagopalan, K., Haas, J.D., Finkelstein, J.L., Knight, R., Mehta, S. (2020) Nutrition and the gut microbiota in 10- to 18-month-old children living in urban slums of Mumbai, India. *mSphere* 5, e00731-00720

S29 Younge, N.E., Newgard, C.B., Cotten, C.M., Goldberg, R.N., Muehlbauer, M.J., Bain, J.R., Stevens, R.D., O'Connel, T.M., Rawls, J.F., Seed, P.C., Ashley, P.L. (2019) Disrupted maturation of the microbiota and metabolome among extremely preterm infants with postnatal growth failure. *Scientific Reports* 9

S30 Varal, I.G., Koksal, N., Ozkan, H., Bagci, O., Dogan, P. (2018) Potential use of multi-strain synbiotics for improving postnatal head circumference. *Pakistan Journal of Medican Sciences* 34, 1502-1506

S31 Farras, M., Chandwe, K., Mayneris-Perxachs, J., Amadi, B., Louis-Auguste, J., Besa, E., Zyambo, K., Guerrant, R., Kelly, P., Swann, J.R. (2018) Characterizing the metabolic phenotype of intestinal villus blunting in Zambian children with severe acute malnutrition and persistent diarrhea. *PLoS ONE* 13, e0192092

S32 Mayneris-Perxachs, J., Lima, A.A.M., Guerrant, R.L., Leite, A.M., Moura, A.F., Lima, N.L., Soares, A.M., Havt, A., Moore, S.R., Pinkerton, R., Swann, J.R. (2016) Urinary N-methylnicotinamide and β-aminoisobutyric acid predict catch-up growth in undernourished Brazilian children. *Scientific Reports* 6

S33 Bartz, S., Mody, A., Hornik, C., Bain, J., Muehlbauer, M., Kiyimba, T., Kiboneka, E., Stevens, R., Bartlett, J., St Peter, J.V., Newgard, C.B., Freemark, M. (2014) Severe Acute Malnutrition in Childhood: Hormonal and Metabolic Status at Presentation, Response to Treatment, and Predictors of Mortality. *The Journal of Clinical Endocrinology & Metabolism* 99, 2128-2137

S34 Charbonneau, M.R., O'Donnell, D., Blanton, L.V., Totten, S.M., Davis, J.C.C., Barratt, M.J., Cheng, J., Guruge, J., Talcott, M., Bain, J.R., Muehlbauer, M.J., Ilkayeva, O., Wu, C., Struckmeyer, T., Barile, D., Mangani, C., Jorgensen, J., Fan, Y., Maleta, K., Dewey, K.G., Ashorn, P., Newgard, C.B., Lebrilla, C., Mills, D.A., Gordon, J.I. (2016) Sialylated Milk OligosaccharidesPromote Microbiota-Dependent Growthin Models of Infant Undernutrition. *Cell* 164, 859-871

S35 Ekici, F., Tekbas, G., Hattapoglu, S., Yaramis, A., Onder, H., Bilici, A. (2016) Brain MRI and MR Spectroscopy Findings in Children with Nutritional Vitamin B12 Deficiency. *Clinical Neuroradiology* 26, 215-220

S36 Yilmaz, C., Yuca, S.A., Yilmaz, N., Bektas, M.S., Caksen, H. (2009) Intracranial hemorrhage due to vitamin K deficiency in infants: a clinical study. *International Journal of Neuroscience* 119, 2250-2256

S37 Peter, C.J., Fischer, L.K., Kundakovic, M., Garg, P., Jakovcevski, M., Dincer, A., Amaral, A.C., Ginns, E.I., Galdzicka, M., Bryce, C.P., Ratner, C., Waber, D.P., Mokler, D., Medford, G., Champagne, F.A., Rosene, D.L., McGaughy, J.A., Sharp, A.J., Galler, J.R., Akbarian, S. (2016) DNA Methylation Signatures of Early Childhood Malnutrition Associated With Impairments in Attention and Cognition. *Biological Psychiatry* 80, 765-774

S38 Monthe-Dreze, C., Rifas-Shiman, S.L., Gold, D.R., Oken, E., Sen, S. (2019) Maternal obesity and offspring cognition: the role of inflammation. *Pediatric Research* 85, 799-806

S39 Norr, M.E., Hect, J.L., Lenniger, C.J., Van den Heuvel, M., Thomason, M.E. (2020) An examination of maternal prenatal BMI and human fetal brain development. *Journal of Child Psychology and Psychiatry*

S40 Spann, M.N., Scheinost, D., Feng, T., Barbato, K., Lee, S., Monk, C., Peterson, B.S. (2020) Association of Maternal Prepregnancy Body Mass Index With Fetal Growth and Neonatal Thalamic Brain Connectivity Among Adolescent and Young Women. *JAMA Network Open* 3, e2024661

S41 Chu, D.M., Antony, K.M., Ma, J., Prince, A.L., Showalter, L., Moller, M., Aagaard, K.M. (2016) The early infant gut microbiome varies in association with a maternal high-fat diet. . *Genomic Medicine* 8

S42 Isganaitis, E., Venditti, S., Matthews, T.J., Lerin, C., Demerath, E.W., Fields, D.A. (2019) Maternal obesity and the human milk metabolome: associations with infant body composition and postnatal weight gain. *American Journal of Clinical Nutrition* 110, 111-120

S43 Leon-Aguilar, L.F., Croyal, M., Ferchaud-Roucher, V., Huang, F., Marchat, L.A., Barraza-Villarreal, A., Romieu, I., Ramakrishnan, U., Krempf, M., Ouguerram, K., Mercado-Camargo, R., Bolanos-Jimenez, F. (2019) Maternal obesity leads to long-term altered levels of plasma ceramides in the offspring as revealed by a longitudinal lipidomic study in children. *International Journal of Obesity* 43, 1231-1243

S44 Liu, X., Li, X., Xia, B., Jin, X., Zou, Q., Zeng, Z., Zhao, W., Yan, S., Li, L., Yuan, S., Zhao, S., Dai, X., Yin, F., Cadenas, E., Liu, R.H., Zhao, B., Hou, M., Liu, Z., Liu, X. (2021) High-fiber diet mitigates maternal obesity-induced cognitive and social dysfunction in the offspring via gut-brain axis. *Cell Metabolism* 33, 923-938

S45 Reyes-Castro, R., J.S., Rodriguez-Gonzalez, G.L., Wimmer, R.D., McDonald, T.J., Larrea, F., Nathanielsz, P.W., Zambrano, E. (2011) Pre- and/or postnatal protein restriction in rats impairs learning and motivation in male offspring. *International Journal of Developmental Neuroscience* 29, 177-182

S46 Reyes-Castro, L.A., Rodriguez, J.S., Charco, R., Bautista, C.J., Larrea, F., Nathanielsz, P.W., Zambrano, E. (2012) Maternal protein restriction in the rat during pregnancy and/or lactation alters cognitive and anxiety behaviors of female offspring. *International Journal of Developmental Neuroscience* 30, 39-45

S47 Burgos, H., Hernandez, A., Constandil, L., Rios, M., Flores, O., Puentes, G., Hernandez, K., Morgan, C., Valladares, L., Castillo, A., Cofre, C., Milla, L.A., Saez-Briones, P., Barra, R. (2019) Early postnatal environmental enrichment restores neurochemical and functional plasticities of the cerebral cortex and improves learning performance in hidden-prenatally-malnourished young-adult rats. *Behavioral Brain Research* 2, 182-190

S48 Reyes-Castro, L.A., Padilla-Gomez, E., Parga-Martinez, N.J., Castro-Rodriguez, D.C., Quirarte, G.L., Diaz-Cintra, S., Nathanielsz, P.W., Zambrano, E. (2018) Hippocampal mechanisms in impaired spatial learning and memory in male offspring of rats fed a low-protein isocaloric diet in pregnancy and/or lactation. *Hippocampus* 28, 18-30

S49 Patro, N., Naik, A.A., Patro, I.K. (2019) Developmental Changes in Oligodendrocyte Genesis, Myelination, and Associated Behavioral Dysfunction in a Rat Model of Intra-generational Protein Malnutrition. *Molecular Neurobiology* 56, 595-610

S50 Reyes-Castro, L.A., Rodriguez, J.S., Rodriguez-Gonzalez, G.L., Chavira, R., Bautista, C.J., MacDonald, T.J., Nathanielsz, P.W., Zambrano, E. (2012) Pre- and/or postnatal protein restriction developmentally programs affect and risk assessment behaviors in adult male rats. *Behavioral Brain Research* 227, 324-329

S51 Nunez, H., Ruiz, S., Soto-Moyano, R., Navarette, M., Valladares, L., White, A., Perez, H. (2008) Fetal undernutrition induces overexpression of CRH mRNA and CRH protein in hypothalamus and increases CRH and corticosterone in plasma during postnatal life in the rat. *Neuroscience Letters* 448, 115-119

S52 Ghaly, A., Maki, Y., Nygard, K., Hammond, R., Hardy, D.B., Richardson, B.S. (2019) Maternal nutrient restriction in guinea pigs leads to fetal growth restriction with increased brain apoptosis. *Pediatric Research* 85, 105-112

S53 Antonow-Schlorke, I., Schwab, M., Cox, L.A., Li, C., Stuchlik, K., Witte, O.W., Nathanielsz, P.W., McDonald, T.J. (2011) Vulnerability of the fetal primate brain to moderate reduction in maternal global nutrient availability. *PNAS* 108, 3011-3016

S54 Gould, J.M., Smith, P.J., Airey, C.J., Mort, E.J., Airey, L.E., Warricker, F.D.M., Pearson-Farr, J.E., Weston, E.C., Gould, P.J.W., Semmence, O.G., Restall, K.L., Watts, J.A., McHugh, P.C., Smith, S.J., Dewing, J.M., Fleming, T.P., Willaime-Morawek, S. (2018) Mouse maternal protein restriction during preimplantation alone permanently alters brain neuron proportion and adult short-term memory. *PNAS* 115, E7398–E7407

S55 Schwarzer, M., Makki, K., Storelli, G., Machuca-Gayet, I., Srutkova, D., Hermanova, P., Martino, M.E., Balmand, S., Hudcovic, T., Heddi, A., Rieusset, J., Kozakova, H., Vidal, H., Leulier, F. (2016) Lactobacillus plantarum strain maintains growth of infant mice during chronic undernutrition. *Science* 351, 854-857

S56 Kesby, J.P., Turner, K.M., Alexander, S., Eyles, D.W., McGrath, J.J., Burne, T.H.J. (2017) Developmental vitamin D deficiency alters multiple neurotransmitter systems in the neonatal rat brain. *International Journal of Developmental Neuroscience* 62

S57 Overeem, K., Alexander, S., Burne, T.H.J., Ko, P., Eyles, D.W. (2019) Developmental Vitamin D Deficiency in the Rat Impairs Recognition Memory, but Has No Effect on Social Approach or Hedonia. *Nutrients* 11, 2713

S58 Yu, X., Jin, L., Zhang, Z., Yu, X. (2013) Effects of maternal mild zinc deficiency and zinc supplementation in offspring

on spatial memory and hippocampal neuronal ultrastructural changes. *Nutrition* 29, 457-461

S59 Craciunescu, C.N., Johnson, A.R., Zeisel, S.H. (2010) Dietary choline reverses some, but not all, effects of folate deficiency on neurogenesis and apoptosis in fetal mouse brain. *Journal of Nutrition* 140, 1162-1166

S60 Yu, L., Zhong, X., He, Y., Shi, Y. (2020) Butyrate, but not propionate, reverses maternal diet-induced neurocognitive deficits in offspring. *Pharmacological Research* 160

S61 Getty, C.M.D., R.N. (2015) Moderate Perinatal Choline Deficiency Elicits Altered Physiology and Metabolomic Profiles in the Piglet. *PLoS ONE* 10, e0133500

S62 Edlow, A.G., Glass, R.M., Smith, C.J., Tran, P.K., James, K., Bilbo, S. (2019) Placental Macrophages: A Window Into Fetal Microglial Function in Maternal Obesity. *International Journal of Developmental Neuroscience* 77, 60-68

S63 Sarker, G., Litwan, K., Kastli, R., Peleg-Raibstein, D. (2019) Maternal overnutrition during critical developmental periods leads to different health adversities in the offspring: relevance of obesity, addiction and schizophrenia. *Scientific Reports* 9, 17322

S64 Ma, J., Prince, A.L., Bader, D., Hu, M., Ganu, R., Baquero, K., Blundell, P., Harris, R.A., Frias, A.E., Grove, K.L., Aagaard, K.M. (2014) High-fat maternal diet during pregnancy persistently alters the offspring microbiome in a primate model. *Nature Communications* 5

S65 Sanguinetti, E., Guzzardi, M.A., Tripodi, M., Panetta, D., Selma-Royo, M., Zega, A., Telleschi, M., Collado, M.C., Iozzo, P. (2019) Microbiota signatures relating to reduced memory and exploratory behaviour in the offspring of overweight mothers in a murine model. *Scientific Reports* 9, 12609

S66 Buffington, S.A., Di Prisco, G.V., Auchtung, T.A., Ajami, N.J., Petrosino, J.F., Costa-Mattioli, M. (2016) Microbial Reconstitution Reverses Maternal Diet-Induced Social and Synaptic Deficits in Offspring. *Cell* 165, 1762-1775

S67 Val-Laillet, D., Besson, M., Guerin, S., Coquery, N., Randuineau, G., Kanzari, A., Quesnel, H., Bonhomme, N., Bolhuis, J.E., Kemp, B., Blat, S., Le Huerou-Luron, I., Clouard, C. (2017) A maternal Western diet during gestation and lactation modifies offspring's microbiota activity, blood lipid levels, cognitive responses, and hippocampal neurogenesis in Yucatan pigs. *FASEB J* 31, 2037-2049

S68 Connor, K.L., Chehoud, C., Altrichter, A., Chan, L., DeSantis, T.Z., Lye, S.J. (2018) Maternal metabolic, immune, and microbial systems in late pregnancy vary with malnutrition in mice. *Biology of Reproduction* 98, 579-592

Text References

1 Schwarzenberg, S.J., Georgieff, M.K., AAP Committee on Nutrition (2018) Advocacy for Improving Nutrition in the First 1000 Days To Support Childhood Development and Adult Health. *Pediatrics* 141, e20173716

2 Yan, X., Zhao, X., Li, J., He, L., Xu, M. (2018) Effects of early-life malnutrition on neurodevelopment and neuropsychiatric disorders and the potential mechanisms. *Progress in Neuro-Psychopharmacology & Biological Psychiatry* 83, 64-75

3 Georgieff, M.K., Ramel, S.E., Cusick, S.E. (2018) Nutritional Influences on Brain Development. *Acta Paediatrica* 107, 1310-1321

4 Kane, A.V., Dinh, D.M., Ward, H.D. (2015) Childhood malnutrition and the intestinal microbiome. *Pediatric Research* 77, 256-262

5 Garcia-Mantrana, I., Bertua, B., Martinez-Costa, C., Collado, M.C. (2016) Perinatal nutrition: How to take care of the gut microbiota? *Clinical Nutrition Experimental* 6, 3-16

6 Borre, Y.E., O'Keeffe, G.W., Clarke, G., Stanton, C., Dinan, T.G., Cryan, J.F. (2014) Microbiota and neurodevelopmental windows: implications for brain disorders. *Trends in Molecular Medicine* 20, 509-518

7 Pronovost, G.N., Hsiao, E.Y. (2019) Perinatal Interactions between the Microbiome, Immunity, and Neurodevelopment. *Immunity* 50, 18-36

8 Ratsika, A., Codagnone, M.C., O'Mahony, S., Stanton, C., Cryan, J.F. (2021) Priming for Life: Early Life Nutrition and the Microbiota-Gut-Brain Axis. *Nutrients* 13

9 Bordeleau, M., de Cossio, L.F., Chakravarty, M.M., Tremblay, M. (2021) From Maternal Diet to Neurodevelopmental Disorders: A Story of Neuroinflammation. *Frontiers in Cellular Neuroscience* 14

10 Ahmed, T., Hossain, M., Sanin, K.I. (2012) Global Burden of Maternal and Child Undernutrition and Micronutrient Deficiencies. *Annals of Nutrition and Metabolism* 61, 8-17

11 Neves, P.A.R., Gatica-Dominguez, G., Santos, I.A., Bertoldi, A.D., Domingues, M., Murray, J., Silveira, M.F. (2020) Poor maternal nutritional status before and during pregnancy is associated with suspected child developmental delay in 2-year old Brazilian children. *Scientific Reports* 10, 1851

12 Liu, J.R., A. (2017) Nutritional status and social behavior in preschool children: the mediating effects of neurocognitive functioning. *Maternal & Child Nutrition* 13, e12321

13 Coviello, C., Kuenen, K., Kersbergen, K.J., Groenendaal, F., Leemans, A., Peels, B., Isgum, I., Viergever, M.A., de Vries, L.S., Buonocore, G., Carnielli, V.P., Benders, M.J.N.L. (2018) Effects of early nutrition and growth on brain volumes, white matter microstructure, and neurodevelopmental outcome in preterm newborns. *Pediatric Research* 83, 102-110

14 Odabas, D., Caksen, H., Sar, S., Tombul, T., Kisli, M., Tuncer, O., Yuca, K., Yilmaz, C. (2005) Auditory brainstem potentials in children with protein energy malnutrition. *International Journal of Pediatric Otorhinolaryngology* 69, 923-928

15 Odabas, D., Caksen, H., Sar, S., Unal, O., Tuncer, O., Atas, B., Yilmaz, C. (2005) Cranial MRI findings in children with protein energy malnutrition. *International Journal of Neuroscience* 115, 829-837

16 Atalabi, O.M., Lagunju, I.A., Tongo, O.O., Akinyinka, O.O. (2010) Cranial Magnetic Resonance Imaging Findings in Kwashiorkor. *International Journal of Neuroscience* 120, 23-27

17 Benitez-Bribiesca, L., De la Rosa-Alvarez, I., Mansilla-Olivares, A. (1999) Dendritic spine pathology in infants with severe protein-calorie malnutrition. *Pediatrics* 104, e21

18 Waber, D.P., Eaglesfield, D., Fitzmaurice, G.M., Bryce, C.P., Harrison, R.H., Galler, J.R. (2011) Cognitive impairment as a mediator in the developmental pathway from infant malnutrition to adolescent depressive symptoms in Barbadian youth. *Journal of Developmental and Behavioral Pediatrics* 32, 225-232

19 Galler, J.R., Bryce, C.P., Waber, D., Hock, R.S., Exner, N., Eaglesfield, D., Fitzmaurice, G., Harrison, R. (2010) Early childhood malnutrition predicts depressive symptoms at ages 11-17. *Journal of Child Psychology and Psychiatry* 51, 789-798

20 Schneider, J., Fumeaux, C.J.F., Duerden, E.G., Guo, T., Foong, J., Graz, M.B., Hagmann, P., Chakravarty, M.M., Huppi, P.S., Beauport, L., Truttmann, A.C., Miller, S.P. (2018) Nutrient Intake in the First Two Weeks of Life and Brain Growth in Preterm Neonates. *Pediatrics* 141, e20172169

21 de Rooij, S.R., Mutsaerts, H.J.M.M., Petr, J., Asllani, I., Caan, M.W.A., Groot, P., Nederveen, A.J., Schwab, M., Roseboom, T.J. (2019) Late-life brain perfusion after prenatal famine exposure. *Neurobiology of Aging* 82, 1-9

22 Franke, K., Gaser, C., Roseboom, T.J., Schwab, M., de Rooij, S.R. (2018) Premature brain aging in humans exposed to maternal nutrient restriction during early gestation. *Neuroimage* 173, 460-471

23 Galler, J.R., Bryce, C.P., Zichlin, M.L., Fitzmaurice, G., Eaglesfield, G.D., Waber, D.P. (2012) Infant malnutrition is associated with persisting attention deficits in middle adulthood. *Journal of Nutrition* 142, 788-794

24 Waber, D.P., Bryce, C.P., Fitzmaurice, G.M., Zichlin, M.L., McGaughy, J., Girard, J.M., Galler, J.R. (2014) Neuropsychological outcomes at midlife following moderate to severe malnutrition in infancy. *Neuropsychology* 28, 530-540

25 Ekici, F., Tekbas, G., Hattapoglu, S., Yaramis, A., Onder, H., Bilici, A. (2016) Brain MRI and MR Spectroscopy Findings in Children with Nutritional Vitamin B12 Deficiency. *Clinical Neuroradiology* 26, 215-220

26 Black, M.M. (2008) Effects of vitamin B12 and folate deficiency on brain development in children. *Food and Nutrition Bulletin* 29, S126-S131

27 Yilmaz, C., Yuca, S.A., Yilmaz, N., Bektas, M.S., Caksen, H. (2009) Intracranial hemorrhage due to vitamin K deficiency in infants: a clinical study. *International Journal of Neuroscience* 119, 2250-2256

28 WHO (2020) Obesity and Overweight Fact Sheet. In *who.int* (WorldHealthOrganization, ed)

29 Monthe-Dreze, C., Rifas-Shiman, S.L., Gold, D.R., Oken, E., Sen, S. (2019) Maternal obesity and offspring cognition: the role of inflammation. *Pediatric Research* 85, 799-806

30 Liu, X., Li, X., Xia, B., Jin, X., Zou, Q., Zeng, Z., Zhao, W., Yan, S., Li, L., Yuan, S., Zhao, S., Dai, X., Yin, F., Cadenas, E., Liu, R.H., Zhao, B., Hou, M., Liu, Z., Liu, X. (2021) High-fiber diet mitigates maternal obesity-induced cognitive and social dysfunction in the offspring via gut-brain axis. *Cell Metabolism* 33, 923-938

31 Norr, M.E., Hect, J.L., Lenniger, C.J., Van den Heuvel, M., Thomason, M.E. (2020) An examination of maternal prenatal BMI and human fetal brain development. *Journal of Child Psychology and Psychiatry*

32 Spann, M.N., Scheinost, D., Feng, T., Barbato, K., Lee, S., Monk, C., Peterson, B.S. (2020) Association of Maternal Prepregnancy Body Mass Index With Fetal Growth and Neonatal Thalamic Brain Connectivity Among Adolescent and Young Women. *JAMA Network Open* 3, e2024661

33 Nunez, H., Ruiz, S., Soto-Moyano, R., Navarette, M., Valladares, L., White, A., Perez, H. (2008) Fetal undernutrition induces overexpression of CRH mRNA and CRH protein in hypothalamus and increases CRH and corticosterone in plasma during postnatal life in the rat. *Neuroscience Letters* 448, 115-119

34 Ghaly, A., Maki, Y., Nygard, K., Hammond, R., Hardy, D.B., Richardson, B.S. (2019) Maternal nutrient restriction in guinea pigs leads to fetal growth restriction with increased brain apoptosis. *Pediatric Research* 85, 105-112

35 Antonow-Schlorke, I., Schwab, M., Cox, L.A., Li, C., Stuchlik, K., Witte, O.W., Nathanielsz, P.W., McDonald, T.J. (2011) Vulnerability of the fetal primate brain to moderate reduction in maternal global nutrient availability. *PNAS* 108, 3011-3016

36 Reyes-Castro, R., J.S., Rodriguez-Gonzalez, G.L., Wimmer, R.D., McDonald, T.J., Larrea, F., Nathanielsz, P.W., Zambrano, E. (2011) Pre- and/or postnatal protein restriction in rats impairs learning and motivation in male offspring. *International Journal of Developmental Neuroscience* 29, 177-182

37 Reyes-Castro, L.A., Rodriguez, J.S., Charco, R., Bautista, C.J., Larrea, F., Nathanielsz, P.W., Zambrano, E. (2012) Maternal protein restriction in the rat during pregnancy and/or lactation alters cognitive and anxiety behaviors of female offspring. *International Journal of Developmental Neuroscience* 30, 39-45

38 Burgos, H., Hernandez, A., Constandil, L., Rios, M., Flores, O., Puentes, G., Hernandez, K., Morgan, C., Valladares, L., Castillo, A., Cofre, C., Milla, L.A., Saez-Briones, P., Barra, R. (2019) Early postnatal environmental enrichment restores neurochemical and functional plasticities of the cerebral cortex and improves learning performance in hidden-prenatally-malnourished young-adult rats. *Behavioral Brain Research* 2, 182-190

39 Reyes-Castro, L.A., Padilla-Gomez, E., Parga-Martinez, N.J., Castro-Rodriguez, D.C., Quirarte, G.L., Diaz-Cintra, S., Nathanielsz, P.W., Zambrano, E. (2018) Hippocampal mechanisms in impaired spatial learning and memory in male offspring of rats fed a low-protein isocaloric diet in pregnancy and/or lactation. *Hippocampus* 28, 18-30

40 Patro, N., Naik, A.A., Patro, I.K. (2019) Developmental Changes in Oligodendrocyte Genesis, Myelination, and Associated Behavioral Dysfunction in a Rat Model of Intra-generational Protein Malnutrition. *Molecular Neurobiology* 56, 595-610

41 Reyes-Castro, L.A., Rodriguez, J.S., Rodriguez-Gonzalez, G.L., Chavira, R., Bautista, C.J., MacDonald, T.J., Nathanielsz, P.W., Zambrano, E. (2012) Pre- and/or postnatal protein restriction developmentally programs affect and risk assessment behaviors in adult male rats. *Behavioral Brain Research* 227, 324-329

42 Gould, J.M., Smith, P.J., Airey, C.J., Mort, E.J., Airey, L.E., Warricker, F.D.M., Pearson-Farr, J.E., Weston, E.C., Gould, P.J.W., Semmence, O.G., Restall, K.L., Watts, J.A., McHugh, P.C., Smith, S.J., Dewing, J.M., Fleming, T.P., Willaime-Morawek, S. (2018) Mouse maternal protein restriction during preimplantation alone permanently alters brain neuron proportion and adult short-term memory. *PNAS* 115, E7398–E7407

43 Kesby, J.P., Turner, K.M., Alexander, S., Eyles, D.W., McGrath, J.J., Burne, T.H.J. (2017) Developmental vitamin D deficiency alters multiple neurotransmitter systems in the neonatal rat brain. *International Journal of Developmental Neuroscience* 62

44 Overeem, K., Alexander, S., Burne, T.H.J., Ko, P., Eyles, D.W. (2019) Developmental Vitamin D Deficiency in the Rat Impairs Recognition Memory, but Has No Effect on Social Approach or Hedonia. *Nutrients* 11, 2713

45 Yu, X., Jin, L., Zhang, Z., Yu, X. (2013) Effects of maternal mild zinc deficiency and zinc supplementation in offspring on spatial memory and hippocampal neuronal ultrastructural changes. *Nutrition* 29, 457-461

46 Craciunescu, C.N., Johnson, A.R., Zeisel, S.H. (2010) Dietary choline reverses some, but not all, effects of folate deficiency on neurogenesis and apoptosis in fetal mouse brain. *Journal of Nutrition* 140, 1162-1166

47 Edlow, A.G., Glass, R.M., Smith, C.J., Tran, P.K., James, K., Bilbo, S. (2019) Placental Macrophages: A Window Into Fetal Microglial Function in Maternal Obesity. *International Journal of Developmental Neuroscience* 77, 60-68

48 Sarker, G., Litwan, K., Kastli, R., Peleg-Raibstein, D. (2019) Maternal overnutrition during critical developmental periods leads to different health adversities in the offspring: relevance of obesity, addiction and schizophrenia. *Scientific Reports* 9, 17322

49 Dalby, M.J., Ross, A.W., Walker, A.W., Morgan, P.J. (2017) Dietary Uncoupling of Gut Microbiota and Energy Harvesting from Obesity and Glucose Tolerance in Mice. *Cell Reports* 21, 1521-1533

50 Zou, J., Chassaing, B., Singh, V., Pellizzon, M., Ricci, M., Fythe, M.D., Kumar, M.V., Gewirtz, A.T. (2018) Fiber-Mediated Nourishment of Gut Microbiota Protects against Diet-Induced Obesity by Restoring IL-22-Mediated Colonic Health. *Cell Host & Microbe* 23, 41-53

51 Subramanian, S., Huq, S., Yatsunenko, T., Haque, R., Mahfuz, M., Alam, M.A., Benezra, A., DeStefano, J., Meier, M.F., Muegge, B.D., Barratt, M.J., VanArendonk, L.G., Zhang, Q., Province, M.A., Petri, W.A., Ahmed, T., Gordon, J.I. (2014) Persistent Gut Microbiota Immaturity in Malnourished Bangladeshi Children. *Nature* 510, 417-421

52 Mirzaei, M.K., Khan, M.A.A., Ghosh, P., Taranu, Z.E., Taguer, M., Ru, J., Chowdhury, R., Kabir, M.M., Deng, L., Mondal, D., Maurice, C.F. (2020) Bacteriophages Isolated from Stunted Children Can Regulate Gut Bacterial Communities in an Age-Specific Manner. *Cell Host & Microbe* 27, 199-212

53 Pham, T.P.T., Alou, M.T., Bachar, D., Levasseur, A., Brah, S., Alhousseini, D., Sokhna, C., Diallo, A., Wieringa, F., Million, M., Raoult, D., (2019) Gut Microbiota Alteration is Characterized by a Proteobacteria and Fusobacteria Bloom in Kwashiorkor and a Bacteroidetes Paucity in Marasmus. *Scientific Reports* 9, 9084

54 Alou, M.T., Million, M., Traore, S.I., Mouelhi, D., Khelaifia, S., Bachar, D., Caputo, A., Delerce, J., Brah, S., Alhousseini, D., Sokhna, C., Robert, C., Diallo, B.A., Diallo, A., Parola, P., Golden, M., Lagier, J., Raoult, D.` (2017) Gut Bacteria Missing in Severe Acute Malnutrition, Can We Identify Potential Probiotics by Culturomics? *Frontiers in Microbiology* 8, 899

55 Million, M., Alou, M.T., Khelaifia, S., Bachar, D., Lagier, J., Dione, N., Brah, S., Hugon, P., Lombard, V., Armougom, F., Fromonot, J., Robert, C., Michelle, C., Diallo, A., Fabre, A., Guieu, R., Sokhna, C., Henrissat, B., Parola, P., Raoult, D. (2016) Increased Gut Redox and Depletion of Anaerobic and Methanogenic Prokaryotes in Severe Acute Malnutrition. *Scientific Reports* 6, 26051

56 Ghosh, T.S., Gupta, S.S., Bhattacharya, T., Yadav, D., Barik, A., Chowdhury, A., Das, B., Mande, S.S., Nair, G.B. (2014) Gut Microbiomes of Indian Children of Varying Nutritional Status. *PLOS ONE* 9, e95547

57 Kristensen, K.H.S., Wiese, M., Rytter, M.J.H., Ozcam, M., Hansen, L.H., Namusoke, H., Friis, H., Nielsen, D.S. (2016) Gut Microbiota in Children Hospitalized with Oedematous and Non-Oedematous Severe Acute Malnutrition in Uganda. *PLoS Neglected Tropical Diseases* 10, e0004369

58 Castro-Mejia, J.L., O'Ferrall, S., Krych, L., O'Mahoney, E., Namusoke, H., Lanyero, B., Kot, W., Nabukeera-Barungi, N., Michaelsen, K.F., Molgaard, C., Friis, H., Grenov, B., Nielsen, D.S. (2020) Restitution of gut microbiota in Ugandan children administered with probiotics (Lactobacillus rhamnosus GG and Bifidobacterium animalis subsp. lactis BB-12) during treatment for severe acute malnutrition. *Gut Microbes* 11, 855-867

59 Chu, D.M., Antony, K.M., Ma, J., Prince, A.L., Showalter, L., Moller, M., Aagaard, K.M. (2016) The early infant gut microbiome varies in association with a maternal high-fat diet. *Genome Medicine* 8

60 Ma, J., Prince, A.L., Bader, D., Hu, M., Ganu, R., Baquero, K., Blundell, P., Harris, R.A., Frias, A.E., Grove, K.L., Aagaard, K.M. (2014) High-fat maternal diet during pregnancy persistently alters the offspring microbiome in a primate model. *Nature Communications* 5, 3899

61 Smith, M.I., Yatsunenko, T., Manary, M.J., Trehan, I., Mkakosya, R., Cheng, J., Kau, A.L., Rich, S.S., Concannon, P., Mychaleckyj, J.C., Liu, J., Houpt, E., Li, J.V., Holmes, E., Nicholson,

J., Knights, D., Ursell, L.K., Knight, R., Gordon, J.I. (2013) Gut microbiomes of Malawian twin pairs discordant for kwashiorkor. *Science* 339, 548-554

62 Schwarzer, M., Makki, K., Storelli, G., Machuca-Gayet, I., Srutkova, D., Hermanova, P., Martino, M.E., Balmand, S., Hudcovic, T., Heddi, A., Rieusset, J., Kozakova, H., Vidal, H., Leulier, F. (2016) Lactobacillus plantarum strain maintains growth of infant mice during chronic undernutrition. *Science* 351, 854-857

63 Kara, S.S., Volkan, B., Erten, I. (2019) Lactobacillus rhamnosus GG can protect malnourished children. *Beneficial Microbes* 10, 237-244

64 Gehrig, J.L., Venkatesh, S., Chang, H.W., Hibberd, M.C., Kung, V.L., Cheng, J., Chen, R.Y., Subramanian, S., Cowardin, C.A., Meier, M.F., O'Donnell, D., Talcott, M., Spears, L.D., Semenkovich, C.F., Henrissat, B., Giannone, R.J., Hettich, R.L., Ilkayeva, O., Muehlbauer, M., Newgard, C.B., Sawyer, C., Head, R.D., Rodionov, D.A., Arzamasov, A.A., Leyn, S.A., Osterman, A.L., Hossain, M.I., Islam, M., Choudhury, N., Sarker, S.A., Huq, S., Mahmud, I., Mostafa, I., Mahfuz, M., Barratt, M.J., Ahmen, T., Gordon, J.I. (2019) Effects of microbiota-directed foods in gnotobiotic animals and undernourished children. *Science* 365, 139

65 Zambrana, L.E., McKeen, S., Ibrahim, H., Zarei, I., Borresen, E.C., Doumbia, L., Bore, A., issoko, A., Douyon, S., Kone, K., Perez, J., Perez, C., Hess, A., Abdo, Z., Sangare, L., Maiga, A., Becker-Dreps, S., Yuan, L., Koita, O., Vilchez, S., Ryan, E.P. (2019) Rice bran supplementation modulates growth, microbiota and metabolome in weaning infants: a clinical trial in Nicaragua and Mali. *Scientific Reports* 9, 13919

66 Huey, S.L., Jiang, L., Fedarko, M.W., McDonald, D., Martino, C., Ali, F., Russel, D.G., Udipi, S.A., Thorat, A., Thakker, V., Ghugre, P., Potdar, R.D., Chopra, H., Rajagopalan, K., Haas, J.D., Finkelstein, J.L., Knight, R., Mehta, S. (2020) Nutrition and the gut microbiota in 10- to 18-month-old children living in urban slums of Mumbai, India. *mSphere* 5, e00731-00720

67 Chen, R.Y., Mostafa, I., Hibberd, M.C., Das, S., Mahfuz, M., Naila, N.N., Islam, M.M., Huq, S., Alam, M.A., Zaman, M.U., Raman, A.S., Webber, D., Zhou, C., Sundaresan, V., Ahsan, K., Meier, M.F., Barratt, M.J., Ahmed, T., Gordon, J.I. (2021) A microbiota-directed food intervention for undernourished children. *The New England Journal of Medicine* 384, 1517-1528

68 Younge, N.E., Newgard, C.B., Cotten, C.M., Goldberg, R.N., Muehlbauer, M.J., Bain, J.R., Stevens, R.D., O'Connel, T.M., Rawls, J.F., Seed, P.C., Ashley, P.L. (2019) Disrupted maturation of the microbiota and metabolome among extremely preterm infants with postnatal growth failure. *Scientific Reports* 9

69 Varal, I.G., Koksal, N., Ozkan, H., Bagci, O., Dogan, P. (2018) Potential use of multi-strain synbiotics for improving postnatal head circumference. *Pakistan Journal of Medican Sciences* 34, 1502-1506

70 Sanguinetti, E., Guzzardi, M.A., Tripodi, M., Panetta, D., Selma-Royo, M., Zega, A., Telleschi, M., Collado, M.C., Iozzo, P. (2019) Microbiota signatures relating to reduced memory and exploratory behaviour in the offspring of overweight mothers in a murine model. *Scientific Reports* 9, 12609

71 Buffington, S.A., Di Prisco, G.V., Auchtung, T.A., Ajami, N.J., Petrosino, J.F., Costa-Mattioli, M. (2016) Microbial Reconstitution Reverses Maternal Diet-Induced Social and Synaptic Deficits in Offspring. *Cell* 165, 1762-1775

72 Jasarevic, E., & Bale, T.L. (2019) Prenatal and postnatal contributions of the maternal microbiome on offspring programming. *Frontiers in Neuroendocrinology* 55, 100797

73 Silva, Y.P., Bernardi, A., Frozza, R.L. (2020) The Role of Short-Chain Fatty Acids From Gut Microbiota in Gut-Brain Communication. *Frontiers in Endocrinology* 11, 25

74 Yu, L., Zhong, X., He, Y., Shi, Y. (2020) Butyrate, but not propionate, reverses maternal diet-induced neurocognitive deficits in offspring. *Pharmacological Research* 160

75 Val-Laillet, D., Besson, M., Guerin, S., Coquery, N., Randuineau, G., Kanzari, A., Quesnel, H., Bonhomme, N., Bolhuis, J.E., Kemp, B., Blat, S., Le Huerou-Luron, I., Clouard, C. (2017) A maternal Western diet during gestation and lactation modifies offspring's microbiota activity, blood lipid levels, cognitive responses, and hippocampal neurogenesis in Yucatan pigs. *FASEB J* 31, 2037-2049

76 Farras, M., Chandwe, K., Mayneris-Perxachs, J., Amadi, B., Louis-Auguste, J., Besa, E., Zyambo, K., Guerrant, R., Kelly, P., Swann, J.R. (2018) Characterizing the metabolic phenotype of intestinal villus blunting in Zambian children with severe acute maInutrition and persistent diarrhea. *PLoS ONE* 13, e0192092

77 Mayneris-Perxachs, J., Lima, A.A.M., Guerrant, R.L., Leite, A.M., Moura, A.F., Lima, N.L., Soares, A.M., Havt, A., Moore, S.R., Pinkerton, R., Swann, J.R. (2016) Urinary N-methylnicotinamide and β-aminoisobutyric acid predict catch-up growth in undernourished Brazilian children. *Scientific Reports* 6, 19780

78 Vuong, H.E., Pronovost, G.N., Williams, D.W., Coley, E.J.L., Siegler, E.L., Qui, A., Kazantsev, M., Wilson, C.J., Rendon, T., Hsiao, E.Y. (2020) The maternal microbiome modulates fetal neurodevelopment in mice. *Nature* 586, 281-286

79 Bartz, S., Mody, A., Hornik, C., Bain, J., Muehlbauer, M., Kiyimba, T., Kiboneka, E., Stevens, R., Bartlett, J., St Peter, J.V., Newgard, C.B., Freemark, M. (2014) Severe Acute Malnutrition in Childhood: Hormonal and Metabolic Status at Presentation, Response to Treatment, and Predictors of Mortality. *The Journal of Clinical Endocrinology & Metabolism* 99, 2128-2137

80 Getty, C.M.D., R.N. (2015) Moderate Perinatal Choline Deficiency Elicits Altered Physiology and Metabolomic Profiles in the Piglet. *PLoS ONE* 10, e0133500

81 Isganaitis, E., Venditti, S., Matthews, T.J., Lerin, C., Demerath, E.W., Fields, D.A. (2019) Maternal obesity and the human milk metabolome: associations with infant body composition and postnatal weight gain. *American Journal of Clinical Nutrition* 110, 111-120

82 Hegar, B., Wibowo, Y., Basrowi, R.W., Ranuh, R.G., Sudarmo, S.M., Munasir, Z., Atthiyah, A.F., Widodo, A.D., Supriatmo, Kadim, M., Suryawan, A., Diana, N.R., Manoppo, C., Vanderplas, Y. (2019) The Role of Two Human Milk Oligosaccharides, 2′-Fucosyllactose and Lacto-N-Neotetraose, in Infant Nutrition. *Pediatric Gastroenterology Hepatology Nutrition* 22, 330-340

83 Charbonneau, M.R., O'Donnell, D., Blanton, L.V., Totten, S.M., Davis, J.C.C., Barratt, M.J., Cheng, J., Guruge, J., Talcott, M., Bain, J.R., Muehlbauer, M.J., Ilkayeva, O., Wu, C., Struckmeyer, T., Barile, D., Mangani, C., Jorgensen, J., Fan, Y., Maleta, K., Dewey, K.G., Ashorn, P., Newgard, C.B., Lebrilla, C., Mills, D.A., Gordon, J.I. (2016) Sialylated Milk OligosaccharidesPromote Microbiota-Dependent Growthin Models of Infant Undernutrition. *Cell* 164, 859-871

84 Wang, B., Brand-Miller, J. (2003) The role and potential of sialic acid in human nutrition. *European Journal of Clinical Nutrition* 57, 1351-1369

85 Hasko, G., Pacher, P., Vizi, E.S., Illes, P. (2005) Adenosine receptor signaling in the brain immune system. *Trends in Pharmacological Science* 26, 511-516

86 Doyle, C., Cristofaro, V., Sullivan, M.P., Adam, R.M. (2018) Inosine – a Multifunctional Treatment for Complications of Neurologic Injury. *Cellular Physiology and Biochemistry* 49, 2293-2303

87 Leon-Aguilar, L.F., Croyal, M., Ferchaud-Roucher, V., Huang, F., Marchat, L.A., Barraza-Villarreal, A., Romieu, I., Ramakrishnan, U., Krempf, M., Ouguerram, K., Mercado-Camargo, R., Bolanos-Jimenez, F. (2019) Maternal obesity leads to long-term altered levels of plasma ceramides in the offspring as revealed by a longitudinal lipidomic study in children. *International Journal of Obesity* 43, 1231-1243

88 Johnson, E.L., Heaver, S.L., Waters, J.L., Kim, B.I., Bretin, A., Goodman, A.L., Gewirtz, A.T., Worgall, T.S., Ley, R.E. (2020) Sphingolipids produced by gut bacteria enter host metabolic pathways impacting ceramide levels. *Nature Communications* 11, 2471

89 Olsen, A.S.B., Faergeman, N.J. (2017) Sphingolipids: membrane microdomains in brain development, function and neurological diseases. *Open Biology* 7, 170069

90 Fischer, D.D., Kandasamy, S., Paim, F.C., Langel, S.N., Alhamo, M.A., Shao, L., Chepngeno, J., Miyazaki, A., Huang, H., Kumar, A., Rajashekara, G., Saif, L.J., Vlasova, A.N. (2017) Protein Malnutrition Alters Tryptophan and Angiotensin-Converting Enzyme 2 Homeostasis and Adaptive Immune Responses in Human Rotavirus-Infected Gnotobiotic Pigs with Human Infant Fecal Microbiota Transplant. *Clinical and Vaccine Immunology* 24, e00172-00117

91 Connor, K.L., Chehoud, C., Altrichter, A., Chan, L., DeSantis, T.Z., Lye, S.J. (2018) Maternal metabolic, immune, and microbial systems in late pregnancy vary with malnutrition in mice. *Biology of Reproduction* 98, 579-592

92 Kim, S., Kim, H., Yim, Y.S., Ha, S., Atarashi, K., Tan, T.G., Longman, R.S., Honda, K., Littman, D.R., Choi, G.B., Huh, J.R. (2017) Maternal gut bacteria promote neurodevelopmental abnormalities in mouse offspring. *Nature* 549, 528-532

93 Hsiao, E.Y., McBride, S.W., Hsien, S., Sharon, G., Hyde, E.R., McCue, T., Codelli, J.A., Chow, J., Reisman, S.E., Petrosino, J.F., Patterson, P.H., Mazmanian, S.K. (2013) The microbiota modulates gut physiology and behavioral abnormalities associated with autism. *Cell* 155, 1451-1463

94 Foster, J.A., Rinaman, L., Cryan, J.F. (2017) Stress & the gut-brain axis: Regulation by the microbiome. *Neurobiology of Stress* 7, 124-136

95 Vaughan, O.R., Sferruzzi-Perri, A.N., Fowden, A.L. (2012) Maternal corticosterone regulates nutrient allocation to fetal growth in mice. *The Journal of Physiology* 190, 5529-5540

96 Jasarevic, E., Howerton, C.L., Howard, C.D., Bale, T.L. (2015) Alterations in the Vaginal Microbiome by Maternal Stress Are Associated With Metabolic Reprogramming of the Offspring Gut and Brain. *Endocrinology* 156, 3265-3276

97 Jasarevic, E., Howard, C.D., Morrison, K., Misic, A., Weinkopff, T., Scott, P., Hunter, C., Beiting, D., Bale, T.L. (2018) The maternal vaginal microbiome partially mediates the effects of prenatal stress on offspring gut and hypothalamus. *Nature Neuroscience* 21, 1061-1071

98 Miro-Blanch, J., Yanes, O. (2019) Epigenetic regulation at the interplay between gut microbiota and host metabolism. *Frontiers in Genetics* 10

99 Dempsey, J., Zhang, A., Cui, J.Y. (2018) Coordinate regulation of long non-coding RNAs and protein-coding genes in germ-free mice. *BMC Genomics* 19

100 Peter, C.J., Fischer, L.K., Kundakovic, M., Garg, P., Jakovcevski, M., Dincer, A., Amaral, A.C., Ginns, E.I., Galdzicka, M., Bryce, C.P., Ratner, C., Waber, D.P., Mokler, D., Medford, G., Champagne, F.A., Rosene, D.L., McGaughy, J.A., Sharp, A.J., Galler, J.R., Akbarian, S. (2016) DNA Methylation Signatures of Early Childhood Malnutrition Associated With Impairments in Attention and Cognition. *Biological Psychiatry* 80, 765-774

101 Blusztajn, J.K.M., T.J. (2012) Choline nutrition programs brain development via DNA and histone methylation. *Central Nervous System Agents in Medicinal Chemistry* 12, 82-94

102 Haithar, S., Kuria, M.W., Sheikh, A., Kumar, M., Vander Stoep, A. (2018) Maternal depression and child severe acute malnutrition: a case-control study from Kenya. *BMC Pediatrics* 18, 289

103 Khan, S., Zaheer, S., Safdar, N.F. (2019) Determinants of stunting, underweight and wasting among children < 5 years of age: evidence from 2012-2013 Pakistan demographic and health survey. *BMC Public Health* 19, 358

Chapter 3: The maternal microbiome modifies adverse effects of protein undernutrition on offspring neurobehavioral impairment in mice

Abstract: Protein undernutrition is a global risk factor for impaired growth and neurobehavioral development in children. However, the critical periods, environmental interactions, and maternal versus neonatal influences on programming lasting behavioral abnormalities are poorly understood. In a mouse model of fetal growth restriction, limiting maternal protein intake particularly during pregnancy leads to cognitive and anxiety-like behavioral abnormalities in adult offspring, indicating a critical role for the gestational period. By cross-fostering newborn mice to dams previously exposed to either low protein or standard diet, we find that the adult behavioral impairments require diet-induced conditioning of both fetal development and maternal peripartum physiology, rather than either alone. This suggests that protein undernutrition during pregnancy directly disrupts fetal neurodevelopment and indirectly alters maternal state in ways that interact postnatally to precipitate behavioral deficits. Consistent with this, maternal protein restriction during pregnancy reduces the diversity of the maternal gut microbiome, modulates maternal serum metabolomic profiles, and yields widespread alterations in fetal brain transcriptomic and metabolomic profiles, including subsets of microbiome-dependent metabolites. Depletion of the maternal microbiome in protein-restricted dams further alters fetal brain gene expression and exacerbates neurocognitive behavior in adult offspring, suggesting that the maternal microbiome modifies the impact of gestational protein undernutrition on risk for neurobehavioral impairment in the offspring. To explore the potential for microbiome-targeted interventions, we find that maternal treatment with short chain fatty acids or a cocktail of 10 diet- and microbiome-dependent metabolites each yield differential effects on fetal development and/or postnatal behavior. Results from this study highlight impactful prenatal influences of maternal protein undernutrition on fetal neurodevelopment and adverse neurobehavioral trajectories in offspring, which are mitigated by microbiome-targeted interventions during pregnancy.

Main

Protein undernutrition is a global risk factor for childhood stunting[1], which is co-morbid with lasting neurological disabilities, including cognitive impairment and anxiety[2–4]. In humans and animal models, abnormalities in the maturation and function of the gut microbiome contribute to malnutrition-induced stunting[5], but standard therapeutic foods have limited effectiveness in supporting persistent microbial rehabilitation[5–7]. There is increasing evidence that bacterial treatments and custom microbiota-directed diets ameliorate growth restriction in animal models of malnutrition and in malnourished children[8–11]. This raises the prospect of using microbiome-based treatments to combat malnutrition-induced growth defects. However, current medical and nutritional interventions that treat childhood stunting are often inadequate to ameliorate co-morbid neurobehavioral impairments[12]. Individuals who experienced protein-energy malnutrition during the first year of life displayed cognitive impairment and depressive symptoms during adolescence and adulthood, despite adequate nutritional rehabilitation and growth recovery during childhood[13–16]. Similarly, supplementing stunted infants with a milk-based formula failed to ameliorate heightened anxiety and cognitive impairments in adolescence[3,4]. Whether alterations in the microbiome contribute to the neurological comorbidities caused by protein undernutrition, and whether microbiome-based interventions can be used to ameliorate them, is poorly understood.

Brain abnormalities, such as cerebral atrophy, ventricular dilation, and myelin-related deficits, are seen in protein malnourished infants as young as 3 months of age and through 36 months of age[17,18], highlighting an early critical period during which protein undernutrition impairs neurodevelopment. In animal models, restricting protein intake particularly during pregnancy yields persistent neurological and neurobehavioral impairments in the offspring, including abnormalities in neuronal proliferation and apoptosis[19], neocortical activity[20], hippocampal morphology[21], learning and memory, and anxiety-like behaviors[19–22]. These results indicate that adverse neurological consequences of protein undernutrition can originate from gestational influences[23]. In considering potential contributions of the microbiome, evidence from animal

models indicate that alterations in the maternal microbiome contribute to adverse effects of immune activation, stress, and high-fat diet on neurological and behavioral deficits in the offspring[24–26], either by directing fetal neurodevelopment during pregnancy[27,28] or by shaping early postnatal neural development via vertical transmission at birth and postpartum[28,29]. These findings align with human studies reporting that alterations in the maternal microbiome during pregnancy are associated with abnormalities in offspring behavior[30,31] and that postpartum nursing supports cognitive, language, and microbiome development in the first years of life[32]. However, mechanisms by which maternal protein undernutrition leads to lasting neurobehavioral deficits in the offspring, and how these processes may be modified by the microbiome, are unknown.

Herein, we examine effects of maternal protein undernutrition during pregnancy on maternal-fetal health and offspring behavior in mice. We use a cross-fostering paradigm to evaluate the ability of maternal protein restriction to directly alter fetal neurodevelopment and indirectly condition maternal physiology to engender lasting cognitive and anxiety-related behaviors in adult offspring. We profile effects of maternal protein restriction on the maternal microbiome, and further assess the impact of maternal microbiome depletion and microbial metabolite supplementation on maternal-fetal and offspring behavioral responses to maternal protein restriction. Results from this study highlight the importance of the gestational period in protein undernutrition altering both maternal health and fetal developmental trajectories. Furthermore, results reveal a role for the maternal microbiome in modulating the severity of fetal developmental and adult neurobehavioral impairments induced by maternal protein undernutrition. These advances in illuminating molecular underpinnings of adverse behavioral outcomes of protein undernutrition could potentially lead to new approaches to ameliorate neurological disorders that co-occur with impaired growth in malnourished children.

Results

Maternal protein restriction yields behavioral abnormalities in adult offspring by altering both fetal development and maternal postpartum physiology

Protein undernutrition is associated with both childhood stunting and neurological dysfunction, but the etiopathogenesis of lasting neurobehavioral deficits remains poorly understood. To explore this relationship, we first evaluated effects of maternal protein restriction particularly during pregnancy on behavior in adult offspring. To model maternal protein undernutrition, male and female C57Bl/6J mice were fed a 6% protein diet (protein restriction, PR) or 20% protein control diet (CD) for 2 weeks prior to timed-mating and throughout gestation (**Fig. 3.1a**). PR and CD formulations were isocaloric, where the 14% protein content lacking in PR was replaced by carbohydrates, mainly sucrose and cellulose (**Fig. 3.S1a, Table 3.S1**). Consistent with existing literature using this paradigm as a model of fetal growth restriction (FGR)[33,34], maternal consumption of a PR diet prior to and throughout pregnancy resulted in reduced fetal weight at late gestation (embryonic day (E) 18.5) and maternal net weight loss with no difference in diet consumption, in addition to elevated maternal serum corticosterone and reduced litter size at birth (**Fig. 3.S1b-f**). These findings suggest a state of maternal physiological stress.

To decouple lasting effects of maternal protein restriction during pregnancy on maternal postpartum physiology versus fetal neurodevelopment, pups were cross fostered at birth to dams gestationally exposed to PR or CD to form the following groups: CD pups fostered to CD dams (CD → CD), PR pups fostered to CD dams (PR → CD), CD pups fostered to PR dams (CD → PR), PR pups fostered to PR dams (PR → PR) (**Fig. 3.1a**). Moreover, to examine effects of maternal protein undernutrition, specifically during pregnancy, on postnatal health of the offspring, PR-fed dams were switched to CD at parturition, and all pups were reared on CD from birth in order to isolate PR to the gestational period. Of all the experimental groups, PR pups fostered to PR dams exhibited the smallest litter sizes by weaning age (**Fig. 3.S1g**) and the lowest total litter survival at 26.5% (**Fig. 3.S1h**). CD pups fostered to PR dams exhibited intermediate reductions in litter survival to 46.7%, whereas PR pups fostered to CD dams exhibited 100% survival, as did

CD pups fostered to CD dams. These results indicate that offspring survival is determined by an interaction between direct effects of gestational PR on fetal health and indirect effects of gestational PR on maternal health persisting into the postnatal period. It further indicates that gestational PR-induced alterations in maternal, but not fetal health, are sufficient to reduce offspring survival. There were no significant differences in pup weights in the first two weeks of life (**Fig. 3.S1i**), suggesting that fetuses from PR dams exhibit weight recovery with postnatal rearing on CD.

To assess lasting effects of maternal protein restriction during pregnancy on adverse neurobehavioral outcomes in the offspring, fostered offspring were weaned, reared to adulthood, and tested in behavioral assays related to anxiety and cognition (**Fig. 3.1b**). The open field assay is a benchmark test for stress-induced thigmotaxis as an endophenotype of anxiety-like behavior[35,36]. Adult PR offspring previously fostered to PR dams and reared since birth on CD (PR→PR) displayed significantly reduced time and distance in the center of open field (**Fig. 3.1c-d**), as compared to other experimental groups, with no difference in average speed or total distance traveled (**Fig. 3.S2a**). This anxiety-like phenotype was more striking in females than males, with postnatal influence of CD rearing appearing to be sex-discriminatory (**Fig. 3.S2b**). This female-bias in anxiety-like response was similarly reported in a multi-hit pre- and postnatal adversity model[37]. This finding suggests that adverse postnatal interactions between maternal and fetal responses to gestational PR lead to anxiety-like behavior. The Barnes maze test is a benchmark assay of spatial learning and memory[38], wherein mice are trained over repeated trials to identify which out of 20 holes contains an escape box (acquisition phase) and their ability to recall the spatial location of the escape is tested in a final probe trial 24 hours post-training. During the acquisition phase, adult PR→PR offspring exhibited increased latency to escape (**Fig. 3.1e**), but no significant difference in primary latency to target zone (**Fig. 3.1f**), suggesting deficient learning. During the probe phase, these PR→PR offspring displayed increased time in the target zone (**Fig. 3.1g**), but no significant difference in errors made (**Fig. 3.1h**), suggesting adequate

24-hour recall, but increased perseveration. There were no overt sex differences in cognitive deficits seen in offspring of PR-fed dams (**Fig. 3.S2c-f**). These findings suggest that maternal PR during pregnancy alters both maternal physiology and fetal development in ways that interact postnatally to engender lasting behavioral impairments in offspring with adequate postnatal nutrition.

Maternal protein restriction alters functional signatures in the fetal brain

Maternal malnutrition can alter the trajectory of fetal neurodevelopment to result in long-term changes in brain function and behavior[19–22]. To uncover mechanisms by which maternal protein undernutrition programs adverse behavioral outcomes in the offspring, we first examined the effects of maternal PR on E18.5 fetal brains by transcriptomic profiling. We identified 505 significantly up-regulated and 423 significantly down-regulated genes in response to maternal PR (**Fig. 3.2a**). By gene ontology analysis, the upregulated genes related to biological processes such as neuronal apoptosis (reported to be increased in fetal brain following protein restriction[19]), ion and amino acid transport, and response to growth factor (**Fig. 3.2b**), suggesting compensatory mechanisms related to brain sparing[33,39]. Downregulated genes related to biological processes such as T-cell differentiation and nervous system development potentially highlight immune or neuroimmune disruptions, as previously implicated in malnourished children[40]. Particular neurobehaviorally-relevant genes were significantly altered in fetal brains from PR dams, including downregulated serotonin transporter (*Slc64a)* and serotonin receptor (*Htr3a)*, insulin-like growth factor 1 (*Igf1*), which modulates anxiety and stress response[41], and Ataxin 1 (*Atxn1*), related to learning and hippocampal deficits[42]. Conversely, activity-dependent neuroprotective protein (*Adnp*), implicated in cognitive and social impairments and stress response[43], and dopamine beta hydroxylase (*Dbh*), relevant to learning and memory[44] were upregulated in fetal brains from PR dams**.**

These PR-induced alterations in fetal gene expression corresponded with widespread changes in levels of fetal brain metabolites. Liquid chromatography tandem mass spectrometry-based metabolomic profiling of E18.5 brains yielded detectable levels of 681 identified compounds, spanning amino acid, peptide, carbohydrate, energy, lipid, nucleotide, cofactor and vitamin, and xenobiotic super pathways. By principal component analysis, metabolomic profiles of fetal brains from PR dams were clearly discriminated from CD controls along PC1 (**Fig. 3.2c**), with statistically significant alterations in 220 metabolites. The most highly affected metabolite classes were amino acids (98) and lipids (84) (**Fig. 3.2d**). Of the amino acid-related metabolites that were significantly altered in fetal brains from PR dams relative to CD controls, 50% were increased (and 50% were decreased), suggesting complex regulation of amino acids. By comparison, we further profiled metabolomics in maternal serum and found 332 serum metabolites that were statistically significantly altered by PR consumption (**Fig. 3.S3a**). As in fetal brains, the majority were amino acids (107) and lipids (144) (**Fig. 3.S3b**). However, in contrast to fetal brains, the alterations in amino acid-related metabolites seen in maternal serum were mostly reductions (81.3%, as compared to 50% in fetal brain), which is consistent with low protein intake and evidence of fetal brain sparing[39]. In line with this, all essential amino acids and glucose showed significant reductions in PR maternal serum compared to CD (**Fig. 3.S3d-m**). However, glucose, lysine, and phenylalanine showed no significant difference between PR and CD fetal brain, and tryptophan showed a significant increase in PR fetal brain compared to CD, further supporting a metabolite-specific brain-sparing phenotype. (**Fig. 3.S3d, h, j, l**).

By metabolite set enrichment analysis, fetal brain metabolites that were reduced by maternal PR mapped to 14 metabolic pathways, with histidine metabolism, glycine and serine metabolism, methionine metabolism, and homocysteine degradation persisting after statistical correction (**Fig. 3.2e**). The fetal brain metabolites that were increased by maternal PR mapped to 4 pathways, including pyrimidine metabolism and tryptophan metabolism, although none survived statistical correction (**Fig. 3.2e**). Similar to fetal brain metabolites, maternal serum metabolites

related to pyrimidine metabolism were upregulated by PR, whereas pathways related to tryptophan metabolism and valine, leucine, and isoleucine degradation were downregulated (**Fig. 3.S3c**). The most severely depleted individual metabolites in PR fetal brains included urea (10.1% the levels of CD fetal brains), a product of protein catabolism, and hypotaurine (24.0% the levels of CD fetal brains), a precursor of taurine, which directly supports synaptic formation and transmission in the developing brain[45]. Conversely, PR fetal brains had a 276.9% increase in corticosterone, which is consistent with increased corticosterone in maternal serum by ELISA (**Fig. 3.S1e**). Synthetic corticosteroids which mimic glucocorticoid activity during gestation have been previously reported to impair hippocampal synaptic development in primates[46], and myelination and brain growth in sheep[47,48]. Furthermore, maternal cortisol has been correlated with sex-specific amygdala connectivity and internalizing symptoms in humans[49]. Taken together, these results indicate that maternal protein undernutrition during pregnancy modifies transcriptional and metabolomic profiles in the late gestational fetal brain, which can contribute to fetal neurodevelopmental programming in ways that interact postnatally with maternal factors to yield behavioral abnormalities in adult offspring.

Murine maternal protein restriction and human fetal growth restriction are associated with reduced diversity of the maternal and infant gut microbiome

Maternal behavioral and physiological care during early life has profound and persistent effects on offspring neurobehavioral development[50,51]. Results from our cross-fostering experiments indicate that PR-induced alterations in offspring behavior require antenatal exposure of both fetuses and mothers to PR during gestation (**Fig. 3.1**). To gain insight into how protein undernutrition during pregnancy impacts maternal health to disrupt offspring behavioral development, we first tested dams for postpartum behavior related to maternal care. The pup retrieval test is a benchmark behavioral assay that assesses the mother's response to retrieve pups upon their removal from the nest[52,53]. There were no statistically significant differences

between PR and CD dams in their latency to full retrieval of their fostered pups, either PR or CD (**Fig. 3.S1j**). Consistent with this, there were no differences in pup righting reflex or ultrasonic vocalizations upon maternal separation (**Fig. 3.S1k-l**). These results suggest no overt difference in pup-directed maternal care across dams previously fed PR or CD during pregnancy.

In addition to maternal care, the maternal gut microbiome is increasingly appreciated for its roles in promoting healthy neonatal development by supporting nutrition and immune development[23,54]. Alterations in the maternal microbiome, observed in various models of malnutrition[55,56], can disrupt early neurodevelopment and elicit lasting changes in offspring behavior[24,25,27,28,30,31,57,58]. To determine effects of protein restriction on the composition of the maternal gut microbiota, we performed 16S rRNA gene sequencing of fecal samples collected over the course of gestation from dams fed PR or CD. Consistent with previous reports[59] bacterial alpha-diversity increased with pregnancy in CD-fed dams (**Fig. 3.3a**). However, this was prevented by PR, as fecal microbiota from PR dams displayed significantly decreased Shannon diversity [a measure of both richness (the number of different species) and evenness (the amount within each species)] and Pielou's evenness as compared to CD controls (**Fig. 3.3a**). Principal coordinates analysis of weighed Unifrac distances discriminates microbiota from PR dams away from CD controls by E10.5 (**Fig. 3.3b**). Differences in beta diversity were driven by statistically significant alterations in the relative abundances of 31 bacterial taxa (**Fig. 3.3c**), which were dominated by *Clostridia* species. Reductions align with the finding that *Clostridia* are the main metabolizers of dietary protein and amino acids[60]. Altogether, these results indicate that maternal protein undernutrition during pregnancy reduces diversity of the maternal microbiota, which corresponds with alterations in functional profiles in the fetal brain and neurobehavioral deficits in adult offspring despite being reared on a standard protein diet since birth.

Microorganisms from the maternal microbiota seed the infant gut microbiota at birth, serving as initial colonizers that inform infant metabolic and immune development[29]. We find in the maternal protein restriction mouse model for FGR that alterations in the maternal microbiota

precede the development of neurobehavioral abnormalities in adult offspring. To gain insight into whether similar relationships are seen in a related human condition, we examined associations between the early life microbiome and neurocognitive outcomes in individuals from a cohort of preterm infants with or without FGR. Compared to 37 non-FGR preterm controls, 16 FGR preterm infants exhibited decreased alpha diversity of the fecal microbiota, with reduced Shannon diversity at week 3 of life, but no difference in subsequent weeks (**Fig. 3.3d**), suggesting delayed maturation of the gut microbiome. Taxonomic data did not show visible clustering of FGR vs non-FGR samples by principal coordinates analysis (**Fig. 3.3e**), indicating no widespread alterations in beta diversity. However, FGR samples exhibited significant alterations in select bacterial taxa, with increased *Staphylococcus* at 2 weeks of life (**Fig. 3.3f**). These alterations in microbiota were not attributable to statistically significant differences in infant sex, pregnancy induced hypertension, mode of delivery, day of life for first enteral feed, number of days on parenteral nutrition, antibiotics before or after delivery, early or late onset sepsis, or necrotizing enterocolitis (the latter showed a negative trending correlation with *Staphylococcus*) (**Fig. 3.3g**). When 28 non-FGR preterm infants were compared to 15 FGR preterm infants in a follow-up across 24 months corrected gestational age, the FGR subset scored significantly lower in the cognitive composite score on the Bayley Scales of Infant and Toddler Development III (BSID III), which is used to assess and diagnose developmental delays[61] (**Fig. 3.3h**). Compared to non-FGR preterm controls, FGR preterm infants exhibited no statistical difference in language composite scores and a trending decrease in motor composite scores (**Fig. 3.3h**). In the subset of participants with both microbiota and BSID III outcome measures (15 non-FGR and 10 FGR), Shannon diversity at 3 weeks of life correlated positively with the language composite score at 12 months corrected gestational age and the cognitive composite score at 18-24 months corrected gestational age, while *Staphylococcus* at 2 weeks of life correlated negatively with cognitive composite score at 6, 12, and 18-24 months corrected gestational age, and trended towards a negative correlation with the motor composite score at 6 months corrected gestational age (**Fig. 3.3i**). *Staphylococcus*-

dominated microbiota in preterm infants has previously been correlated to developmental delays and poor health outcomes[62]. Overall, these results reveal associations between human FGR, reduced alpha diversity of the early life gut microbiota, and reduced scores in infant neurodevelopmental measures, particularly in the cognitive domain. Despite the heterogenous nature and limited sample size of this human FGR cohort, and the difference in sampling timepoint, these findings mirror our observations from the maternal protein restriction mouse model for FGR.

Depletion of the maternal gut microbiome modifies effects of dietary protein restriction on functional signatures in the fetal brain

The maternal gut microbiome guides normal fetal neurodevelopment and modifies effects of maternal environmental exposures, such as immune activation, antidepressant treatment, and prenatal stress on the fetal brain[24,25,58,63]. To examine influences of the maternal gut microbiome on fetal neurodevelopmental responses to maternal protein undernutrition, we examined functional signatures in the fetal brain after depletion of the maternal microbiome in PR-fed dams. Dams were treated with a cocktail of broad-spectrum antibiotics (ABX) by oral gavage twice daily for one week before breeding, and subsequently maintained on ABX in water throughout gestation[27,64] (**Fig. 3.4a**). RNA sequencing revealed 1564 genes that were differentially expressed in E18.5 fetal brains from ABX-treated dams fed PR compared to conventional PR controls (specific pathogen free, SPF PR) (**Fig. 3.4b**), suggesting widespread fetal brain responses to depletion of the maternal microbiome. Of these, only 160 (10.2%) of the genes differentially expressed by maternal ABX treatment were similarly dysregulated by maternal PR relative to CD controls (**Fig. 3.4b**). By gene ontology analysis, fetal brain genes that were upregulated by ABX and PR mapped to pathways related to central nervous system development, neuron migration, synapse organization, and cellular response to amino acid starvation, whereas downregulated genes mapped to pathways including cerebral cortex and hippocampal development, as well as

neuron migration (**Fig. 3.4c**). The minor overlap between the ABX and PR sets of differentially expressed genes suggests that the maternal microbiome has widespread influence on fetal brain gene expression that *modifies* responses to maternal protein restriction, but is unlikely to *mediate* adverse effects of maternal protein restriction.

In addition to modifying the fetal brain transcriptome, depleting the maternal microbiome in protein undernourished dams altered fetal brain metabolomic profiles. E18.5 brains from fetuses of antibiotic-treated PR dams exhibited significant alterations in 70 metabolites relative to SPF PR controls (**Fig. 3.4d**). Of these, 40 metabolites overlapped with those altered by maternal PR relative to CD controls, reflecting 18.2% of metabolites altered by PR relative to CD (**Fig. 3.4d**). Metabolites altered by ABX were primarily amino acids (47.1%) and lipids (28.6%) (**Fig. 3.4e**), with significantly reduced metabolites mapping to 8 pathways, including phenylacetate metabolism (**Fig. 3.4f**). Maternal ABX-induced reductions in fetal brain metabolites related to glutamate metabolism, and glycine and serine metabolism (**Fig. 3.4f**), were similarly seen with maternal PR relative to CD (**Fig. 3.2e**), suggesting an exacerbating effect of maternal microbiome deficiency on these PR-induced alterations in the fetal brain. This finding is in line with work suggesting a role for the gut microbiome in supplying the host with essential amino acids[65]. Metabolites that were significantly elevated by depletion of the maternal microbiome mapped to 7 pathways, including taurine and hypotaurine metabolism and homocysteine degradation (**Fig. 3.4f**). Taken together, these results suggest that the diversity of the maternal microbiome alters the fetal brain in ways that modify effects of maternal protein undernutrition on offspring neurodevelopment.

Microbiome-based interventions during pregnancy differentially modify adverse effects of maternal protein restriction on offspring growth or behavior

Alterations in the maternal microbiome during pregnancy are increasingly associated with impaired fetal and postnatal development of the offspring[27,30,31,66], raising the question of whether

manipulating the maternal microbiome during pregnancy can change offspring health trajectories. We found that maternal protein restriction alters maternal health status, including reductions in diversity of the maternal microbiota, which interacts with fetal development to yield abnormal behavior in adult offspring. Following the observation that ABX microbial depletion modifies PR-indued fetal brain signatures, we aimed to assess causal effects of the maternal microbiome during pregnancy on offspring developmental responses to maternal protein restriction. To this end, we investigated growth and behavior of offspring reared from ABX-treated and PR-fed dams, fed CD at birth, and cross-fostered to untreated SPF dams fed PR during pregnancy (**Fig. 3.5a**). This experimental design isolates the effect of maternal microbial depletion and PR to the pregnancy period, and evaluates their influences on offspring developmental programming. There was no significant effect of maternal microbial depletion on PR-induced reductions in fetal size, maternal gestational weight loss, or maternal diet consumption (**Fig. 3.S4a-c**). However, there was a partial attenuation of PR-induced elevation of maternal serum corticosterone levels at E18.5 (**Fig. 3.S4d**). This corresponded with a trending decrease in litter size (**Fig. 3.S4e**), despite overall increases in rates of litter survival at weaning (**Fig. 3.S4f**). Offspring of microbiota-depleted dams fed PR during pregnancy exhibited gradual sub-significant reductions in postnatal weight over the first two weeks of life (**Fig. 3.S4g**), with statistically significant decreases in weight by adulthood despite being fed CD since birth (**Fig. 3.S4h**). Maternal microbiome depletion and protein restriction during pregnancy yielded adult offspring with anxiety-like behavior that was not statistically different from that seen in control offspring from SPF and PR-fed dams (**Fig. 3.S5a and 3.S6a**). However, adult offspring of ABX PR dams exhibited exacerbated learning deficits, with increased latency to target zone during the acquisition phase of the Barnes maze assay relative to cognitively impaired control offspring of SPF dams fed PR (**Fig. 3.5b**). In other parameters of the Barnes maze test, offspring of microbiome-depleted and PR-fed dams exhibited deficiencies in performance that were not statistically significantly different from those seen in control offspring from PR-fed SPF dams (**Fig. 3.S5b-d**). When analyzing data for male and female

offspring separately, male offspring were especially affected by maternal microbiome depletion, with more pronounced exacerbation of cognitive behavior, which did not reach statistical significance (**Fig. 3.S6b-e**). These results indicate that further reducing the diversity of the maternal microbiome, as shaped by protein restriction during pregnancy, yields offspring developmental programs that lead to deficient postnatal weight gain and exacerbated cognitive impairment during adulthood. These findings further suggest that interventions to improve the diversity and function of the maternal microbiome may aid in preventing the adverse effects of maternal protein undernutrition on offspring growth and behavior.

Short chain fatty acids (SCFAs) produced by bacterial fermentation of complex carbohydrates promote normal gastrointestinal and immune function[67,68], and their supplementation is reported to counter adverse effects of high fat or low fiber diets on behavioral development[55,56]. To explore potential microbiome-based interventions for preventing adverse effects of maternal protein undernutrition on offspring growth and behavior, we first tested supplementation with SCFAs, which we previously utilized to prevent placental insufficiencies induced by maternal protein restriction[64]. PR-fed dams were supplemented with a cocktail of SCFAs (acetate, butyrate, and propionate), or a sodium-matched vehicle control, in water throughout gestation[64] (**Fig. 3.S7a**). There were no significant effects of maternal SCFA supplementation during pregnancy on maternal PR-induced reductions in fetal and maternal weight and elevations in maternal serum corticosterone, despite significant effects of SCFA supplementation on increasing maternal dietary intake (**Fig. 3.S7b-e**). Maternal SCFA supplementation had no statistically significant effects on litter size at birth, but modestly increased rates of litter survival postnatally, and promoted a gradual increase in pup weight over the first two weeks of life, which was reversed in adulthood (**Fig. 3.S7f-i**). Consistent with our previous observations (**Fig. 3.1**), adult offspring of vehicle-treated and gestational PR-fed dams exhibited anxiety-like behavior in the open field and cognitive impairment in the Barnes maze despite rearing since birth on CD (**Fig. 3.S8a-e**). There were no statistically significant effects of

maternal SCFA supplementation on the behavioral abnormalities induced by maternal PR during pregnancy (**Fig. 3.S8a-e, 3.S9a-e**). These results indicate that while maternal SCFA supplementation during pregnancy may effectively prevent adverse effects of maternal protein restriction on placental development[64] and promote early postnatal growth (**Fig. 3.S7h**), it fails to avert diet-induced neurodevelopmental programming of behavioral abnormalities in adult offspring. This aligns with human studies, wherein children subject to early life protein undernutrition remain at risk for mood and neurocognitive disorders despite subsequent nutritional rehabilitation and adequate postnatal growth[13–16].

The maternal microbiome regulates numerous metabolites in the maternal blood, fetal blood, and fetal brain, a subset of which aid in guiding normal fetal neurodevelopment[23,27,64]. We further explored the possibility that microbial metabolites aside from SCFAs could be used to attenuate adverse effects of maternal protein undernutrition on offspring development. To do so, we identified 10 microbially-modulated metabolites (10M: 3-indoxul sulfate, phenylacetylglycine, imidazole propionate, alpha-hydroxyisocaproate, 2-hydroxy-3-methylvalerate, alpha-hydroxyisovalerate, 1-methylhistamine, beta-hydroxyisovalerate, 2R, 3R-dihydroxybutyrate, and N-acetylleucine) that were reduced in the fetal brain by maternal PR, similarly reduced by maternal PR in maternal serum, and additionally altered by maternal ABX treatment, indicating dependence on the maternal microbiome (**Fig. 3.5c**). Pregnant dams were fed PR and treated with 10M, or vehicle control, throughout gestation via a daily subcutaneous injection (**Fig. 3.5d**). There were no statistically significant effects of maternal 10M supplementation on PR-induced reductions in fetal weight, maternal weight, and maternal food consumption (**Fig. 3.S10a-c**). However, maternal 10M supplementation significantly attenuated PR-induced increases in maternal serum corticosterone and drastically increased offspring survival (**Fig. 3.S10d, f**), with no effect on litter size at birth, pup weight, or adult weight (**Fig. 3.S10e, g-h**). Adult offspring of vehicle-treated dams fed PR exhibited anxiety-like behavior in the open field and cognitive behavioral impairment in the Barnes maze (**Fig. 3.S11a-e**), which reproduced effects of maternal

protein undernutrition that were seen in initial PR experiments (**Fig. 3.1**) and in vehicle control groups for SCFA treatment (**Fig. 3.S8**). Adult offspring of 10M-supplemented and PR-fed dams displayed sexually dimorphic behavioral responses relative to control offspring of vehicle-treated and PR-fed dams (**Fig. 3.5e-h, Fig. 3.S12a-b**). In particular, female offspring of 10M-supplemented dams exhibited increased time and distance in the center during open field test without any motor effects (**Fig. 3.5e-f, Fig. 3.S11a**)), suggesting reduced anxiety-like behavior which aligns with the female-bias in anxiety-like behavior seen in response to maternal PR (**Fig. 3.S2b**). In contrast, male offspring of 10M-supplemented dams exhibited increased time in target zone and decreased errors during the probe phase of Barnes maze (**Fig. 3.5g-h**), suggesting better 24-hour recall without an effect on learning during the acquisition phase (**Fig. 3.S11b-e, 3.S12a-b**). These results indicate that maternal 10M supplementation during pregnancy partially attenuates adverse effects of maternal protein undernutrition on abnormal cognitive and anxiety-related behavior in adult offspring in a sex-specific manner. These sex- and domain-specific improvements are seen in the absence of normalized fetal or postnatal growth, again providing evidence that amelioration of neurobehavioral trajectories can occur independently of restoration of physical growth.

Discussion

Findings from this study identify the maternal microbiome as a modifier of adverse neurological outcomes in offspring of protein undernourished dams. Maternal protein restriction reduces diversity of the maternal microbiome and elicits widespread alterations in maternal-fetal metabolomic profiles and fetal brain gene expression, including subsets of maternal microbiome-dependent metabolites and genes. Further depleting the maternal microbiome of protein-restricted dams substantially alters transcriptomic and metabolomic profiles in fetal brains, where only a small fraction of metabolites and genes differentially regulated by maternal microbiome depletion overlap with those altered by protein restriction alone. Furthermore, depleting the

maternal microbiome exacerbates cognitive, but not anxiety-like, behavioral impairments observed in adult offspring of protein-restricted dams. These results suggest that wholesale depletion of the maternal microbiome elicits select brain and behavioral changes in offspring of protein-restricted dams through mechanisms that are largely independent of those caused by maternal protein restriction alone. As such, reductions in microbial diversity likely modify, but do not directly mediate, adverse effects of maternal protein restriction on offspring neurodevelopment. These findings may have translational implications, as human preterm infants with FGR display early postnatal decreases in microbial diversity which correlate with reduced infant cognitive scores compared to non-FGR counterparts.

We find that supplementing protein-restricted dams with a cocktail of ten diet- and microbiome-dependent metabolites during pregnancy prevents anxiety-like behavior and cognitive impairment in their adult offspring. The metabolites were selected based on their significant decreases in both fetal brain and maternal serum of protein-restricted dams compared to standard protein-fed controls, and their further modulation by depletion of the maternal microbiome. It is unclear precisely how 10M is acting to protect offspring from behavioral impairments induced by maternal protein undernutrition. However, many of these metabolites have been previously shown to support neurological and behavioral functioning, in addition to being linked to the gut microbiome. Five of the ten metabolites (alpha-hydroxyisocaproate, 2-hydroxy-3-methylvalerate, alpha-hydroxyisovalerate, beta-hydroxyisovalerate, and N-acetylleucine) are dietary catabolites of the branched chain amino acids (BCAAs) leucine, isoleucine, and valine. The gut microbiota is capable of both producing and breaking down BCAAs[69]. BCAAs are also implicated in neural development and function following insult: alpha-hydroxyisocaproate, 2-hydroxy-3-methylvalerate, alpha-hydroxyisovalerate, and N-acetylleucine were increased in fetal brain following exposure to intrauterine inflammation[70], and N-acetylleucine reduced cortical inflammation and apoptosis and increased memory in novel object recognition task after traumatic brain injury[71]. In addition to these five BCAA-related metabolites,

3-indoxyl sulfate, imidazole propionate, and phenylacetylglycine are well established metabolites of the gut microbiome produced by sulfonation of bacterially-derived indole, direct bacterial synthesis from histidine, and bacterial conversion of phenylalanine, respectively[72–74]. They have also been implicated in neurodevelopment: imidazole propionate promoted thalamocortical axonogenesis in fetal brains from offspring of antibiotic-depleted dams[27], and all three have been reported to vary across postnatal development in mouse forebrain[75]. The final 10M metabolites, 1-methylhistamine and 2R,3R-dihydroxybutyrate (commonly referred to as 4-deoxyerythronic acid), have only correlational ties to the gut microbiome and brain development. The former, a major metabolite of histamine, has been correlated with microbes, primarily of the order *Clostridiales* and genus *Lactobacillus*[76], while the latter, a metabolite of L-threonine[77], was downregulated in the plasma of MDD patients after escitalopram treatment[78]. Specific microbial metabolites are increasingly linked to neurodevelopment and behavior. In addition to the examples discussed above, individual microbially-modulated metabolites have recently been reported to induce anxiety-like behaviors by preventing oligodendrocyte maturation and altering myelination[79], and promote cognitive decline by precipitating microglial apoptosis[80]. However, more research is needed to identify neuromodulatory microbial metabolites, and further understand the diverse mechanisms by which they engage in direct or indirect communication with the brain during critical temporal windows to guide neurodevelopment and influence behavioral outcomes.

Although the exact mechanisms by which PR induces behavioral deficits, and by which 10M ameliorates them are unclear, transcriptomic and metabolomic profiling of fetal brains of PR-fed dams revealed some possibilities. For one, tryptophan and tryptophan-related metabolic pathways were significantly downregulated in maternal serum, but significantly upregulated in fetal brain in response to gestational PR. Additionally, the *Slc6a4* gene encoding the serotonin transporter and the *Htr3a* gene encoding a serotonin receptor are significantly decreased in PR fetal brains. Finally, a tryptophan catabolite, 3-indoxyl sulfate, was among the 10M group that

normalized behavior in offspring. These findings suggest abnormal tryptophan and serotonin signaling pathways as candidate contributors to subsequent behavioral deficits in offspring. Indeed, tryptophan and serotonin were altered by protein restriction during gestation and lactation in rats[81], serotonin regulates many neurodevelopmental processes, and altered levels during gestation have been linked to behavioral impairments, including anxiety and cognitive, in offspring[82]. In addition, disruptions to the hypothalamic-pituitary-adrenal axis could be at play, as we observe elevated corticosterone in maternal serum and in fetal brains of protein-restricted dams, the former of which is attenuated by 10M supplementation. Stress during critical periods can be neurotoxic, is known to interact with both maternal microbiome and fetal neurodevelopment[25,59], and to precipitate anxiety- and cognitive-related behavioral deficits in offspring[83]. Finally, neuroimmune processes may be disrupted, as we observed downregulated T-cell differentiation in PR fetal brains by transcriptomic pathway analysis. Indeed, T-cell differentiation promoted by maternal gut bacteria has been reported to underlie behavioral deficits in offspring following maternal immune activation[24,84]. Although we interpret these changes to be due to low levels of protein in the PR diet, high-sucrose diets during gestation have also been shown to alter offspring brain and behavior[85,86]. While the PR diet has comparably lower sucrose levels than used in high-sucrose models (15% kcal coming from increased sucrose and cellulose in PR compared to CD, versus 25% kcal from sucrose alone in a high-sucrose model[85]), and we see minimal carbohydrate metabolites affected in PR maternal serum and fetal brains, sucrose is significantly higher in PR fetal brain compared to CD**.** We are therefore unable to rule out an effect of high sucrose on the reported results.

This study showed sexual dimorphism in behavioral responses to both PR alone, where female offspring showed a more severe anxiety-like phenotype, and to 10M intervention, where female offspring showed restoration of anxiety-like behavior, and male offspring showed restoration of memory deficits. These findings highlight the importance of examining both males and females, and including sex as a biological variable[87]. Sex biases have been well-documented

in various neurodevelopmental conditions, including a male skew in autism spectrum disorder and attention deficit hyperactivity disorder[88] and a female skew in anxiety and mood disorders[89]. Furthermore, findings from this study support the ability of sex to influence susceptibility to, or presentation of, prenatal programming from environmental stressors or maternal microbial shifts[59]. The biological basis for this interaction with sex is unclear, but theories have been raised to explain sexually dimorphic responses to prenatal perturbations, including slower maturation and increased intrauterine immunoreactive responses to male fetuses, differences in placental function by sex, and contributions of sex steroids and *SRY* programming[90,91]. These different presentations of behavioral domain by sex also raise the question of different biological underpinnings of anxiety-like versus cognitive behaviors. Projections from the basolateral amygdala to the central amygdala[92] and ventral hippocampus[93] underlie anxiety-related behaviors, while spatial learning and memory rely on hippocampal CA3-medial prefrontal cortex circuits[94]. Based on the sexually dimorphic and domain-specific behavioral responses of offspring treated with 10M during gestation, it may be the case that these interventions are acting in a sex- and circuit-specific manner to ameliorate select phenotypes of gestational protein restriction. There is more work to be done in understanding the role of microbes and microbial metabolites in supporting or disrupting neurodevelopment, and how biological sex interacts with and facilitates this process.

Although maternal supplementation with 10 diet- and microbiome-dependent metabolites prevented impairments in particular anxiety-like and cognitive behavioral parameters in adult offspring, not all behavioral deficits induced by maternal protein restriction were prevented, suggesting that they are mediated by additional, as yet undefined, microbiome-dependent or -independent mechanisms. Results from our cross-fostering experiments indicate that maternal protein restriction alters offspring behavior through mechanisms that require diet-induced programming of both fetal neurodevelopment and maternal physiology, as only offspring born to and fostered by dams on PR during gestation show behavioral deficits. One way in which maternal

programming could translate is via maternal care behaviors, which are well-known to inform offspring neurodevelopment and behavior[50,51]. Although we do not see significant differences in maternal retrieval behavior, which is altered in other gestational stress models[95], there may be changes in other domains of stress-sensitive maternal care that warrant further investigation, such as licking/grooming and nursing behaviors[95,96]. Additionally, milk volume or nutrient content may be persistently altered by gestational PR, and may therefore create inconsistencies in postnatal nutrition between cross-fostering groups to inform long-term behavioral trajectories. Indeed, protein content of milk and size of offspring was reduced in dams fed a low protein diet during gestation and lactation[97], and sialylated milk oligosaccharides, found to be decreased in mothers of undernourished infants, were sufficient to promote growth in humanized mouse and pig models of early postnatal malnutrition[98]. The impact of malnutrition and other peri-gestational stressors on both maternal and infant health underscores the importance of further research on women's health and investigation of lasting implications of the postpartum period.

Nutritional support, and even growth and gross physiological restoration, are often inadequate to prevent long-term microbial, neurological, and behavioral impairments caused by early malnutrition[5–7,12–16]. Indeed, results from this study show consistent decoupling of early growth trajectories with later behavioral impairments. Restricting protein undernutrition to the pregnancy period in mice induces anxiety-like and impaired cognitive behavior in adult offspring that are fed standard nutritive diet since birth and exhibit typical growth trajectories by body weight. Depletion of the maternal microbiome exacerbates, whereas maternal supplementation with select microbes or microbially modulated metabolites prevents, select behavioral deficits in adult offspring without influencing pre- and postnatal growth. In contrast, maternal supplementation with short-chain fatty acids promotes feto-placental[64] and offspring growth, but does not effectively prevent neurobehavioral deficits in adult offspring of dams that were protein restricted during pregnancy. As malnutrition continues to be a prevalent and severe global health burden[23], additional interventions beyond nutritional rehabilitation alone are needed to target

adverse effects of malnutrition on child neurobehavioral development. Findings from this study reveal that the maternal microbiome modifies adverse neurobehavioral outcomes of gestational protein undernutrition, which are partially prevented by maternal supplementation with select microbial metabolites. These results suggest that microbiome-based interventions should be further evaluated for their ability to reduce malnutrition-associated neurobehavioral disorders, which are not adequately addressed with current nutrition-focused standards of care.

Methods

Mice

8-week old male and female C57Bl/6J mice were purchased from Jackson Laboratories and maintained on 12-h light-dark cycle in temperature- and humidity-controlled environment. All mice were kept under sterile conditions (autoclaved cages, bedding, water bottles, and water). All experiments were performed in accordance with the NIH Guide for the Care and Use of Laboratory Animals using protocols approved by the Institutional Animal Care and Use Committee at UCLA.

Protein restriction

Mice were first subjected to a microbiota normalization, where two scoops of bedding were removed from each cage, mixed together, and deposited back in each cage to normalize microbiota between all mice in each testing cohort. At least 5 days after normalization, male and female mice were given either 6% protein diet (Teklad Envigo; TD.90016) or 20% control diet (Teklad Envigo; TD.91352) *ad libitum* for at least 2 weeks. Following this habituation period, mice were paired and time-mated. At E0.5, determined by observation of copulation plug, pregnant dams were individually housed and continued to be fed the same diet through gestation. Weights and fecal samples were collected from each dam at E0.5 and 18.5, with a subset collected at E0.5, 7.5, 10.5, 14.5, 18.5.

Antibiotic treatment

For “ABX” treatment groups, SPF male and female mice were gavaged twice daily for one week with neomycin (100 mg/kg), metronidazole (100 mg/kg) and vancomycin (50 mg/kg), as previously described[27,64]. During this time, ampicillin (1 mg/mL) was provided *ad libitum* in drinking water. Mice were then time-mated as described above. Following gavage, mice were maintained on ampicillin (1 mg/mL), neomycin (1 mg/mL) and vancomycin (0.5 mg/mL) *ad libitum* in drinking water for the duration of the experiment.

Fetal tissue collections

At E18.5, dams were sacrificed by cervical dislocation. Fecal samples were extracted from the colon. Blood was collected by cardiac puncture into vacutainer SST tubes (Becton Dickinson) and allowed to clot for 1 hour at room temperature, before centrifuging at 1500xg, 4°C for 10 minutes. Serum supernatant was collected and stored at -20°C. The entire uterine horn, including all conceptuses, was removed and placed in ice cold 1x PBS. Dams were weighed once again to record post-transection weight. Each fetus was dissected from the amniotic sac and weighed. Brains were microdissected and either placed into RNAlater (Invitrogen) for subsequent RNA sequencing, or snap-frozen in liquid nitrogen for subsequent metabolomics analysis. All samples were stored at -80°C.

Behavioral testing

For behavioral cohorts, dams were given shepherd shacks on E17.5 to reduce stress ahead of birth. At P0, dams and diet were weighed, pups were counted, and all diet groups were switched to CD. Complete litters were cross-fostered, as denoted in figures (**Fig. 3.1a, Fig. 3.5a,d, Fig. 3.S7a**). Subsequently, litters were checked daily for pup survival. Litters were denoted as not

survived if <4 pups remained at weaning (as previously done[64]). Pups were weighed on P3, 5, 7, 9, 11, 13, and toe-tattooed P4-P6, for identification purposes. Pups were weaned at P24-P26, and separated into cages with same-sex littermates. Adult behaviors were run beginning when mice were ~90 days old. All mice were habituated in the testing room 30 minutes prior to test start. Tests were run in order of least to most stressful, in the order described below, with at least 3 days separating each test. All equipment was cleaned with 70% ethanol and allowed to dry in between trials.

Righting reflex & maternal retrieval – SPF cohorts only

The righting reflex and maternal retrieval tests were utilized to examine early neurological development[99] and maternal care-giving and responsiveness[53], respectively. Pups were subjected to righting reflex and maternal retrieval tests on P3, 5, 9, 11. All pups from each litter were placed one-by-one on their backs and the time it took for them to right themselves (with all four paws on the ground) was recorded, capped at 30 seconds. Pups were then placed back into their home cage all at once, in the opposite corner of the nest. The latency to first pup retrieval and full litter retrieval by the dam was measured, capped at 5 minutes.

Ultrasonic vocalizations – SPF cohorts only

Ultrasonic vocalizations in pups were analyzed as a response to separation from the litter [100]. Pups were tested for USVs at P7 and P13. Four pups were randomly chosen (when possible, 2 males and 2 females) for USV testing, and the same pups were used at both timepoints. Pups were habituated in the recording chambers for 5 minutes, and then recorded for 5 minutes. Number and duration of calls, in addition to inter-call latency, were analyzed. Recording and analysis were performed using SASLab Pro (Avisoft Bioacoustics).

Open field test – all cohorts

Open field test was employed to assess locomotion and thigmotaxis as a proxy for anxiety-like behavior[35,36]. Mice were placed into open field arenas (27.5 cm^2) for 10 minutes under bright light. Videos were recorded using an overhead camera, and the first 5 minutes of each test were analyzed using AnyMaze 7.1 for time spent in center zone, distance traveled in center zone/total distance traveled, total distance traveled, and mean speed.

Barnes maze – all cohorts

Barnes maze was employed to assess spatial learning and memory[38]. The Barnes maze apparatus has an elevated round surface (90 cm diameter) with 20 holes evenly spaced around the perimeter. One hole was denoted as the "escape" hole, and an escape box was attached below the hole. The position of the escape hole was kept consistent within mice, but counterbalanced between mice. Spatial cues (black and white geometric shapes printed on 9x11in paper) were placed around the maze, and kept consistent throughout training and testing. On day 1 of the testing protocol, each mouse was allowed to freely explore the Barnes maze apparatus for 5 minutes with no white noise under mild light, with no escape box present. Immediately following, each mouse was placed under a wire cup in the center of the apparatus, with white noise and bright light for 1 minute. Finally, each mouse was gently guided to the escape hole and into the escape box, and white noise and bright light were removed, for 1 minute. On days 2-5, each mouse was subject to three training trials, with an inter-trial latency of 20-45 minutes. The training trials consisted of 15s habituation, where mice were placed under a wire cup in the center of the apparatus with bright light and white noise. The cup was then lifted, and mice were given 180s to escape into the escape hole, thereby ending the test. If the mouse did not escape by 180s, they were gently guided into the escape hole. At the end of each trial, mice were left for 1 minute in the escape hole, with no white noise. On day 6, a probe test was run to assess long-term memory. Each mouse was subject to one probe trial, consisting of a 15s habituation, and then a 180s test without the escape box. Videos were recorded using an

overhead camera and analyzed in AnyMaze 7.1. For the training trials, latency to find the escape hole and latency to enter the escape box were analyzed. For the probe trial, time spent in the escape hole vicinity, and errors, defined as non-escape hole vicinities a mouse entered *before* entering the escape hole vicinity, were analyzed.

Human Infants

This prospective cohort study was conducted at the University of California Los Angeles (UCLA) neonatal intensive care units (UCLA Ronald Reagan Hospital/UCLA Mattel Children's Hospital, Los Angeles, CA and UCLA Santa Monica Hospital, Santa Monica, CA). The UCLA Institutional Review Board granted approval for this study (IRB #15 00718). Verbal informed consent was obtained from parents/legal guardians. Inclusion criteria included infants with a birth weight <2 kilograms (kg), <14 days of age, who were predicted to require parenteral nutrition for ≥2 weeks, and follow-up at the UCLA High Risk Infant Clinic (HRIF). The exclusion criteria included infants who were unlikely to survive and infants with congenital anomalies and congenital infections. Infants missing prenatal medical records with which to diagnose FGR were also excluded.

Demographic and clinical data was collected from the electronic medical chart. FGR was determined as previously described[101] by the obstetric team who documented fetal growth deceleration on repeated prenatal ultrasounds. Full feeds were defined as 100 mL/kg/d of enteral nutrition or *ad libitum* feeding, whichever occurred first. Early onset sepsis was defined as a positive blood culture before 72 hours of age and antibiotics for ≥5 days. Late onset sepsis was defined as a positive blood culture after 72 hours of age and antibiotics for ≥5 days. Necrotizing enterocolitis was defined by Bell's stage II or III. Neurodevelopment was assessed using composite cognitive, language, and motor scores from the Bayley Scales of Infant Development (BSID) III[61], which was conducted by doctorally trained clinicians who work in the HRIF. These

clinicians have established inter-rater reliability for the BSIS-III examination, which is monitored for recertification research projects and clinical assessments..

16S rRNA gene sequencing

Fecal samples were collected from CD and PR dams throughout gestation at the following timepoints: E0.5, E7.5, E10.5, E14.5, E18.5 and stored at -80°C until processing. The same dams were collected from at each timepoint. Bacterial genomic DNA was isolated according to manufacturer instructions using the DNeasy PowerSoil Kit (Qiagen). Additionally, fecal samples were collected from preterm infants with and without FGR during their hospital stay. Specimens were collected shortly after study enrollment, then weekly while on parenteral nutrition, and for four weeks after parenteral nutrition was discontinued. Samples were collected from infant diapers using sterile collection kits and stored at -80°C until processing. Because of intestinal dysmotility, preterm infants have delayed passage of meconium and do not stool frequently in the first couple weeks of life, resulting in missing samples disproportionately at early timepoints. Approximately 50mg per sample was aliquoted in liquid nitrogen, bead-beat in buffer RLT using Lysing Matrix E tubes (MP Biomedicals), and extracted using AllPrep DNA/RNA/Protein Mini kit (Qiagen), as previously described[102].

For both mouse and human samples,16S rRNA gene sequencing was performed as previously described[27,64]. Briefly, sequencing libraries were generated according to methods adapted from Caporaso et al. 2011[103], amplifying the V4 regions of the 16S rRNA gene by PCR. The final PCR product was purified using the Qiaquick PCR purification kit (Qiagen). 250 ng of purified, PCR product from each individually barcoded sample were pooled and sequenced by Laragen, Inc. using the Illumina MiSeq platform and 2 x 250bp reagent kit for paired-end sequencing. All analyses were performed using QIIME2 2023.7[104], including DADA2[105] for quality control, taxonomy assignment, alpha-rarefaction and beta-diversity analyses. 29,152 reads were

analyzed per sample. Operational taxonomic units (OTUs) were assigned based on 99% sequence similarity compared to the SILVA 138 database. Beta-diversity principal coordinates analysis plots were generated with QIIME2 View, and other bacterial metrics, including correlation analyses with clinical metadata were performed and plotted in Prism 9.0 (Graphpad).

Corticosterone ELISAs

Total corticosterone levels were determined by a corticosterone ELISA assay (Enzo Life Sciences). The assay was run per manufacturer's instructions, following the small volume protocol. All experimental samples were run in triplicate; blanks and controls were run in duplicate. Mean optical density was read on a Synergy H1 plate reader (Agilent BioTek), and corticosterone concentrations were determined in ug/mL based on a standard curve.

Fetal brain RNA sequencing

Whole fetal brains were randomly chosen from each litter, dissected, and immediately placed into 400uL RNA*later* (ThermoFisher Scientific) and stored at -80°C. RNA was extracted and cDNA synthesized using the PureLink RNA Mini Kit (Invitrogen) and qScript cDNA synthesis kit (Quantabio), respectively. Equal amounts of RNA were pooled from 2 brains per litter, resulting in 1522ng RNA per sample, except for one which had 508ng. An RNA integrity number (RIN) of at least 8.7 was confirmed for each sample using the 4200 Tapestation system (Agilent). RNA was prepared as previously described[64] using the TruSeq RNA Library Prep kit and Lexogen QuantSeq 3' forward-sequencing was performed using the Illumina HiSeq 4000 platform by the UCLA Neuroscience Genomics Core. Sequences were quality filtered, trimmed, and mapped using FastQC v0.11.5, bbduk v35.92, and RSeQC v2.6.4. Reads were aligned to UCSC Genome Browser assembly ID: mm10 using STAR v2.5.2a, indexed using samtools v1.3, and aligned using HTSeq-count v0.6.0. Differential expression analysis was conducted using DESeq2 v1.24.041. Heatmaps were generated using the pheatmap v1.0.12 package for R. DAVID

2021[106,107] was used to conduct GO term enrichment analysis of differentially expressed genes with non-adjusted p-value < 0.05.

Metabolomics

Whole fetal brains were randomly chosen from each litter, dissected, and immediately snap-frozen in liquid nitrogen and stored at -80°C. 1.5-2 brains were pooled for subsequent analysis. Untargeted metabolomics was run on fetal brain and maternal serum by Metabolon Inc. as previously described[27,64]. Briefly, samples were prepared using the automated MicroLab STAR system (Hamilton Company) and analyzed on GC/MS, LC/MS and LC/MS/MS platforms. Organic aqueous solvents were used to perform serial extractions for protein fractions, concentrated using a TurboVap system (Zymark) and vacuum dried. For LC/MS and LC-MS/MS, samples were reconstituted in acidic or basic LC-compatible solvents containing > 11 injection 25 standards and run on a Waters ACQUITY UPLC and Thermo-Finnigan LTQ mass spectrometer, with a linear ion-trap frontend and a Fourier transform ion cyclotron resonance mass spectrometer back-end. For GC/MS, samples were derivatized under dried nitrogen using bistrimethyl-silyl-trifluoroacetamide and analyzed on a Thermo-Finnigan Trace DSQ fast-scanning single-quadrupole mass spectrometer using electron impact ionization. Chemical entities were identified 30 by comparison to metabolomic library entries of purified standards. Following log transformation and imputation with minimum observed values for each compound, data were analyzed using two-way ANOVA to test for group effects. P- and q-values were calculated based on two-way ANOVA contrasts. Principal components analysis was used to visualize variance distribution with the ggplot2 R package[108]. The Metaboanalyst 5.0[109] platform's metabolite set enrichment analysis (MSEA) was performed on whole fetal brain and maternal serum metabolites that were statistically significantly altered (non-adjusted p-value < 0.05) between SPF PR and SPF CD treatment groups and ABX PR and SPF PR treatment groups. Metabolites sets were

analyzed for metabolite pathway enrichment using the Small Molecule Pathway Database (SMPDB).

In vivo short-chain fatty acid supplementation

All mice were habituated on PR diet, and bred as described above. Once copulation plugs were observed, SCFA were supplemented *ad libitum* in drinking water from E0.5-E18.5 (prenatal cohort) or E19.5 (behavior cohort), as previously described[64]. SCFA water cocktail contained 25mM sodium propionate, 40mM sodium butyrate, and 67.5mM sodium acetate. SCFA water was changed at least every 4 days. Sodium-matched controls were given water supplemented with 7.745g/L sodium chloride. All supplemented water was sterile-filtered before administration. SCFA and Na-matched litters were then used for E18.5 tissue collections, or for postnatal cross-fostering and behavioral testing, as described above.

In vivo metabolite supplementation

Metabolite selection for in vivo supplementation

Metabolites were first filtered for significant differences between SPF CD and SPF PR. Those that were decreased in SPF PR compared to SPF CD were further checked for microbiome modulation, as denoted by significant change in any direction in ABX PR relative to SPF PR, or in ABX CD relative to SPF CD. This set of filters was applied to metabolomic results from both fetal brain and maternal serum. Metabolites that met these criteria from *both* tissue compartments were used for supplementation.

Metabolite supplementation

All mice were habituated on PR diet, and bred as described above. Once copulation plugs were observed, sterile filtered metabolite mixture (10M) was injected subcutaneously once per day from E0.5-E17.5. Control dams were injected with vehicle. Physiological concentrations were

determined as previously described[27] based on literature[72,110–118], estimated blood volume, and on the relative differences in metabolite fold change between CD and PR dams. The 10M injections contained 0.76ug imidazole propionate, 7.3ug alpha-hydroxyisocaproate, 7.24ug alpha-hydroxyisovalerate, 0.0094uL beta-hydroxyisovalerate, 11.68ug N-acetylleucine, 2.16ug 2-hydroxy-3-methylvalerate, 6.3ug phenylacetylglycine, 29.16ug 3-indoxyl sulfate, 0.04ug 1-methylhistamine, and 6.66ug 2R,3R-dihydroxybutyrate in 200uL 1X sterile PBS. Vehicle injections contained 8.66ug potassium chloride, 0.012nL hydrochloric acid, and 1.7ug sodium hydroxide in 200uL 1X sterile PBS. 10M and vehicle litters were then used for E18.5 tissue collections, or for postnatal cross-fostering and behavioral testing, as described above.

Statistical Methods and Sample Sizes

Statistical analyses were performed using Prism 9.0 (Graphpad). Assays with two groups were assessed for normality and subsequently analyzed by either an unpaired two-tailed t-test with Welch's correction, or by a Mann-Whitney test. Tests on three or more groups were assessed by a one-way ANOVA, and when there were two factors, with a two-way ANOVA. Data over time were assessed with a repeated measures ANOVA or mixed measures analysis. Tukey or Sidak post-hoc tests were used, based on Prism recommendations. All prenatal weight measures and postnatal behavioral measures were run using litter as a biological replicate, with all fetuses or offspring averaged within each litter. For prenatal weights and maternal metrics, at least 9 litters per group were analyzed. For behavioral experiments, 4-7 litters per group were tested. To assess sex differences in the behavioral results, and in adult weights, individual male and female offspring were treated as biological replicates. For metabolomics, 1.5-2 fetal brains were randomly chosen and pooled per litter, from 6 litters per group. For RNAseq, 2 fetal brains were randomly chosen and pooled per litter, from 5 litters per group. Whole litters were excluded from all analyses if they had fewer than 4 fetuses or pups (as done previously[64]). For prenatal measures, no viable fetuses within any litters were excluded from reported analyses. For behavioral measures, individual

offspring were occasionally excluded from all tests due to health reasons (i.e. developing malocclusion) or from a specific test or trial due to a test-related event (i.e. escaping the testing chamber). These occasions were rare, and not associated with a particular group or condition. All data are plotted as mean +/- SEM. Significant differences are denoted as follows: *$p < 0.05$, **$p < 0.01$, ***$p < 0.001$, ****$p < 0.0001$, n.s. not significant.

Data Availability

Transcriptomic data have been deposited to the Sequence Read Archive (SRA) repository with accession number PRJNA1074327. Untargeted metabolomic data have been deposited to Mendeley Data (DOI: 10.17632/2pdwjm85tb.1. 16S rRNA gene sequencing data have been deposited to the SRA repository with accession number PRJNA1074327. Other data available upon reasonable request.

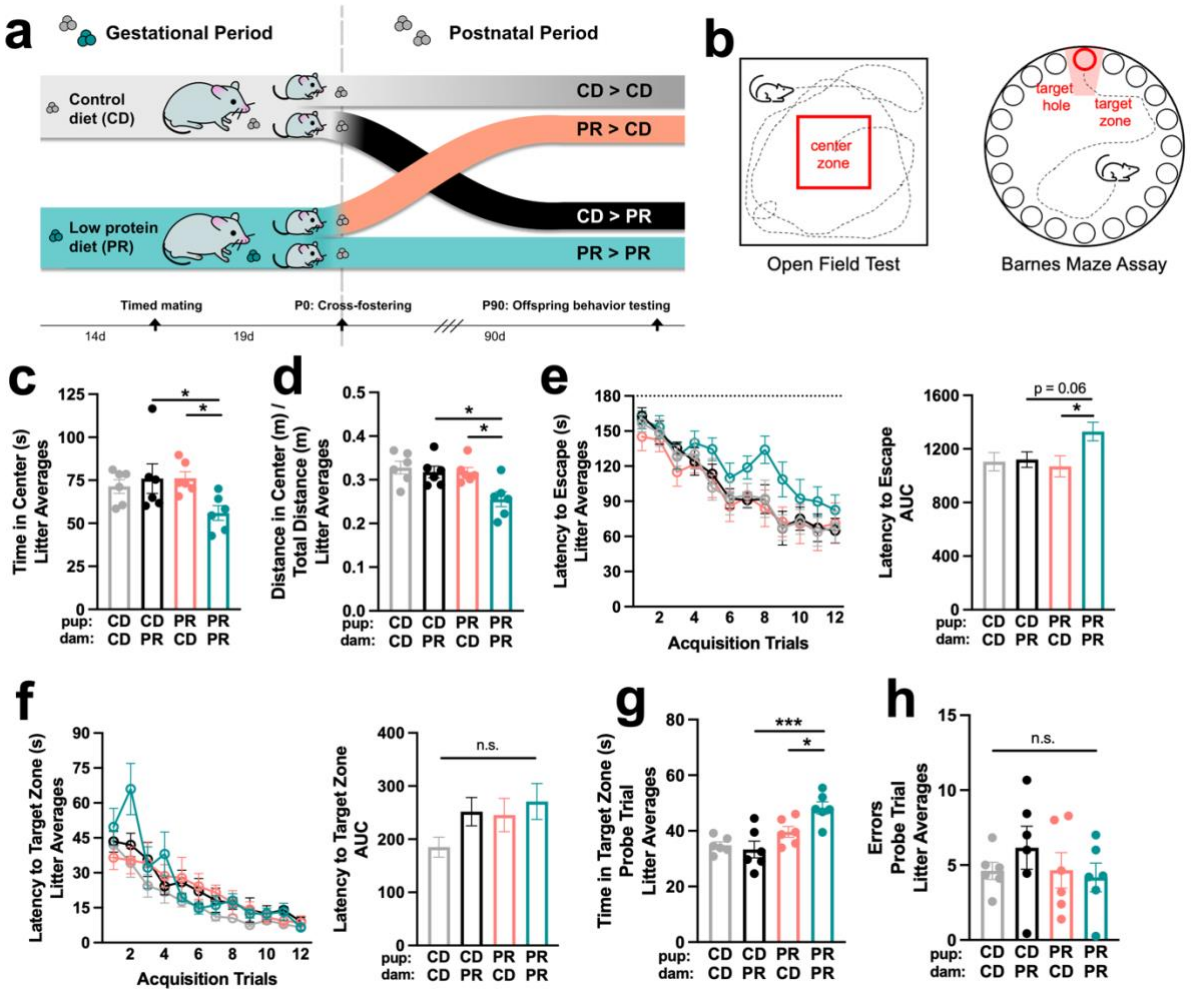

Figure 3.1: The prenatal period of maternal protein restriction is critical for programming cognitive and anxiety-like behavioral deficits in adult offspring. a, Graphic of cross-fostering paradigm. **b,** Graphic of behavioral tests, open field test (left), Barnes maze (right). **c,** Time in center in open field test, all offspring averaged within each litter (two-way ANOVA with Sidak, n = 6 litters per group). Top row refers to pup condition, bottom row refers to dam condition. **d,** Distance in center in open field test, controlled by total distance traveled, all offspring averaged within each litter (two-way ANOVA with Sidak, n = 6 litters per group). Top row refers to pup condition, bottom row refers to dam condition. **e,** Left: Latency to escape in Barnes maze acquisition phase, all offspring averaged within each litter (n = 6 litters per group). Right: AUC of latency to escape (two-way ANOVA with Sidak). Top row refers to pup condition, bottom row refers to dam condition. **f,** Left: Latency to target zone in Barnes maze acquisition phase, all offspring averaged within each litter (n = 6 litters per group). Right: AUC of latency to target zone (two-way ANOVA with Sidak). Top row refers to pup condition, bottom row refers to dam condition. **g,** Time in target zone in Barnes maze probe trial, all offspring averaged within each litter (two-way ANOVA with Sidak, n = 6 litters per group). **h,** Errors made in Barnes maze probe trial, all offspring averaged within each litter (two-way ANOVA with Sidak, n = 6 litters per group). Mean +/- SEM, *p < 0.05, **p < 0.01, ***p < 0.001, ****p < 0.0001, n.s. not significant.

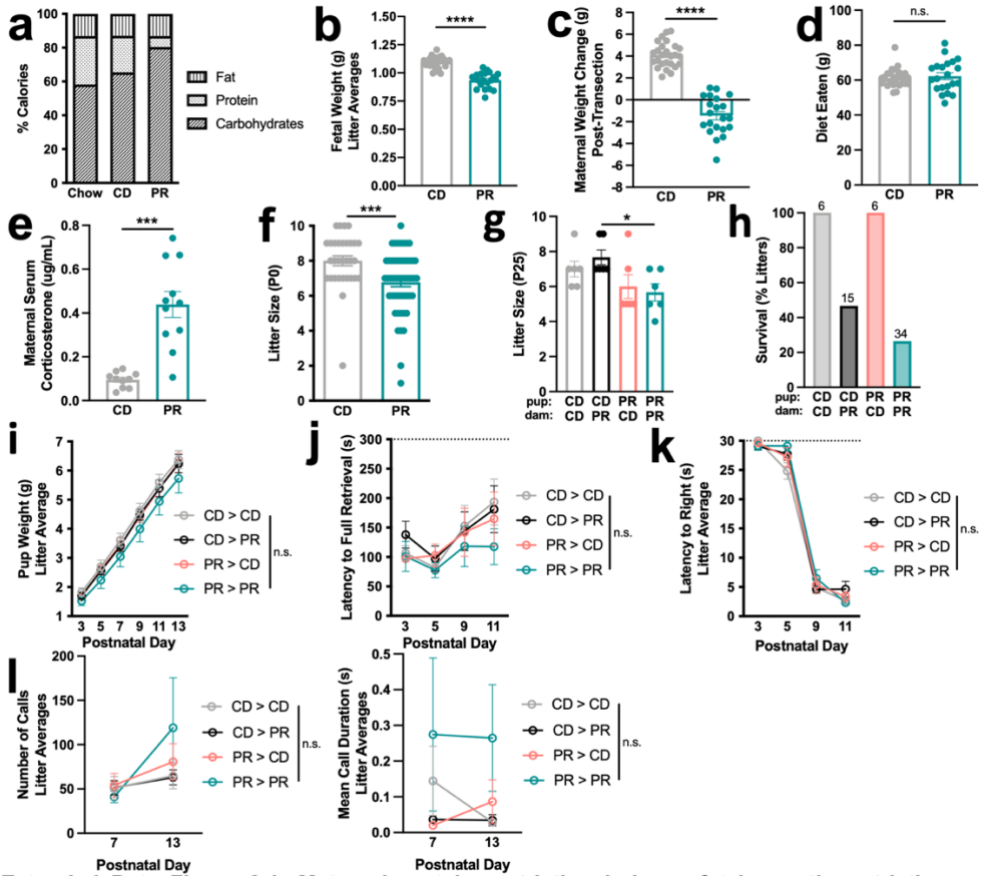

Figure 3.S1: Maternal protein restriction induces fetal growth restriction and maternal stress, and reduces postnatal survival, but does not influence early postnatal growth or maternal behavior. a, Macronutrient breakdown of CD and PR diets compared to standard lab chow. **b,** Fetal weight at E18.5 from SPF CD and SPF PR dams, all fetuses averaged within each litter (unpaired Welch's t-test, n = 28, 21, from left to right). **c,** Maternal weight change, from E0.5 to E18.5, in SPF CD and SPF PR dams (unpaired Welch's t-test, n = 26, 21, from left to right). **d,** Maternal diet eaten, from E0.5 to E18.5 in SPF CD and SPF PR dams (Mann Whitney test, n = 26, 21, from left to right). **e,** Corticosterone measured in serum in SPF CD, SPF PR dams at E18.5 (unpaired Welch's t-test, n = 10, 11, from left to right). **f,** Litter size at P0, from SPF CD and SPF PR dams (Mann Whitney test, n = 31, 50, from left to right). **g,** Litter size, pups per litters, measured at weaning, from cross-fostered groups SPF CD pups > CD dams, SPF CD pups > PR dams, SPF PR pups > CD dams, SPF PR pups > PR dams (two-way ANOVA with Sidak, n = 6 litters per group). Top row refers to pup condition, bottom row refers to dam condition. **h,** Litter survival (percentage of total litters), from SPF CD pups > CD dams, SPF CD pups > PR dams, SPF PR pups > CD dams, SPF PR pups > PR dams (n = 6, 15, 6, 34, from left to right). Top row refers to pup condition, bottom row refers to dam condition. **i,** Pup weights, all offspring averaged within each litter (two-way repeated measures ANOVA with Tukey, n = 6 litters per group). **j,** Latency to retrieve in maternal retrieval test (two-way repeated measures ANOVA with Tukey, n = 6 dams per group). **k,** Latency to right in pup righting reflex test, all offspring averaged within each litter (two-way repeated measures ANOVA with Tukey, n = 6 litters per group). **l,** Left: Number of calls, ultrasonic vocalizations, 4 offspring averaged within each litter (two-way repeated measures ANOVA with Tukey, n = 6 litters per group). Right: Mean duration of calls, ultrasonic vocalizations, 4 offspring averaged within each litter (two-way repeated measures ANOVA with Tukey, n = 6 litters per group). Mean +/- SEM, *p < 0.05, **p < 0.01, ***p < 0.001, ****p < 0.0001, n.s. not significant.

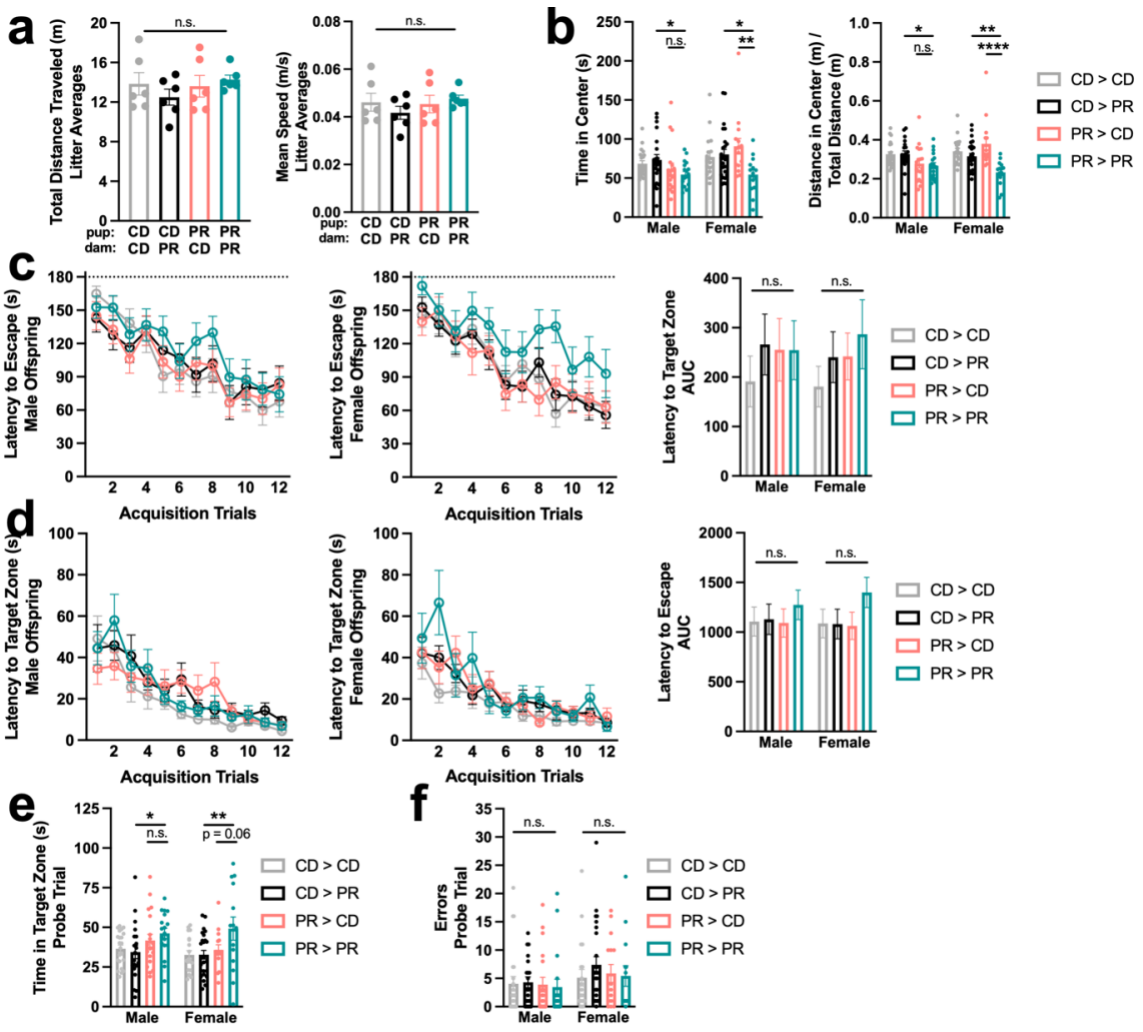

Figure 3.S2: Adult female offspring exhibit behavioral differences based on both gestational and rearing-associated protein restriction, whereas male offspring are based on gestational alone. a, Left: Total distance traveled in open field test, all offspring averaged within each litter (two-way ANOVA with Sidak, n = 6 litters per group). Right: Mean speed in open field test, all offspring averaged within each litter (two-way ANOVA with Sidak, n = 6 litters per group). Top row refers to pup condition, bottom row refers to dam condition. **b,** Left: Time in center in open field test, male and female offspring (two-way ANOVA with Sidak for each sex, n = 22, 20, 18, 18, 19, 25, 15, 14, from left to right). Right: Distance in center in open field test, controlled by total distance traveled, male and female offspring (two-way ANOVA with Sidak for each sex, n = 22, 20, 18, 18, 19, 25, 15, 14, from left to right). **c,** Left: Latency to escape in Barnes maze acquisition phase, male offspring (n = 22, 20, 19, 18). Middle: Latency to escape in Barnes maze acquisition phase, female offspring (n = 19, 25, 15, 14). Right: AUC of latency to escape (two-way ANOVA with Sidak for each sex). **d,** Left: Latency to target zone in Barnes maze acquisition phase, male offspring (n = 22, 20, 19, 18). Middle: Latency to target zone in Barnes maze acquisition phase, female offspring (n = 19, 25, 15, 14). Right: AUC of latency to target zone (two-way ANOVA with Sidak for each sex). **e,** Time in target zone in Barnes maze probe trial, male and female offspring (two-way ANOVA with Sidak for each sex, n = 22, 20, 19, 18, 19, 25, 15, 14, from left to right). **f,** Errors made in Barnes maze probe trial, male and female offspring (two-way ANOVA with Sidak for each sex, n = 22, 20, 19, 18, 19, 25, 15, 14, from left to right). Mean +/- SEM, *p < 0.05, **p < 0.01, ***p < 0.001, ****p < 0.0001, n.s. not significant.

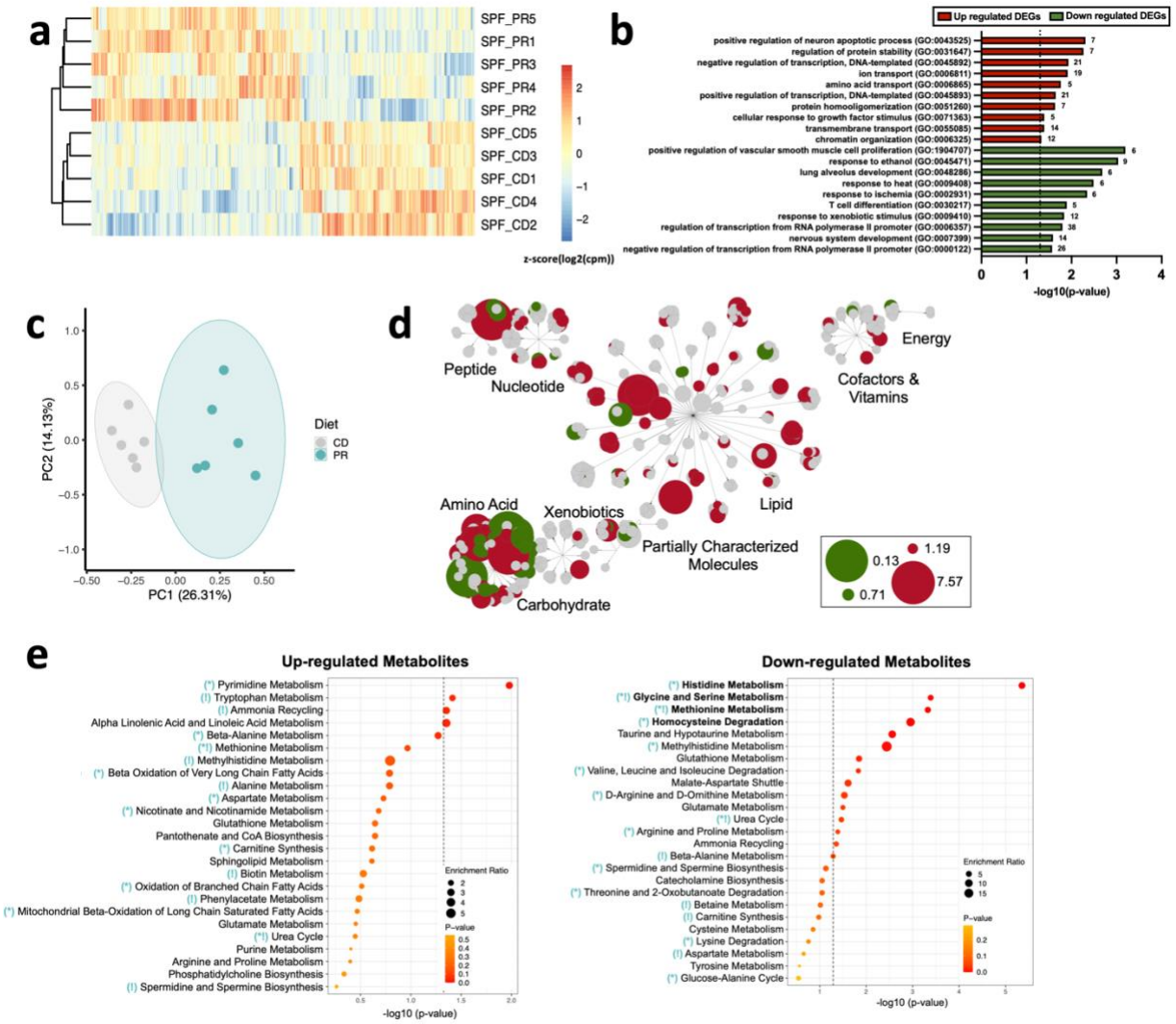

Figure 3.2: Maternal protein restriction alters transcriptional and metabolomic profiles in the fetal brain. a, Heatmap of differentially expressed genes (DEGs) (505 up-regulated, 423 down-regulated; $p < 0.05$) of E18.5 fetal brains from SPF CD or SPF PR dams with Euclidean clustering on rows (n = 5 litters per group, 2 brains pooled per litter). **b,** Biological Process gene ontology (GO) of upregulated DEGs ($p < 0.05$, red) and downregulated DEGs ($p < 0.05$, green) of transcripts from E18.5 fetal brains from SPF CD or SPF PR dams (n = 5 litters per group, 2 brains pooled per litter). **c,** PCA of untargeted metabolomics from E18.5 fetal brains from SPF CD and SPF PR dams (n= 6 litters per group, 1.5-2 brains pooled per litter). **d,** Metabolon network map showing positive and negative fold change. **e,** Top enriched Small Molecule Pathway Database pathways for significantly upregulated metabolites ($p < 0.05$, left) and downregulated metabolites ($p < 0.05$, right) for E18.5 fetal brains from SPF PR dams compared to SPF CD dams (bold pathways have $q < 0.05$; teal symbols relate to analogous enriched pathways in SPF PR vs SPF CD maternal serum [see Fig. 3.S3c]; * = enriched pathway in same direction; ! = enriched pathway in opposite direction).

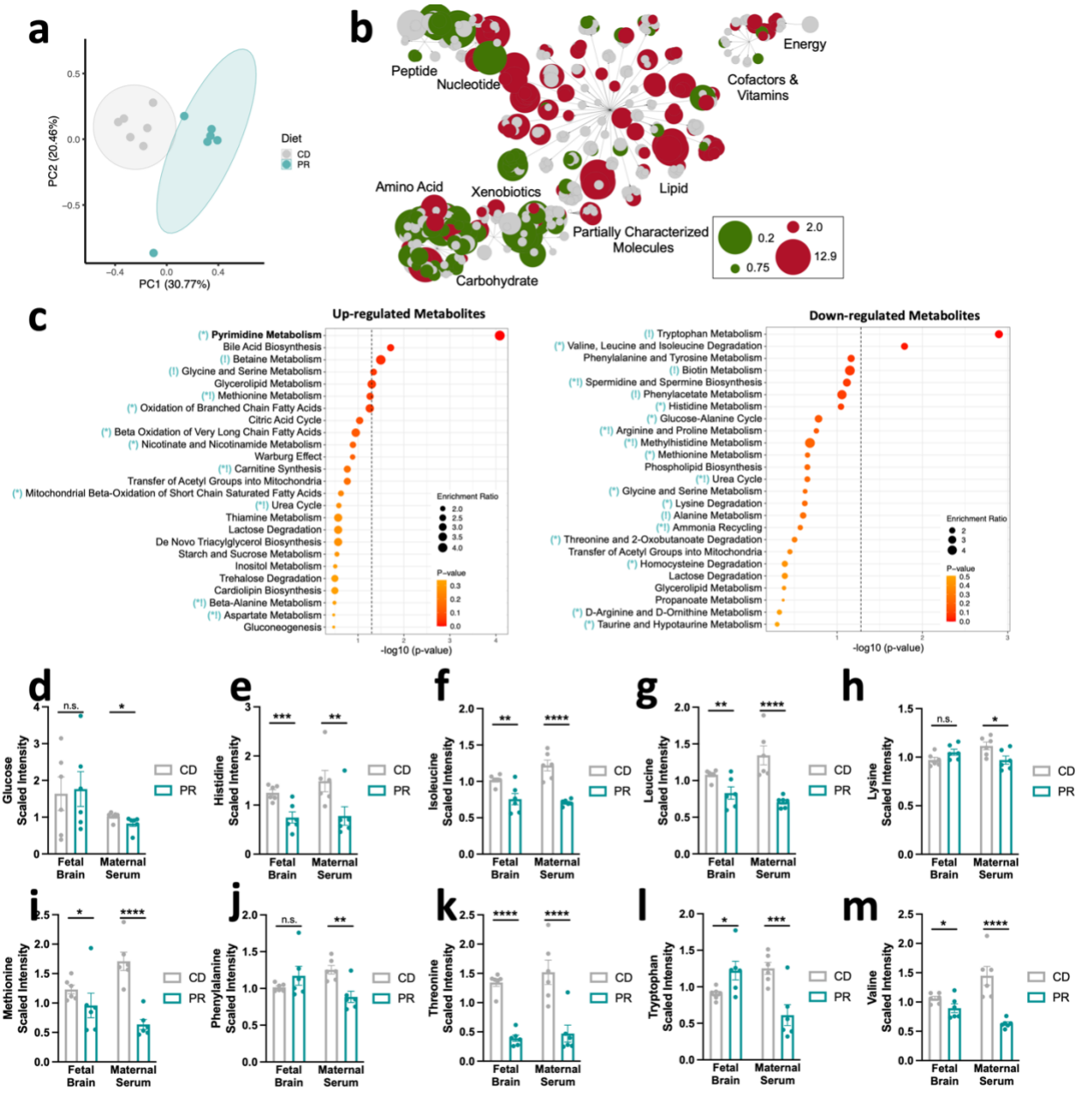

Figure 3.S3: Maternal protein restriction alters metabolomic profiles in maternal serum, and induces nutrient brain sparing in fetal brains at late gestation. **a,** Untargeted metabolomics PCA comparing serum from SPF CD and SPF PR dams (n = 6 dams per group). **b,** Metabolon network map showing positive and negative fold change. **c,** Top enriched Small Molecule Pathway Database pathways for significantly upregulated metabolites ($p < 0.05$, left) and downregulated metabolites ($p < 0.05$, right) for serum from SPF PR dams compared to SPF CD dams (bold pathways have $q < 0.05$; teal symbols relate to analogous enriched pathways in SPF PR vs SPF CD fetal brain [see Figure 2e]; * = enriched pathway in same direction; ! = enriched pathway in opposite direction). **d-m,** Untargeted metabolomics of essential amino acids and glucose from E18.5 fetal brains from SPF CD and SPF PR dams (n= 6 litters per group, 1.5-2 brains pooled per litter) and E18.5 serum from SPF CD and SPF PR dams (n = 6 dams per group). Mean +/- SEM, *$p < 0.05$, **$p < 0.01$, ***$p < 0.001$, ****$p < 0.0001$, n.s. not significant.

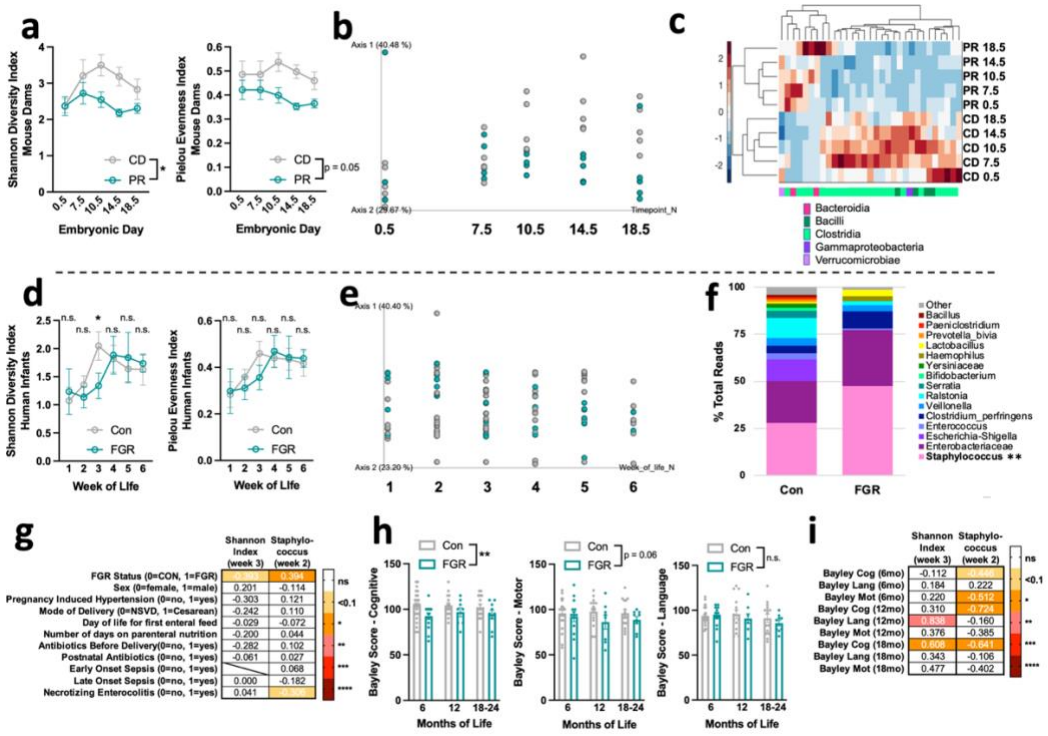

Figure 3.3: Murine maternal protein restriction or human fetal growth restriction reduces diversity of the gut microbiome. a, Left: Shannon diversity index across gestation in SPF CD and SPF PR dams (two-way repeated measures ANOVA with Sidak, n = 5 dams per group). Right: Pielou evenness index across gestation in SPF CD and SPF PR dams (two-way repeated measures ANOVA with Sidak, n = 5 dams per group). **b,** PCA of weighted unifrac across gestation in SPF CD and SPF PR dams (n = 5 dams per group). Axis 3 = time pseudo-axis. **c,** Heatmap of significantly different taxa across gestation in SPF CD and SPF PR dams (Qiime2 Kruskal Wallis test, $q < 0.05$, n = 5 dams per group). **d,** Left: Shannon diversity index in the first 6 weeks of life in Con and FGR infants (unpaired Welch's t-test per timepoint, n = 37 (with 1-4 timepoints each), 16 (with 1-5 timepoints each) infants from top to bottom). Right: Pielou evenness index in the first 6 weeks of life in Con and FGR infants (unpaired Welch's t-test per timepoint, n = 37 (with 1-4 timepoints each), 16 (with 1-5 timepoints each) infants from top to bottom). **e,** PCA of weighted unifrac of Con and FGR infants across the first six weeks of life (n = 34 Con with 1-4 timepoints each, 16 IUGR with 1-5 timepoints each). **f,** Taxa bar plots of taxa >1% total reads in Con or FGR infants in week 2 of life (n = 26, 10, infants from left to right, ** survived correction by Kruskal Wallis test in Qiime2). **g,** Spearman correlation matrix of Shannon diversity index at week 3 and Staphylococcus genus % reads at week 2, against clinical metadata (Con n = 16, 22; FGR n = 9, 10, from left to right). Displayed values are R^2. **h,** Left: Bayley Cognitive assessment scores across the first two years of life in Con and FGR infants (2-way ANOVA Sidak, n = 28 Con with 1-3 visits each, 15 IUGR with 1-3 visits each). Middle: Bayley Motor assessment scores across the first two years of life in Con and FGR infants (2-way ANOVA Sidak, n = 28 Con with 1-3 visits each, 15 IUGR with 1-3 visits each). Right: Bayley Language assessment scores across the first two years of life in Con and FGR infants (2-way ANOVA Sidak, n = 28 Con with 1-3 visits each, 15 IUGR with 1-3 visits each). **i,** Spearman correlation matrix of Shannon diversity index at week 3 and Staphylococcus genus % reads at week 2 against Bayley cognitive, motor, and language composite scores from 6 months (Con n = 10, FGR = 7; Con n = 10, FGR = 8, from left to right), 12 months (Con n = 8, FGR = 3; Con n = 7, FGR = 2, from left to right), and 18-24 months (Con n = 8, FGR = 4; Con n = 7, FGR = 4, from left to right). Displayed values are R^2. Mean +/- SEM, *p < 0.05, **p < 0.01, ***p < 0.001, ****p < 0.0001, n.s. not significant.

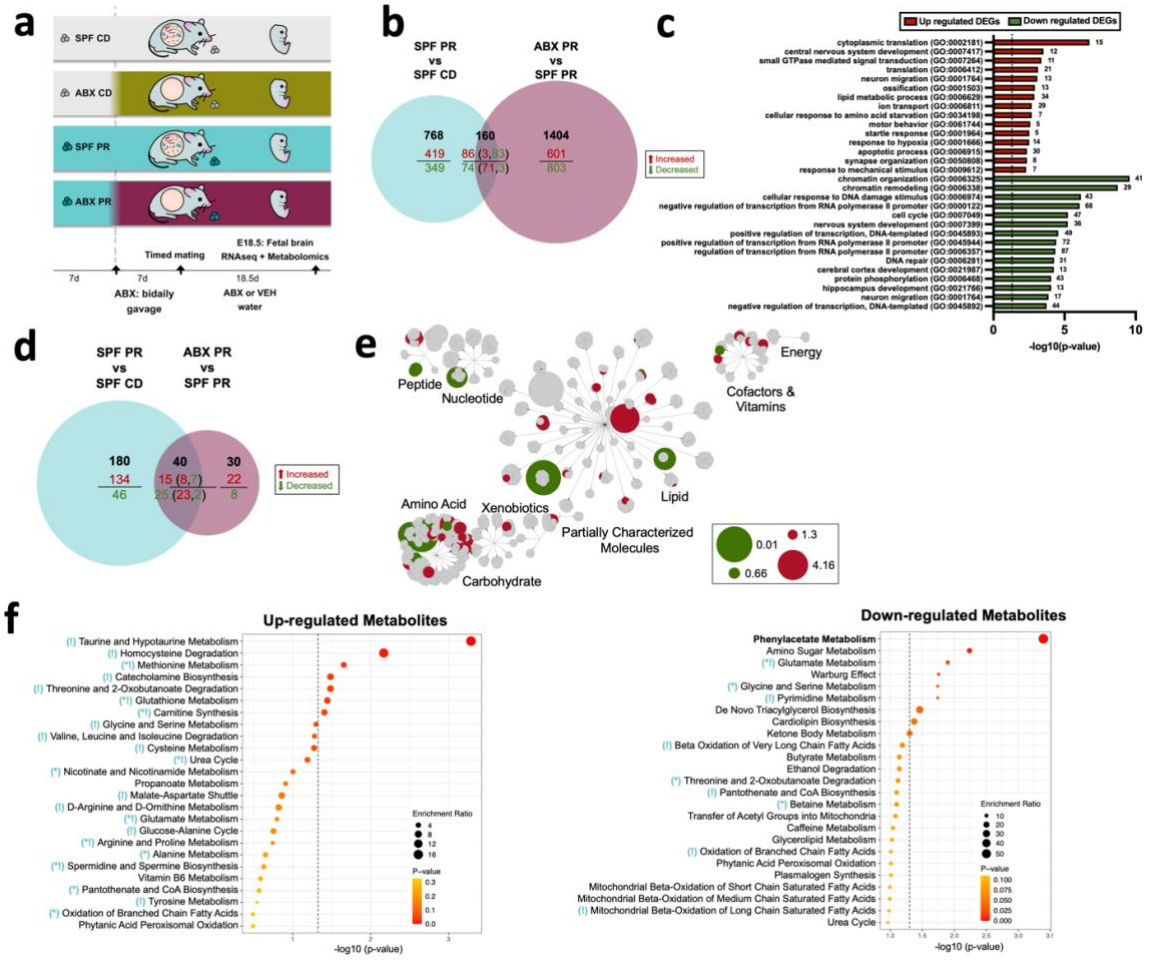

Figure 3.4: Depletion of the maternal gut microbiome induces distinct and additive fetal brain transcriptomic and metabolomic responses to maternal protein restriction. a, Timeline of ABX treatment prior to and throughout gestation. **b,** Venn diagram of DEGs ($p < 0.05$) in the fetal brains from SPF PR compared to SPF CD dams and in the fetal brains from ABX PR compared to SPF PR dams (n = 5 litters per group, 2 brains pooled per litter). Red = up-regulated, green = down-regulated. For the overlapping genes from both comparisons (center of the venn), red = up-regulated and green = down-regulated in SPF PR vs. SPF CD and in parentheses the colored numbers match the directionality of the metabolite in ABX PR vs SPF PR. **c,** Biological Process gene ontology (GO) of upregulated DEGs ($p < 0.05$, red) and downregulated DEGs ($p < 0.05$, green) of fetal brain transcripts from ABX PR dams and SPF PR dams (n = 5 litters per group, 2 brains pooled per litter). **d,** Venn diagram of differential metabolites ($p < 0.05$) in the fetal brains from SPF PR compared to SPF CD dams and in the fetal brains from ABX PR compared to SPF PR dams (n = 5 litters per group, 1.5-2 brains pooled per litter). Red = up-regulated, green = down-regulated. For the overlapping metabolites from both comparisons (center of the venn), red = up-regulated and green = down-regulated in SPF PR vs. SPF CD and in parentheses the colored numbers match the directionality of the metabolite in ABX PR vs SPF PR. **e,** Metabolon network map showing positive and negative fold change. **f,** Top enriched Small Molecule Pathway Database pathways for significantly up-regulated metabolites ($p < 0.05$, left) and down-regulated metabolites ($p < 0.05$, right) from fetal brains of ABX PR dams compared to SPF PR dams (bold pathways have $q < 0.05$; teal symbols relate to analogous enriched pathways in SPF PR vs SPF CD fetal brain [see Figure 2e]; * = enriched pathway in same direction; ! = enriched pathway in opposite direction).

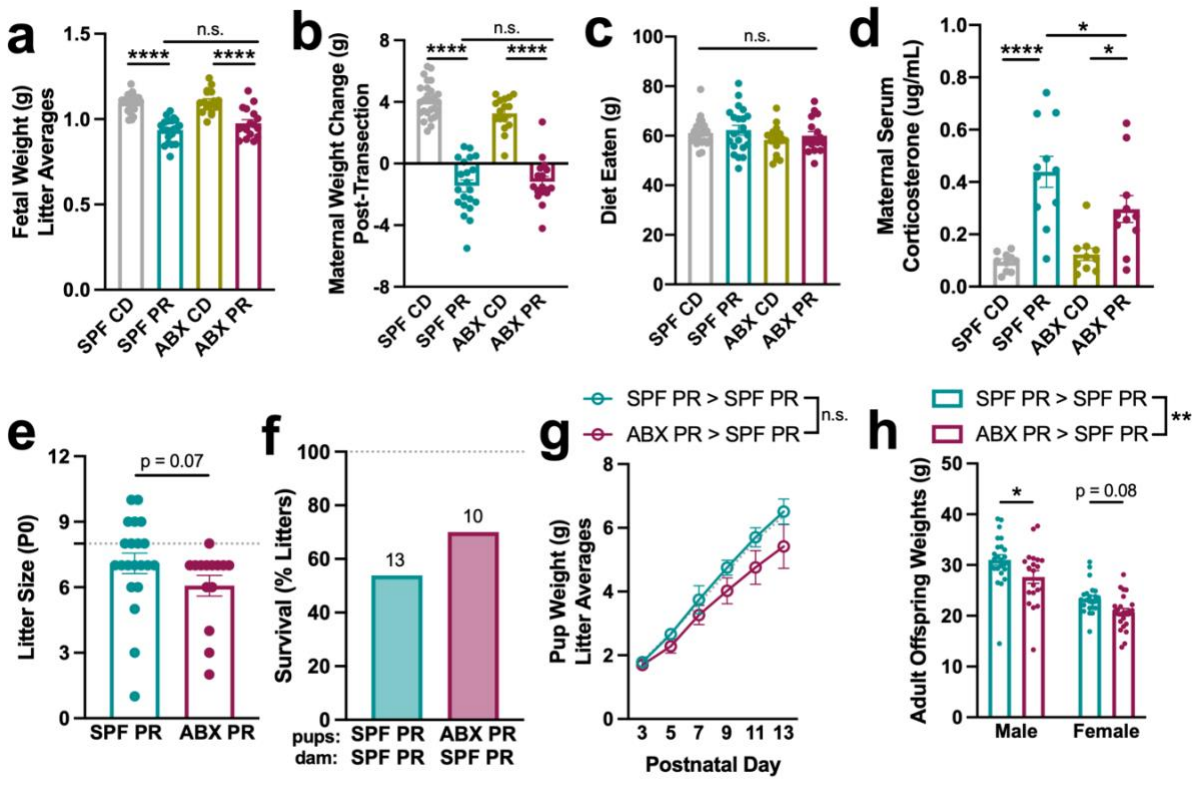

Figure 3.S4: Maternal microbial depletion moderately impacts gross measures of maternal and offspring health. a, Fetal weight at E18.5 from SPF CD, SPF PR, ABX CD, ABX PR dams, all fetuses averaged within each litter (two-way ANOVA with Sidak, n = 28, 21, 16, 17, from left to right). SPF data same as in Fig. 3.S1b. **b,** Maternal weight change, from E0.5 to E18.5 post-transection, in SPF CD, SPF PR, ABX CD, ABX PR dams (two-way ANOVA with Sidak, n = 26, 21, 16, 17, from left to right). SPF data same as in Fig. 3.S1c. **c,** Diet eaten, from E0.5 to E18.5, in SPF CD, SPF PR, ABX CD, ABX PR dams (two-way ANOVA with Sidak, n = 26, 21, 16, 17, from left to right). SPF data same as in Fig. 3.S1d. **d,** Corticosterone measured in serum in SPF CD, SPF PR, ABX CD, ABX PR dams at E18.5 (two-way ANOVA with Sidak, n = 10, 11, 10, 11, from left to right). SPF data same as in Fig. 3.S1e. **e,** Litter size, pups per litters, measured at P0, from SPF PR and ABX PR dams (Mann-Whitney test, n = 21, 14, from left to right). Dotted line indicates average value for SPF CD litters. **f,** Litter survival (percentage of total litters), from SPF PR pups > SPF PR dams and ABX PR pups > SPF PR dams (n = 13, 10, from left to right). Dotted line indicates average value for SPF CD litters. Top row refers to pup condition, bottom row refers to dam condition. **g,** Pup weights, all offspring averaged within each litter (two-way mixed effects analysis with Sidak, n = 7 litters per group). Dotted line indicates average value for SPF CD litters. **h,** Adult weights, male and female offspring (two-way ANOVA with Sidak, n = 24, 20, 23, 23, from left to right). Mean +/- SEM, *p < 0.05, **p < 0.01, ***p < 0.001, ****p < 0.0001, n.s. not significant.

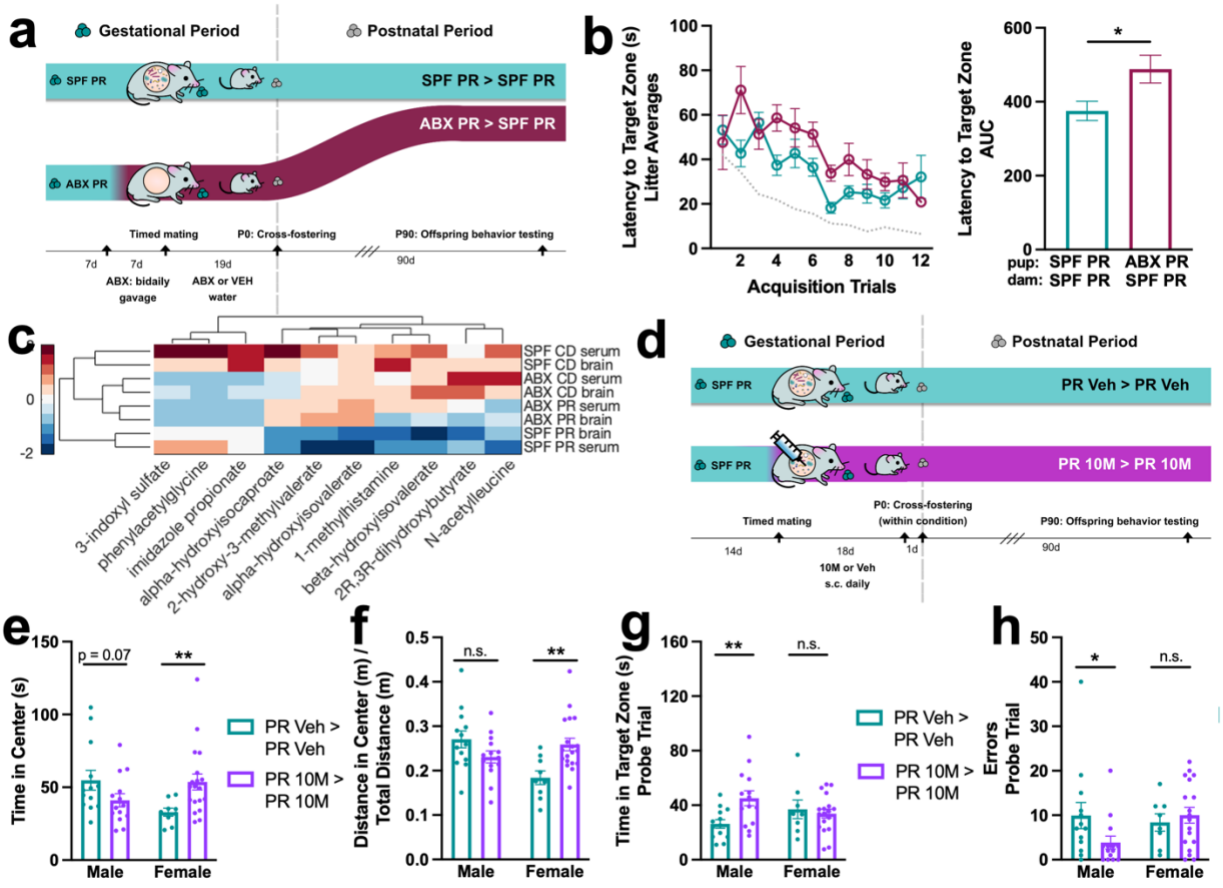

Figure 3.5: Maternal microbiome-informed interventions differentially modify risk for neurobehavioral deficits induced by maternal protein restriction during pregnancy. a, Graphic of cross-fostering paradigm for ABX experiments. **b,** Left: Latency to target zone in Barnes maze, all offspring averaged within each litter (n = 5 litters per group). Dotted line indicates average value for SPF CD litters. Right: AUC of latency to target zone (unpaired Welch's t-test). Top row refers to pup condition, bottom row refers to dam condition. **c,** Heatmap of metabolites chosen for 10M supplementation, hierarchical clustering around 0, SD = 1 (n = 6 litters for each group/tissue type, 2 fetal brains or 1 dam serum pooled per litter). **d,** Graphic of cross-fostering paradigm for 10M experiments. **e,** Time in center in open field test, male and female offspring (Mann Whitney test for each sex, n = 13, 14, 9, 19, from left to right). **f,** Distance in center in open field test, controlled by total distance traveled, male and female offspring (Mann Whitney test for each sex, n = 13, 14, 9, 19, from left to right). **g,** Time in target zone in Barnes maze probe trial, male and female offspring (unpaired Welch's t-test for each sex, n = 13, 14, 8, 18, from left to right). **h,** Errors in Barnes maze probe trial, male and female offspring (Mann-Whitney test for each sex, n = 13, 14, 8, 18, from left to right). Mean +/- SEM, *p < 0.05, **p < 0.01, ***p < 0.001, ****p < 0.0001, n.s. not significant.

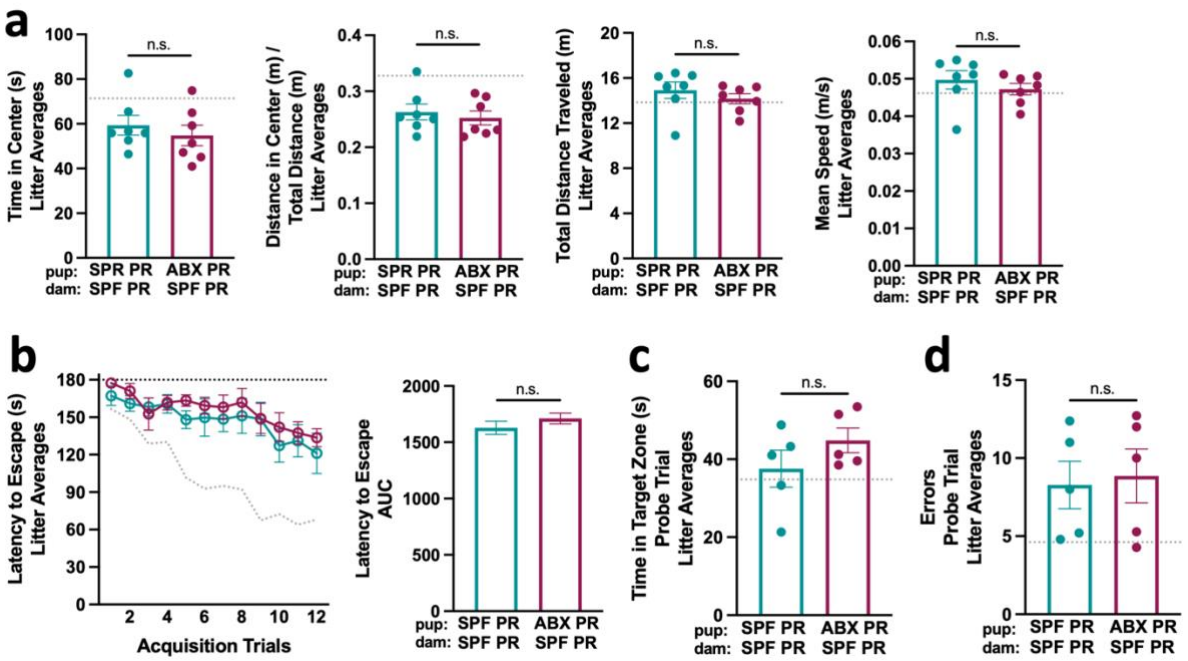

Figure 3.S5: Maternal microbiome depletion does not influence anxiety-like, locomotor, or cognitive behavioral measures in adult offspring exposed to gestational protein restriction. a, Left: Time in center in open field test, all offspring averaged within each litter (Mann Whitney test, n = 7 litters per group). Top row refers to pup condition, bottom row refers to dam condition. Dotted line indicates average value for SPF CD litters. Left-middle: Distance in center in open field test, controlled by total distance traveled, all offspring averaged within each litter (unpaired Welch's t-test, n = 7 litters per group). Top row refers to pup condition, bottom row refers to dam condition. Dotted line indicates average value for SPF CD litters. Right-middle: Total distance traveled in open field test, all offspring averaged within each litter (Mann Whitney test, n = 7 litters per group). Top row refers to pup condition, bottom row refers to dam condition. Dotted line indicates average value for SPF CD litters. Right: Mean speed in open field test, all offspring averaged within each litter (Mann Whitney test, n = 7 litters per group). Top row refers to pup condition, bottom row refers to dam condition. Dotted line indicates average value for SPF CD litters. **b,** Left: Latency to escape in Barnes maze, all offspring averaged within each litter (n = 5 litters per group). Dotted line indicates average value for SPF CD litters. Right: AUC of latency to escape (unpaired Welch's t-test). Top row refers to pup condition, bottom row refers to dam condition. **c,** Time in target zone in Barnes maze probe phase, all offspring averaged within each litter (unpaired Welch's t-test, n = 5 litters per group). Dotted line indicates average values for SPF CD litters. **d,** Errors made in Barnes maze probe phase, all offspring averaged within each litter (unpaired Welch's t-test, n = 5 litters per group). Dotted line indicates average values for SPF CD litters. Mean +/- SEM, *p < 0.05, **p < 0.01, ***p < 0.001, ****p < 0.0001, n.s. not significant.

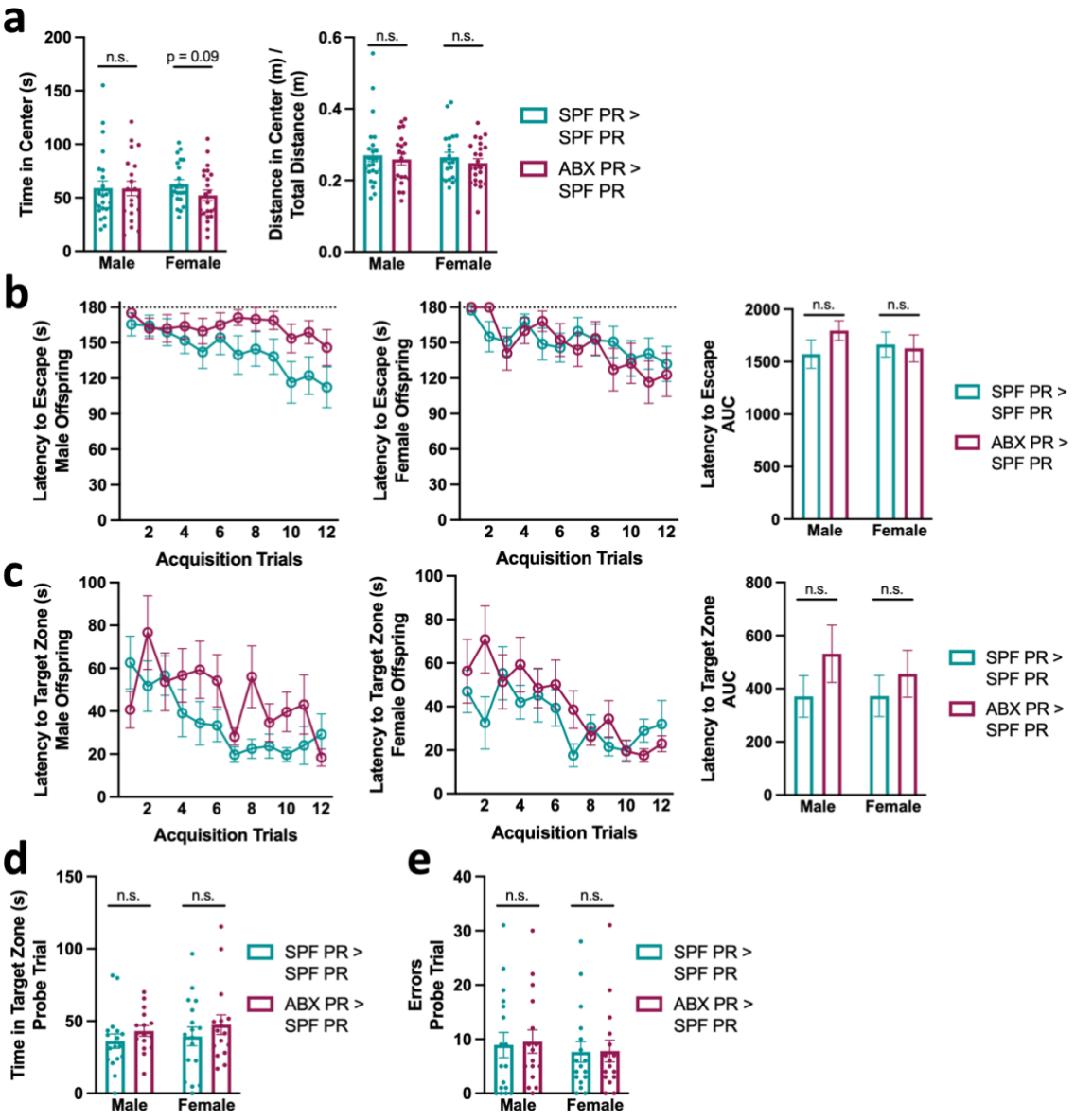

Figure 3.S6: Adult offspring do not exhibit sexually dimorphic behavioral responses to gestational protein restriction and maternal microbiome depletion. a, Left: Time in center in open field test, male and female offspring (Mann Whitney test for each sex, n = 24, 20, 23, 23, from left to right). Right: Distance in center in open field test, controlled by total distance traveled, male and female offspring (Mann Whitney test for each sex, n = 24, 20, 23, 23, from left to right). **b,** Left: Latency to escape in Barnes maze acquisition phase, male offspring (n = 17, 16). Middle: Latency to escape in Barnes maze acquisition phase, female offspring (n = 17, 16). Right: AUC of latency to escape (unpaired Welch's t-test for each sex). **c,** Left: Latency to target zone in Barnes maze acquisition phase, male offspring (n = 17, 16). Middle: Latency to target zone in Barnes maze acquisition phase, female offspring (n = 17, 16). Right: AUC of latency to target zone (unpaired Welch's t-test for each sex). **d,** Time in target zone in Barnes maze probe trial, male and female offspring (Mann-Whitney test for each sex, n = 17, 17, 16, 16, from left to right). **e,** Errors made in Barnes maze probe trial, male and female offspring (Mann-Whitney test for each sex, n = 17, 17, 16, 16, from left to right). Mean +/- SEM, *p < 0.05, **p < 0.01, ***p < 0.001, ****p < 0.0001, n.s. not significant.

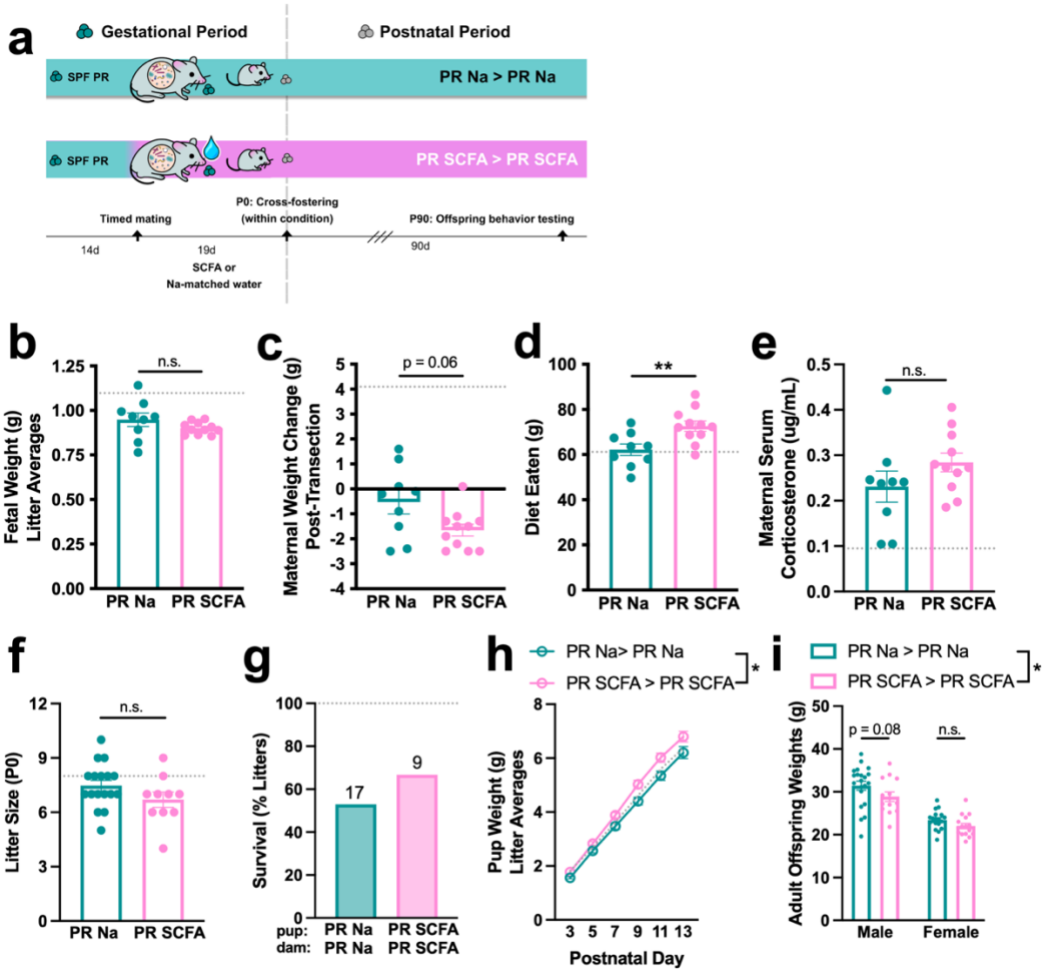

Figure 3.S7: Maternal microbial SCFA supplementation has limited impact on gross measures of maternal and offspring health. a, Graphic of gestational supplementation and cross-fostering paradigm for SCFA experiments. **b,** Fetal weight at E18.5 from SPF PR + Na and SPF PR + SCFA dams, all fetuses averaged within each litter (unpaired Welch's t-test, n = 9, 11, from left to right). Dotted line indicates average value for SPF CD fetuses. **c,** Maternal weight change, from E0.5 to E18.5 post-transection, in SPF PR + Na and SPF PR + SCFA dams (unpaired Welch's t-test, n = 9, 11, from left to right). Dotted line indicates average value for SPF CD dams. **d,** Diet eaten, from E0.5 to E18.5 in SPF PR + Na and SPF PR + SCFA dams (unpaired Welch's t-test, n = 9, 11, from left to right). Dotted line indicates average value for SPF CD dams. **e,** Corticosterone measured in serum in SPF PR + Na and SPF PR + SCFA dams at E18.5 (unpaired Welch's t-test, n = 9, 11, from left to right). Dotted line indicates average value for SPF CD dams. **f,** Litter size, pups per litters, measured at P0, from SPF PR + Na and SPF PR + SCFA dams (unpaired Welch's t-test, n = 17, 10, from left to right). Dotted line indicates average value for SPF CD litters. **g,** Litter survival (percentage of total litters), from SPF PR + Na pups > SPF PR + Na dams and SPF PR + SCFA pups > SPF PR + SCFA dams (n = 17, 9, from left to right). Dotted line indicates average value for SPF CD litters. Top row refers to pup condition, bottom row refers to dam condition. **h,** Pup weights, all offspring averaged within each litter (two-way repeated measures ANOVA with Sidak, n = 9, 6 litters per group, from top to bottom). Dotted line indicates average value for SPF CD litters. **i,** Adult weights, male and female offspring (two-way ANOVA with Sidak, n = 21, 14, 18, 16, from left to right). Mean +/- SEM, *p < 0.05, **p < 0.01, ***p < 0.001, ****p < 0.0001, n.s. not significant.

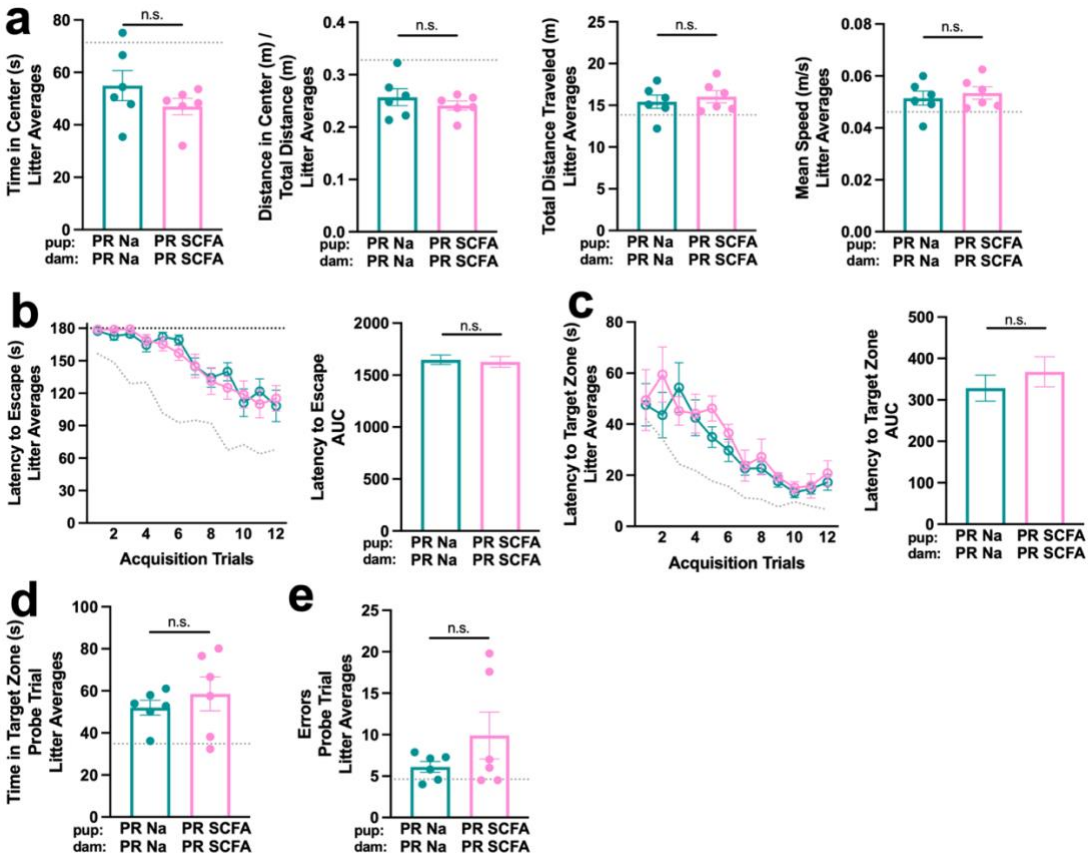

Figure 3.S8: Maternal microbial SCFA supplementation does not influence anxiety-like, locomotor, or cognitive behavioral measures in adult offspring exposed to gestational protein restriction. a, Left: Time in center in open field test, all offspring averaged within each litter (Mann Whitney test, n = 6 litters per group). Top row refers to pup condition, bottom row refers to dam condition. Dotted line indicates average value for SPF CD litters. Left-middle: Distance in center in open field test, controlled by total distance traveled, all offspring averaged within each litter (unpaired Welch's t-test, n = 6 litters per group). Top row refers to pup condition, bottom row refers to dam condition. Dotted line indicates average value for SPF CD litters. Right-middle: Total distance traveled in open field test, all offspring averaged within each litter (unpaired Welch's t-test, n = 6 litters per group). Top row refers to pup condition, bottom row refers to dam condition. Dotted line indicates average value for SPF CD litters. Right: Mean speed in open field test, all offspring averaged within each litter (unpaired Welch's t-test, n = 6 litters per group). Top row refers to pup condition, bottom row refers to dam condition. Dotted line indicates average value for SPF CD litters. **b,** Left: Latency to escape in Barnes maze, all offspring averaged within each litter (n = 6 litters per group). Dotted line indicates average value for SPF CD litters. Right: AUC of latency to escape (unpaired Welch's t-test). Top row refers to pup condition, bottom row refers to dam condition. **c,** Left: Latency to target zone in Barnes maze, all offspring averaged within each litter (n = 6 litters per group). Dotted line indicates average value for SPF CD litters. Right: AUC of latency to target zone (unpaired Welch's t-test). Top row refers to pup condition, bottom row refers to dam condition. **d,** Time in target zone in Barnes maze probe trial, all offspring averaged within each litter (unpaired Welch's t-test, n = 6 litters per group). Dotted line indicates average values for SPF CD litters. **e,** Errors made in Barnes maze probe trial, all offspring averaged within each litter (unpaired Welch's t-test, n = 6 litters per group). Dotted line indicates average values for SPF CD litters. Mean +/- SEM, *p < 0.05, **p < 0.01, ***p < 0.001, ****p < 0.0001, n.s. not significant.

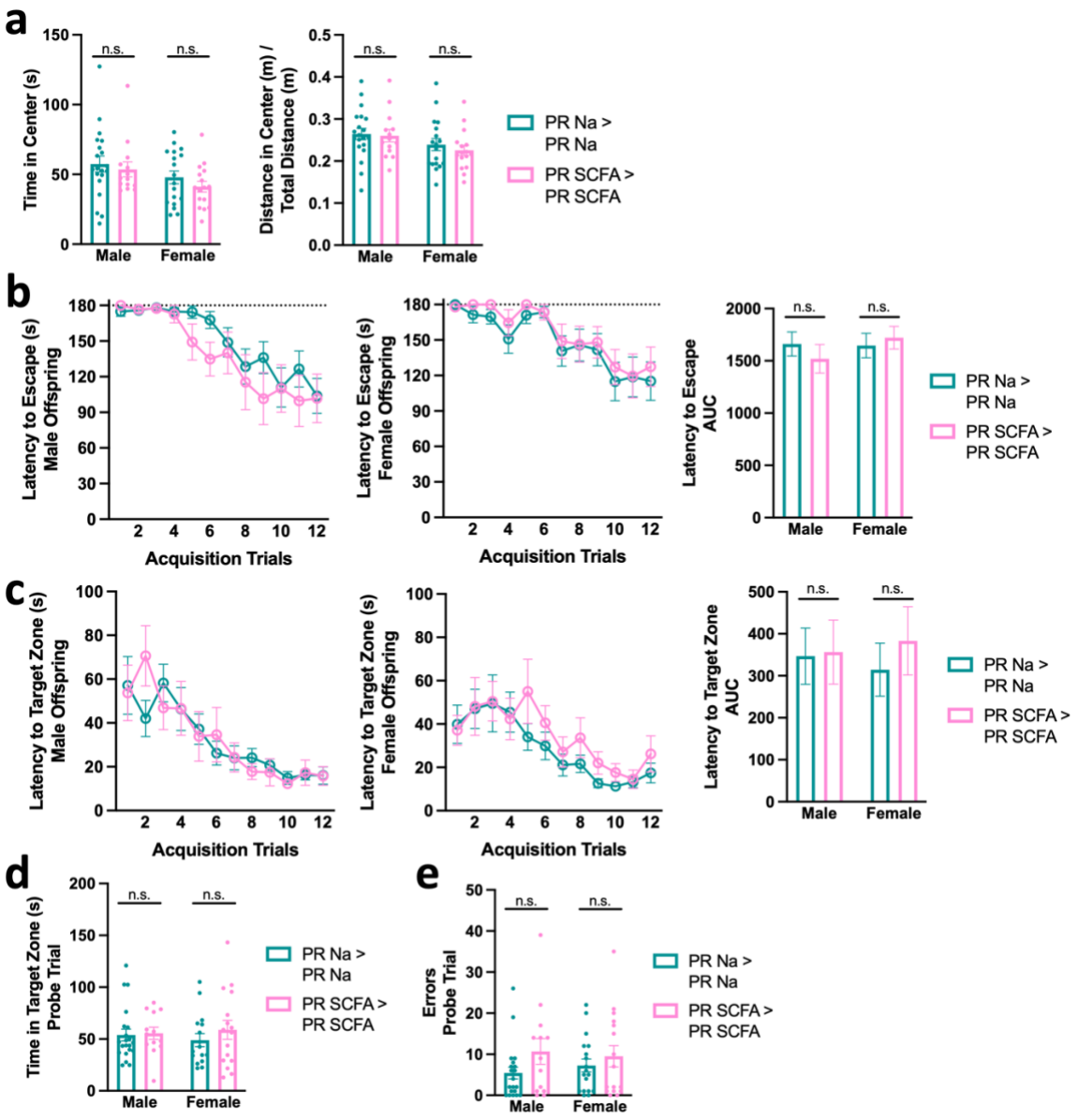

Figure 3.S9: Adult offspring do not exhibit sexually dimorphic behavioral responses to gestational protein restriction and microbial SCFA supplementation. a, Left: Time in center in open field test, male and female offspring (Mann Whitney test for each sex, n = 20, 14, 18, 16, from left to right). Right: Distance in center in open field test, controlled by total distance traveled, male and female offspring (unpaired Welch's t-test for each sex, n = 20, 14, 18, 16, from left to right). **b,** Left: Latency to escape in Barnes maze acquisition phase, male offspring (n = 21, 13). Middle: Latency to escape in Barnes maze acquisition phase, female offspring (n = 18, 16). Right: AUC of latency to escape (unpaired Welch's t-test for each sex). **c,** Left: Latency to target zone in Barnes maze acquisition phase, male offspring (n = 21, 13). Middle: Latency to target zone in Barnes maze acquisition phase, female offspring (n = 18, 16). Right: AUC of latency to target zone (unpaired Welch's t-test for each sex). **d,** Time in target zone in Barnes maze probe trial, male and female offspring (Mann-Whitney test for each sex, n = 21, 13, 18, 16, from left to right). **e,** Errors made in Barnes maze probe trial, male and female offspring (Mann-Whitney test for each sex, n = 21, 13, 18, 16, from left to right). Mean +/- SEM, *p < 0.05, **p < 0.01, ***p < 0.001, ****p < 0.0001, n.s. not significant.

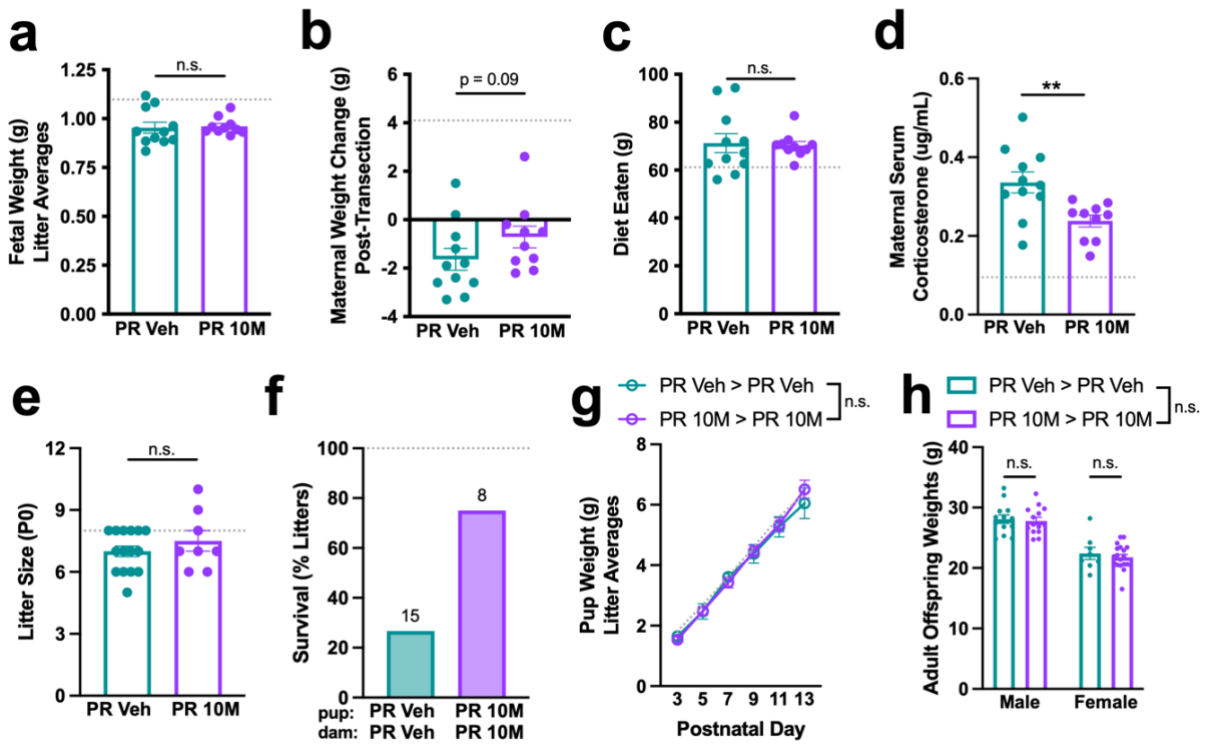

Figure 3.S10: Maternal 10M supplementation has limited impact on gross measures of maternal and offspring health. a, Fetal weight at E18.5 from SPF PR + Veh and SPF PR + 10M dams, all fetuses averaged within each litter (unpaired Welch's t-test, n = 11, 10, from left to right). Dotted line indicates average value for SPF CD fetuses. **b,** Maternal weight change, from E0.5 to E18.5 post-transection, in SPF PR + Veh and SPF PR + 10M dams (Mann-Whitney test, n = 11, 10, from left to right). Dotted line indicates average value for SPF CD dams. **c,** Diet eaten, from E0.5 to E18.5 in SPF PR + Veh and SPF PR + 10M dams (Mann-Whitney test, n = 11, 10, from left to right). Dotted line indicates average value for SPF CD dams. **d,** Corticosterone measured in serum in SPF PR + Veh and SPF PR + 10M dams at E18.5 (unpaired Welch's t-test, n = 11, 10, from left to right). Dotted line indicates average value for SPF CD dams. **e,** Litter size, pups per litters, measured at P0, from SPF PR + Veh and SPF PR + 10M dams (Mann-Whitney test, n = 15, 8, from left to right). Dotted line indicates average value for SPF CD litters. **f,** Litter survival (percentage of total litters), from SPF PR + Veh pups > SPF PR + Veh dams and SPF PR + 10M pups > SPF PR + 10M dams (n = 15, 8, from left to right). Dotted line indicates average value for SPF CD litters. Top row refers to pup condition, bottom row refers to dam condition. **g,** Pup weights, all offspring averaged within each litter (two-way repeated measures mixed effects analysis with Sidak, n = 4, 6 litters per group, from top to bottom). Dotted line indicates average value for SPF CD litters. **h,** Adult weights, male and female offspring (two-way ANOVA with Sidak, n = 13, 14, 8, 19, from left to right). Mean +/- SEM, *p < 0.05, **p < 0.01, ***p < 0.001, ****p < 0.0001, n.s. not significant.

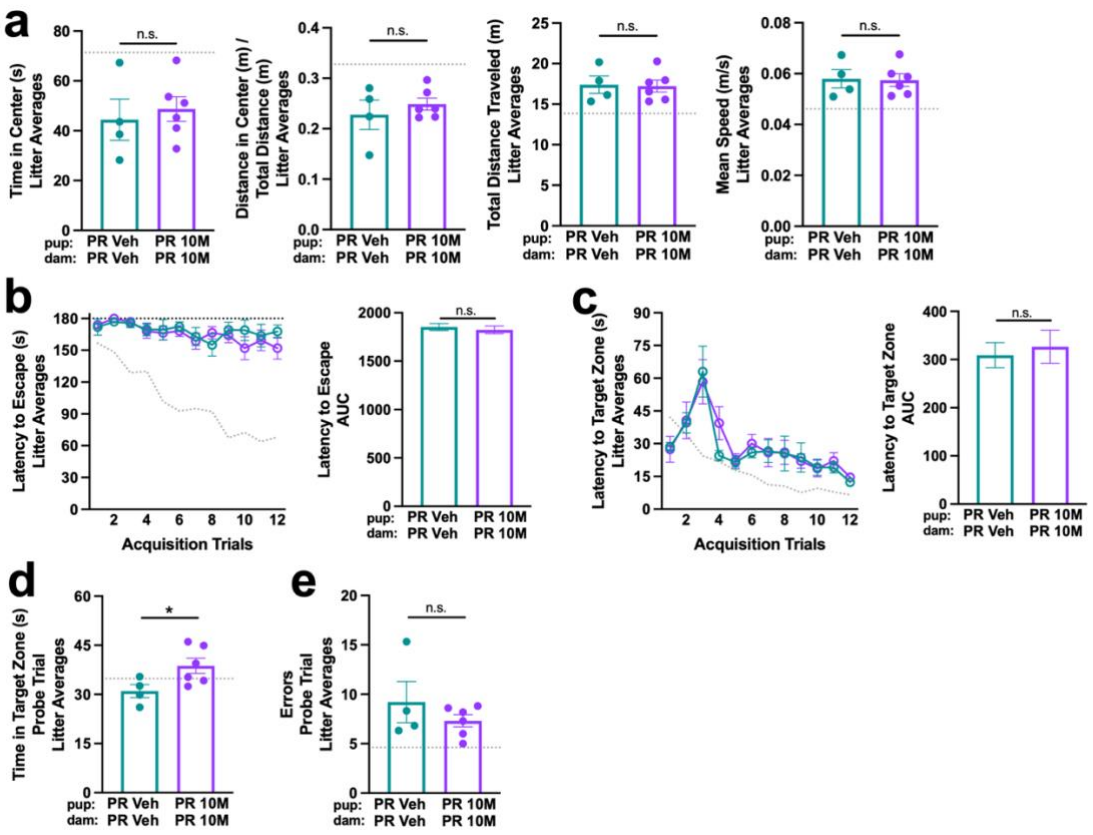

Figure 3.S11: Maternal 10M supplementation does not influence anxiety-like, locomotor, or cognitive behavioral measures in adult offspring exposed to gestational protein restriction. a, Left: Time in center in open field test, all offspring averaged within each litter (unpaired Welch's t-test, n = 4, 6 litters per group, from left to right). Top row refers to pup condition, bottom row refers to dam condition. Dotted line indicates average value for SPF CD litters. Left-middle: Distance in center in open field test, controlled by total distance traveled, all offspring averaged within each litter (unpaired Welch's t-test, n = 4, 6 litters per group, from left to right). Top row refers to pup condition, bottom row refers to dam condition. Dotted line indicates average value for SPF CD litters. Right-middle: Total distance traveled in open field test, all offspring averaged within each litter (unpaired Welch's t-test, n = 4, 6 litters per group, from left to right). Top row refers to pup condition, bottom row refers to dam condition. Dotted line indicates average value for SPF CD litters. Right: Mean speed in open field test, all offspring averaged within each litter (unpaired Welch's t-test, n = 4, 6 litters per group, from left to right). Top row refers to pup condition, bottom row refers to dam condition. Dotted line indicates average value for SPF CD litters. **b,** Left: Latency to escape in Barnes maze, all offspring averaged within each litter (n = 4, 6 litters per group, from top to bottom). Dotted line indicates average value for SPF CD litters. Right: AUC of latency to escape (unpaired Welch's t-test). Top row refers to pup condition, bottom row refers to dam condition. **c,** Left: Latency to target zone in Barnes maze, all offspring averaged within each litter (n = 4, 6 litters per group, from top to bottom). Dotted line indicates average value for SPF CD litters. Right: AUC of latency to target zone (unpaired Welch's t-test). Top row refers to pup condition, bottom row refers to dam condition. **d,** Time in target zone in Barnes maze probe trial, all offspring averaged within each litter (unpaired Welch's t-test, n = 4, 6 litters per group, from left to right). Dotted line indicates average values for SPF CD litters. **e,** Errors made in Barnes maze probe trial, all offspring averaged within each litter (unpaired Welch's t-test, n = 4, 6 litters per group, from left to right). Dotted line indicates average values for SPF CD litters. Mean +/- SEM, *p < 0.05, **p < 0.01, ***p < 0.001, ****p < 0.0001, n.s. not significant.

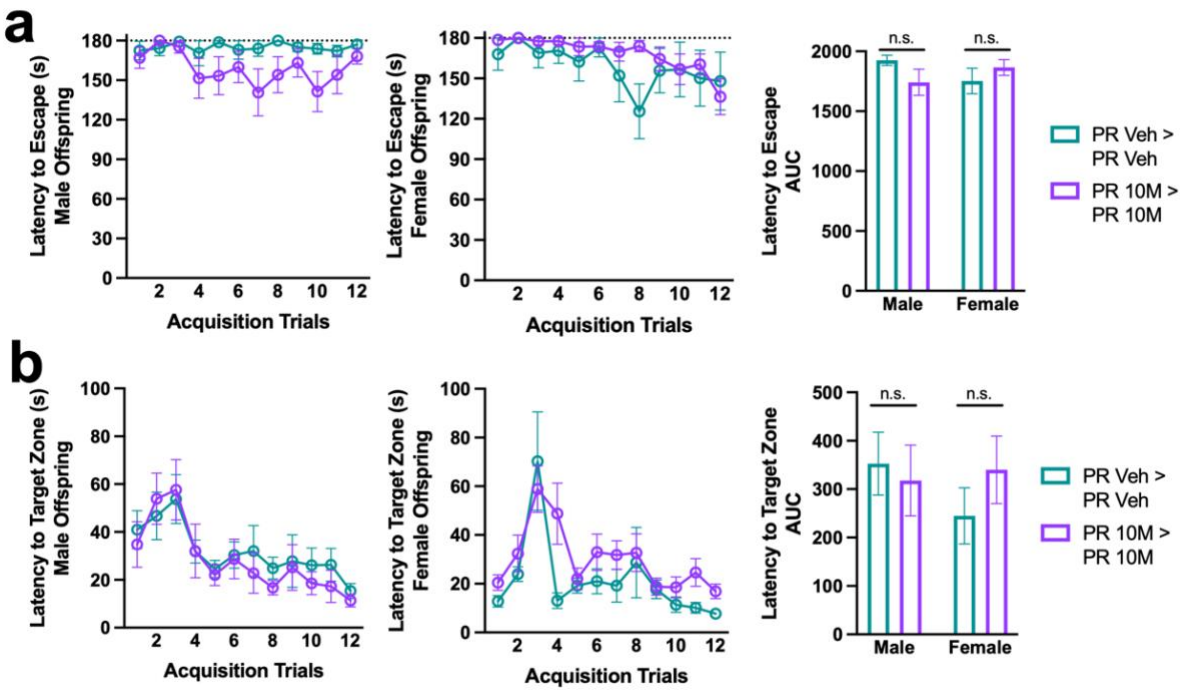

Figure 3.S12: Adult offspring do not exhibit sexually dimorphic behavioral responses to gestational protein restriction and microbial 10M supplementation. a, Left: Latency to escape in Barnes maze acquisition phase, male offspring (n = 13, 14). Middle: Latency to escape in Barnes maze acquisition phase, female offspring (n = 9, 18). Right: AUC of latency to escape (unpaired Welch's t-test for each sex). **b,** Left: Latency to target zone in Barnes maze acquisition phase, male offspring (n = 13, 14). Middle: Latency to target zone in Barnes maze acquisition phase, female offspring (n = 9, 18). Right: AUC of latency to target zone (unpaired Welch's t-test for each sex). Mean +/- SEM, *p < 0.05, **p < 0.01, ***p < 0.001, ****p < 0.0001, n.s. not significant.

Nutrient	20% Protein Diet (CD)		6% Protein Diet (PR)	
	g/Kg		g/Kg	
Casein	230		69	
DL-Methionine	3		0.9	
Sucrose	431.7		571.8	
Corn Starch	200		200	
Corn Oil	52.3		53.9	
Cellulose	37.86		57.82	
Vitamin Mix, Teklad (40060)	10		10	
Ethoxyquin, antioxidant	0.01		0.01	
Mineral Mix, Ca-P Deficient (79055)	13.37		13.37	
Calcium Phosphate, dibasic	16.66		21.6	
Calcium Carbonate	5.1		1.6	
	% by weight	**% kcal from**	**% by weight**	**% kcal from**
Protein	20.3	21.6	6.1	6.5
Carbohydrate	61.6	65.4	75.6	80.4
Fat	5.5	13	5.5	13.1

Table 3.S1: Nutritional information for control and low-protein diets.

References

1. Ghosh, et al., S. Assessment of protein adequacy in developing countries: quality matters. *Br. J. Nutr.* **108**, S77–S87 (2012).

2. Miller, et al., A. C. How consistent are associations between stunting and child development? Evidence from a meta-analysis of associations between stunting and multidimensional child development in fifteen low- and middle-income countries. *Public Health Nutr.* **19**, 1339–1347 (2015).

3. Walker, et al., S. P. Early Childhood Stunting Is Associated with Poor Psychological Functioning in Late Adolescence and Effects Are Reduced by Psychosocial Stimulation. *J. Nutr.* **137**, 2464–2469 (2007).

4. Walker, et al., S. P. Effects of early childhood psychosocial stimulation and nutritional supplementation on cognition and education in growth-stunted Jamaican children: prospective cohort study. *The Lancet* **366**, 1804–1807 (2005).

5. Smith, et al., M. I. Gut microbiomes of Malawian twin pairs discordant for kwashiorkor. *Science* **339**, 548–554 (2013).

6. Subramanian, et al., S. Persistent gut microbiota immaturity in malnourished Bangladeshi children. *Nature* **510**, 417–421 (2014).

7. Hendrixson, et al., D. T. An Alternative Oat–Containing, Ready-To-Use, Therapeutic Food Does Not Alter Intestinal Permeability or the 16S Ribosomal RNA Fecal Microbiome Configuration Among Children With Severe Malnutrition in Sierra Leone: A Randomized Controlled Trial. *J. Nutr.* **152**, 2744–2753 (2022).

8. Schwarzer, et al., M. Lactobacillus plantarum strain maintains growth of infant mice during chronic undernutrition. *Science* **351**, 854–857 (2016).

9. Barratt, et al., M. J. Bifidobacterium infantis treatment promotes weight gain in Bangladeshi infants with severe acute malnutrition. *Sci. Transl. Med.* **14**, (2022).

10. Gehrig, et al., J. L. Effects of microbiota-directed foods in gnotobiotic animals and undernourished children. *Science* **365**, (2019).

11. Chen, R. Y. A Microbiota-Directed Food Intervention for Undernourished Children. *N. Engl. J. Med.* **384**, 1517–1528 (2021).

12. Prado, et al., E. L. Do effects of early life interventions on linear growth correspond to effects on neurobehavioural development? A systematic review and meta-analysis. *Lancet Glob. Health* **7**, E1398–E1413 (2019).

13. Waber, et al., D. P. Cognitive impairment as a mediator in the developmental pathway from infant malnutrition to adolescent depressive symptoms in Barbadian youth. *J. Dev. Behav. Pediatr.* **32**, 225–232 (2011).

14. Waber, et al., D. P. Neuropsychological outcomes at midlife following moderate to severe malnutrition in infancy. *Neuropsychology* **28**, 530–540 (2014).

15. Galler, et al., J. R. Early childhood malnutrition predicts depressive symptoms at ages 11-17. *J. Child Psychol. Psychiatry* **51**, 789–798 (2010).

16. Galler, et al., J. R. Infant malnutrition is associated with persisting attention deficits in middle adulthood. *J. Nutr.* **142**, 788–794 (2012).

17. Odabas, et al., D. Cranial MRI findings in children with protein energy malnutrition. *Int. J. Neurosci.* **115**, 829–837 (2005).

18. Odabas, et al., D. Auditory brainstem potentials in children with protein energy malnutrition. *Int. J. Pediatr. Otorhinolaryngol.* **69**, 923–928 (2005).

19. Gould, et al., J. M. Mouse maternal protein restriction during preimplantation alone permanently alters brain neuron proportion and adult short-term memory. *PNAS* **115**, E7398–E7407 (2018).

20. Burgos, et al., H. Early postnatal environmental enrichment restores neurochemical and functional plasticities of the cerebral cortex and improves learning performance in hidden-prenatally-malnourished young-adult rats. *Behav. Brain Res.* **2**, 182–190 (2019).

21. Reyes-Castro, et al., L. A. Hippocampal mechanisms in impaired spatial learning and memory in male offspring of rats fed a low-protein isocaloric diet in pregnancy and/or lactation. *Hippocampus* **28**, 18–30 (2018).

22. Reyes-Castro, et al., L. A. Maternal protein restriction in the rat during pregnancy and/or lactation alters cognitive and anxiety behaviors of female offspring. *Int. J. Dev. Neurosci.* **30**, 39–45 (2012).

23. Coley, E. Y., E. J. L. &. Hsiao. Malnutrition and the microbiome as modifiers of early neurodevelopment. *Trends Neurosci.* **44**, 753–764 (2021).

24. Kim, et al., S. Maternal gut bacteria promote neurodevelopmental abnormalities in mouse offspring. *Nature* **549**, 528–532 (2017).

25. Jasarevic, et al., E. The maternal vaginal microbiome partially mediates the effects of prenatal stress on offspring gut and hypothalamus. *Nat. Neurosci.* **21**, 1061–1071 (2018).

26. Buffington, et al., S. A. Microbial reconstitution reverses maternal diet-induced social and synaptic deficits in offspring. *Cell* **165**, 1762–1775 (2016).

27. Vuong, H. E. *et al.* The maternal microbiome modulates fetal neurodevelopment in mice. *Nature* **586**, 281–286 (2020).

28. Jasarevic, T. L., E. &. Bale. Prenatal and postnatal contributions of the maternal microbiome on offspring programming. *Front. Neuroendocrinol.* **55**, (2019).

29. Dominguez-Bello, et al., M. G. Delivery mode shapes the acquisition and structure of the initial microbiota across multiple body habitats in newborns. *Proc. Natl. Acad. Sci.* **107**, 11971–11975 (2010).

30. Dawson, et al., S. L. Maternal prenatal gut microbiota composition predicts child behaviour. *EBioMedicine* **68**, (2021).

31. Sun, et al., Z. Revealing the importance of prenatal gut microbiome in offspring neurodevelopment in humans. *EBioMedicine* **90**, (2023).

32. Guo, et al., S. Regulation of gut microbiota through breast milk feeding benefits language and cognitive development in preterm toddlers. *Microorganisms* **11**, 866 (2023).

33. Gonzalez, et al., P. N. Chronic Protein Restriction in Mice Impacts Placental Function and Maternal Body Weight before Fetal Growth. *PLOS ONE* **11**, e0152227 (2016).

34. Sutton, et al., G. M. Protein Malnutrition during Pregnancy in C57BL/6J Mice Results in Offspring with Altered Circadian Physiology before Obesity. *Endocrinology* **151**, 1570–1580 (2010).

35. Seibenhener, M. C., M. L. &. Wooten. Use of the Open Field Maze to Measure Locomotor and Anxiety-like Behavior in Mice. *J. Vis. Exp.* **96**, 52434 (2015).

36. Hall, C. S. Emotional behavior in the rat: I. Defecation and urination as measures of individual differences in emotionality. *J. Comp. Psychol.* **18**, 385–403 (1934).

37. Rincel, et al., M. Multi-hit early life adversity affects gut microbiota, brain and behavior in a sex-dependent manner. *Brain. Behav. Immun.* **80**, 179–192 (2019).

38. Barnes, C. A. Memory deficits associated with senescence: A neurophysiological and behavioral study in the rat. *J. Comp. Physiol. Psychol.* **93**, 74–104 (1979).

39. Serpente, et al., P. Quantification of fetal organ sparing in maternal low-protein dietary models. *Wellcome Open Res.* **6**, (2022).

40. Bourke, et al., C. D. Immune Dysfunction as a Cause and Consequence of Malnutrition. *Trends Immunol.* **37**, 386–398 (2016).

41. Santi, et al., A. Circulating insulin-like growth factor I modulates mood and is a biomarker of vulnerability to stress: from mouse to man. *Transl. Psychiatry* **8**, (2018).

42. Matilla, et al., A. Mice lacking ataxin-1 display learning deficits and decreased hippocampal paired-pulse facilitation. *J. Neurosci.* **18**, 5508–5516 (1998).

43. Sragovich, et al., S. The autism-mutated ADNP plays a key role in stress response. *Transl. Psychiatry* **9**, (2019).

44. Thomas, R. D., S. A. &. Palmiter. Disruption of the dopamine beta-hydroxylase gene in mice suggests roles for norepinephrine in motor function, learning, and memory. *Behav.*

Neurosci. **111**, 579–589 (1997).

45. Mersman, et al., B. Taurine Promotes Neurite Outgrowth and Synapse Development of Both Vertebrate and Invertebrate Central Neurons. *Front. Synaptic Neurosci.* **12**, (2020).

46. Uno, et al., H. Brain damage induced by prenatal exposure to dexamethasone in fetal rhesus macaques. I. Hippocampus. *Dev. Brain Res.* **53**, 157–167 (1990).

47. Huang, et al., W. L. Effect of corticosteroids on brain growth in fetal sheep. *Obstet. Gynecol.* **94**, 213–218 (1999).

48. Huang, et al., W. L. Repeated prenatal corticosteroid administration delays myelination of the corpus callosum in fetal sheep. *Int. J. Dev. Neurosci.* **19**, 415–425 (2001).

49. Graham, et al., A. M. Maternal Cortisol Concentrations During Pregnancy and Sex Specific Associations with Neonatal Amygdala Connectivity and Emerging Internalizing Behaviors. *Biol. Psychiatry* **85**, 172–181 (2019).

50. Davis, et al., E. P. Across continents and demographics, unpredictable maternal signals are associated with children's cognitive function. *eBIOMedicine* **46**, (2019).

51. Weaver, et al., I. C. G. Epigenetic programming by maternal behavior. *Nat. Neurosci.* **7**, 847–854 (2004).

52. Thomas, R. D., S. A. &. Palmiter. Impaired Maternal Behavior in Mice Lacking Norepinephrine and Epinephrine. *Cell* **91**, 583–592 (1997).

53. Rosenblatt, J. S. Nonhormonal basis of maternal behavior in the rat. *Science* **156**, 1512–1514 (1967).

54. Pronovost, E. Y., G. N. &. Hsiao. PDF [2 MB] Figures Save Share Reprints Request Perinatal Interactions between the Microbiome, Immunity, and Neurodevelopment. *Immunity* **50**, 18–36 (2019).

55. Yu, et al., L. Butyrate, but not propionate, reverses maternal diet-induced neurocognitive deficits in offspring. *Pharmacol. Res.* **160**, (2020).

56. Liu, et al., X. High-fiber diet mitigates maternal obesity-induced cognitive and social dysfunction in the offspring via gut-brain axis. *Cell Metab.* **33**, 923–938 (2021).

57. Lee, et al., Y. M. Microbiota control of maternal behavior regulates early postnatal growth of offspring. *Sci. Adv.* **7**, (2021).

58. Hsiao, et al., E. Y. Microbiota Modulate Behavioral and Physiological Abnormalities Associated with Neurodevelopmental Disorders. *Cell* **155**, 1451–1463 (2013).

59. Jasarevic, E. *et al.* Stress during pregnancy alters temporal and spatial dynamics of the maternal and offspring microbiome in a sex-specific manner. *Sci. Rep.* **7**, 44182 (2017).

60. Guo, et al., P. Clostridium species as probiotics: potentials and challenges. *J. Anim. Sci. Biotechnol.* **11**, 24 (2020).

61. Bayley, N. *Bayley Scales of Infant and Toddler Development, Third Edition*. (Harcourt Assessment, San Antonio (TX), 2006).

62. Rozé, J. C. *et al.* Assessment of Neonatal Intensive Care Unit Practices and Preterm Newborn Gut Microbiota and 2-Year Neurodevelopmental Outcomes. *JAMA Netw. Open* **3**, e2018119 (2020).

63. Vuong, et al., H. E. Interactions between maternal fluoxetine exposure, the maternal gut microbiome and fetal neurodevelopment in mice. *Behav. Brain Res.* **410**, 113353 (2021).

64. Pronovost, et al., G. N. The maternal microbiome promotes placental development in mice. *Sci. Adv.* **9**, (2023).

65. Kim, B. *et al.* Response of the microbiome–gut–brain axis in Drosophila to amino acid deficit. *Nature* **593**, 570–574 (2021).

66. Lebovitz, et al., Y. Lactobacillus rescues postnatal neurobehavioral and microglial dysfunction in a model of maternal microbiome dysbiosis. *Brain. Behav. Immun.* **81**, 617–629 (2019).

67. Erny, et al., D. Host microbiota constantly control maturation and function of microglia in the CNS. *Nat. Neurosci.* **18**, 965–977 (2015).

68. Smith, et al., P. M. The microbial metabolites, short-chain fatty acids, regulate colonic Treg cell homeostasis. *Science* **341**, 569–573 (2013).

69. Gojda, M., J. &. Cahova. Gut Microbiota as the Link between Elevated BCAA Serum Levels and Insulin Resistance. *Biomolecules* **11**, 1414 (2021).

70. Brown, et al., A. G. Exposure to intrauterine inflammation alters metabolomic profiles in the amniotic fluid, fetal and neonatal brain in the mouse. *PLOS One* **12**, (2017).

71. Hegdekar, et al., N. N-Acetyl-L-leucine improves functional recovery and attenuates cortical cell death and neuroinflammation after traumatic brain injury in mice. *Sci. Rep.* **11**, 9249 (2021).

72. Koh, et al., A. Microbially produced imidazole propionate impairs insulin signaling through mTORC1. *Cell* **175**, 947–961 (2018).

73. Wikoff, et al., W. R. Metabolomics analysis reveals large effects of gutmicroflora on mammalian blood metabolites. *Proc. Natl. Acad. Sci.* **106**, 3698–3703 (2009).

74. Aronov, et al., P. A. Colonic Contribution to Uremic Solutes. *J. Am. Soc. Nephrol.* **22**, 1769–1776 (2011).

75. Swann, R. D., J. R. ,. Spitzer, S. O. ,. Heijtz. Developmental Signatures of Microbiota-

Derived Metabolites in the Mouse Brain. *Metabolites* **10**, 172 (2020).

76. Liu, et al., F. Mechanistic insights into the attenuation of intestinal inflammation and modulation of the gut microbiome by krill oil using in vitro and in vivo models. *Microbiome* **8**, (2020).

77. Appiah-Amponsah, et al., E. Identification of 4-deoxythreonic acid present in human urine by combining HPLC and NMR techniques. *J. Pharm. Biomed. Anal.* **50**, 878–885 (2009).

78. Wang, et al., Y. Multi-omics reveal microbial determinants impacting the treatment outcome of antidepressants in major depressive disorder. *Microbiome* **11**, (2023).

79. Needham, et al., B. D. A gut-derived metabolite alters brain activity and anxiety behaviour in mice. *Nature* **602**, 647–653 (2022).

80. Teng, et al., Y. Gut bacterial isoamylamine promotes age-related cognitive dysfunction by promoting microglial cell death. *Cell Host Microbe* **30**, 944–960 (2022).

81. Martimiano, et al., P. H. M. Maternal protein restriction during gestation and lactation in the rat results in increased brain levels of kynurenine and kynurenic acid in their adult offspring. *J. Neurochem.* **140**, 68–81 (2017).

82. Kepser, J. R., L. J. &. Homberg. The neurodevelopmental effects of serotonin: A behavioural perspective. *Behav. Brain Res.* **277**, 3–13 (2015).

83. Weinstock, M. The long-term behavioural consequences of prenatal stress. *Neurosci. Biobehav. Rev.* **32**, 1073–1086 (2008).

84. Choi, et al., G. B. The maternal interleukin-17a pathway in mice promotes autismlike phenotypes in offspring. *Science* **351**, 933–939 (2016).

85. Tobiansky, et al., D. J. Maternal sucrose consumption alters behaviour and steroids in adult rat offspring. *J. Endocrinol.* **251**, 161–180 (2021).

86. Choi, et al., C. S. High sucrose consumption during pregnancy induced ADHD-like behavioral phenotypes in mice offspring. *J. Nutr. Biochem.* **26**, 1520–1526 (2015).

87. Shansky, A. Z., R. M. &. Murphy. Considering sex as a biological variable will require a global shift in science culture. *Nat. Neurosci.* **24**, 457–464 (2021).

88. May, et al., T. Sex differences in neurodevelopmental disorders. *Curr. Opin. Neurol.* **32**, 622–626 (2019).

89. Brown, et al., C. M. Origin of Sex-Biased Mental Disorders: Do Males and Females Experience Different Selective Regimes? *J. Mol. Evol.* **90**, 401–417 (2022).

90. Bale, T. L. Sex differences in prenatal epigenetic programing of stress pathways. *Int. J. Biol. Stress* **14**, 348–356 (2011).

91. Dipietro, K. M., J. A. &. Voegtline. The gestational foundation of sex differences in development and vulnerability. *Neuroscience* **342**, 4–20 (2017).

92. Tye, et al., K. M. Amygdala circuitry mediating reversible and bidirectional control of anxiety. *Nature* **471**, 358–362 (2011).

93. Felix-Ortiz, et al., A. C. BLA to vHPC inputs modulate anxiety-related behaviors. *Neuron* **79**, 658–664 (2013).

94. Jo, et al., Y. S. The Medial Prefrontal Cortex Is Involved in Spatial Memory Retrieval under Partial-Cue Conditions. *J. Neurosci.* **27**, 13567–13578 (2007).

95. Meek, et al., L. R. Effects of stress during pregnancy on maternal behavior in mice. *Physiol. Behav.* **72**, 473–479 (2001).

96. Champagne, M. J., F. A. &. Meaney. Stress during gestation alters postpartum maternal care and the development of the offspring in a rodent model. *Biol. Psychiatry* **59**, 1227–1235 (2006).

97. Derrickson, S. R., E. M. &. Lowas. The Effects of Dietary Protein Levels on Milk Protein Levels and Postnatal Growth in Laboratory Mice (Mus musculus). *J. Mammal.* **88**, 1475–1481 (2007).

98. Charbonneau, et al., M. R. Sialylated Milk Oligosaccharides Promote Microbiota-Dependent Growth in Models of Infant Undernutrition. *Cell* **164**, 859–871 (2016).

99. Fox, W. M. Reflex-ontogeny and behavioural development of the mouse. *Anim. Behav.* **13**, 234–241 (1965).

100. Zippelius, W. M., H. M. &. Schleidt. Ultrasonic vocalization in infant mice. *Naturwissenschaften* **43**, 502–503 (1956).

101. Chu, et al., A. Prenatal intrauterine growth restriction and risk of retinopathy of prematurity. *Sci. Rep.* **10**, (2020).

102. Wu, A. J. *et al.* Impact of Clinical Factors on the Intestinal Microbiome in Infants With Gastroschisis. *J. Parenter. Enter. Nutr.* **45**, 818–825 (2021).

103. Caporaso, et al., J. G. Global patterns of 16S rRNA diversity at a depth of millions of sequences per sample. *PNAS* **108**, 4516–4522 (2011).

104. Bolyen, et al., E. Reproducible, interactive, scalable and extensible microbiome data science using QIIME 2. *Nat. Biotechnol.* **37**, 852–857 (2019).

105. Callahan, et al., B. J. DADA2: High-resolution sample inference from Illumina amplicon data. *Nat. Methods* **13**, 581–583 (2016).

106. Huang, et al., D. W. Systematic and integrative analysis of large gene lists using DAVID bioinformatics resources. *Nat. Protoc.* **4**, 44–57 (2008).

107. Sherman, et al., B. T. DAVID: a web server for functional enrichment analysis and functional annotation of gene lists (2021 update). *Nucleid Acids Res.* **50**, W216–W221 (2022).

108. Ginestet, C. ggplot2: Elegant Graphics for Data Analysis. *J. R. Stat. Soc. Ser. A Stat. Soc.* **174**, 245–246 (2011).

109. Pang, et al., Z. MetaboAnalyst 5.0: narrowing the gap between raw spectra and functional insights. *Nucleic Acids Res.* **49**, W388–W396 (2021).

110. Sugimoto, et al., M. MMMDB: Mouse Multiple Tissue Metabolome Database. *Nucleic Acids Res.* **40**, D809–D814 (2012).

111. Mishima, et al., E. Evaluation of the impact of gut microbiota on uremic solute accumulation by a CE-TOFMS–based metabolomics approach. *Kidney Int.* **92**, P634–P645 (2017).

112. Khandelwal, et al., J. K. Measurement of tele-methylhistamine and histamine in human cerebrospinal fluid, urine, and plasma. *Agents Actions* **12**, 583–590 (1982).

113. Daniel, et al., N. Gut microbiota and fermentation-derived branched chain hydroxy acids mediate health benefits of yogurt consumption in obese mice. *Nat. Commun.* **13**, (2022).

114. Kahanovitz, et al., L. Type 1 Diabetes – A Clinical Perspective. *Point Care* **16**, 37–40 (2017).

115. Arazi, et al., H. A Review of the Effects of Leucine Metabolite (β-Hydroxy-β-methylbutyrate) Supplementation and Resistance Training on Inflammatory Markers: A New Approach to Oxidative Stress and Cardiovascular Risk Factors. *Antioxidants* **7**, 148 (2018).

116. Bahado-Singh, et al., R. O. First-trimester metabolomic detection of late-onset preeclampsia. *Am. J. Obstet. Gynecol.* **208**, 58.E1-58.E7 (2013).

117. Bahado-Singh, et al., R. O. Metabolomics and first-trimester prediction of early-onset preeclampsia. *J. Matern. Fetal Neonatal Med.* **25**, 1840–1847 (2012).

118. Bahado-Singh, R. O. Metabolomic analysis for first-trimester trisomy 18 detection. *Am. J. Obstet. Gynecol.* **209**, 65.E1-65.E9 (2013).

Chapter 4: Interactions between maternal fluoxetine exposure, the maternal gut microbiome and fetal neurodevelopment in mice

Abstract

Selective serotonin reuptake inhibitors (SSRIs) are the most widely used treatment by women experiencing depression during pregnancy. However, the effects of maternal SSRI use on early offspring development remain poorly understood. Recent studies suggest that SSRIs can modify the gut microbiota and interact directly with particular gut bacteria, raising the question of whether the gut microbiome impacts host responses to SSRIs. In this study, we investigate effects of prenatal SSRI exposure on fetal neurodevelopment and further evaluate potential modulatory influences of the maternal gut microbiome. We demonstrate that maternal treatment with the SSRI fluoxetine induces widespread alterations in the fetal brain transcriptome during midgestation, including increases in the expression of genes relevant to synaptic organization and neuronal signaling and decreases in the expression of genes related to DNA replication and mitosis. Notably, maternal fluoxetine treatment from E7.5 to E14.5 has no overt effects on the composition of the maternal gut microbiota. However, maternal pretreatment with antibiotics to deplete the gut microbiome substantially modifies transcriptional responses of the fetal brain to maternal fluoxetine treatment. In particular, maternal fluoxetine treatment elevates localized expression of the opioid binding protein/cell adhesion molecule like gene Opcml in the fetal thalamus and lateral ganglionic eminence, which is prevented by maternal antibiotic treatment. Together, these findings reveal that maternal fluoxetine treatment alters gene expression in the fetal brain through pathways that are impacted, at least in part, by the presence of the maternal gut microbiota.

1. Introduction

Major depression occurs in 8–12 % of pregnant women, and the number of pregnant women with symptoms of depression has continued to increase [1–3]. Identifying safe and effective treatments for depression is of key importance, especially for pregnant women, given that factors such as maternal stress and anxiety can increase risk for adverse developmental

outcomes in the offspring [4–7]. Among treatment options, selective serotonin reuptake inhibitors (SSRIs) are the most widely used class of antidepressants during pregnancy [8]. SSRI use is reported to protect against symptoms of maternal mood disorders, with the potential to buffer against negative consequences of maternal depression on offspring health [9–15]. However, maternal use of SSRIs has also been associated with a number of obstetric outcomes, including preterm birth, low birth weight, smaller head circumference, poor neonatal adaptation postdelivery and low Apgar scores [16–20]. Neurodevelopmental changes in the offspring have also been reported: infants of mothers treated with SSRIs during pregnancy exhibited reduced global integration in the frontal brain, increased gray matter in the amygdala and increased white matter connectivity in the insular cortex, compared to matched controls [21,22]. Animal studies examining the consequences of maternal SSRI exposure on offspring brain and behavior have yielded disparate and sometimes conflicting results, pointing to complex context-specific effects of maternal SSRI use on developing offspring [23–28]. Exactly how maternal SSRI treatment during pregnancy may interact with other physiological factors to influence early neurodevelopment in the offspring remains poorly understood.

Despite the widespread use of SSRIs as a first-line treatment for depression, patient responses to SSRIs are highly variable [29,30]. This highlights a need to identify physiological factors that modify responses to SSRIs in order to understand the biological basis of treatment efficacy. The maternal gut microbiome is one such variable that is increasingly recognized for its important roles in the metabolic, immune, and nervous systems [31–37] and for its capacity to modulate patient responses to various common medications [38–41]. Indeed, SSRI use is associated with alterations in the gut microbiome [42–44] and select gut bacteria can interact directly with SSRIs [45,46], which raises the question of whether the maternal microbiome may modify host responses to SSRI treatment during pregnancy.

This study addresses these open questions by investigating the effects of maternal SSRI treatment on fetal neurodevelopment and by further evaluating roles for the maternal gut

microbiome in modulating observed responses to SSRIs. The results reveal widespread influences of maternal fluoxetine treatment on fetal brain gene expression during midgestation, which are modified by the maternal gut microbiota, likely through indirect host-microbial interactions with SSRIs.

2. Materials and methods

2.1. Mice

6–8 week-old specific pathogen-free (SPF) C57BL/6 J mice from the Jackson laboratory were group-housed in ventilated cages, with free access to standard rodent chow and water. The holding room maintained a controlled temperature (22− 25 ◦C) and humidity, as well as a 12 -h light/dark cycle. Prior to breeding, bedding from all cages was mixed every 3 days over 14 days to normalize the gut microbiota across mice. Mice were randomly divided into four groups: SPF mice treated with saline (SPF + Veh), SPF mice treated with fluoxetine (SPF + FLX), SPF mice pre-treated with antibiotics and treated with saline (ABX + Veh) and SPF mice pre-treated with antibiotics and treated with fluoxetine (ABX + FLX). All experiments were performed in accordance with the NIH Guide for the Care and Use of Laboratory Animals using protocols approved by the Institutional Animal Care and Use Committee at UCLA.

2.2. Antibiotic pre-treatment and timed-matings

All male and female mice in the ABX + Veh and ABX + FLX groups were orally gavaged with an antibiotic cocktail of vancomycin (50 mg/ kg), neomycin (100 mg/kg), and metronidazole (100 mg/kg) twice daily at 8:00 and 17:00, for 7 days, while being maintained on drinking water supplemented with ampicillin (1 mg/mL). SPF controls were gavaged with saline and maintained on standard drinking water. Males and females in each group were then paired for timed-matings. Mice in the ABX + Veh and ABX + FLX groups were maintained on drinking water supplemented with ampicillin (1 mg/mL), neomycin (1 mg/mL) and vancomycin (0.5 mg/mL).

Females were checked daily for vaginal plugs. The day of plug observation was considered embryonic day 0.5 (E0.5), after which dams were housed individually and monitored for weight gain over 14 days.

2.3. Fluoxetine treatment and tissue collection

On day E7.5, individually housed dams that gained 2− 3 g denoting successful pregnancy were assigned randomly to a specific experimental group to either be gavaged daily at 8:00 over 8 days with 10 mg/kg fluoxetine hydrochloride [7,8] (FLX, Santa Cruz) or saline as the vehicle control (Veh). On E14.5, dams were sacrificed by cervical dislocation to preclude any effects of hypoxic stress from CO2 euthanasia on maternal and fetal physiology. Whole embryos or embryonic brains were collected for downstream analyses.

2.4. Serotonin and tryptophan measurements

Maternal blood samples were collected by cardiac puncture and spun through serum separation tubes (Becton Dickinson) for 10 min at 1000 RCF (g) at 4 ◦C. E14.5 placenta and fetal brains were sonicated on ice for 10 s at 50 mV in enzyme-linked immunosorbent assay (ELISA) standard buffer supplemented with 10 % ascorbic acid (Eagle Biosciences). Serotonin levels were detected by ELISA assay according to the manufacturer's instructions (Eagle Biosciences, SEU39-K01). Tryptophan levels were measured using the Bridge-IT L-Tryptophan fluorescence assay (Mediomics, 1-1-1001) according to the manufacturer's protocol. Readings from tissue samples were normalized to total protein content as detected by the 660 nm Protein Assay (Thermo Pierce, 22662). All samples were run in triplicate, and controls and standards were run in duplicate. Optical density was read at 405 nm on a Synergy H1 Hybrid Multimodal plate reader (BioTek). Mean absorbance per sample was calculated based on a standard curve of serial dilutions and triplicates were confirmed to exhibit a coefficient of variability of less than 10 %.

2.5. Fluoxetine quantitation

Fluoxetine (1 μM, 10 μM, and 100 μM) was added to water to confirm detection and retention time (RT) =1.89 min. For standards, fluoxetine (10 μM, 1 μM, 100 nM, and 10 nM) was added to control serum samples before metabolite extraction. 50 μL standard and experimental serum samples were mixed with 50 μL H2O and 400 μL of 100 % methanol, the samples were vortexed for 10 s, placed at − 80 ◦C for 20 min. Samples were centrifuged and the cell free supernatant was mixed with 300 μL H2O and 400 μL chloroform. The aqueous layer containing fluoxetine was transferred to glass vials (Thermo Fisher Scientific, 13-622-351) and dried in a Genevac EZ-2 Elite evaporator. At the UCLA Metabolomics core facility, dried samples were resuspended in 50 % Acetonitrile (ACN):water. Utilizing a Vanquish Flex (Thermo Scientific) UPLC, 1/ 10th of the sample was loaded onto a Luna 3um NH2 100A (150 × 2.0 mm) column (Phenomenex) equilibrated to 15 % mobile phase A (5 mM NH4AcO pH 9.9) and 85 % B (ACN). Metabolite was eluted with a 4 min gradient of 15 %–90 % A at a flow rate of 200 μl/min, followed by reequilibration to 15 % A. Metabolite was detected with a Q Exactive (Thermo Scientific) mass spectrometer in full MS mode with positive ionization mode and at 70 K resolution. The data files were then converted to mzXML files with MSConvert and extracted with Maven (v8.1.27.5) for fluoxetine ([M+H]+ = 310.14133).

2.6. 16S rRNA gene sequencing and analysis

Fecal samples were collected for the SPF + Veh and SPF + FLX groups on gestational days E3.5, E6.5, E8.5, E11.5 and E14.5, and kept frozen at − 80 ◦C. Bacterial genomic DNA was extracted from frozen fecal samples using the Qiagen DNeasy Powersoil Kit, and purified using the QIAquick PCR Purification Kit. The sequencing library was generated according to methods adapted from Caporaso et al. [47]. The V4 regions of the 16S rRNA gene were amplified by PCR using universal primers barcoded with unique oligonucleotides, Illumina

adaptors, and 30 ng of the extracted genomic DNA. The PCR reaction was set up in triplicates, and the product was then purified again using the QIAquick PCR purification kit (Qiagen). DNA concentration was quantified using a BioTek Synergy H1 Multimodal microplate reader, and 250 ng of purified PCR product from each sample was pooled and sequenced by Laragen, Inc. Sequencing was performed using the Illumina MiSeq platform and 2 × 250 bp reagent kit for paired-end sequencing. Operational taxonomic units (OTUs) were chosen by open reference OTU picking based on 99 % sequence similarity to the most recent SILVA 132 database [48,49]. Taxonomy assignment and rarefaction were performed using QIIME2− 2020.2.0 [50].

2.7. Fetal brain RNA sequencing and analysis

Embryonic brains were dissected on E14.5 and homogenized in Trizol Reagent (Invitrogen), using three biological replicates per group as the minimum for inferential analysis [51]. RNA was extracted using the RNAeasy Mini kit with on-column genomic DNA-digest (Qiagen). RNA quality of RIN > 8.0 was confirmed using the 4200 Tapestation system (Agilent). RNA was prepared using the TruSeq RNA Library Prep kit, and 2 × 69 bp paired-end sequencing was performed using the Illumina HiSeq 4000 platform by the UCLA Neuroscience Genomics core facility. FastQC v0.11.8 and HiSAT2 2.1.0 [52,53] were used for quality filtering and mapping. Reads were aligned to UCSC Genome Browser assembly ID: mm10. Differential expression analysis of $p < 0.05$ was conducted using DESeq2 1.24.0 [54]. Heatmaps were generated using the pheatmap package for R. GO term enrichment analysis of differentially expressed genes with $q < 0.05$ (Benjamini-Hochberg correction) was conducted using DAVID v6.8 [55]. Protein interaction networks were generated using STRING v10.5 using a minimum required interaction score of highest confidence (0.900) and maximum number of interactions of no more than 5 interactors, and line thickness is based on confidence of interaction. Functional enrichments nodes were categorized by GO: biological process, molecular function, and cellular

component and/or KEGG pathways using a false discovery rate (FDR) less than 0.05 (Benjamini-Hochberg correction).

2.8. Quantitative RT-PCR

E14.5 brains were dissected and sonicated in Trizol for RNA isolation using the RNAeasy Mini kit with on-column genomic DNA-digest (Qiagen). cDNA synthesis was performed using the qScript cDNA synthesis kit (Quantabio). qRT-PCR was performed on a QuantStudio 5 thermocycler (ThermoFisher Scientific) using SYBR green master mix with Rox passive reference dye and validated primer sets obtained from Primerbank (Harvard).

2.9. Microcomputed tomography (μCT)

Whole embryos were serially dehydrated in 30 %, 50 %, and 70 % ethanol overnight at 4 ◦C eachand incubated in 4% (w/v) phosphotungstic acid (EPTA) diluted in 70 % EtOH for 4 days at 4 ◦C. Embryos were scanned at 80 kVp/140 μA with 500 ms exposure and a 5-frame average at a resolution of 20 μm using a μCT scanner (HiCT) developed by the Chatziioannou Lab at the Crump Institute for Molecular Imaging at UCLA. 2-dimensional images were reconstructed following dynamic range adjustment using gaussian smoothing. Regions of interest (ROI) for embryo and brain volume measurements were selected manually, and EPTA-stained tissue was segmented based on contrast to give a final embryo and brain volume measurement (mm3) within the ROI. Whole embryo and brain volumes were reconstructed and measured using Amide software (amide.exe 1.0.4).

2.10. Fluorescence in situ hybridization

E14.5 embryos were harvested, immediately frozen in liquid nitrogen and then embedded in cryo-embedding medium OCT (Tissue-Tek, VWR). Fetal brains were cut into 15 μm sections, mounted onto SuperFrost Plus slides and post-fixed in 4 % paraformaldehyde for

15 min at 4 ◦C. Sections were then serially dehydrated in 50 %, 70 %, 100 % and 100 % ethanol for 5 min each at room temperature and processed using the RNAscope Multiplex Fluorescent Kit V2 (Advanced Cell Diagnostics Inc, 323100). Sections were incubated for 2 h at 40 ◦C with 3-plex positive control probe (320881), 3-plex negative control probe (320871) or customized target probes for mouse gene Mm-Opcml (824171). Following probe hybridization, sections were washed twice with wash buffer (ACD, 310091), and then sequentially hybridized with amplifier 1, 2, and 3 at 40 ◦C for 30 min, 30 min, and 15 min, respectively. HRP signal was developed and visualized in Opal Dye 690 channel. Sections were then counterstained with the nuclear marker DAPI and mounted using ProLong Gold Antifade Mountant.

2.10.1. Fluorescence in situ hybridization imaging

Slides were imaged using a 20X objective on a Zeiss LSM780 confocal microscope, equipped with a Diode 405 (1 %) and HeNe 633 nm at 17 %. Images were acquired with 0.7 and 1X zoom, average line 2, pixel dwell of 3.15 µs at a 1024 × 1024 pixel resolution. Scans were exported using the Zen 2.1 (Blue Edition) software.

2.10.2. Fluorescence in situ hybridization image analysis

Images of somatosensory neocortex, thalamus, lateral ganglionic eminence, striatum and hippocampus were deidentified and analyzed using ImageJ (version: 2.0.0-rc-69/1.52p) by a researcher blinded to experimental group. Channels were split into different windows, and the scale was set to 1.2 pixels/ µm. Raw integrated density of Opcml in each image was measured to assess total fluorescence. Then, the DAPI channel of each image was thresholded to 30/255, and the area was measured to ascertain total brain area. Opcml integrated density was divided by the DAPI area for that image, to calculate total raw integrated density per µm2 . For somatosensory neocortex, thalamus and striatum, the whole image was quantified, and for

lateral ganglionic eminence and hippocampus, an ROI was drawn to isolate the region from adjacent tissue.

2.11. Fluorescence immunohistochemistry

E14.5 embryos were quickly collected and fixed in 4 % paraformaldehyde for 24 h at 4 ◦C, after which they are transferred to a 30 % sucrose solution for cryoprotection. After a week in sucrose, embryos were frozen in OCT (Tissue-Tek, VWR) and stored at − 80 ◦C. Embryos were sectioned sagittally at 10 μm, mounted on Superfrost Ultra Plus glass slides (ThermoFisher Scientific) and stored at − 20 ◦C. Slides were incubated in DAKO antigen retrieval solution (Agilent) at 90 ◦C for 2 min, washed with 1X PBS, and then incubated for 1 h at room temperature with 10 % normal donkey serum. Slides were then incubated with primary antibodies for 30 h at 4 ◦C: anti-5-HT (rat monoclonal, Abcam, ab6336, 1:100), anti-SERT (rabbit polyclonal, Abcam, ab9726, 1:500), or anti-Tph2 (goat polyclonal, US Biological 208476, 1:500). Slides were incubated with the respective secondary antibody for 1 h at room temperature: donkey anti-rat Alexa Fluor 488, 1:1000; donkey anti-goat, Alexa Fluor 568, 1:1000; donkey anti-rabbit, Alexa Fluor 647, 1:1000 (ThermoFisher Scientific). Slides were mounted with Prolong Gold antifade reagent with DAPI (ThermoFisher Scientific), air-dried for 1 h, and maintained at 4 ◦C.

2.11.1. Fluorescence immunohistochemistry imaging

Slides were imaged using a 20X objective on a Zeiss LSM780 confocal microscope, equipped with an Argon laser (488 nm) at 14 %, a Diode 561 nm at 10 % and HeNe 633 nm at 15 %. Images were acquired across eight z-sections, scanning a total of 5.31 μm at a 1024 × 1024 pixel resolution. Scans were tiled in the Zen Black Edition software and stitched using the Zen 2.1 (Blue Edition) software.

2.11.2. Fluorescence immunohistochemistry image analysis

To compare 5-HT+, SERT + and Tph2+ expression in each group, sagittal E13.5 and E15.5 brain sections from the Allen Developing Mouse Brain Atlas (2008) were used as a reference to locate the dorsal raphe nucleus (DRN) and axons. DRN neurons were counted using the ImageJ Puncta Analyzer plugin [56]. A DRN standard region of interest (ROI) was used to measure cells that colocalized with 5-HT+ and SERT+ fluorescence, or 5-HT+ and Tph2+ fluorescence in the DRN. Separately, three standard ROIs were used to measure the number of 5-HT+, SERT+ and Tph2+ puncta and integrated density in DRN axon projections. Quantifications were normalized to the area of the ROIs and background noise was subtracted.

2.12. Statistical analysis

Statistical analyses were performed in Prism 8 software. Given that maternal fluoxetine treatment and microbiome status are the primary experimental variables across experiments, biological sample sizes reflect the number of maternal biological replicates. Experiments evaluating fetal outcomes include at least 2 randomly selected embryos per dam, where data from offspring from a single dam were averaged to represent the dam as the biological “n”. Therefore, data in quantitative RT-PCR, immunofluorescence staining, fluorescence in situ hybridization, maternal weight, fetal numbers and size, and ELISA experiments are represented as n = independent maternal dam. Differences among ≥ 2 groups with only one variable were assessed using one-way ANOVA with Tukey’s or Sidak’s post-hoc test. Two-way ANOVA with Tukey’s or Sidak’s post-hoc test was used for ≥ 2 groups with two variables. Taxonomic comparisons from 16S rRNA gene sequencing analysis were analyzed by Kruskal-Wallis test with Tukey’s post-hoc test. Significant differences emerging from the above tests are indicated in the figures by *$p < 0.05$, **$p < 0.01$, ***$p < 0.001$, ****$p < 0.0001$. Notable nonsignificant differences are indicated in the figures by “n.s.”.

3. Results

3.1. Maternal fluoxetine treatment from E7.5 to E14.5 has no significant effects on maternal weight, litter size, fetal volume or fetal brain volume

To first examine effects of maternal fluoxetine treatment from E7.5 to E14.5 on gross metrics of maternal and fetal health, conventionally-colonized pregnant dams were orally gavaged with fluoxetine (10 mg/ kg; SPF + FLX) or saline as a vehicle control (SPF + Veh) once daily from E7.5–14.5 (**Fig. 4.1A**). The E7.5 to E14.5 timeframe was chosen because of its clinical relevance to prenatal SSRI exposure [18,57,58]. Mass spectrometry-based assessment of maternal serum indicated that oral fluoxetine treatment of pregnant dams yielded serum fluoxetine concentrations of 1.597 ± 0.1618 μM (mean ± s.e.m.) on E14.5 (**Fig. 4.S1A, B**, $p = 0.0001$, $F = 23.92$). There were no statistically significant differences in maternal weight before fluoxetine treatment, but a modest decrease following fluoxetine treatment (**Fig. 4.S2A-C**, $p = 0.039$, $F = 6.625$). Interestingly, pregnant dams that were treated with fluoxetine exhibited modest, though statistically significant, increases in cecal weight on E14.5 (**Fig. 4.S2D**, $p = 0.0305$, $F = 77.79$), which may align with expected responses to the proposed antibacterial effects of fluoxetine [59]. Contrary to a previous report that treated pregnant dams of a different mouse strain (129/SvEvTac) with fluoxetine in drinking water (approximately 10 mg/kg/day) for 14 days [60], we observed no statistically significant alterations in average litter size after maternal fluoxetine treatment during midgestation (**Fig. 4.S2E**). Microcomputed tomography (μCT)-based imaging indicated no statistically significant effects of maternal fluoxetine treatment on embryo or brain volume (**Fig. 4.S2F-H**). Altogether, these data reveal modest effects of maternal fluoxetine treatment during midgestation on gross metrics of maternal weight, and no overt effects on fetal health.

3.2. Maternal fluoxetine treatment from E7.5 to E14.5 alters the fetal brain transcriptome

In the absence of overt effects of maternal fluoxetine treatment on fetal brain size, we next asked whether maternal fluoxetine treatment alters gene expression in the fetal brain. Fetal brains were harvested on E14.5 from dams treated with fluoxetine or vehicle, and processed for RNA sequencing and differential gene expression analysis. E14.5 was selected as a time point reflecting several active early neurodevelopmental events, including neurogenesis, neuronal migration, axon outgrowth, and synapse formation [61]. Transcriptomic analysis revealed that maternal fluoxetine treatment significantly altered the expression of 864 genes in the fetal brain, with 451 upregulated and 413 downregulated in fetal brains from offspring of fluoxetine-treated dams relative to those from saline-treated controls (**Fig. 4.1B**). In particular, maternal fluoxetine treatment increased the expression of genes that clustered into pathways related to synapse organization, cognition, locomotory behavior, and neurotransmission in the fetal brain (**Fig. 4.1C, Fig. 4.S3A**) and decreased the expression of genes most relevant to cell cycle, mitosis, DNA repair and DNA replication pathways in the fetal brain (**Fig. 4.1D, Fig. 4.S3B**). Among the differentially expressed genes, maternal fluoxetine treatment induced widespread reductions in the expression of several histone-related genes in the fetal brain (Hist1h4k, Hist1h3a, Hist1h4b, Hist1h3c, Hist1h4j, Hist1h3bj, Hist1h2ac, Hist1h3e, and Hist1h2bk), which encode nuclear proteins that play a central role in transcription regulation, DNA repair, DNA replication, and chromosomal stability (**Fig. 4.1E, F**). In contrast, maternal fluoxetine treatment increased the expression of select genes that encode for zinc finger proteins (Zfp455 and Zfp804b) and calcium ion binding proteins (Syn1 and Necab1) (**Fig. 4.1E, F**). In addition, maternal fluoxetine treatment increased the gene expression of Opcml, which is part of a family of cell adhesion molecules that regulate neurite outgrowth, dendritic arborization and synapse formation [1] (**Fig. 4.1E, F**). These data reveal that maternal fluoxetine treatment elicits global alterations in the fetal brain transcriptome that have the potential to impact early neurodevelopment.

3.3. Maternal fluoxetine treatment from E7.5 to E14.5 has no significant effect on the fetal serotonergic system

5-HT is an important signaling molecule in the fetal brain that is derived from both central and peripheral sources [62–64]. The development of the serotonergic system in the fetal brain begins with the neurogenesis of 5-HT neurons from E9.5–12, followed by a series of neuro-maturational events that continue through the third postnatal week of life [65]. SSRIs inhibit the 5-HT transporter SERT to modulate the bioavailability of 5-HT and shape key components of the serotonergic system [27,66,67]. In light of reports that fluoxetine, and other SSRIs, can cross the placenta, we asked if the effects of maternal fluoxetine treatment on fetal brain gene expression could be due to direct effects of fluoxetine on the fetal serotonergic system. To gain insight, we first assessed effects of maternal fluoxetine treatment on levels of 5-HT and its precursor tryptophan in maternal serum and fetal brain at E14.5. As an expected response to the inhibition of SERT-dependent uptake of 5-HT by blood platelets [68], maternal fluoxetine treatment significantly decreased maternal serum levels of 5-HT relative to vehicle-treated controls ($p = 0.0333$, $F = 4.336$), with no effects on levels of maternal tryptophan (**Fig. 4.S4A, B**). While maternal fluoxetine could act on placental SERT to regulate development of the fetal brain [66,69,70], maternal fluoxetine treatment did not alter levels of 5-HT and tryptophan in the placenta relative to vehicle-treated controls (**Fig. 4.S4C, D**). Notably, maternal fluoxetine treatment had no statistically significant effects on levels of 5-HT or tryptophan in the fetal brain, suggesting no direct effects of maternal fluoxetine on the bioavailability of 5-HT in the fetal brain (**Fig. 4.S4E, F**). To further evaluate the possibility for maternal fluoxetine treatment to alter fetal development of the central serotonergic system, serotonergic neurons of the fetal dorsal raphe nucleus (DRN) were stained and imaged for 5-HT, SERT, and Tph2, the rate-limiting enzyme for neuronal 5-HT synthesis. Compared to vehicle-treated controls, there were no statistically significant effects of maternal fluoxetine treatment on the density of 5-HT-, SERT, or Tph2-positive neurons in the DRN (**Fig. 4.S5A-G**), or on the integrated density and number of 5-HT-,

SERT-, or Tph2-positive axonal projections from DRN to the prefrontal cortex (**Fig. 4.S5H-N**). Together, these results indicate that maternal fluoxetine treatment has no significant effect on levels of 5-HT or development of serotonergic DRN neurons in the fetal brain. These findings further suggest that the observed transcriptional responses to maternal fluoxetine treatment in the fetal brain are likely not due to direct effects of fluoxetine on the fetal serotonergic system.

3.4. Maternal fluoxetine treatment has no overt effects on the maternal gut microbiota

SSRI use is associated with alterations in the composition of the human gut microbiome [42–44], and select bacterial members of the gut microbiota can interact directly with fluoxetine [45,46,71]. To examine effects of maternal fluoxetine treatment on the composition of the maternal gut microbiota, we performed 16S rRNA gene sequencing on maternal fecal samples collected before treatment, on E3.5 and E6.5, and during fluoxetine or vehicle treatment on E8.5, E11.5, and E14.5. There was no significant effect of maternal fluoxetine treatment on the alpha diversity of the gut microbiota (**Fig. 4.S6A**). Of note, we observed a modest but not statistically significant reduction in fecal microbial Shannon diversity after 1 and 7 days of maternal fluoxetine treatment (**Fig. 4.S6A**, E8.5 and E14.5), which may align with the modest fluoxetine-associated increases in maternal cecal weight on E14.5 (**Fig. 4.S2D**). There was also no overt effect of maternal fluoxetine treatment on global beta diversity of the gut microbiota, as assessed by principal coordinate analysis of weighted Unifrac distances (**Fig. 4.S6B**). Despite no significant changes in the relative levels of abundant bacterial taxa (**Fig. 4.S6C, D**), select rare microbial taxa were significantly altered in the fecal microbiota of fluoxetine-treated dams compared to vehicle-treated controls (**Fig. 4.S6E-H**). In particular, maternal fluoxetine treatment correlated with significant increases in the relative abundance of Lachnospiraceae bacterium COE1, a short-chain fatty acid-producing bacterium [3] (**Fig. 4.S6E**, p(E8.5) = 0.008, p(E11.5) = 0.005, p(E14.5) = 0.039). The relative abundances of Blautia and Lachnoclostridium were significantly increased on select days after maternal fluoxetine treatment (**Fig. 4.S6F** p(E6.5) =

0.036, p(E8.5) = 0.033, p(E14.5) = 0.03, 6 G, p(E11.5) = 0.03). Lachnospiraceae UCG-006 was increased in the fecal microbiota of dams from the fluoxetine-treated group, compared to the vehicle-treated group, at baseline, before initiating treatments (**Fig. 4.S6H**, p(E3.5) = 0.04, p(E8.5) = 0.02). Whether these modest alterations in select low-abundance bacterial taxa will be reproducible across independent iterations of maternal fluoxetine treatment is uncertain. Overall, these results reveal that maternal fluoxetine treatment from E7.5-E14.5 has no overt effect on the composition of the maternal gut microbiota in mice.

3.5. Depletion of the maternal gut microbiome modifies fetal brain transcriptomic responses to maternal fluoxetine treatment

While the results from this study indicate that maternal fluoxetine treatment from E7.5-E14.5 does not substantially alter the composition of the maternal gut microbiota (**Fig. 4.S6**), whether the presence of a complex gut microbiota impacts fetal responses to maternal fluoxetine treatment is unclear. To address this question, female mice were pre-treated with broad spectrum antibiotics to deplete the microbiota from pre-conception through midgestation, or treated with vehicle as a negative control. Pregnant dams were subjected to oral fluoxetine or saline treatment as in experiments described above, and E14.5 fetal brains were subjected to RNA sequencing and analysis (**Fig. 4.2A**). Compared to vehicle controls (**Fig. 4.1**), maternal pre-treatment with antibiotics to deplete the gut microbiome induced widespread alterations in fetal brain transcriptomic responses to maternal fluoxetine treatment (**Fig. 4.2B**). Notably, the gene expression profiles from fetal brains belonging to antibiotic- and fluoxetine-treated dams (ABX + FLX) clustered closely with those from conventional vehicle-treated controls (SPF + Veh), and apart from antibiotic-treated controls (ABX + Veh), suggesting that the transcriptional changes occur, at least in part, in response to interactions between maternal antibiotic and fluoxetine treatment rather than additive effects of the two independent variables (**Fig. 4.2B**). Consistent with this, maternal fluoxetine treatment significantly altered 864 genes in the fetal

brain (**Figs. 4.1 and 4.2C**), and the differential expression of 264 (~30 %) of the 864 genes was prevented by maternal antibiotic pre-treatment (**Fig. 4.2C, D**). Of these 264 genes, the 161 that were upregulated in response to maternal fluoxetine treatment and prevented by maternal antibiotic pre-treatment mapped to pathways related to the regulation of membrane potential, synapse organization, and cognition (**Fig. 4.2E, Fig. 4.S7A, C**), whereas the 101 genes that were downregulated in response to maternal fluoxetine treatment and prevented by maternal antibiotic pretreatment aligned with pathways related to cell cycle, nuclear division, and DNA repair and replication pathways (**Fig. 4.2F, Fig. 4.S7B, D**). In addition to these, maternal antibiotic pre-treatment yielded an additional 840 differentially expressed genes in the fetal brains of offspring from fluoxetine-treated dams (**Fig. 4.2C**). Notably, maternal fluoxetine exposure also elicited many gene expression alterations in the fetal brain that were non-overlapping: of the 864 genes that were differentially expressed in response to fluoxetine treatment, 600 were not affected by maternal antibiotic treatment (**Fig. 4.2C, Fig. 4.S8**). Taken together, these data strongly suggest that the presence of the maternal gut microbiota conditions host physiologies that impact fetal responses to maternal fluoxetine exposure during pregnancy.

3.6. Maternal fluoxetine treatment from E7.5-E14.5 elevates Opcml expression, which is prevented by maternal antibiotic treatment

Maternal pre-treatment with antibiotics modified fetal brain transcriptomic responses to maternal fluoxetine treatment, preventing the differential expression of ~30 % of fluoxetine-induced alterations in gene expression and further inducing statistically significant changes in an additional 840 genes (**Fig. 4.2, Fig. 4.S7**). A subset of the genes that were upregulated by maternal fluoxetine treatment and prevented by antibiotic pre-treatment were relevant to pathways for cell adhesion and synapse organization, key processes for neurite outgrowth and circuit wiring (**Fig. 4.2E, G, H, Fig. 4.S7A, C, Fig. 4.S9**). In particular, maternal fluoxetine

treatment increased gene expression of the neural adhesion molecule, Opcml, in E14.5 fetal brains, as compared to vehicle-treated controls, which was prevented by maternal antibiotic pre-treatment (**Fig. 4.S9B**). These alterations were confirmed by quantitative RT-PCR of a larger set of fetal brain samples across each experimental group (**Fig. 4.S9C**). Opcml encodes the opioid binding cell adhesion molecule, a member of the IgLON subfamily, which is important for dendritic spine maturation, synaptogenesis and axonal outgrowth [72–75].

Neurite outgrowth and synapse formation are critical processes for prenatal neural circuit development [4]. To further examine effects of maternal fluoxetine treatment and antibiotic pre-treatment on localized expression of Opcml, we performed RNAScope-based in situ hybridization in E14.5 fetal brain sections using transcript-specific probes. Consistent with previous reports [72,76], Opcml transcript was distributed prominently within the developing somatosensory neocortex, thalamus, lateral ganglionic eminence, and striatum, and sparsely in the hippocampus (**Fig. 4.3A–E**). Consistent with findings from RNA sequencing (**Fig. 4.2G, Fig. 4.S9B**) and quantitative RT-PCR (**Fig. 4.S9C**), quantification of Opcml integrated density indicated that maternal fluoxetine treatment increased Opcml transcript in the fetal thalamus ($p = 0.0133$, $F = 4.751$) and lateral ganglionic eminence ($p = 0.0018$, $F = 8.260$) compared to vehicle-treated controls (**Fig. 4.3A–D, F–I**), with near significance in fetal somatosensory neocortex ($p = 0.0763$) and striatum ($p = 0.0631$), and no significant differences in the hippocampus (**Fig. 4.3E, J**). The localized increases in Opcml transcript were prevented by maternal antibiotic pre-treatment (**Fig. 4.3A–D, F–I**), indicating that depletion of the maternal microbiome abrogates this particular fetal response to maternal fluoxetine treatment.

3.7. Antibiotic pre-treatment of fluoxetine-treated dams has no significant effects on gross metrics of maternal and fetal health, maternal serum fluoxetine levels, or components of the fetal serotonergic system

The gut microbiome has the capacity to modify host responses to SSRIs directly or indirectly through myriad mechanisms. Particular gut microbes are reported to respond to, metabolize, or biotransform fluoxetine [45,71,77]. To assess the possibility of such direct effects of the maternal gut microbiome on the bioavailability of fluoxetine in the host, fluoxetine concentrations were measured by mass spectrometry in fluoxetine-treated dams that were pre-treated with antibiotics. There was no statistically significant effect of maternal antibiotic pre-treatment on E14.5 serum fluoxetine levels in fluoxetine-treated dams (**Fig. 4.S1A, B**). This suggests that the effects of maternal gut microbiome on modifying fetal responses to maternal fluoxetine treatment are likely not due to direct interactions between gut bacteria and antibiotics or fluoxetine. It further suggests that any indirect effects of the maternal gut microbiome on modulating host physiological processes that impact fluoxetine bioavailability, such as host xenobiotic metabolism or transport [38,40,41,78], are also not responsible.

We next considered if the maternal gut microbiome may impact the fetal serotonergic system to modify responses to maternal fluoxetine treatment. Maternal antibiotic pre-treatment had no significant effects on concentrations of 5-HT or tryptophan in the fetal brain (**Fig. 4.S4C, D**), or on numbers of 5-HT-, Tph2-, or SERT-positive neurons in the fetal DRN (**Fig. 4.S5**). This suggests that the maternal gut microbiome does not modify fetal transcriptomic responses to fluoxetine via alterations to the fetal serotonergic system. There were also no significant effects of maternal antibiotic pretreatment on maternal weight, litter size or fetal volume (**Fig. 4.S2**), suggesting that the ability of the maternal gut microbiota to modify fetal responses to maternal fluoxetine treatment are not due to overt microbial influences on gross metrics of maternal or fetal health. Taken together, these data support the notion that the maternal gut microbiome modifies fetal responses to maternal fluoxetine treatment through indirect effects on host physiologies that impact fetal neurodevelopment.

4. Discussion

While maternal depression is a growing medical concern, precisely how SSRI use during pregnancy impacts maternal and offspring health remains a controversial issue [10,12,18]. Results from this study demonstrate that effects of maternal SSRI use on offspring development can begin prenatally, as maternal treatment with the common SSRI fluoxetine during pregnancy induces global changes in the fetal brain transcriptome by midgestation in mice. In addition, we find that the effects of maternal SSRI exposure on gene expression in the fetal brain are modified by maternal treatment with antibiotics. This suggests that the maternal gut microbiome is a physiological factor that influences host responses to SSRI exposure.

Notably, the experimental paradigms used in this study isolate maternal SSRI exposure and maternal antibiotic treatment to determine their individual vs. combined effects on fetal neurodevelopment. A major caveat of the study is that the interventions are administered to conventional dams in the absence of a model of maternal adversity. This detracts from the clinical relevance of the system, as the study does not capture effects of SSRIs that may be unique to the context of a maternal affective disorder. Rather, the findings from the study provide fundamental proof-of-principle that maternal exposure to fluoxetine during midgestation can impact gene expression in the brain, independently of maternal adversities such as depression, stress or anxiety. They further reveal interactions between the effects of maternal fluoxetine exposure and the effects of the maternal microbiome which together determine outcomes on fetal brain transcriptomes. Based on these results, future efforts are warranted to explore interactions between maternal SSRI use and the gut microbiome in the context of a maternal depression and/or anxiety model.

Interestingly, the influences of maternal fluoxetine treatment on gene expression in the fetal brain occur independently of alterations in the fetal serotonergic system. Although prior studies report that fluoxetine can readily cross the placenta to enter the fetus in humans, mice and rats [79–81], findings from our experimental paradigm of oral fluoxetine treatment of dams suggest that effects on the fetal brain are likely not due to direct entry of fluoxetine to inhibit fetal

SERT. In addition, previous studies in rodents reported that prenatal fluoxetine treatment induces maternal weight loss, reduced live birth rate, decreased litter size, and increased neonatal mortality [60,82], which we also did not observe. The discrepancies could be due to differences in length of fluoxetine treatment (previous studies treated for 14 days from early to midgestation or mid to late gestation vs. in our experiments we treated for 7 days from early to midgestation), route of administration (previous studies, drinking water vs. in our experiments, via oral gavage), or dosage (previous studies, 10− 12 mg/kg vs. in our experiments, 10 mg/kg reflecting clinically relevant doses of fluoxetine, as scaled to mice). Overall, the lack of overt disruptions to maternal and fetal health in the experimental paradigm used in this study offer the opportunity to examine effects of maternal fluoxetine treatment on fetal neurodevelopment in the absence of potentially confounding developmental alterations.

We observe that maternal fluoxetine treatment from E7.5 to E14.5 induces widespread changes in the fetal brain transcriptome during midgestation, characterized by differential expression of genes relevant to synapse organization, cognition, locomotory behavior, regulation of mitotic cell cycle and DNA repair pathways. Interestingly, a previous study of maternally stressed Slc6a4-/- mice, which are deficient in SERT, the molecular target for fluoxetine, reported that E13.5 fetal brains exhibited increased expression of genes involved in neuron projection and forebrain development pathways [83]. A comparison of the gene expression changes reported in the Slc6a4-/- study relative to those observed herein suggest some common phenotypes, in genes related to synapse organization, synaptic vesicle, cell cycle, and DNA replication, but also many differing phenotypes. For example, we observe substantial alterations in genes related to developmental cell growth, regulation of microtubule organization, ribosome organization and RNA splicing in fetal brains of offspring from dams treated with fluoxetine, which were not reported in offspring of Slc6a4-/- dams. Many factors may contribute to the discrepancies, including developmental influences of constitutive SERT deficiency as opposed to the brief SSRI intervention used in this study. Another potential

consideration is the possibility that fluoxetine has physiological effects that occur independently of SERT inhibition. Indeed, fluoxetine is reported to exhibit “off-target” interactions with serotonin 5-HT2B receptor, dopamine D2 receptor, TREK-1 potassium channel, and purine P2X4 receptor [84–88] and to influence many physiological systems outside of the nervous system, such as the immune and vascular systems [89,90]. Further, fluoxetine could potentially regulate fetal brain development through a SERT-independent pathways, by binding to tyrosine kinase receptor 2, the brain-derived neurotrophic factor receptor, to regulate embryonic cortical cell cycle, neuronal proliferation, and neurogenesis [91,92] or act on the dopamine D2 receptor in the developing brain to impact organization of neuronal networks [93].

The gut microbiome modulates the peripheral serotonergic system, promoting 5-HT biosynthesis from enterochromaffin cells in the gastrointestinal tract [94–97], as well as the central serotonergic system, altering the expression of subsets of 5-HT receptors and levels of 5-HT in select brain regions [98,99]. Recent studies suggest that the gut microbiome can also interact with SSRIs, through direct or indirect mechanisms [45,100–102]. We find that pre-treating dams with antibiotics to deplete the maternal gut microbiome substantially modifies fetal brain transcriptomic responses to maternal fluoxetine treatment. In particular, ~30 % of the gene expression changes induced by maternal fluoxetine treatment are prevented by maternal antibiotic pre-treatment, and an additional 840 genes are differentially expressed when fluoxetine-treated dams are pre-treated with antibiotics.

Notably, the transcriptomic profiles induced by the combined maternal treatments are distinct from those seen in response to maternal fluoxetine alone or antibiotics alone. This suggests that there are interactions between the two variables, maternal SSRI exposure and maternal gut microbiome, that together alter gene expression in the fetal brain. Notably, these influences of the maternal gut microbiome appear to be conferred via its homeostatic effects on host physiology, rather than select taxonomic or functional shifts in response to fluoxetine treatment. Indeed, we observe no striking effects of maternal fluoxetine treatment from E7.5-

E14.5 on the composition of the gut microbiota, with Lachnospiraceae COE1 being the only taxon that was persistently and significantly increased in response to maternal fluoxetine treatment. While this could align with previous reports that UC Lachnospiraceae is increased with fluoxetine treatment and decreased in depressed patients [39,45,101,103], another study suggests that fluoxetine-induced changes in the maternal gut microbiome occur primarily after treatment from gestation through the lactation period [6]. In the absence of fluoxetine-induced shifts in the composition of the gut microbiota, our data reveal that the presence of the complex maternal gut microbiome, rather than select shifts in the microbiota, influences host responses to maternal fluoxetine treatment. In considering potential pathways involved, we observed no effects of maternal antibiotic treatment on the serum bioavailability of fluoxetine and also no effects of maternal antibiotic treatment on the fetal serotonergic system. These results render unlikely the possibility that the maternal microbiome interacts directly with fluoxetine to alter its downstream actions on the serotonergic system. The finding that maternal antibiotic treatment does not alter fluoxetine bioavailability also renders unlikely the possibility that the maternal microbiome alters pathways for host xenobiotic metabolism of fluoxetine. While exact mechanisms remain unclear, one hypothesis is that the maternal microbiome conditions host physiological states that modify responses to fluoxetine, such as immune homeostasis [104] or stress response [105,106]. Future studies are warranted to identify the mechanisms by which the maternal gut microbiome modifies fetal neurodevelopmental responses to maternal SSRI use.

We observe that maternal fluoxetine treatment induces widespread changes in the fetal brain transcriptome that are modified by maternal antibiotic treatment. We highlight, validate and localize Opcml in particular, based on its key role in regulating synapse formation and neurite outgrowth during fetal neurodevelopment [107–109]. Notably, recent large-scale genome-wide association studies identify key polymorphisms in Opcml (i.e., rs3016384, rs1941213, and rs132568126) that are associated with schizophrenia [110–112]. In addition, Opcml deficiency in

mice results in immature spine formation and deficits in sensorimotor gating and cognitive behaviors [75]. Interestingly, Opcml expression is temporally regulated, suggesting that increased Opcml during development may impact downstream developmental milestones and behavior [75,113]. These findings suggest that alterations in Opcml during development may contribute to the effects of perinatal fluoxetine treatment on offspring brain development and behavior. Moreover, Opcml is expressed in both neurons and astrocytes [72,85,114,115], providing the further opportunity to examine cell-type specific effects of maternal fluoxetine treatment and the maternal gut microbiome on gene expression and cellular function.

Notably, the findings in this study reveal widespread effects of maternal fluoxetine exposure on gene expression profiles in the fetal brain, including Opcml in particular, that are modified by maternal antibiotic treatment. However, it remains unclear whether these changes result in meaningful alterations in fetal neurodevelopment and brain and behavioral outcomes in the offspring. Studies on maternal SSRI use during pregnancy have reported disparate and sometimes conflicting results, spanning negative [116–122], positive [113] and neutral (no) effects [10,13–15] on offspring neurophysiology and behavior. Future research is needed to evaluate the downstream cellular and functional consequences of maternal fluoxetine-induced changes in fetal brain transcriptomes, including the modifying effects of maternal microbiome status.

Overall, understanding effects of the gut microbiome in modifying host responses to SSRI treatment could reveal fundamental insights into the biological bases of SSRI efficacy and the variability therein. Furthermore, examining interactions between the maternal gut microbiome and SSRI use during pregnancy is critical for identifying risks and informing best practices for clinical depression, toward ensuring the health of both mother and offspring.

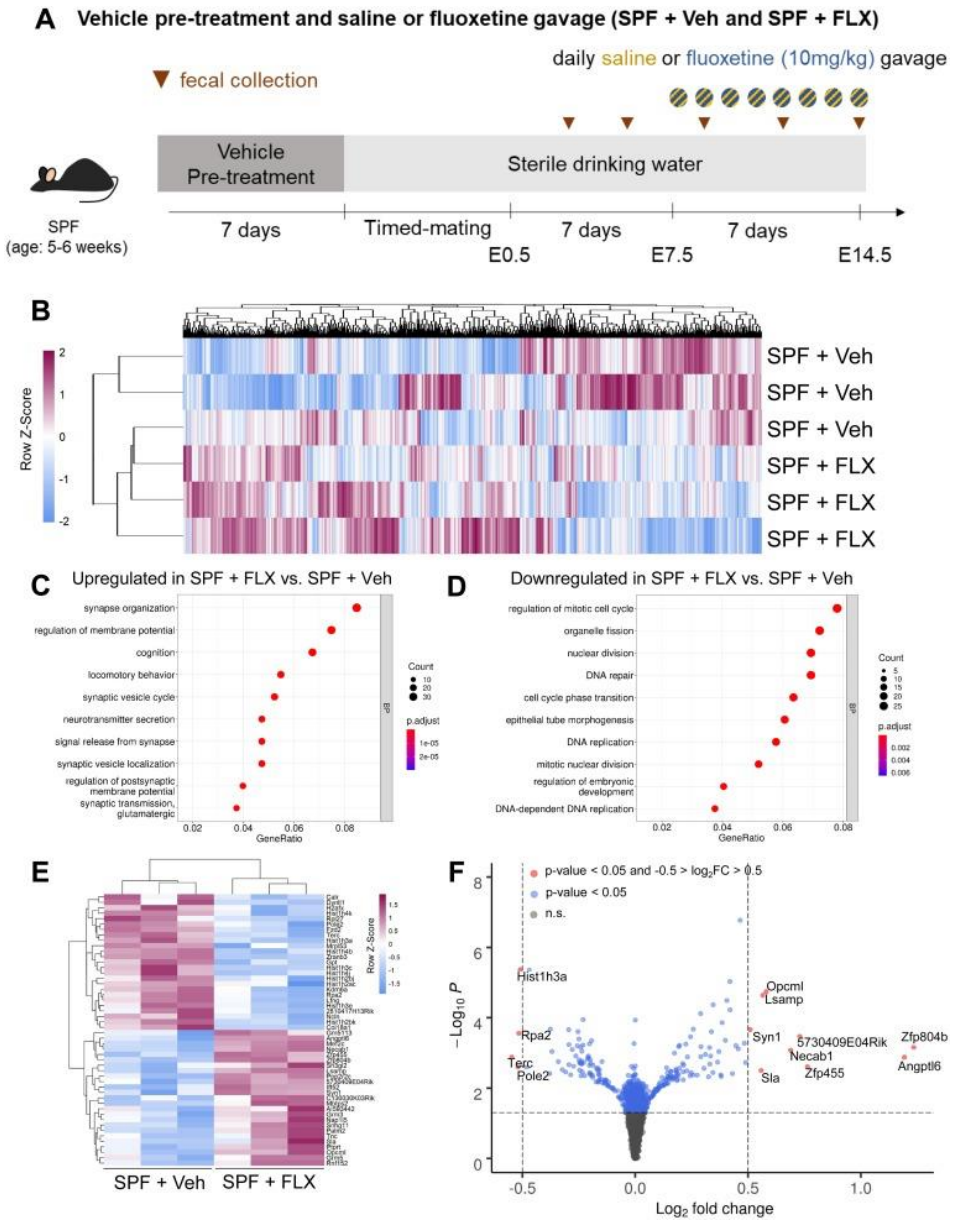

Figure 4.1. Maternal fluoxetine treatment alters fetal brain gene expression. A, Experimental timeline of SPF + Veh and SPF + FLX groups. **B,** Heatmap of 864 differentially expressed genes ($p < 0.05$) in E14.5 fetal brains from SPF + FLX compared to SPF + Veh dams (Wald test, n = 3, 3, respectively). **C,** Top 10 biological process (BP) gene ontology (GO) terms that are upregulated in E14.5 fetal brains from SPF + FLX compared to SPF + Veh dams (Fisher's Exact test, n = 3, 3, respectively). Gene ratio: number of genes present in dataset vs present in GO term. **D,** GO term enrichment analysis of top 10 biological process (BP) that are downregulated in E14.5 fetal brains of SPF + FLX compared to SPF + Veh dams (Fisher's Exact test, n = 3, 3, respectively). **E,** Heatmap of 25 most upregulated and 25 most downregulated differentially expressed genes ($p < 0.05$) in E14.5 fetal brains from SPF + Veh compared to SPF + FLX dams (Wald test, n = 3, 3, respectively). **F,** Volcano plot of differentially expressed genes in E14.5 fetal brain of embryos from SPF + FLX compared to SPF + Veh dams. Blue: Differentially expressed genes that are $p < 0.05$. Red: Differentially expressed genes that have log2fold change greater than 0.5 and $p < 0.05$.

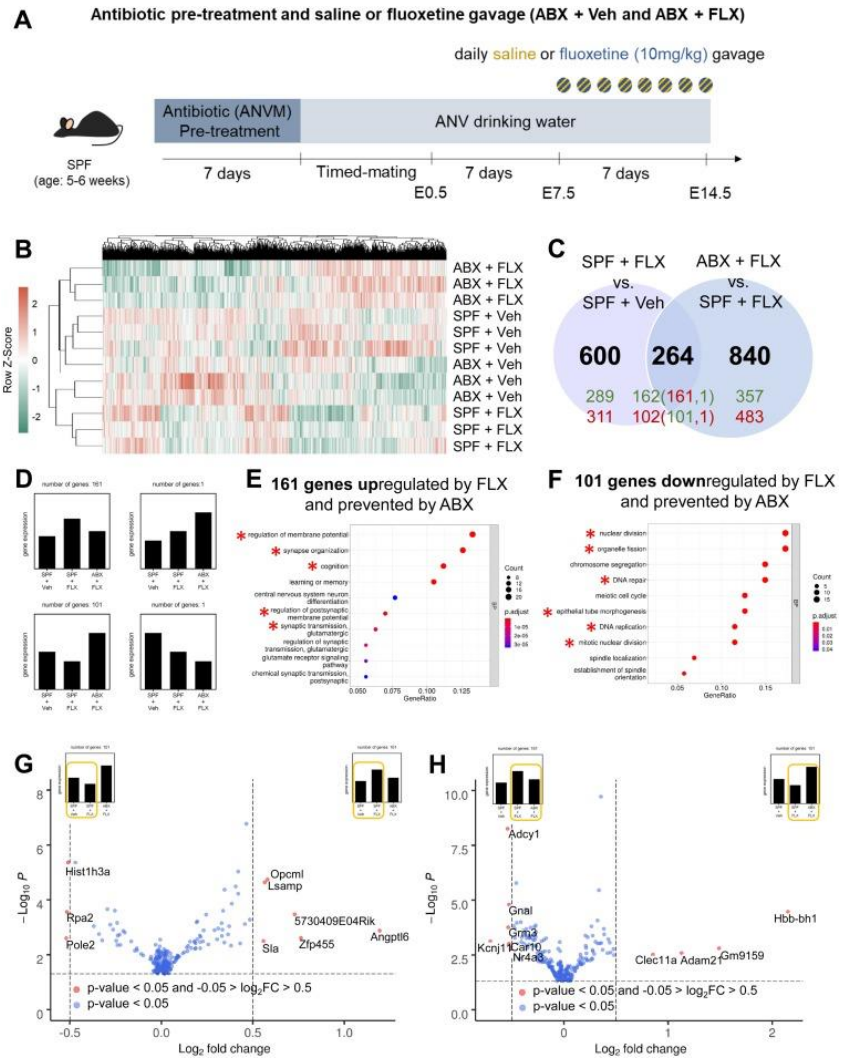

Figure 4.2. Depletion of the maternal microbiome modifies the effects of maternal fluoxetine treatment on gene expression in the fetal brain. A, Antibiotic depletion treatment and vehicle or fluoxetine exposure during pregnancy. **B,** Heatmap of differentially expressed genes ($p < 0.05$) in E14.5 fetal brain from SPF + Veh, SPF + FLX, ABX + Veh, and ABX + FLX dams ($p < 0.05$). **C,** Venn diagram of differentially expressed genes in E14.5 fetal brains from SPF + FLX compared to SPF + Veh dams and ABX + FLX compared to SPF + FLX dams ($p < 0.05$). Black: total genes, Green: Upregulated genes, Red: Downregulated genes. **D,** Schematic representation of comparative expression levels of genes in the center of the venn diagram. **E,** Gene ontology analysis of upregulated genes in SPF + FLX compared to both SPF + Veh and ABX + FLX (161 genes). **F,** Gene ontology analysis of downregulated genes in E14.5 fetal brains from SPF + FLX compared to ABX + FLX and SPF + Veh (101 genes). **G**, Volcano plot of differentially expressed genes in E14.5 fetal brains from SPF + FLX compared to SPF + Veh dams. Differentially expressed genes that are $p < 0.05$ (blue) and differentially expressed genes that have log2fold change greater than 0.5 (red). **H**, Volcano plot of differentially expressed genes in E14.5 fetal brains from ABX + FLX compared to SPF + FLX (right) dams. Differentially expressed genes that are $p < 0.05$ (blue) and differentially expressed genes that have log2fold change greater than 0.5 (red). ANVM: ampicillin, neomycin, vancomycin, and metronidazole. ANV: ampicillin, neomycin, and vancomycin.

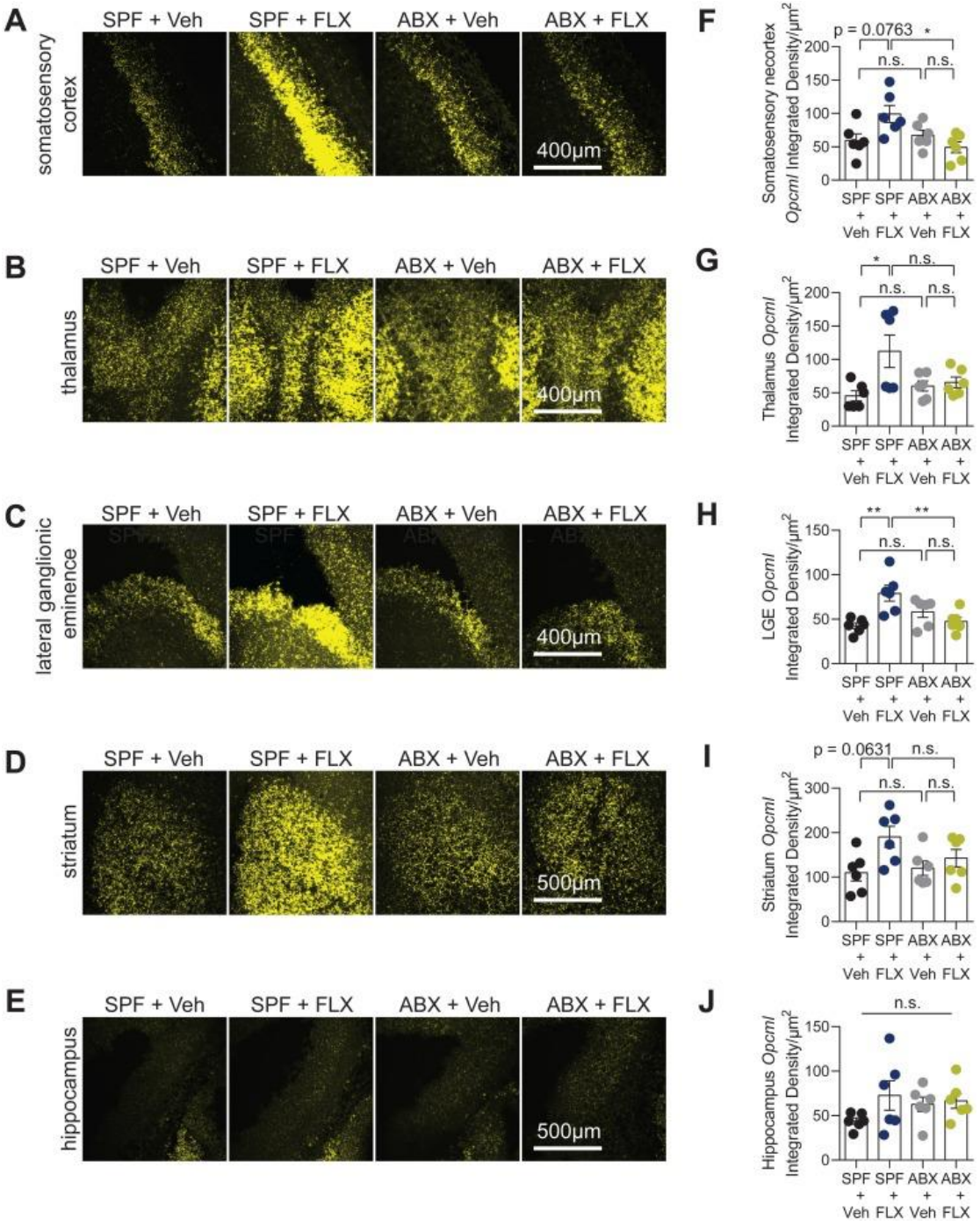

Figure 4.3. Maternal fluoxetine treatment alters *Opcml* gene expression in the embryonic brain. Representative images of Opcml transcript (yellow) in the somatosensory neocortex (**A**), thalamus (**B**), lateral ganglionic eminence (**C**), striatum (**D**), and hippocampus (*E*) in E14.5 embryonic brains from SPF + Veh, SPF + FLX, ABX + Veh, and ABX + FLX dams. Quantification of Opcml integrated density normalized to area in the somatosensory neocortex (**F**), thalamus (**G**), lateral ganglionic eminence (**H**), striatum (**I**), and hippocampus (*J*) of E14.5 embryonic brains from SPF + Veh, SPF + FLX, ABX + Veh, and ABX + FLX dams (two-way ANOVA with Tukey's, n = 6, 6, 6, 6 dams). Scale bar: 400 μm and 500 μm. n.s.: not significant, * $p < 0.05$, ** $p < 0.01$, *** $p < 0.001$.

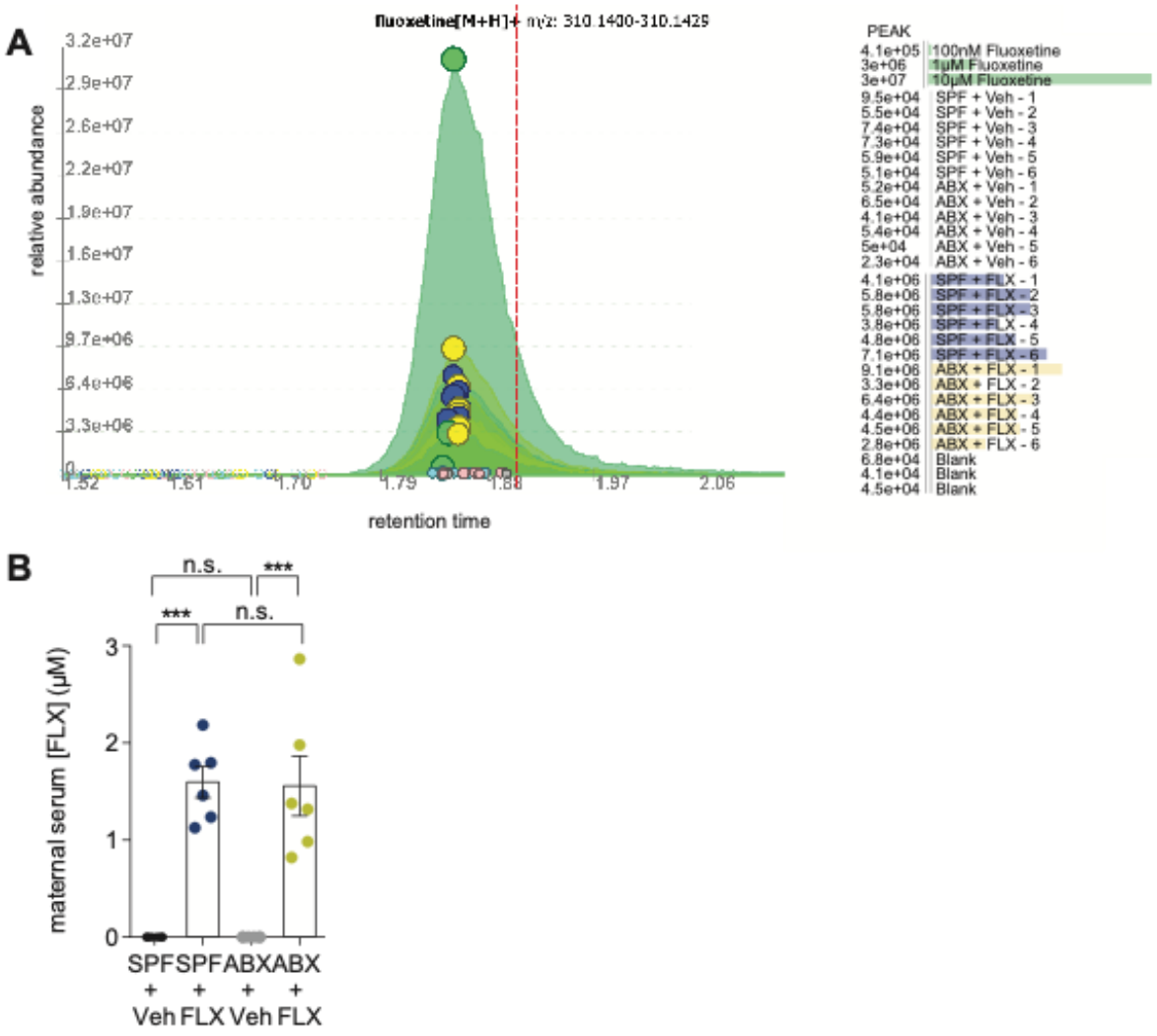

Figure 4.S1. Levels of fluoxetine in maternal serum. A, Mass spectrometry dose-response of 100nM, 1µM, and 10µM fluoxetine in maternal serum, maternal sera of SPF+ Veh, ABX + Veh, SPF+ FLX, ABX + FLX groups at E14.5. **B,** Concentration of fluoxetine in maternal serum of SPF + Veh, SPF + FLX, ABX + Veh and ABX + FLX groups (two-way ANOVA with Tukey's, n = 6, 6, 6, 6, respectively). n.s.: not significant, *** $p < 0.001$

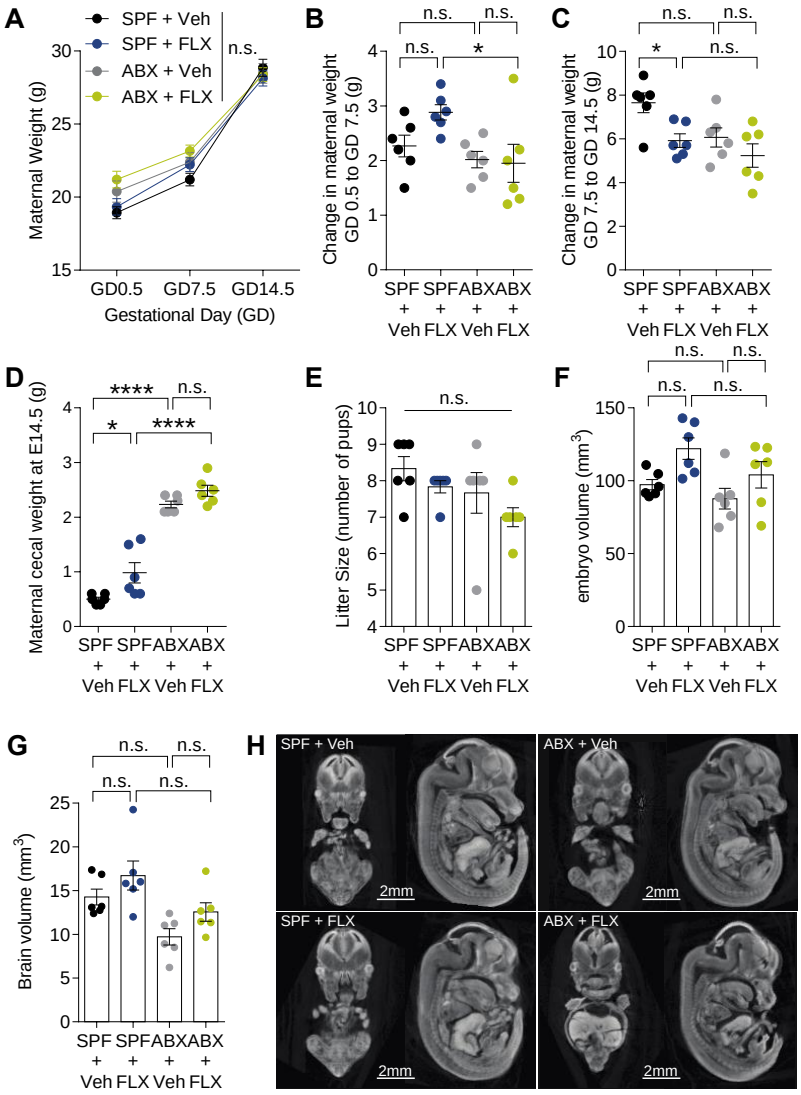

Figure 4.S2. Effects of maternal fluoxetine treatment with microbiome depletion on maternal weight, litter size, embryo size and brain volume. A, Maternal weight of SPF + Veh, SPF + FLX, ABX + Veh and ABX + FLX groups on gestational day 0.5, 7.5, and 14.5 (two-way ANOVA with Tukey's, n = 6, 6, 6, 6, respectively). **B,** Change in maternal weight of SPF+ Veh, SPF + FLX, ABX + Veh and ABX + FLX groups from gestational day 0.5 to 7.5. (two-way ANOVA with Tukey's, n = 6, 6, 6, 6 respectively). **C,** Change in maternal weight of SPF+ Veh, SPF + FLX, ABX + Veh and ABX + FLX groups from gestational day 7.5 to 14.5. (two-way ANOVA with Tukey's, n = 6, 6, 6, 6 respectively). **D,** Maternal cecal weight of SPF+ Veh, SPF + FLX, ABX + Veh and ABX + FLX at E14.5. (two-way ANOVA with Tukey's, n = 6, 6, 6, 6 respectively). **E,** Number of pups born to dams of SPF + Veh, SPF + FLX, ABX + Veh and ABX + FLX. (two-way ANOVA with Tukey's, n = 6, 6, 6, 6 respectively). **F,** Volume of SPF+ Veh, SPF + FLX, ABX + Veh and ABX + FLX embryos at E14.5. (two-way ANOVA with Tukey's, n = 6, 6, 6, 6 respectively) **G,** Volume of SPF+ Veh, SPF + FLX, ABX + Veh and ABX + FLX embryonic brain at E14.5. (two-way ANOVA with Tukey's, n = 6, 6, 6, 6 respectively) **H,** Representative coronal and sagittal microcomputed tomography images of SPF+ Veh, SPF + FLX, ABX + Veh and ABX + FLX embryos at E14.5. (n = 6, 6, 6, 6 respectively). n.s.: not significant, * $p < 0.05$, **** $p < 0.0001$.

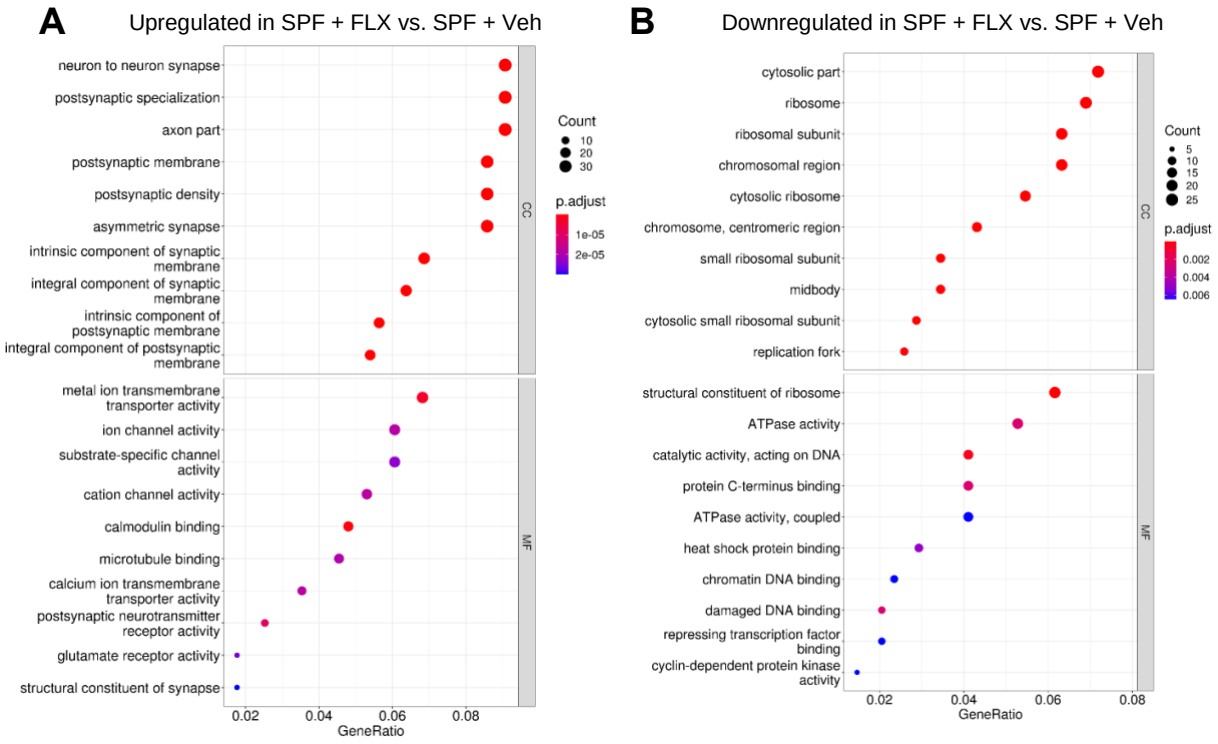

Figure 4.S3. Maternal fluoxetine treatment alters fetal brain molecular function and cellular component pathways. A and B, Top 10 molecular function (MF) and cellular component (CC) gene ontology (GO) terms enrichment analysis of genes upregulated (**A**) and downregulated (**B**) in E14.5 fetal brain from SPF+FLX compared to SPF+Veh dams.

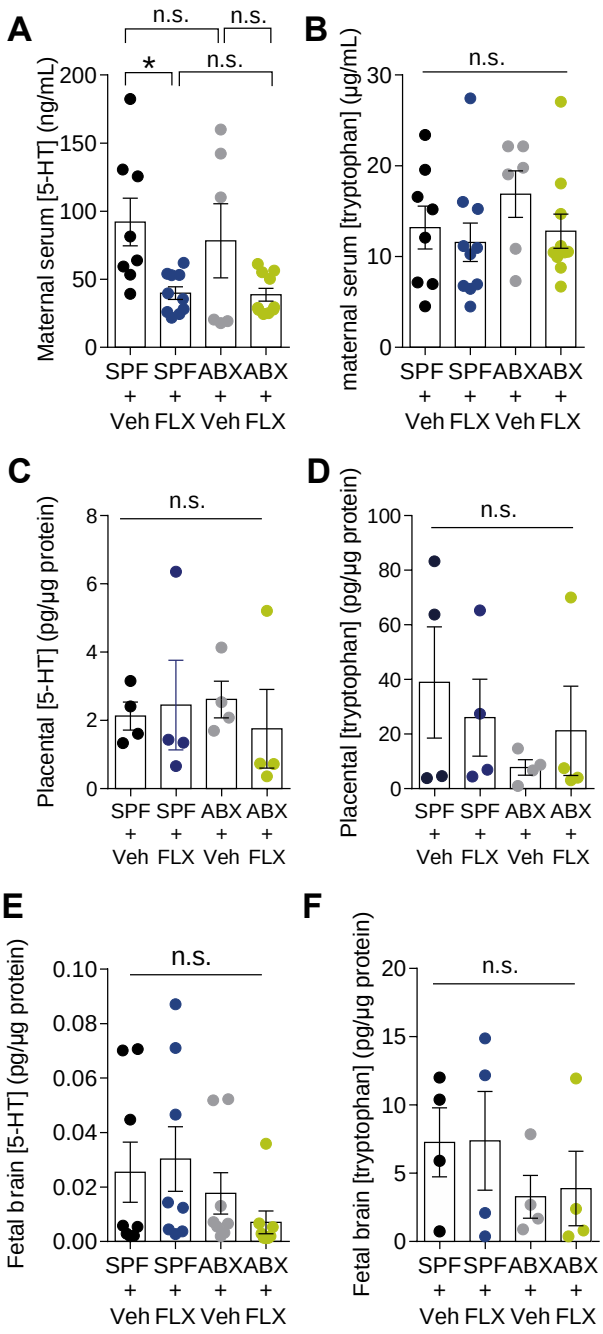

Figure 4.S4. Effects of maternal fluoxetine treatment on maternal, placental, and fetal brain serotonin and tryptophan levels. A, B, Serum levels of serotonin (5-HT) (**A**) and tryptophan (**B**) in gestational day 14.5 murine dams that were conventionally colonized with vehicle (SPF + Veh) or fluoxetine (SPF + FLX) gavage and antibiotic treated with vehicle (ABX + Veh) or fluoxetine (ABX + FLX) gavage. (one- way ANOVA with Tukey's, n = 8, 10, 6, 10 dams, respectively) **C**, **D**, Placental levels of 5-HT (**C**) and tryptophan (**D**) on gestational day E14.5 (two-way ANOVA with Tukey's, n = 4 dams respectively). **E, F,** Fetal brain levels of 5-HT (two-way ANOVA with Tukey's, n = 8) (**E**) and tryptophan (**F**) on gestational day E14.5 (two-way ANOVA with Tukey's, n = 4). n.s.: not significant, * $p < 0.05$

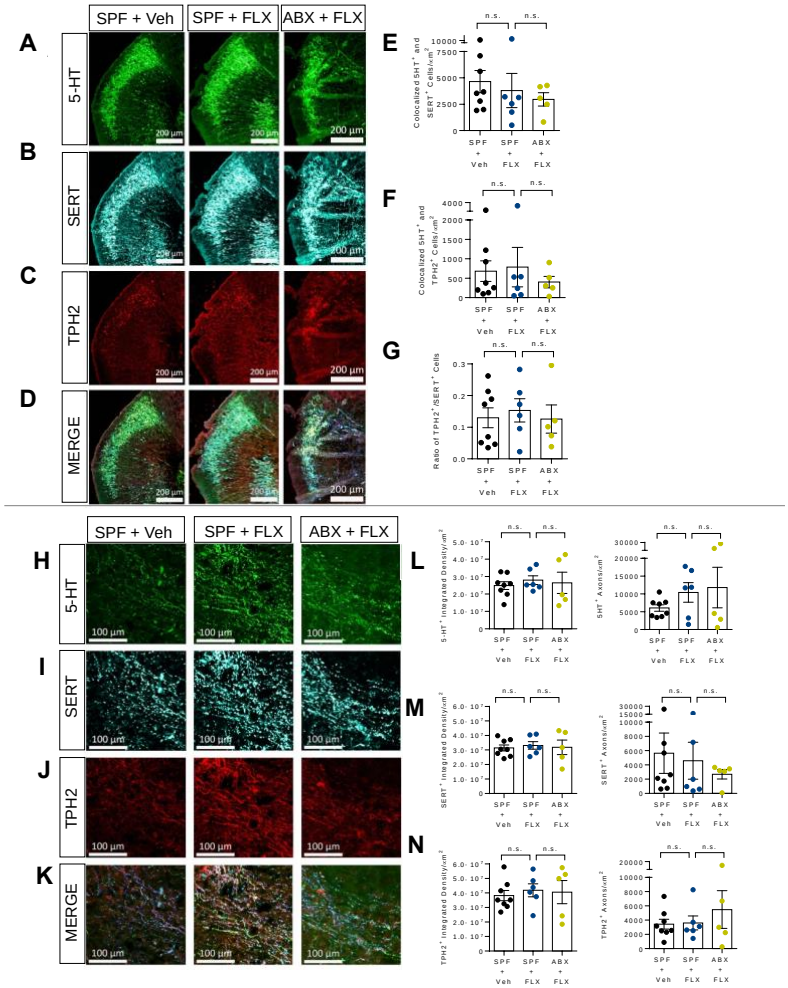

Figure 4.S5. Gestational fluoxetine exposure has no significant effect on the fetal brain serotonergic system. Representative images of SPF + Veh, SPF + FLX, and ABX + FLX sagittal sections showing 5-HT (**A**), SERT (**B**), Tph2 (**C**), and overlay (**D**) staining for cells in the dorsal raphe nucleus (DRN). Quantification of colocalized 5-HT+ & SERT+ (**E**) and 5-HT+ & Tph2+ (**F**) cells in the DRN of SPF + Veh, SPF + FLX, and ABX + FLX embryo brains (One-way ANOVA, n = 8, 6, 5). **G**, The ratio of Tph2+ cells to SERT+ cells in DRN of SPF + Veh, SPF + FLX, and ABX + FLX embryo brains. (one-way ANOVA, n = 8, 6, 5). Representative images of 5-HT (**H**), SERT (**I**), Tph2 (**J**), and overlay (**K**) axon projections from the DRN to the prefrontal cortex (PFC) in sagittal SPF + Veh, SPF + FLX, and ABX + FLX embryonic brain sections. **L,** (Left) Quantification of 5-HT integrated density in DRN to PFC axon projections in SPF + Veh, SPF + FLX, and ABX + FLX sagittal embryo brain sections (one-way ANOVA, n = 8, 6, 5). (Right) Quantification of number of 5-HT+ axons in SPF + Veh, SPF + FLX, and ABX + FLX sagittal embryo brain sections (one-way ANOVA, n = 8, 6, 5). **M,** (Left) Quantification of SERT integrated density in DRN to PFC axon projections in SPF + Veh, SPF + FLX, and ABX + FLX sagittal embryo brain sections (one-way ANOVA, n = 8, 6, 5). (Right) Quantification of SERT+ puncta in DRN to PFC axon projections in SPF + Veh, SPF + FLX, and ABX + FLX sagittal embryo brain sections (one-way ANOVA, n = 8, 6, 5). **N,** (Left) Quantification of Tph2 integrated density in DRN to PFC axon projections in SPF + Veh, SPF + FLX, and ABX + FLX sagittal embryo brain sections (one-way ANOVA, n = 8, 6, 5). (Right) Quantification of number of TPH2+ axons in SPF + Veh, SPF + FLX, and ABX + FLX sagittal embryo brain sections (one-way ANOVA, n = 8, 6, 5). Scale bar: 100 µm. n.s.: not statistically significant

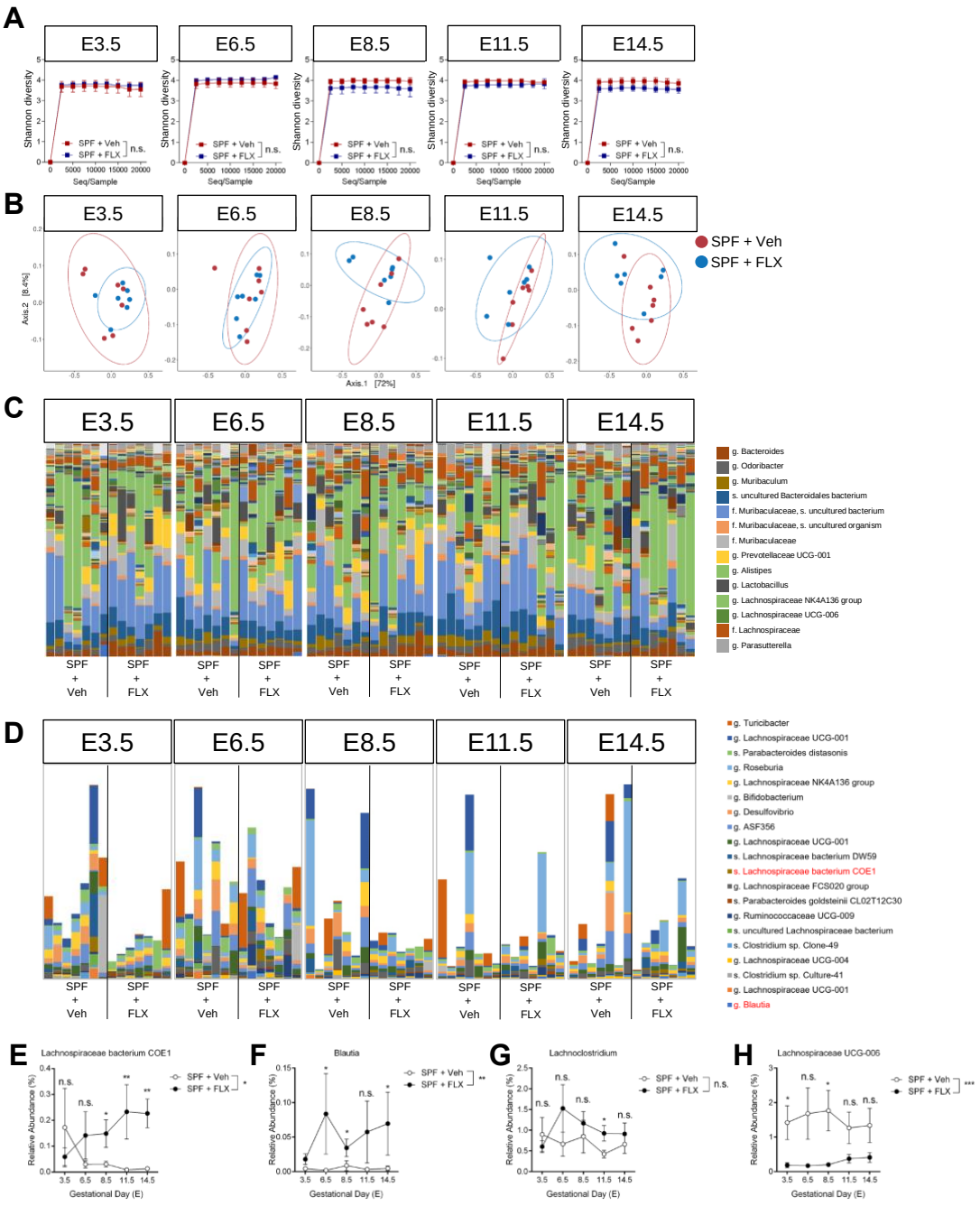

Figure 4.S6. Maternal fluoxetine treatment has no overt effect on the composition of the maternal gut microbiota. A, Alpha rarefaction plots of Shannon diversity of fecal samples from E3.5, E6.5, E8.5, E11.5, and E14.5 SPF+Veh and SPF+FLX dams. **B,** Weighted Unifrac PCoA plots of fecal samples from E3.5, E6.5, E8.5, E11.5, and E14.5 SPF+Veh and SPF+FLX dams. **C,** Taxa bar plots and **D,** Relative abundance of 20 rarest taxa identified with SILVA database in fecal samples from E3.5, E6.5, E8.5, E11.5, and E14.5 SPF+Veh and SPF+FLX dams. Relative abundance of *Lachnospiraceae* bacterium COE1 (**E**), *Blautia* (**F**), *Lachnoclostridium* (**G**), and *Lachnospiraceae* UCG-006 (**H**) based on 16S rRNA gene sequencing of fecal samples from SPF+Veh and SPF+FLX dams on gestational day E3.5, E6.5, E8.5, E11.5, and E14.5 (Kruskal-Wallis Test, n = 7, 7, respectively). n.s.: not significant, * $p < 0.05$, ** $p < 0.01$.

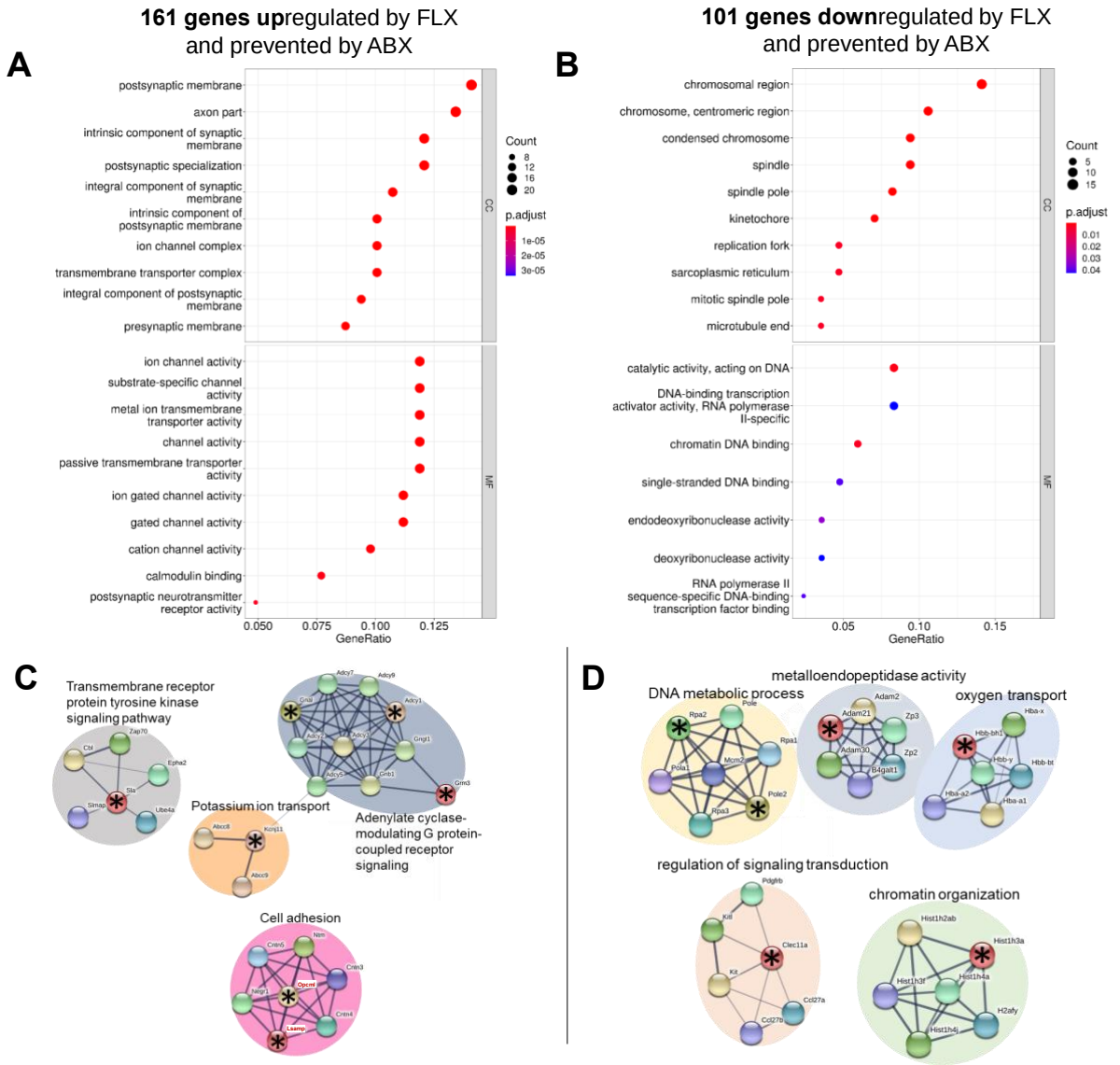

Figure 4.S7. Interactions between maternal fluoxetine treatment and the maternal microbiome regulate gene ontology pathways. A, Top 10 molecular function (MF) and cellular component (CC) gene ontology (GO) terms that are upregulated in E14.5 fetal brains from SPF+FLX compared to SPF+Veh and ABX+FLX dams, selected by most abundant and p.adjust < 0.05 Gene ratio: number of genes present in dataset vs present in GO term. **B,** Top 10 molecular function (MF) and cellular component (CC) gene ontology (GO) terms that are downregulated in E14.5 fetal brains from SPF+FLX compared to SPF+Veh and ABX+FLX dams. **C,** STRING protein interaction network of genes significantly upregulated, greater than 0.5-fold, in E14.5 fetal brain from SPF+FLX compared to SPF+Veh and ABX+FLX dams. **D,** STRING protein interaction network of genes significantly downregulated (>0.5 fold) in E14.5 fetal brains from SPF+FLX compared to SPF+Veh and ABX+FLX dams.

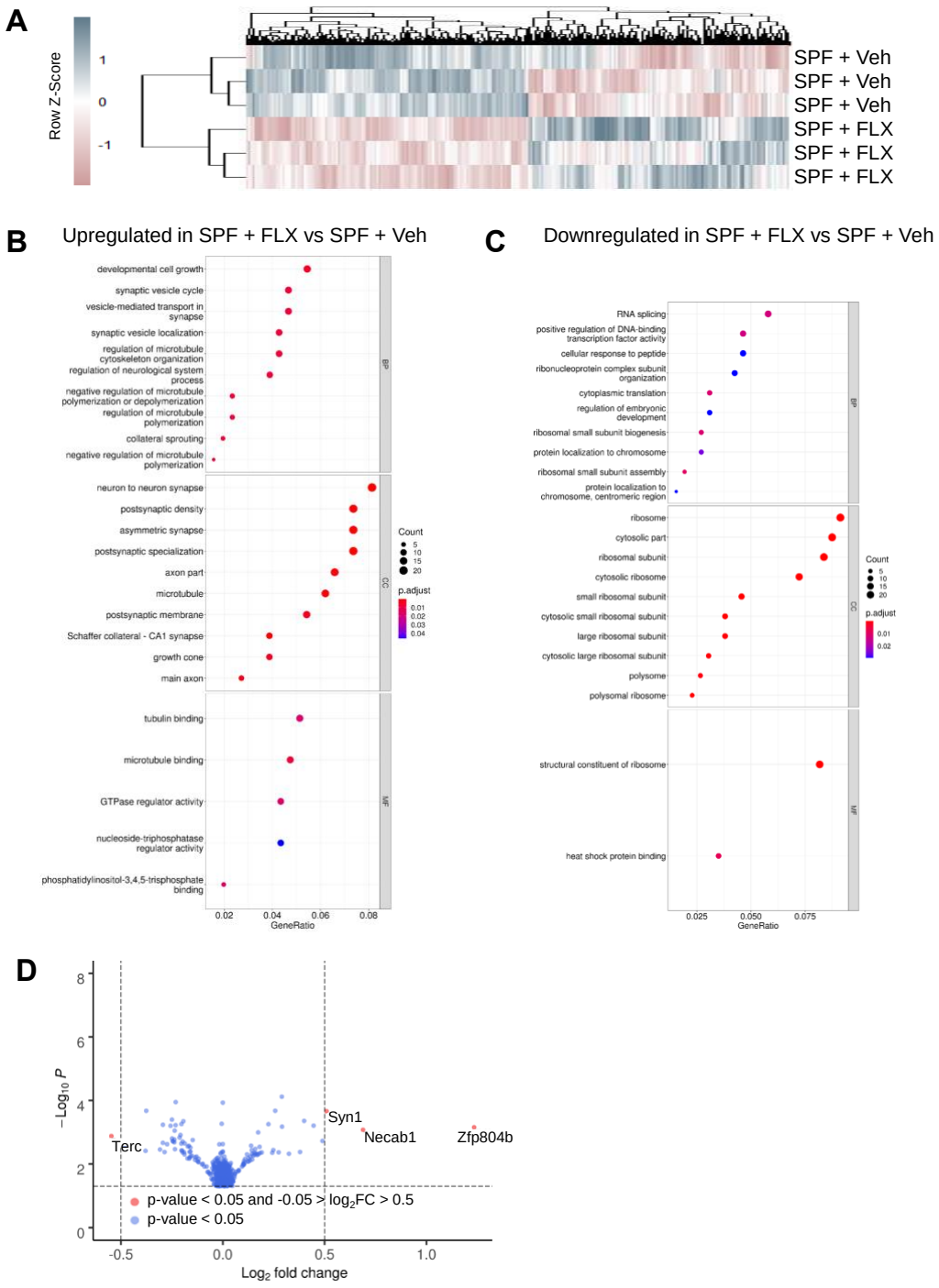

Figure 4.S8. Effects of maternal fluoxetine treatment on fetal brain gene expression that occur independently of the maternal microbiota. A, Heatmap of 600 differentially expressed genes in E14.5 fetal brain from SPF + Veh compared to SPF + FLX dams. **B, C,** GO enrichment analysis of upregulated (**B**) and downregulated (**C**) genes in E14.5 fetal brains from SPF + FLX compared to SPF + Veh dams. **D,** Volcano plot of 600 differentially expressed genes (p<0.05) in E14.5 fetal brains from SPF + FLX compared to SPF + Veh dams. Red, significant and greater than 0.5-fold or less than -0.5-fold, blue, significant (p<0.05).

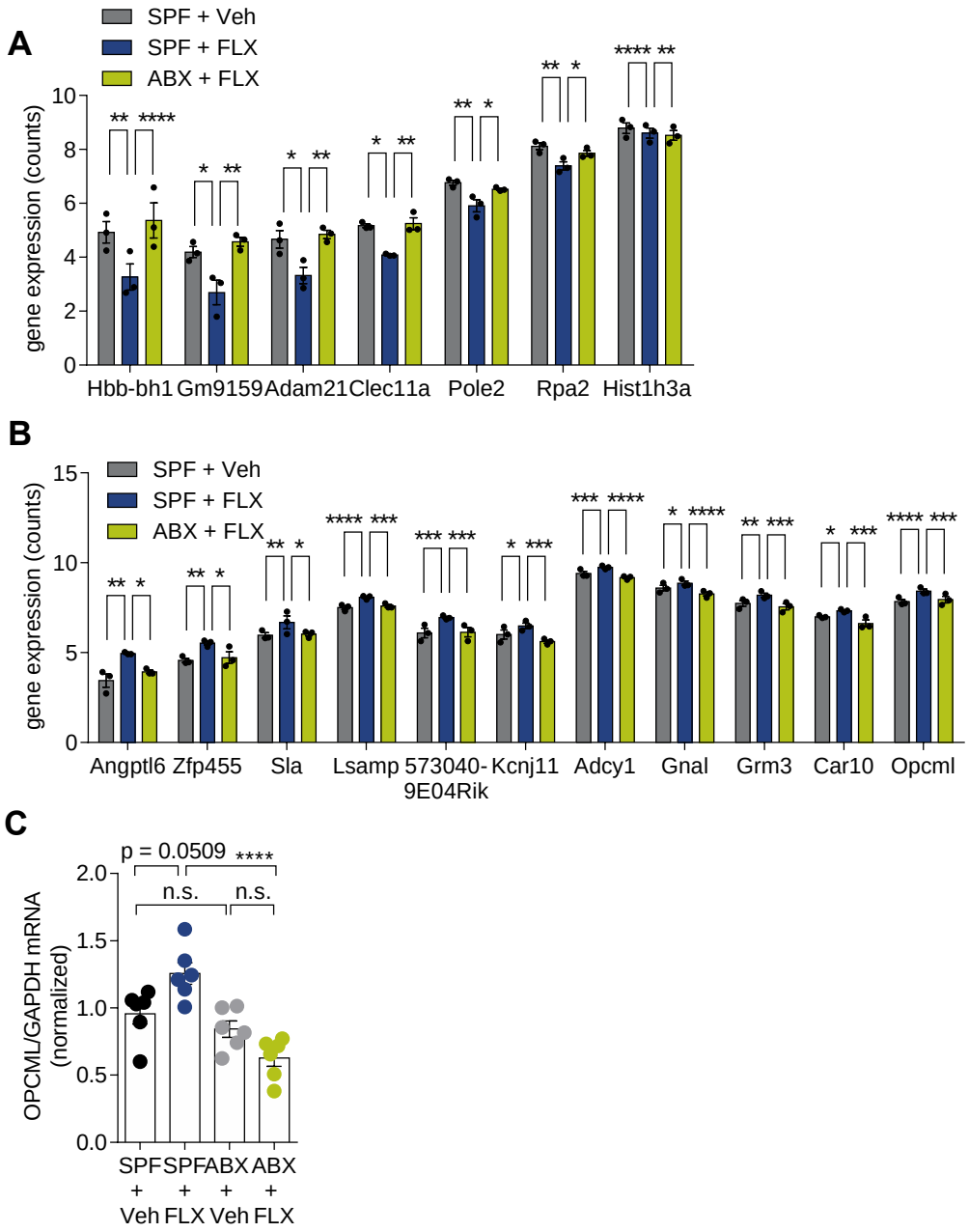

Figure 4.S9. Expression of select genes altered by maternal fluoxetine exposure and maternal microbiota status. A, Gene expression of *Hbb-bh1*, *Gm9159*, *Adam21*, and *Clec11a* that are upregulated in ABX+FLX compared to SPF+FLX greater than 0.5-fold and *Pole2*, *Rpa2*, and *Hist1h3a* that are upregulated in SPF+Veh compared to SPF+FLX greater than 0.5-fold. **B,** Gene expression of *Angptl6*, *Zfp455*, *Sla*, *Lsamp*, 5730409E04Rik, *Opcml* that are upregulated in SPF+FLX compared to SPF+Veh and greater than 0.5-fold ($p<0.05$), and *Kcnj11*, *Adcy1*, *Gnal*, *Grm3*, *Car10* that are upregulated in SPF+FLX compared to ABX+FLX and greater than 0.5-fold ($p<0.05$). **C,** Quantitative RT-PCR measurement of *Opcml* gene expression in SPF + Veh, SPF + FLX, ABX + Veh, and ABX + FLX embryo brains. (two-way ANOVA with Tukey's, n = 6, 6, 6, 6 dams). n.s.: not significant, * $p < 0.05$, ** $p < 0.01$, *** $p < 0.001$, **** $p < 0.0001$

References

[1] J.L. Melville, A. Gavin, Y. Guo, M.Y. Fan, W.J. Katon, Depressive disorders during pregnancy: prevalence and risk factors in a large urban sample, Obstet. Gynecol. 116 (2010) 1064–1070, https://doi.org/10.1097/AOG.0b013e3181f60b0a.

[2] N.I. Gavin, et al., Perinatal depression: a systematic review of prevalence and incidence, Obstet. Gynecol. 106 (2005) 1071–1083, https://doi.org/10.1097/01. AOG.0000183597.31630.db.

[3] S.C. Haight, N. Byatt, T.A. Moore Simas, C.L. Robbins, J.Y. Ko, Recorded diagnoses of depression during delivery hospitalizations in the United States, 2000–2015, Obstet. Gynecol. 133 (2019) 1216–1223, https://doi.org/10.1097/ AOG.0000000000003291.

[4] R.M. Graham, et al., Maternal anxiety and depression during late pregnancy and newborn brain white matter development, AJNR Am. J. Neuroradiol. 41 (2020) 1908–1915, https://doi.org/10.3174/ajnr.A6759.

[5] Y. Wu, et al., Association of prenatal maternal psychological distress with fetal brain growth, metabolism, and cortical maturation, JAMA Netw. Open 3 (2020), e1919940, https://doi.org/10.1001/jamanetworkopen.2019.19940.

[6] K.J. O'Donnell, V. Glover, E.D. Barker, T.G. O'Connor, The persisting effect of maternal mood in pregnancy on childhood psychopathology, Dev. Psychopathol. 26 (2014) 393–403, https://doi.org/10.1017/S0954579414000029.

[7] K. Walsh, et al., Maternal prenatal stress phenotypes associate with fetal neurodevelopment and birth outcomes, Proc. Natl. Acad. Sci. U. S. A. 116 (2019) 23996–24005, https://doi.org/10.1073/pnas.1905890116.

[8] E. Jimenez-Solem, et al., Prevalence of antidepressant use during pregnancy in Denmark, a nation-wide cohort study, PLoS One 8 (2013), e63034, https://doi. org/10.1371/journal.pone.0063034.

[9] C.H. Bourke, Z.N. Stowe, M.J. Owens, Prenatal antidepressant exposure: clinical and preclinical findings, Pharmacol. Rev. 66 (2014) 435–465, https://doi.org/ 10.1124/pr.111.005207.

[10] H.K. Brown, et al., Association between serotonergic antidepressant use during pregnancy and autism Spectrum disorder in children, JAMA 317 (2017) 1544–1552, https://doi.org/10.1001/jama.2017.3415.

[11] S.M. Hutchison, L.C. Masse, J.L. Pawluski, T.F. Oberlander, Perinatal selective serotonin reuptake inhibitor (SSRI) effects on body weight at birth and beyond: a review of animal and human studies, Reprod. Toxicol. 77 (2018) 109–121, https://doi.org/10.1016/j.reprotox.2018.02.004.

[12] S.M. Hutchison, L.C. Masse, J.L. Pawluski, T.F. Oberlander, Perinatal selective serotonin reuptake inhibitor (SSRI) and other antidepressant exposure effects on anxiety and depressive

behaviors in offspring: a review of findings in humans and rodent models, Reprod. Toxicol. 99 (2021) 80–95, https://doi.org/10.1016/j. reprotox.2020.11.013.

[13] I. Nulman, et al., Neurodevelopment of children exposed in utero to antidepressant drugs, N. Engl. J. Med. 336 (1997) 258–262, https://doi.org/ 10.1056/NEJM199701233360404.

[14] I. Nulman, et al., Child development following exposure to tricyclic antidepressants or fluoxetine throughout fetal life: a prospective, controlled study, Am. J. Psychiatry 159 (2002) 1889–1895, https://doi.org/10.1176/appi. ajp.159.11.1889.

[15] G.E. Simon, M.L. Cunningham, R.L. Davis, Outcomes of prenatal antidepressant exposure, Am. J. Psychiatry 159 (2002) 2055–2061, https://doi.org/10.1176/ appi.ajp.159.12.2055.

[16] R.M. Hayes, et al., Maternal antidepressant use and adverse outcomes: a cohort study of 228,876 pregnancies, Am. J. Obstet. Gynecol. 207 (49) (2012) e41–49, https://doi.org/10.1016/j.ajog.2012.04.028.

[17] R. Levinson-Castiel, P. Merlob, N. Linder, L. Sirota, G. Klinger, Neonatal abstinence syndrome after in utero exposure to selective serotonin reuptake inhibitors in term infants, Arch. Pediatr. Adolesc. Med. 160 (2006) 173–176, https://doi.org/10.1001/archpedi.160.2.173.

[18] A.C. Sujan, et al., Associations of maternal antidepressant use during the first trimester of pregnancy with preterm birth, small for gestational age, autism Spectrum disorder, and attention-deficit/hyperactivity disorder in offspring, JAMA 317 (2017) 1553–1562, https://doi.org/10.1001/jama.2017.3413.

[19] S. Davidson, et al., Effect of exposure to selective serotonin reuptake inhibitors in utero on fetal growth: potential role for the IGF-I and HPA axes, Pediatr. Res. 65 (2009) 236–241, https://doi.org/10.1203/PDR.0b013e318193594a.

[20] C.N. van der Veere, N.K.S. de Vries, K. van Braeckel, A.F. Bos, Intra-uterine exposure to selective serotonin reuptake inhibitors (SSRIs), maternal psychopathology, and neurodevelopment at age 2.5years - results from the prospective cohort SMOK study, Early Hum. Dev. 147 (2020), 105075, https:// doi.org/10.1016/j.earlhumdev.2020.105075.

[21] C. Lugo-Candelas, et al., Associations between brain structure and connectivity in infants and exposure to selective serotonin reuptake inhibitors during pregnancy, JAMA Pediatr. 172 (2018) 525–533, https://doi.org/10.1001/ jamapediatrics.2017.5227.

[22] M. Videman, et al., Newborn brain function is affected by fetal exposure to maternal serotonin reuptake inhibitors, Cereb. Cortex 27 (2017) 3208–3216, https://doi.org/10.1093/cercor/bhw153.

[23] C.M. Bond, et al., Perinatal fluoxetine exposure results in social deficits and reduced monoamine oxidase gene expression in mice, Brain Res. 1727 (2020), 146282, https://doi.org/10.1016/j.brainres.2019.06.001.

[24] F. Boulle, et al., Prenatal stress and early-life exposure to fluoxetine have enduring effects on anxiety and hippocampal BDNF gene expression in adult male offspring, Dev. Psychobiol. 58 (2016) 427–438, https://doi.org/10.1002/ dev.21385.

[25] S. Frazer, K. Otomo, A. Dayer, Early-life serotonin dysregulation affects the migration and positioning of cortical interneuron subtypes, Transl. Psychiatry 5 (2015) e644, https://doi.org/10.1038/tp.2015.147.

[26] J. Golebiowska, et al., Serotonin transporter deficiency alters socioemotional ultrasonic communication in rats, Sci. Rep. 9 (2019) 20283, https://doi.org/ 10.1038/s41598-019-56629-y.

[27] M. Soiza-Reilly, et al., SSRIs target prefrontal to raphe circuits during development modulating synaptic connectivity and emotional behavior, Mol. Psychiatry 24 (2019) 726–745, https://doi.org/10.1038/s41380-018-0260-9.

[28] A.S. Ramsteijn, et al., Perinatal selective serotonin reuptake inhibitor exposure and behavioral outcomes: a systematic review and meta-analyses of animal studies, Neurosci. Biobehav. Rev. 114 (2020) 53–69, https://doi.org/10.1016/j. neubiorev.2020.04.010.

[29] T. Frodl, Recent advances in predicting responses to antidepressant treatment, F1000Res 6 (2017), https://doi.org/10.12688/f1000research.10300.1.

[30] S.H. Preskorn, Prediction of individual response to antidepressants and antipsychotics: an integrated concept, Dialogues Clin. Neurosci. 16 (2014) 545–554.

[31] T.A. Ajslev, C.S. Andersen, M. Gamborg, T.I. Sorensen, T. Jess, Childhood overweight after establishment of the gut microbiota: the role of delivery mode, pre-pregnancy weight and early administration of antibiotics, Int. J. Obes. (Lond.) 35 (2011) 522–529, https://doi.org/10.1038/ijo.2011.27.

[32] L. Jostins, et al., Host-microbe interactions have shaped the genetic architecture of inflammatory bowel disease, Nature 491 (2012) 119–124, https://doi.org/ 10.1038/nature11582.

[33] L.V. Hooper, D.R. Littman, A.J. Macpherson, Interactions between the microbiota and the immune system, Science 336 (2012) 1268–1273, https://doi.org/ 10.1126/science.1223490.

[34] I. Kimura, et al., Maternal gut microbiota in pregnancy influences offspring metabolic phenotype in mice, Science 367 (2020), https://doi.org/10.1126/ science.aaw8429.

[35] V. Braniste, et al., The gut microbiota influences blood-brain barrier permeability in mice, Sci. Transl. Med. 6 (2014), 263ra158, https://doi.org/10.1126/ scitranslmed.3009759.

[36] D. Erny, et al., Host microbiota constantly control maturation and function of microglia in the CNS, Nat. Neurosci. 18 (2015) 965–977, https://doi.org/ 10.1038/nn.4030. [37] J. Stokholm, A. Sevelsted, K. Bonnelykke, H. Bisgaard, Maternal propensity for infections and risk of childhood asthma: a registry-based cohort study, Lancet Respir. Med. 2 (2014) 631–637, https://doi.org/10.1016/S2213-2600(14)70152- 3.

[38] V. Maini Rekdal, E.N. Bess, J.E. Bisanz, P.J. Turnbaugh, E.P. Balskus, Discovery and inhibition of an interspecies gut bacterial pathway for Levodopa metabolism, Science 364 (2019), https://doi.org/10.1126/science.aau6323.

[39] A.S. Ramsteijn, E. Jasarevic, D.J. Houwing, T.L. Bale, J.D. Olivier, Antidepressant treatment with fluoxetine during pregnancy and lactation modulates the gut microbiome and metabolome in a rat model relevant to depression, Gut Microbes 11 (2020) 735–753, https://doi.org/10.1080/19490976.2019.1705728.

[40] X. Wang, et al., Sodium oligomannate therapeutically remodels gut microbiota and suppresses gut bacterial amino acids-shaped neuroinflammation to inhibit Alzheimer's disease progression, Cell Res. 29 (2019) 787–803, https://doi.org/ 10.1038/s41422-019-0216-x.

[41] H. Wu, et al., Metformin alters the gut microbiome of individuals with treatmentnaive type 2 diabetes, contributing to the therapeutic effects of the drug, Nat. Med. 23 (2017) 850–858, https://doi.org/10.1038/nm.4345.

[42] M.A. Jackson, et al., Gut microbiota associations with common diseases and prescription medications in a population-based cohort, Nat. Commun. 9 (2018) 2655, https://doi.org/10.1038/s41467-018-05184-7.

[43] L. Maier, et al., Extensive impact of non-antibiotic drugs on human gut bacteria, Nature 555 (2018) 623–628, https://doi.org/10.1038/nature25979.

[44] A. Vich Vila, et al., Impact of commonly used drugs on the composition and metabolic function of the gut microbiota, Nat. Commun. 11 (2020) 362, https:// doi.org/10.1038/s41467-019-14177-z.

[45] T.C. Fung, et al., Intestinal serotonin and fluoxetine exposure modulate bacterial colonization in the gut, Nat. Microbiol. 4 (2019) 2064–2073, https://doi.org/ 10.1038/s41564-019-0540-4.

[46] J.L. Munoz-Bellido, S. Munoz-Criado, J.A. Garcia-Rodriguez, Antimicrobial activity of psychotropic drugs: selective serotonin reuptake inhibitors, Int. J. Antimicrob. Agents 14 (2000) 177–180, https://doi.org/10.1016/s0924-8579 (99)00154-5.

[47] J.G. Caporaso, et al., Global patterns of 16S rRNA diversity at a depth of millions of sequences per sample, Proc. Natl. Acad. Sci. U. S. A. 108 (Suppl. 1) (2011) 4516–4522, https://doi.org/10.1073/pnas.1000080107.

[48] C. Quast, et al., The SILVA ribosomal RNA gene database project: improved data processing and web-based tools, Nucleic Acids Res. 41 (2013) D590–596, https:// doi.org/10.1093/nar/gks1219.

[49] P. Yilmaz, et al., The SILVA and "all-species living tree project (LTP)" taxonomic frameworks, Nucleic Acids Res. 42 (2014) D643–648, https://doi.org/10.1093/ nar/gkt1209.

[50] E. Bolyen, et al., Reproducible, interactive, scalable and extensible microbiome data science using QIIME 2, Nat. Biotechnol. 37 (2019) 852–857, https://doi.org/ 10.1038/s41587-019-0209-9.

[51] A. Conesa, et al., A survey of best practices for RNA-seq data analysis, Genome Biol. 17 (2016) 13, https://doi.org/10.1186/s13059-016-0881-8.

[52] D. Kim, B. Langmead, S.L. Salzberg, HISAT: a fast spliced aligner with low memory requirements, Nat. Methods 12 (2015) 357–360, https://doi.org/ 10.1038/nmeth.3317.

[53] M. Pertea, D. Kim, G.M. Pertea, J.T. Leek, S.L. Salzberg, Transcript-level expression analysis of RNA-seq experiments with HISAT, StringTie and Ballgown, Nat. Protoc. 11 (2016) 1650–1667, https://doi.org/10.1038/nprot.2016.095.

[54] M.I. Love, W. Huber, S. Anders, Moderated estimation of fold change and dispersion for RNA-seq data with DESeq2, Genome Biol. 15 (2014) 550, https:// doi.org/10.1186/s13059-014-0550-8.

[55] W. Huang da, B.T. Sherman, R.A. Lempicki, Systematic and integrative analysis of large gene lists using DAVID bioinformatics resources, Nat. Protoc. 4 (2009) 44–57, https://doi.org/10.1038/nprot.2008.211.

[56] D.M. Ippolito, C. Eroglu, Quantifying synapses: an immunocytochemistry-based assay to quantify synapse number, J. Vis. Exp. (2010), https://doi.org/10.3791/ 2270.

[57] T.F. Oberlander, W. Warburton, S. Misri, J. Aghajanian, C. Hertzman, Effects of timing and duration of gestational exposure to serotonin reuptake inhibitor antidepressants: population-based study, Br. J. Psychiatry 192 (2008) 338–343, https://doi.org/10.1192/bjp.bp.107.037101.

[58] J. Reefhuis, et al., Specific SSRIs and birth defects: Bayesian analysis to interpret new data in the context of previous reports, BMJ 351 (2015) h3190, https://doi. org/10.1136/bmj.h3190.

[59] A. Karine de Sousa, et al., New roles of fluoxetine in pharmacology: antibacterial effect and modulation of antibiotic activity, Microb. Pathog. 123 (2018) 368–371, https://doi.org/10.1016/j.micpath.2018.07.040.

[60] S. Bauer, C. Monk, M. Ansorge, C. Gyamfi, M. Myers, Impact of antenatal selective serotonin reuptake inhibitor exposure on pregnancy outcomes in mice, Am. J. Obstet. Gynecol. 203 (375) (2010) e371–374, https://doi.org/10.1016/j. ajog.2010.05.008.

[61] B.D. Semple, K. Blomgren, K. Gimlin, D.M. Ferriero, L.J. Noble-Haeusslein, Brain development in rodents and humans: identifying benchmarks of maturation and vulnerability to injury across species, Prog. Neurobiol. 106-107 (2013) 1–16, https://doi.org/10.1016/j.pneurobio.2013.04.001.

[62] M. Berger, J.A. Gray, B.L. Roth, The expanded biology of serotonin, Annu. Rev. Med. 60 (2009) 355–366, https://doi.org/10.1146/annurev. med.60.042307.110802.

[63] E.A. Daubert, B.G. Condron, Serotonin: a regulator of neuronal morphology and circuitry, Trends Neurosci. 33 (2010) 424–434, https://doi.org/10.1016/j. tins.2010.05.005.

[64] C. Jonnakuty, C. Gragnoli, What do we know about serotonin? J. Cell. Physiol. 217 (2008) 301–306, https://doi.org/10.1002/jcp.21533.

[65] E. Deneris, P. Gaspar, Serotonin neuron development: shaping molecular and structural identities, Wiley Interdiscip. Rev. Dev. Biol. 7 (2018), https://doi.org/ 10.1002/wdev.301.

[66] J.C. Velasquez, et al., In utero exposure to citalopram mitigates maternal stress effects on fetal brain development, ACS Chem. Neurosci. 10 (2019) 3307–3317, https://doi.org/10.1021/acschemneuro.9b00180.

[67] C.A. Marcinkiewcz, et al., Serotonin engages an anxiety and fear-promoting circuit in the extended amygdala, Nature 537 (2016) 97–101, https://doi.org/ 10.1038/nature19318.

[68] B. Brenner, et al., Plasma serotonin levels and the platelet serotonin transporter, J. Neurochem. 102 (2007) 206–215, https://doi.org/10.1111/j.1471- 4159.2007.04542.x.

[69] A. Bonnin, et al., A transient placental source of serotonin for the fetal forebrain, Nature 472 (2011) 347–350, https://doi.org/10.1038/nature09972.

[70] H.J. Kliman, et al., Pathway of maternal serotonin to the human embryo and fetus, Endocrinology 159 (2018) 1609–1629, https://doi.org/10.1210/en.2017- 03025.

[71] M. Zimmermann, M. Zimmermann-Kogadeeva, R. Wegmann, A.L. Goodman, Mapping human microbiome drug metabolism by gut bacteria and their genes, Nature 570 (2019) 462–467, https://doi.org/10.1038/s41586-019-1291-3.

[72] A. Hachisuka, O. Nakajima, T. Yamazaki, J. Sawada, Localization of opioidbinding cell adhesion molecule (OBCAM) in adult rat brain, Brain Res. 842 (1999) 482–486, https://doi.org/10.1016/s0006-8993(99)01831-4.

[73] C. Sugimoto, S. Maekawa, S. Miyata, OBCAM, an immunoglobulin superfamily cell adhesion molecule, regulates morphology and proliferation of cerebral astrocytes, J. Neurochem. 112 (2010) 818–828, https://doi.org/10.1111/j.1471- 4159.2009.06513.x.

[74] M. Yamada, et al., Synaptic adhesion molecule OBCAM; synaptogenesis and dynamic internalization, Brain Res. 1165 (2007) 5–14, https://doi.org/10.1016/ j.brainres.2007.04.062.

[75] Z. Zhang, et al., The schizophrenia susceptibility gene OPCML regulates spine maturation and cognitive behaviors through Eph-Cofilin signaling, Cell Rep. 29 (2019) 49–61, https://doi.org/10.1016/j.celrep.2019.08.091, e47.

[76] K. Karis, et al., Altered expression profile of IgLON family of neural cell adhesion molecules in the dorsolateral prefrontal cortex of schizophrenic patients, Front. Mol. Neurosci. 11 (2018) 8, https://doi.org/10.3389/fnmol.2018.00008.

[77] Z. Zhou, et al., Antidepressant specificity of serotonin transporter suggested by three LeuT-SSRI structures, Nat. Struct. Mol. Biol. 16 (2009) 652–657, https:// doi.org/10.1038/nsmb.1602.

[78] R.N. Carmody, P.J. Turnbaugh, Host-microbial interactions in the metabolism of therapeutic and diet-derived xenobiotics, J. Clin. Invest. 124 (2014) 4173–4181, https://doi.org/10.1172/JCI72335.

[79] C.W. Noorlander, et al., Modulation of serotonin transporter function during fetal development causes dilated heart cardiomyopathy and lifelong behavioral abnormalities, PLoS One 3 (2008) e2782, https://doi.org/10.1371/journal. pone.0002782.

[80] J.D. Olivier, et al., Fluoxetine administration to pregnant rats increases anxietyrelated behavior in the offspring, Psychopharmacology (Berl.) 217 (2011) 419–432, https://doi.org/10.1007/s00213-011-2299-z.

[81] J. Rampono, et al., Placental transfer of SSRI and SNRI antidepressants and effects on the neonate, Pharmacopsychiatry 42 (2009) 95–100, https://doi.org/ 10.1055/s-0028-1103296.

[82] C.V. Vorhees, et al., A developmental neurotoxicity evaluation of the effects of prenatal exposure to fluoxetine in rats, Fundam. Appl. Toxicol. 23 (1994) 194–205, https://doi.org/10.1006/faat.1994.1098.

[83] C.P. Sjaarda, et al., Interplay between maternal Slc6a4 mutation and prenatal stress: a possible mechanism for autistic behavior development, Sci. Rep. 7 (2017) 8735, https://doi.org/10.1038/s41598-017-07405-3.

[84] K. Nagata, et al., Antidepressants inhibit P2X4 receptor function: a possible involvement in neuropathic pain relief, Mol. Pain 5 (2009) 20, https://doi.org/ 10.1186/1744-8069-5-20.

[85] L. Peng, L. Gu, B. Li, L. Hertz, Fluoxetine and all other SSRIs are 5-HT2B Agonists - Importance for their Therapeutic Effects, Curr. Neuropharmacol. 12 (2014) 365–379, https://doi.org/10.2174/1570159X12666140828221720.

[86] J. Penttila, et al., Effects of fluoxetine on dopamine D2 receptors in the human brain: a positron emission tomography study with [11C]raclopride, Int. J. Neuropsychopharmacol. 7 (2004) 431–439, https://doi.org/10.1017/ S146114570400450X.

[87] L. Pozzi, R. Invernizzi, C. Garavaglia, R. Samanin, Fluoxetine increases extracellular dopamine in the prefrontal cortex by a mechanism not dependent on serotonin: a comparison with citalopram, J. Neurochem. 73 (1999) 1051–1057, https://doi.org/10.1046/j.1471-4159.1999.0731051.x.

[88] C.W. Kim, et al., Dual effects of fluoxetine on mouse early embryonic development, Toxicol. Appl. Pharmacol. 265 (2012) 61–72, https://doi.org/ 10.1016/j.taap.2012.09.020.

[89] M.E. Di Rosso, M.L. Palumbo, A.M. Genaro, Immunomodulatory effects of fluoxetine: A new potential pharmacological action for a classic antidepressant drug? Pharmacol. Res. 109 (2016) 101–107, https://doi.org/10.1016/j. phrs.2015.11.021.

[90] C.A. Pereira, et al., Chronic treatment with fluoxetine modulates vascular adrenergic responses by inhibition of pre- and post-synaptic mechanisms, Eur. J. Pharmacol. 800 (2017) 70–80, https://doi.org/10.1016/j.ejphar.2017.02.029.

[91] K. Bartkowska, A. Paquin, A.S. Gauthier, D.R. Kaplan, F.D. Miller, Trk signaling regulates neural precursor cell proliferation and differentiation during cortical development, Development 134 (2007) 4369–4380, https://doi.org/10.1242/ dev.008227.

[92] P.C. Casarotto, et al., Antidepressant drugs act by directly binding to TRKB neurotrophin receptors, Cell 184 (2021) 1299–1313, https://doi.org/10.1016/j. cell.2021.01.034, e1219.

[93] S.E. Sillivan, C. Konradi, Expression and function of dopamine receptors in the developing medial frontal cortex and striatum of the rat, Neuroscience 199 (2011) 501–514, https://doi.org/10.1016/j.neuroscience.2011.10.004.

[94] Z. Chen, et al., Interleukin-33 promotes serotonin release from enterochromaffin cells for intestinal homeostasis, Immunity 54 (2021) 151–163, https://doi.org/ 10.1016/j.immuni.2020.10.014, e156.

[95] A.D. Mandic, et al., Clostridium ramosum regulates enterochromaffin cell development and serotonin release, Sci. Rep. 9 (2019) 1177, https://doi.org/ 10.1038/s41598-018-38018-z.

[96] C.S. Reigstad, et al., Gut microbes promote colonic serotonin production through an effect of short-chain fatty acids on enterochromaffin cells, FASEB J. 29 (2015) 1395–1403, https://doi.org/10.1096/fj.14-259598.

[97] J.M. Yano, et al., Indigenous bacteria from the gut microbiota regulate host serotonin biosynthesis, Cell 161 (2015) 264–276, https://doi.org/10.1016/j. cell.2015.02.047.

[98] G. Clarke, et al., The microbiome-gut-brain axis during early life regulates the hippocampal serotonergic system in a sex-dependent manner, Mol. Psychiatry 18 (2013) 666–673, https://doi.org/10.1038/mp.2012.77.

[99] M. van de Wouw, et al., Host microbiota regulates central nervous system serotonin receptor 2C editing in rodents, ACS Chem. Neurosci. 10 (2019) 3953–3960, https://doi.org/10.1021/acschemneuro.9b00414.

[100] I. Lukic, et al., Antidepressants affect gut microbiota and Ruminococcus flavefaciens is able to abolish their effects on depressive-like behavior, Transl. Psychiatry 9 (2019) 133, https://doi.org/10.1038/s41398-019-0466-x.

[101] M. Lyte, K.M. Daniels, S. Schmitz-Esser, Fluoxetine-induced alteration of murine gut microbial community structure: evidence for a microbial endocrinology-based mechanism of action responsible for fluoxetine-induced side effects, PeerJ 7 (2019) e6199, https://doi.org/10.7717/peerj.6199.

[102] E. Siopi, et al., Changes in gut microbiota by chronic stress impair the efficacy of fluoxetine, Cell Rep. 30 (2020) 3682–3690, https://doi.org/10.1016/j. celrep.2020.02.099, e3686.

[103] A. Naseribafrouei, et al., Correlation between the human fecal microbiota and depression, Neurogastroenterol. Motil. 26 (2014) 1155–1162, https://doi.org/ 10.1111/nmo.12378.

[104] G.N. Pronovost, E.Y. Hsiao, Perinatal interactions between the microbiome, immunity, and neurodevelopment, Immunity 50 (2019) 18–36, https://doi.org/ 10.1016/j.immuni.2018.11.016.

[105] M. Crumeyrolle-Arias, et al., Absence of the gut microbiota enhances anxiety-like behavior and neuroendocrine response to acute stress in rats, Psychoneuroendocrinology 42 (2014) 207–217, https://doi.org/10.1016/j. psyneuen.2014.01.014.

[106] G. De Palma, et al., Microbiota and host determinants of behavioural phenotype in maternally separated mice, Nat. Commun. 6 (2015) 7735, https://doi.org/ 10.1038/ncomms8735.

[107] T. Hashimoto, S. Maekawa, S. Miyata, IgLON cell adhesion molecules regulate synaptogenesis in hippocampal neurons, Cell Biochem. Funct. 27 (2009) 496–498, https://doi.org/10.1002/cbf.1600.

[108] R.L. Sanz, G.B. Ferraro, M.P. Girouard, A.E. Fournier, Ectodomain shedding of Limbic System-Associated Membrane Protein (LSAMP) by ADAM Metallopeptidases promotes neurite outgrowth in DRG neurons, Sci. Rep. 7 (2017) 7961, https://doi.org/10.1038/s41598-017-08315-0.

[109] R. Sanz, G.B. Ferraro, A.E. Fournier, IgLON cell adhesion molecules are shed from the cell surface of cortical neurons to promote neuronal growth, J. Biol. Chem. 290 (2015) 4330–4342, https://doi.org/10.1074/jbc.M114.628438.

[110] M. Lam, et al., Comparative genetic architectures of schizophrenia in East Asian and European populations, Nat. Genet. 51 (2019) 1670–1678, https://doi.org/ 10.1038/s41588-019-0512-x.

[111] L. Athanasiu, et al., Gene variants associated with schizophrenia in a Norwegian genome-wide study are replicated in a large European cohort, J. Psychiatr. Res. 44 (2010) 748–753, https://doi.org/10.1016/j.jpsychires.2010.02.002.

[112] M.C. O'Donovan, et al., Identification of loci associated with schizophrenia by genome-wide association and follow-up, Nat. Genet. 40 (2008) 1053–1055, https://doi.org/10.1038/ng.201.

[113] W.M. Weikum, T.F. Oberlander, T.K. Hensch, J.F. Werker, Prenatal exposure to antidepressants and depressed maternal mood alter trajectory of infant speech perception, Proc. Natl. Acad. Sci. U. S. A. 109 (Suppl. 2) (2012) 17221–17227, https://doi.org/10.1073/pnas.1121263109.

[114] K. Zinn, E. Ozkan, Neural immunoglobulin superfamily interaction networks, Curr. Opin. Neurobiol. 45 (2017) 99–105, https://doi.org/10.1016/j. conb.2017.05.010.

[115] N. Kubick, D. Brosamle, M.E. Mickael, Molecular evolution and functional divergence of the IgLON family, Evol. Bioinform. Online 14 (2018), 1176934318775081, https://doi.org/10.1177/1176934318775081.

[116] R.C. Casper, et al., Follow-up of children of depressed mothers exposed or not exposed to antidepressant drugs during pregnancy, J. Pediatr. 142 (2003) 402–408, https://doi.org/10.1067/mpd.2003.139.

[117] L.A. Croen, J.K. Grether, C.K. Yoshida, R. Odouli, V. Hendrick, Antidepressant use during pregnancy and childhood autism spectrum disorders, Arch. Gen. Psychiatry 68 (2011) 1104–1112, https://doi.org/10.1001/ archgenpsychiatry.2011.73.

[118] T.F. Oberlander, et al., Hypothalamic-pituitary-adrenal (HPA) axis function in 3- month old infants with prenatal selective serotonin reuptake inhibitor (SSRI) antidepressant exposure, Early Hum. Dev. 84 (2008) 689–697, https://doi.org/ 10.1016/j.earlhumdev.2008.06.008.

[119] T.F. Oberlander, et al., Pain reactivity in 2-month-old infants after prenatal and postnatal serotonin reuptake inhibitor medication exposure, Pediatrics 115 (2005) 411–425, https://doi.org/10.1542/peds.2004-0420.

[120] T.F. Oberlander, et al., Prenatal effects of selective serotonin reuptake inhibitor antidepressants, serotonin transporter promoter genotype (SLC6A4), and maternal mood on child behavior at 3 years of age, Arch. Pediatr. Adolesc. Med. 164 (2010) 444–451, https://doi.org/10.1001/archpediatrics.2010.51.

[121] J.L. Pawluski, U.M. Brain, C.M. Underhill, G.L. Hammond, T.F. Oberlander, Prenatal SSRI exposure alters neonatal corticosteroid binding globulin, infant cortisol levels, and emerging HPA function, Psychoneuroendocrinology 37 (2012) 1019–1028, https://doi.org/10.1016/j.psyneuen.2011.11.011.

[122] P.S. Zeskind, L.E. Stephens, Maternal selective serotonin reuptake inhibitor use during pregnancy and newborn neurobehavior, Pediatrics 113 (2004) 368–375, https://doi.org/10.1542/peds.113.2.368.

Chapter 5: Early Life Adversity Predicts Brain-Gut Alterations Associated with Increased Stress and Mood

Abstract

Alterations in the brain-gut system have been implicated in various disease states, but little is known about how early-life adversity (ELA) impacts development and adult health as mediated by brain-gut interactions. We hypothesize that ELA disrupts components of the brain-gut system, thereby increasing susceptibility to disordered mood. In a sample of 128 healthy adult participants, a history of ELA and current stress, depression, and anxiety were assessed using validated questionnaires. Fecal metabolites were measured using liquid chromatography tandem mass spectrometry-based untargeted metabolomic profiling. Functional brain connectivity was evaluated by magnetic resonance imaging. Sparse partial least squares-discriminant analysis, controlling for sex, body mass index, age, and diet was used to predict brain-gut alterations as a function of ELA. ELA was correlated with four gut-regulated metabolites within the glutamate pathway (5-oxoproline, malate, urate, and glutamate gamma methyl ester) and alterations in functional brain connectivity within primarily sensorimotor, salience, and central executive networks. Integrated analyses revealed significant associations between these metabolites, functional brain connectivity, and scores for perceived stress, anxiety, and depression. This study reveals a novel association between a history of ELA, alterations in the brain-gut axis, and increased vulnerability to negative mood and stress. Results from the study raise the hypothesis that select gut-regulated metabolites may contribute to the adverse effects of critical period stress on neural development via pathways related to glutamatergic excitotoxicity and oxidative stress.

1. Introduction

Early-life adversity (ELA) is a known disruptor capable of inducing a range of developmental changes[1], and is associated with increased vulnerability to a variety of health conditions and psychiatric disorders later in life[2]. Systemic changes in response to stress during critical periods include dysregulation of peripheral gene expression[3], immune function[4], and hormone levels[5], in addition to perturbations of the microbiome[6], all of which may contribute to

and result from direct changes in the developing central nervous system (CNS). The involvement of the gut microbiome and its interactions with the brain during this early programming period remain incompletely understood. We have previously proposed that this may occur in a *bidirectional* manner: while the brain may influence alterations of gut physiology and microbiome composition and function, the resulting altered functional output from the gut microbiome may result in neuroplastic changes in the brain[7-9]. A history of ELA has been reported in conditions ranging from obesity[10] to irritable bowel syndrome[11,12] and inflammation[13,14], but few studies to date have used a systems approach to investigate perturbations in the gut metabolome and the brain in humans exposed to ELA.

A primary pathway by which ELA can influence life-long trajectories is by shaping brain development[1]. Previous studies have shown that a history of ELA is associated with alterations mainly in regions of the emotion regulation and salience networks, which in turn can influence epigenetic processes related to myelination and neurogenesis[15,16]. These neural changes have also been implicated in hyperarousal and difficulties with emotion regulation, and later development of negative mood states[17-19]. In particular, prefrontal cortex and hippocampal volumes were persistently reduced in adolescents adopted from international orphanages[20], and female adolescents with a history of childhood maltreatment displayed altered organization of cortical networks, which mediated psychiatric outcomes[21]. Rodent research has shown similar findings with increased resolution: for instance, maternal separation was associated with accelerated innervation of basolateral amygdala axons into the prefrontal cortex, with females specifically demonstrating reduced functional connectivity between these regions across maturation, and increased anxiety-like behavior[22].

In addition to neural development, the gut is also sensitive to ELA[23]. A number of early developmental factors have been implicated in gut microbiome development, especially factors relating to maternal stress, diet, and disease[24], mode of delivery[25,26], early nutrition/breast-feeding[26,27], and exposure to antibiotics[25]. In a youth cohort, early life adversity was not only

associated with gastrointestinal symptoms and later anxiety, but also correlated with microbial diversity, and taxonomic abundances predicted prefrontal cortex activity[28]. In a sample of pregnant women, early adversity correlated positively with *Prevotella*, and cortisol correlated positively with *Rikenellaceae* and *Dialister*, and negatively with *Bacteroides*, suggesting an interaction between early adversity, current stress, and gut microbiota[29]. Additionally, gut signaling to the brain can be mediated by metabolites produced directly by gut microbes or indirectly from host cells responding to microbial cues[30]. For example, transplantation of microbiota from depressed patients into germ-free mice promoted anxiety- and depression-related behaviors compared to germ-free mice transplanted with a non-depressed microbiota; these interactions were mediated by selective modulation of both microbial and host genes involved in carbohydrate and amino acid metabolism[31]. Additionally, microbiome-derived short-chain fatty acids ameliorate stress-induced cortisol release in humans when delivered directly to the colon[32] and ameliorate early chronic stress in rodents when delivered orally[33], further underscoring potential relationships between the brain-gut-microbiome axis and stress[34].

While findings from animal models support a role for the gut microbiome in mediating adverse effects of ELA on neurodevelopment[35,36], comprehensive investigation of these interactions in humans is lacking. Despite the well-known limitations of cross-sectional and retrospective data, herein we test the primary hypothesis that ELA-related alterations in gut microbial metabolites are associated with alterations in brain connectivity, disordered mood, and increased vulnerability to stress in adulthood.

2. Materials and Methods

2.1. Participants

The study was comprised of 128 right-handed healthy participants (43 males and 85 females), with the absence of significant medical or psychiatric conditions, as assessed by a physical exam, detailed medical history, and a clinical assessment using the modified Mini-

International Neuropsychiatric Interview Plus 5.0 (MINI)[37]. Participants were excluded for the following: pregnant or lactating, substance use, abdominal surgery, tobacco dependence (half a pack or more daily), extreme strenuous exercise (>8h of continuous exercise per week), current or past psychiatric illness, and major medical or neurological conditions. Participants taking medications that interfere with the CNS or using analgesic drugs regularly (e.g. full dose antidepressants including SSRIs, NSRIs, sedatives or anxiolytics, and opioids) were excluded. Participants were also excluded for use of antibiotics or probiotic supplements in the past 3 months. Since female sex hormones such as estrogen are known to effect brain structure and function, we requested females to stop taking hormonal contraceptives for the duration of the study. In addition, we assessed only females who were premenopausal (i.e., women under than or equal to 45 years who reported regular menses for at least 1 year) and were scanned during the follicular phase of the menstrual cycle (i.e., defined as 4-12 days after the first day of the last menstrual period), as assessed by self-report.

All procedures complied with and were approved by the Institutional Review Board (16-000187, 15-001591) at the University of California, Los Angeles's Office of Protection for Research Subjects. All participants provided written informed consent.

2.2. Questionnaires

ELA was measured using the Early Traumatic Inventory-Self Report (ETI-SR)[38], a 27-item questionnaire. This questionnaire assesses the histories of childhood traumatic and adverse life events that occurred before the age of 18 years old and covers four domains: general trauma (11 items), physical punishment (5 items), emotional abuse (5 items), and sexual abuse (6 items). General traumatic events comprise a range of stressful and traumatic events that can be mostly secondary to chance events. Sample items on this scale include death of a parent, discordant relationships or divorce between parents, or death or sickness of a sibling or friend. Physical abuse involves physical contact, constraint, or confinement, with intent to hurt or injure. Sample

items on the physical abuse subscale include being spanked by hand or being hit by objects. Emotional abuse is verbal communication with the intention of humiliating or degrading the victim. Sample items on the ETI-SR emotion subscale include the following, “Often put down or ridiculed,” or “Often told that one is no good.” Sexual abuse is unwanted sexual contact performed solely for the gratification of the perpetrator or for the purposes of dominating or degrading the victim. Sample items on the sexual abuse scale include being forced to pose for suggestive photographs, to perform sexual acts for money, or coercive anal sexual acts against one’s will. The ETI-SR instrument was chosen due to its psychometric properties, ease of administration, time efficiency, and ability to measure ELAs in multiple domains. For subsequent analyses, participants were split into two groups: “High ETI” (ETI-SR total > 4) and “Low ETI” (ETI-SR total ≤ 4). This cut off ETI score was selected based on the median score of this sample versus the mean ETI score in past papers because of the presence of extreme ETI scores in the data. While some studies have reported a higher mean ETI, our cut-off falls in line with previously reported healthy patient samples tested using the short-form version of the tool (mean=3.5, sd=3.3[39]; mean=2.68, sd=2.55[40]).

Additional questionnaires included the Perceived Stress Scale (PSS) and the Hospital Anxiety and Depression Scale (HADS). The PSS is a 10-item scale used to measure stressful demands in a given situation, indicating that demands exceed ability to cope[41]. The questions are based on subjects reporting the frequency of their feelings within the past month to each question, which are scored on a scale of 0 (never) to 4 (very often). The HADS is a 14-item scale used to measure symptoms of anxiety and depression[42]. The questions are scored on a scale of 0 to 3, corresponding to how much the individual identifies with the question for the past week.

Diet was assessed through a self-reported UCLA Diet Checklist, is a questionnaire developed by our institution, intended to represent the diet that best reflects what patients consume on a regular basis. The specific diets incorporated into this checklist include the following options: i) Standard American (characterized by high consumption of processed, frozen,

and packaged foods, pasta and breads, and red meat; vegetables and fruits are not consumed in large quantities), ii) Modified American (high consumption of whole grains including some processed, frozen, and packaged foods; red meat is consumed in limited quantities; vegetables and fruit are consumed in moderate to large quantities), iii) Mediterranean (high consumption of fruits, vegetables, beans, nuts, and seeds; olive oil is the key monounsaturated fat source; dairy products, fish, and poultry are consumed in low to moderate amounts and little red meat is eaten), and iv) all other diets that do not fit into the above categories. If they marked "other" they were asked to describe the components of their individual diet with regards to consumption of meat, dairy, eggs, fruits, vegetables, and grains. If a participant selected "other", their comments regarding intake of food components were individually reviewed, as was that participant's previous 24-hour food intake. Our institution's Diet Checklist was then internally validated against the standardized DHQ-III. For data analysis we had 3 diet categories: We combined standard American and modified American diet as one category. Mediterranean, vegan, vegetarian, and gluten-free were combined into a single category, and all other diets were combined as "other." For the analyses, the three categories (America, Mediterranean/Plant based, Other) were used.

2.3. Gut Microbiome

2.3.1. Collection and Storage

These have been previously described in great detail in recently published papers[43-45]. Participants were given "at home collection kits" which consisted of a standard laboratory supplies such as collection hat over the commode and a urine cup to pack the fresh stool. The participants were given specific instructions regarding time of stool collection (e.g., time of day and within 2-3 days before the MRI scan). In addition, 2-3 consecutive diet diaries were collected from the time of enrollment to the time of the MRI scan and stool collection (1 weekday and 1 weekend). Participants were asked to collect the stool before the first meal of the day. If participants were on antidiarrheal or laxatives, they were asked to refrain from use for 2-3 days before the sample

collection. Participants were asked to store their fresh stool immediately in the freezer immediately upon collection and to bring in the stool to the laboratory on the day of the MRI (note day and time of stool collection and storage). Any deviation from the stool sample collection or storage were documented in order to account for in the analyses. Fecal samples were stored at -80°C, then ground into a coarse powder by mortar and pestle under liquid nitrogen and aliquoted for DNA extraction and metabolomic profiling.

2.3.2. Fecal Microbial Profiling

DNA extraction with bead beating was performed using the QIAGEN Powersoil DNA Isolation Kit (MO BIO Laboratories, Carlsbad, CA) with bead beating following the manufacturers protocol. The V4 hypervariable region of the 16S rRNA gene was then amplified using the 515F and 806R primers to generate a sequencing library according to a published protocol[46]. The PCR products were purified with a commercial kit. The library underwent 2x250 sequencing on an Illumina HiSeq 2500 to a mean depth of 250,000 merged sequences per sample. QIIME 1.9.1 was used to perform quality filtering, merge paired end reads, and cluster sequences into 97% operational taxonomic units (OTUs)[47]. OTUs were classified taxonomically using the Greengenes May 2013 database at the level of domain, phylum, family, genus, and species, depending on the depth of reliable classifier assignments.

Microbial alpha diversity was assessed on datasets rarefied to equal sequencing depth (34,222) using the Chao1 index of richness, Faith's phylogenetic diversity, and the Shannon index of evenness. Microbial composition was compared across samples by weighted UniFrac distances and visualized with principal coordinates analysis[48]. The significance of differences in microbial composition between individuals with high or low ETI scores, adjusting for age, BMI, diet, and sex was assessed using PERMANOVA with 100,000 permutations[49]. Differential abundance of microbial genera was determined using multivariate negative binomial mixed models implemented in DESeq2 that included age, BMI, diet, and sex as covariates[50]. P-values

were adjusted for multiple hypothesis testing to generate q-values, with a significance threshold of $q < 0.05$.

2.3.3. Fecal Metabolomic Profiling

Fecal aliquots were shipped to Metabolon, Inc., and run as a single batch on their global HD4 metabolomics platform[51]. This involved running methanol extracted samples through ultrahigh performance liquid chromatography-tandem mass spectroscopy under four separate chromatography and electrospray ionization conditions to separate compounds with a wide range of chemical properties. Compounds were identified by comparison of spectral features to Metabolon's proprietary library that includes MS/MS spectral data on more than 3300 purified standards. Study specific technical replicates generated by pooling aliquots of all samples were used to measure total process variability (median relative standard deviation 13%). Results were provided as scaled, imputed abundances of 872 known compounds.

Missing values of raw data were filled up using median values, and ineffective peaks were removed through the interquartile range denoising method. In addition, the internal standard normalization method was employed in the data analysis. The dataset for the multiple classification analysis was compiled from the metabolite profiling results and a 3D matrix involving metabolite numbers, sample names, and normalized peak intensities were fed into the MetaboAnlyst web software 3.0 (http://www.metaboanalyst.ca).

2.4. Magnetic Resonance Imaging

Whole brain structural and functional (resting state) data was acquired using a 3.0T Siemens Prisma MRI scanner (Siemens, Erlangen, Germany). Detailed information on the standardized acquisition protocols, quality control measures, and image preprocessing are provided in previously published studies[16,44,45].

2.4.1. Structural MRI Acquisition

High resolution T1-weighted images were acquired: echo time/ repetition time (TE/TR)=3.26ms/2200ms, field of view=220×220mm slice thickness=1mm, 176 slices, 256×256 voxel matrices, and voxel size=0.86×0.86×1mm.

2.4.2. Functional MRI Acquisition

Resting-state scans were acquired with eyes closed and an echo planar sequence with the following parameters: TE/TR=28ms/2000ms, flip angle=77 degrees, scan duration=8m6s–10m6s, FOV=220mm, slices=40 and slice thickness=4.0mm, and slices were obtained with whole-brain coverage.

2.4.3. Preprocessing of MRI images

Preprocessing and quality control of functional images was done using SPM-12 software (Welcome Department of Cognitive Neurology, London, UK). The first two volumes were discarded to allow for stabilization of the magnetic field. Slice timing correction was performed first, followed by rigid six-degree motion-correction for the six realignment parameters. The motion correction parameters in each degree were examined for excessive motion. If any motion was detected above 2 mm translation or 2˚ rotation, the scan, along with the paired structural scan was discarded. In order to robustly take account the effects of motion, root mean squared realignment estimates were calculated as robust measures of motion using publicly available MATLAB code. Any subjects with a greater RMS value than 0.25 was not included in the analysis. The resting state images were then co-registered to their respective anatomical T1 images. Each T1 image was then segmented and normalized to a smoothed template brain in Montreal Neurological Institute[52] template space. Each subject's T1 normalization parameters were then applied to that subject's resting state image, resulting in an MNI space normalized resting state image. The resulting images were smoothed with $5mm^3$ Gaussian kernel. For each subject, a sample of the volumes was inspected for any artifacts and anomalies. Levels of signal dropout were also visually inspected for excessive dropout in a priori regions of interest.

2.4.4. Structural Image Parcellation

T1-image segmentation and cortical and subcortical regional parcellation were conducted using Schaefer 400 atlas[53], Harvard-Oxford subcortical atlas[54], and the Ascending Arousal Network atlas[55]. This parcellation results in the labeling of 430 regions, 400 cortical structures, 14 bilateral subcortical structures, bilateral cerebellum, and 14 brainstem nuclei.

2.4.5. Functional Brain Connectivity Matrix Construction

To summarize, all pre-processed, normalized images were entered into the CONN-fMRI functional connectivity toolbox version 17 in MATLAB. All images were first corrected for noise using the automatic component-based noise correction (aCompCor) method to remove physiological noise without regressing out the global signal. Confounds for the six motion parameters along with their first-order temporal derivatives, along with confounds emerging from white matter and cerebral spinal fluid, and first-order temporal derivatives of motion, and root mean squared values of the detrended realignment estimates were removed using regression. Although the influence of head motion cannot be completely removed, CompCor has been shown to be particularly effective for dealing with residual motion relative to other methods. The images were then band-pass filtered between 0.008 and 0.009 Hz to minimize the effects of low frequency drift and high frequency noise after CompCor regression. Connectivity matrices for each subject, consisting of all the parcellated regions were then computed. This represents the association between two average temporal BOLD time series across all the voxels in each region. The final outputs for each subject consisted of a connectivity matrix between the 430 parcellated regions and was indexed by Fisher transformed Z correlation coefficients between each region of interest.

2.5. Statistical Analysis

2.5.1. Sparse Partial Least Squares — Discriminate Analysis

A partial least squares-discriminant analysis (PLS-DA) was conducted in R (Boston, MA) to explore the group difference between high vs. low ETI groups by incorporating known classifications for the metabolites. Similarly, a sparse PLS-DA for whole brain resting state

connectivity was run to understand the classification in brain signatures related to high vs. low ETI. In order to prevent overfitting of the model, we ran permutation tests. The metabolites with values of the first component of variable importance projection (VIP) greater than 1.0 were assessed, indicating the estimate of the importance of each metabolite used in the model. The brain connectivity regions/brain signatures from the two components of the weighted design matric and contributing to the discrimination between the two groups were summarized using the top variable loadings on the individual dimensions/components and VIP coefficients. T-tests using contrasts in a general linear model controlling for age, BMI, diet (3 categories), and sex (male, female) were conducted. *P*-values were adjusted for with the Benjamini-Hochberg false discovery rate (FDR) procedure and significant *q*-values, were reported[56]. The metabolites with VIPs > 1.0 and $q < 0.05$ were selected as significantly different between the two groups. The fold change was also calculated to investigate the difference by comparing the mean value of the peak area obtained between the two groups.

2.5.2. Network Analysis

Network analysis was performed to integrate information from three data sets: 1) stool-derived metabolites 2) clinical data (ETI, PSS, HADS Anxiety, HADS Depression) and 3) functional connectivity brain data. The interaction between the phenome (clinical measures), microbiome (stool-derived metabolites) and connectome (brain connectivity) was determined by computing Spearman correlations between different data types in R v. 3.6.2, controlling for age, BMI, diet, and sex. These correlations were run separately for 1. All participants 2. the low ETI group and for 3. the high ETI group. Circos images were created to visualize and construct brain, symptom, and gut-derived metabolite interaction networks thresholded at FDR corrected $q < 0.05$. We present the networks by placing nodes of the same type of data together and displaying connecting edges representing correlations. A red edge indicates a significant correlation in the high ETI group. A green edge indicates a significant correlation in the low ETI group. A grey edge represents a significant correlation for all the participants as a function of increasing ETI scores.

3. Results

3.1. Subject Demographics and Clinical Variables

Individuals in the low ETI group had a mean score of 1.2, while those in the high ETI group had a mean score of 8.6. Those with a history of high ELA exposure as indexed by the ETI scale had significantly higher BMI ($p<0.001$) and anxiety ($p=0.032$) levels (**Table 5.1**). Although the high ELA group was older ($p=0.244$), and reported higher levels of depression symptoms ($p=0.284$), and perceived stress ($p=0.069$), these differences were not significant. To account for the significant difference in BMI between low and high ETI groups, we controlled for it in subsequent multivariate analyses. Diet did not differ by ETI group (American: High ETI=15, Low ETI=19, Mediterranean/Plant Based: High ETI=25, Low ETI=39, Other: High ETI=12, Low ETI=18.

3.2. Early Life Adversity and Gut Microbiome Composition

There were no significant relationships between a history of ELA exposure and microbial alpha diversity, the variation of microbes within a sample, (ACE, $p = 0.50749$; Chao1, $p = 0.63385$; Shannon, $p = 0.10209$) (**Fig. 5.S1A**), microbial beta diversity, the variation of microbial communities between samples, (measured by Bray-Curtis-based PCoA; permanova $p = 0.441$) (**Fig. 5.S1B**) or relative taxonomic abundance, at either the phylum or genus levels (**Fig. 5.S1C**).

3.3. Early Life Adversity Associates with Adult Gut Metabolites

The PLS-DA of the gut metabolites showed a defined clustering, based on low or high ETI exposure (**Table 5.2; Fig. 5.1A**). Out of 557 gut metabolites screened, 207 loaded on component 1 > 1.0, and were classified as “VIP” metabolites. Of this narrowed-down list of 207, 33 metabolites showed a significant relationship to ETI exposure ($p < 0.05$), belonging to amino acid, carbohydrate, cofactors and vitamins, energy, lipid, nucleotide, and xenobiotics super pathways (**Table 5.2**). After correcting for multiple comparisons, four metabolites remained significantly

correlated with ETI exposure: glutamate, gamma-methyl ester (p=0.022, q=0.044), in the glutamate metabolism sub-pathway; 5-oxoproline (p=0.020, q=0.044), in the glutathione metabolism sub-pathway; malate (p=0.003, q=0.018), in the tricarboxylic acid (TCA) cycle sub-pathway; and urate (p=0.002, q=0.036), in the purine metabolism sub-pathway. Of these four significant metabolites, all were reduced by approximately two-fold in individuals with high ETI exposure, compared to those with low ETI exposure (**Fig. 5.1B**).

3.4. Early Life Adversity Associates with Brain Functional Connectivity

A sPLS-DA of brain functional connectivity displayed significant clustering based on low or high ETI exposure (**Table 5.3; Fig. 5.2A**). Connectivity between eleven pairs of brain regions were significantly associated with ETI exposure ($p<0.05$), and after correcting for multiple comparisons, ten pairs of regions remained significant ($q<0.05$) (**Table 5.3**). All regions found to be significantly different have been summarized in **Fig. 5.3** (represented by regions in each specific brain network).

High ETI-related connectivity was observed between salience, sensorimotor, central executive, default mode and central autonomic networks. Specific positive relationships included salience (superior segment of the circular sulcus of the insula) with both sensorimotor (superior frontal gyrus ($q<0.001$)) and default mode (inferior temporal gyrus ($q<0.001$)); sensorimotor (post-central gyrus) with central executive (intraparietal sulcus, interparietal sulcus, and transverse parietal sulci ($q<0.001$)); default mode (lateral aspect of the superior temporal gyrus) with sensorimotor (superior frontal sulcus ($q<0.001$)); sensorimotor (paracentral lobule and sulcus) with sensorimotor (thalamus ($q=0.002$)); default mode (middle temporal gyrus and anterior transverse collateral sulcus) with central autonomic (medial orbital sulcus ($q=0.019$) and straight gyrus (gyrus rectus) ($q=0.014$), respectively) (**Fig. 5.2B; Fig. 5.3; Table 5.3**).

Low ETI-related connectivity was observed between occipital, default mode, and emotion regulation networks, including: default mode (precuneus) with occipital (middle occipital gyrus

(q<0.001)); emotion regulation (anterior part of the cingulate gyrus and sulcus) with both sensorimotor (inferior segment of the circular sulcus of the insula (q<0.001)) and occipital (medial occipito-temporal sulcus (collateral sulcus) (q = 0.029)). (**Fig. 5.2B; Fig. 5.3; Table 5.3**). Additionally, low ETI exposure correlated with increased connectivity approaching significance between default mode (precuneus) and sensorimotor (precentral gyrus (q=0.054)).

3.5. Early Life Adversity Correlates with Alterations in the Brain-Gut-Microbiome System and Current Mood Symptoms

Significant relationships were identified between the significant pairs of connected brain regions (**Section 4.3**), four metabolites (glutamate gamma-methyl ester, 5-oxoproline, malate, and urate; **Section 4.2**), and four clinical variables (ETI score, PSS score, HADS anxiety, and HADS depression; **Section 4.1**) (**Table 5.4; Fig. 5.4**). Significant associations between the variables and by ETI exposure are depicted by group (high ETI and low ETI) and after correcting for multiple comparisons (q<0.05).

In the High ETI group, significant negative associations with key regions of the salience (superior segment of the circular sulcus of the insula), emotion regulation (anterior part of the cingulate gyrus and sulcus), central autonomic (gyrus rectus [straight gyrus]), default mode (inferior temporal gyrus, anterior transverse collateral sulcus), and occipital (medial occipito-temporal sulcus [collateral sulcus]) networks were found with malate and glutamate gamma-methyl ester. Glutamate gamma-methyl ester and 5-oxoproline were negatively associated with symptoms of both anxiety and depression, while urate was negatively associated with symptoms of depression. Connectivity between the sensorimotor and default model networks was positively associated with perceived stress. In addition, sensorimotor networks were negatively correlated with BMI, whereas default mode and central autonomic networks were positively correlated with BMI.

In the Low ETI group, significant negative correlations were found between the connectivity of regions in the sensorimotor (paracentral lobule and sulcus, thalamus, and inferior segment of the circular sulcus of the insula) and emotion regulation (anterior part of the cingulate gyrus and sulcus) networks with glutamate gamma-methyl ester, 5-oxoproline, and urate. However, positive correlations between connectivity in regions of the sensorimotor (postcentral gyrus) and central executive (intraparietal sulcus (interparietal sulcus) and transverse parietal sulci) were positively associated with perceived stress, and symptoms of anxiety and depression. 5-oxoproline and urate were positively associated with ETI total score, while glutamate gamma-methyl ester and 5-oxoproline were negatively associated with BMI.

4. Discussion

The current study aimed to test the hypothesis that a history of ELA is associated with altered brain-gut interactions that impact perceived stress, and symptoms of depression and anxiety in adulthood. Our findings support the notion that ELA can lead to persistent disruptions in the brain-gut system, which may contribute to susceptibility to psychological conditions later into adulthood in response to early life adversity. To our knowledge, this is the first study to comprehensively link adversity during childhood to later-life alterations in intestinal metabolites and functional brain connectivity in humans.

4.1. Early Life Adversity is Associated with Adult Gut Metabolites

We identified four fecal metabolites – urate, malate, glutamate gamma-methyl ester, and 5-oxoproline – as significantly negatively correlated with a history of ELA. Although a clear understanding of the role of these metabolites in humans is limited, previous preclinical investigations demonstrate that some of them display sensitivity to environmental disruptors and disease[57], as well as to microbiome alterations[58 58,59]. In particular, high levels of urate in human plasma have been related to protection against Parkinson's disease[60] and associated with a

microbial enterotype dominated by *Prevotella*[59]. Conversely, in a sample of pregnant women, early adversity correlated positively with *Prevotella*[29]. In addition, 5-oxoproline was increased in the livers of mice transplanted with microbiota from patients with major depressive disorder[61], while levels were decreased in the serum of rats treated with antibiotics[62], suggesting a role for the gut microbiota in the regulation of the metabolite.

One potential pathway by which these metabolites may mediate the relationship between ELA, brain connectivity, and mood is via regulation of oxidative stress. ELA has been previously linked to oxidative stress and cellular aging[63]. In a sample of healthy women, oxidative stress index was positively associated with perceived stress and telomere length[64]. Similarly, a history of childhood maltreatment predicted shorter telomeres[65] and greater mitochondrial DNA copies[65], a marker of oxidative damage, in healthy adults. Notably, the four metabolites of interest have previously been implicated in and described within the context of oxidative stress in animal models[66-68]. In particular, 5-oxoproline was reduced in aged rats, and rescued by probiotic treatment, acting as a gut-targeted antioxidant[69]. In this way, disruptions in the four metabolites may play a role in ELA-related brain network alterations that are mediated by oxidative stress pathways.

An alternative, although potentially related mechanism, is supported by the metabolites being intimately involved in the metabolism of glutamate and related compounds. Glutamate gamma-methyl ester is a metabolite of glutamate[70], while 5-oxoproline is a precursor and closely-related analogue of glutamate[68]. Furthermore, 5-oxoproline plays a critical role in glutamate clearance, by stimulating glutamate transport from the brain and inhibiting its uptake by endothelial cells of the blood-brain barrier[71]. The observed reduction in 5-oxoproline may therefore interfere with CNS clearance of glutamate, which at increased concentrations can be particularly excitotoxic[72] in those with a history of high ELA. Additionally, a role for urate-induced, astrocyte-mediated protection against excitotoxicity has been reported *in vitro*[73]. A reduction in

these metabolites may lower the threshold for cytotoxicity while simultaneously increasing CNS concentrations of glutamate, thereby increasing the risk for excitotoxity and cell death.

4.2. Early Life Adversity is Associated with Adult Brain Functional Connectivity

Many types of ELA have previously been associated with altered brain structure and connectivity, including amygdala, prefrontal, limbic, hippocampal, and striatal regions[20,21,74]. Here, we identify additional brain regions wherein connectivity was significantly correlated with greater ELA scores, which may explain the relationship between early life adversity and negative psychological outcomes later in life. In particular, we report reduced connectivity of the precuneus, a default mode network region critical for aspects of social cognition[75], and self-consciousness and interpretation[76], which may point to altered evaluation of self and others underlying anxious feelings. Indeed, default mode efficiency is negatively correlated with anxiety in young adults[77], and default mode connectivity relates to responsiveness during anxiety learning[77] as well as being heavily implicated in depressive symptoms[78]. Additionally, our findings of decreased connectivity involving emotion regulation networks such as the anterior cingulate cortex, which is involved in conflict monitoring[79] and emotional and cognitive attention[80], and increased connectivity of the insula, a key region in the salience network[81], may suggest modified ability to regulate emotional responses. We report increased connectivity of frontal and parietal sensorimotor regions, and central executive and autonomic areas, which is consistent with a meta-analysis implicating executive control, salience, and sensorimotor networks in anxiety[82].

The fact that ELA disrupts many regions involved in cognitive and emotional processes, which are highly vulnerable to persistent deleterious effects of ELA[83], may present a neurological basis underlying our finding that early adversity correlates with later-life stress and anxiety. Similarly, measures of centrality and segregation in brain regions implicated in emotion and salience reportedly correlate with ELA[16], suggesting that these regions may contribute to psychological manifestations of early trauma. This potential interaction is further supported by

findings that functional connectivity of regions, including the amygdala, putamen, and middle frontal gyrus, as well as regions we also identified, such as the middle temporal and superior frontal gyri, differentiated patients with generalized anxiety from healthy controls.[84]

4.3. A History of Early Life Adversity Correlates with Alterations in the Brain-Gut-Microbiome System and Mood Symptoms

We identified significant relationships between fecal metabolites and altered functional brain connectivity measures involving, most notably, the sensorimotor and default mode networks, which have been implicated in both anxiety[82] and depression[78]. Previous work has underscored associations between the brain-gut axis and psychological outcomes across the lifetime. Gut-targeted probiotic treatment in healthy adults was sufficient to reduce resting state connectivity in somatosensory and insular areas during an emotional attention task[85] and to increase prefrontal cortical activity and reduce induced stress[86]. Connectivity of reward regions has been related to microbiome-derived indole metabolites and anxiety and food addiction outcomes in adults[87]. In addition, connectivity of regions involved in salience, emotion regulation, and sensorimotor function correlated with microbial diversity and cognitive outcomes in infants[88]. Interestingly, in pilot analyses, we have also observed relationships between stress and gut health: in particular, we find that increased stress reactivity is associated with a four-fold higher flare frequency in ulcerative colitis patients, and a similar effect in patients with irritable bowel syndrome, both of which are associated with a history of ELA and psychiatric comorbidities. Findings such as these suggest an interaction between psychological well-being and gut microbiome status, both in healthy and in disease populations.

While other studies have found relationships between early adversity, microbial diversity or taxonomic relative abundances, and current stress and anxiety[28,29], we did not see any difference in diversity or relative abundances in our cohort. However, we observe a change in functional output, suggesting that while the levels of microbes are comparable, something about

their functional potential is being altered by early adversity. Gut microbial metabolites may influence brain network connectivity through both direct and indirect mechanisms. While 5-oxoproline decreases entry of amino acids into the brain by interacting with transporters[89], urate is capable of passing across the blood-brain barrier and acts as a pro-inflammatory agent[90]. However, since the metabolites in this study were measured in feces rather than serum, whether these metabolites may have any direct access to the brain remains unclear. Alternatively, these metabolites may act indirectly via vagal afferent nerve pathways[91,92], which in turn may contribute to the observed changes in functional connectivity.

Not only ELA, but other negative emotional and physiological states have the potential to interact with the brain-gut axis as well. We show that symptoms of anxiety and depression and BMI correlate significantly with urate, glutamate gamma-methyl ester, and 5-oxoproline, that these scales as well as current stress relate significantly to brain functional connectivity of sensorimotor, central executive, default mode, and central autonomic regions, and that subsets of these networks, in addition to salience, emotion regulation, and occipital, correlate significantly with the metabolites. These relationships are of significance due to the potential functional influence of altered sensory modalities and orbitofrontal cortex function, which are critical for decision-making[93], on negative psychological states. Similar findings have been reported in the context of food addiction, with amygdala circuitry and the gut microbiota-derived indole skatole correlating with higher food addiction scores[87]. Additionally, stress-related disorders such as PTSD have been related to altered connectivity in the hippocampus[94] as well as in amygdala-insula circuits[95], and acute stress has been related to metabolites, with increased CSF homovanillic acid correlating with induced symptoms in PTSD patients[96]. However, these past studies do not decouple contributions of past adversity from current experiences of stress and anxiety.

4.4. Future Directions

Limitations of this study include its use of retrospective self-reporting through standardized surveys, which can introduce potential bias into the results and may potentially lead to reduced reliability of the findings. This limitation includes the self-reporting for assessment of menstrual phase and menopause status, which future studies will need to address more accurately by measuring female sex hormone levels especially when investigating sex differences. Critically, our measure of early adversity is not temporally specific, but rather covers the broad period of time from birth to 18 years of age. Future research is warranted to refine this time window to examine relationships between brain-gut phenotypes and ELA during more specific critical periods during development. Secondly, our reported microbial and metabolite findings are derived from fecal samples, which include both microbiota- and host-derived metabolites, and do not necessarily give insight into tissue levels within the CNS. Furthermore, we analyzed only a single fecal sample per participant, although the microbiome and metabolome have been reported to be relatively stable across adulthood[97,98]. We chose to focus on gut metabolites as opposed to microbial community composition as most brain-gut interactions are mediated by microbiota products (such as metabolites) rather than an intrinsic characteristic of the particular microbe itself (such as lipopolysaccharide)[99]. Previous high-quality studies[100,101] have underscored the important role of dietary fiber in modulating the gut microbiota and gut-microbiota derived fecal metabolites. Although we controlled for the type of diet consumed in our analysis, we did not quantify the fiber content of our participants' diets, which may confound our results.

Although the associations between ELA and the brain-gut axis were evident, our sample consisted of participants with a relatively "healthy" status, where anyone with clinical level symptoms of anxiety or depression were excluded from the study. We selected these participants with the intent to highlight and isolate the negative outcomes associated with ELA that are distinct from any effects from overt neurological disease. Future studies that expand upon reported brain-gut phenotypes in individuals with ELA-associated conditions, such as anxiety and depression, are of interest. Finally, while the results from this study reveal novel associations between ELA

and later-life alterations in microbiome-related metabolites and functional brain connectivity, the cross-sectional study design precludes the ability to make causal inferences. Longitudinal studies in humans would help to strengthen correlations and shed light on the timing of interactions between early trauma and altered metabolites and functional brain connectivity.

Although we control for BMI in our final analysis exploring the relationship between ELA, metabolites, and clinical measures, it is important to highlight the positive association between ELA and BMI we identify here – a relationship that has also been confirmed in previous work[102,103]. Obesity is increasingly understood as a brain-gut-microbiome disorder, with mechanisms similar to those we identify in this present work with respect to anxiety and depression. Future investigations may benefit from exploring the intersection between ELA and BMI on these clinical measures within the context of brain-gut interactions[104].

4.5. Clinical Implications and Conclusions

Our findings in human subjects with a history of ELA demonstrate associations that may support the hypothesis that traumatic experiences during critical periods of brain and gut development shape long-term changes in brain-gut interactions. We suggest that this may occur via the well characterized effect of ELA on brain networks involved in emotion regulation and autonomic nervous system output to potentially alter gut microbial function, in the form of microbially-modulated metabolites. The observed dysregulation of glutamate pathways may result in excitotoxicity and oxidative stress, disrupting neural circuit assembly and existing brain network connectivity, and increasing the risk of developing anxiety and depression. Overall, findings from the study provide clinical evidence of brain-gut alterations in response to ELA, and further form a solid foundation upon which to assess potential roles for the microbiome in mediating adverse effects of ELA on brain development and later-life behavior.

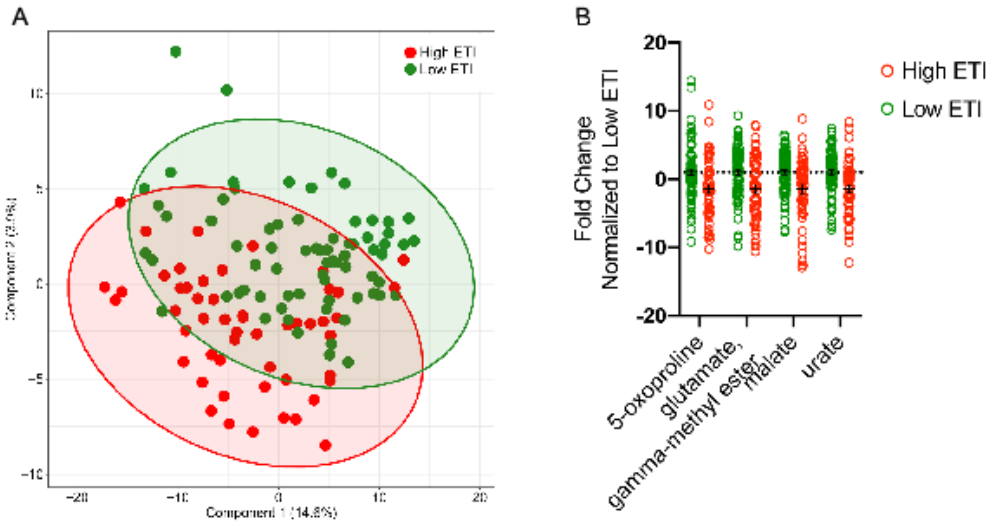

Figure 5.1: Early Life Adversity Differentiates Fecal Metabolite Composition
N=128 total, Low ETI group N=76, High ETI group N=52
A: Gut metabolites cluster by PLS-DA.
B: Fold change of significant metabolites after FDR correction, q < 0.05. Errors bars represent mean +/- SEM.

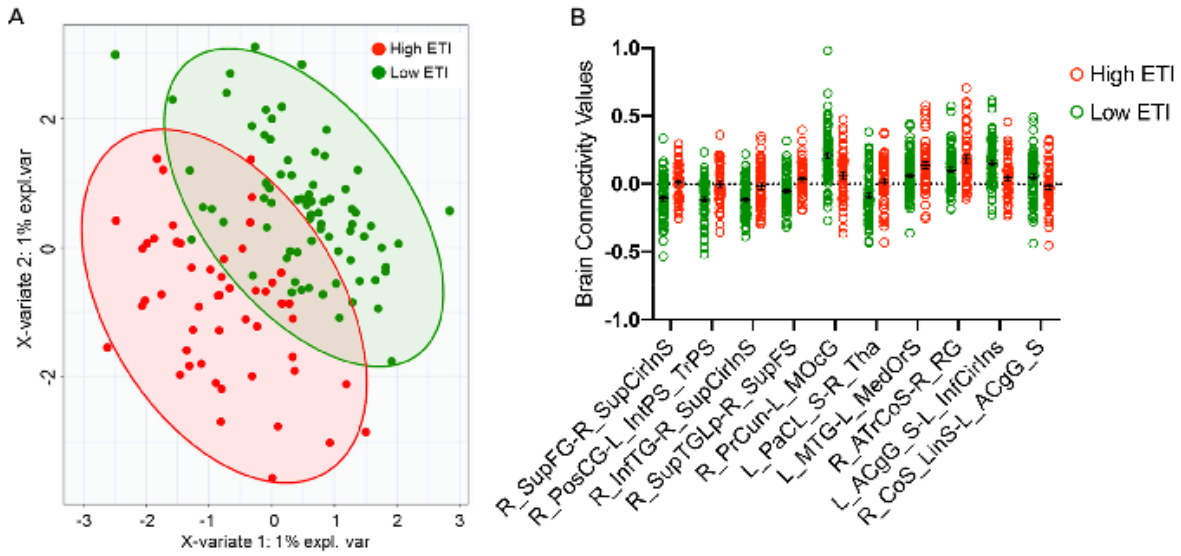

Figure 5.2: Early Life Adversity Differentiates Brain Connectivity
N=128 total, Low ETI group N=76, High ETI group N=52
A: Brain connectivity clusters by SPLS-DA.
B: Significant regions after FDR correction, $q < 0.05$. Error bars represent mean +/- SEM.

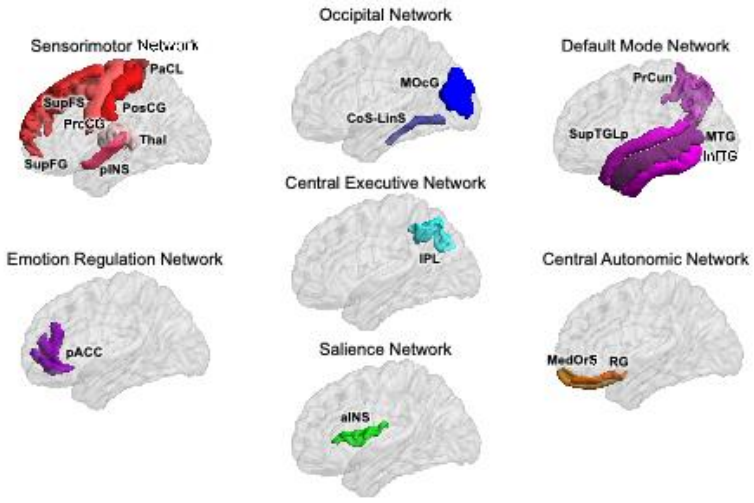

Figure 5.3: Early Life Adversity Impacts Multiple Brain Networks
Brain Regions:
SupFG/S: superior frontal gyrus and sulcus, PreCG: precentral gyrus, PostCG: postcentral gyrus, PaCL: paracentral lobule, pINS: posterior insula; Thal: thalamus, pACC: pregenual anterior cingulate cortex, MOcG: middle occipital gyrus, CoS-LinS: medial occipito-temporal sulcus (collateral sulcus) and lingual sulcus, IPL: inferior parietal lobule, aINS: anterior insula, PrCun: precuneus, SupTGLp: lateral aspect of the superior temporal gyrus, MTG: middle temporal gyrus, InfTG: inferior temporal gyrus, MedOrS: medial orbital sulcus (olfactory sulcus) , RG: gyrus rectus (straight gyrus).

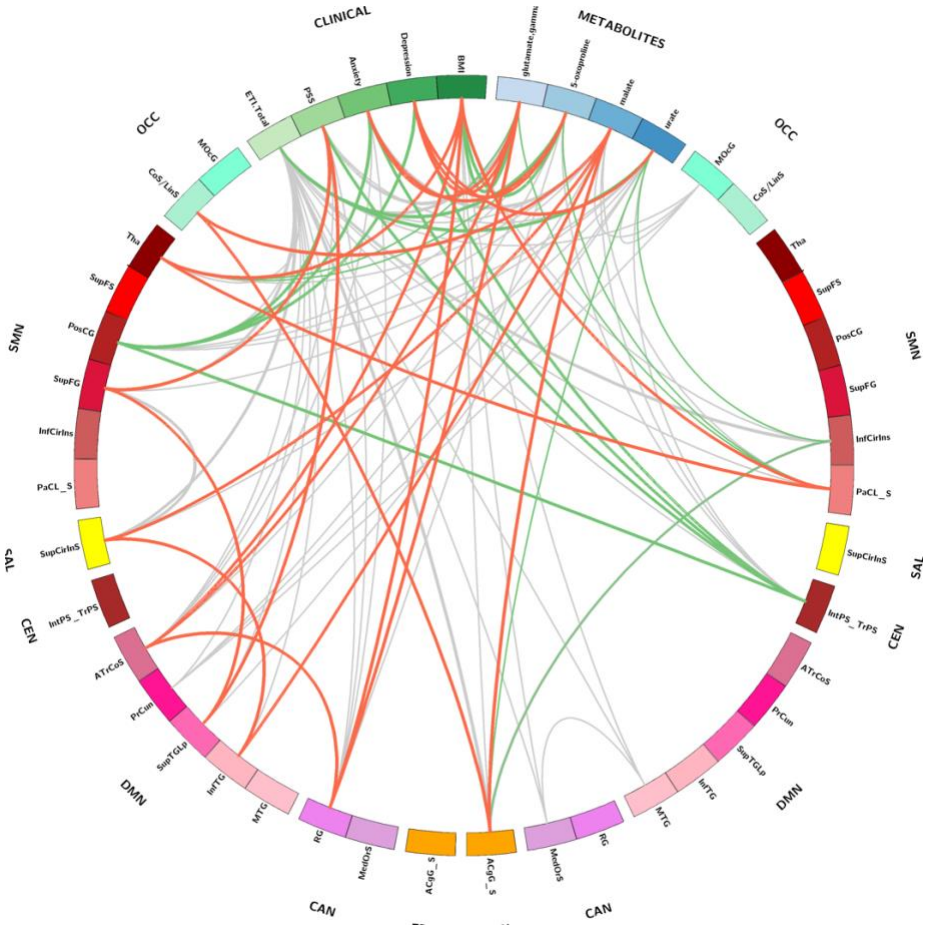

Figure 5.4: Early Life Adversity Interacts with Clinical Variables, Gut Metabolites and Brain Connectivity

N=128 total, Low ETI group N=76, High ETI group N=52

p-value significant <.05

Q-values derived from FDR correction, q-value significant <.05

Red Line: Significant associations in the High ETI group (ETI Total >4)

Green Line: Significant associations in the High ETI group (ETI Total <=4)

Grey Line: Significant associations in the whole sample

Networks:

SMN: sensorimotor, DMN: default mode, SAL: salience, CEN: central executive, CAN: central autonomic, ERN: emotion regulation, OCC: occipital.

Brain Regions:

SupFG: superior frontal gyrus, SupCirInS: superior segment of the circular sulcus of the insula, PosCG: postcentral gyrus, IntPS_TrPS: intraparietal sulcus (interparietal sulcus) and transverse parietal sulci, InfTG: inferior temporal gyrus, SupTGLp: lateral aspect of the superior temporal gyrus, SupFS: superior frontal sulcus, PaCL/S: paracentral lobule and sulcus, Thal: thalamus, ATrCoS: anterior transverse collateral sulcus, RG: straight gyrus (gyrus rectus), ACgG_S: anterior part of the cingulate gyrus and sulcus, InfCirInS: inferior segment of the circular sulcus of the insula; CoS_LinS: medial occipito-temporal sulcus (collateral sulcus) and lingual sulcus.

Clinical Variables:

ETI: early traumatic inventory; BMI: body mass index, PSS: Perceived Stress Scale, HADS: Hospital Anxiety and Depression Scale.

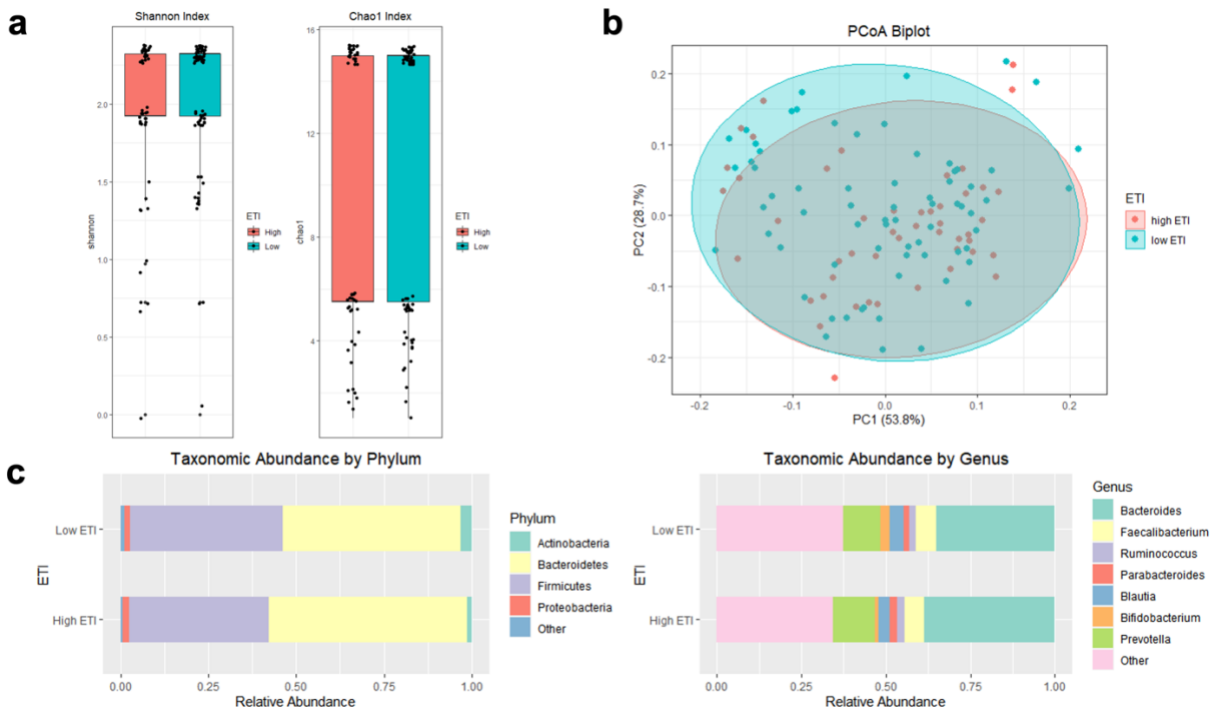

Figure 5.S1: Early Life Adversity Does Not Differentiate Alpha and Beta Diversity or Taxonomic Relative Abundances

A. Alpha diversity metrics, from left to right: ACE ($p = 0.50749$), Chao1 ($p = 0.63385$), Shannon ($p = 0.10209$).

B. Beta diversity: Bray-Curtis-based PCoA (permanova $p = 0.441$).

C: Taxanomic relative abundances: left displays results at the phylum level, right displays results at the genus level.

Psychological Measures	Low ETI		N	High ETI		N	t-value	p-value
	Mean	SD		Mean	SD			
Sex	48 Female	28 Male	76	37 Female	15 Male	52	-	-
Age	27.28	7.55	76	28.81	7.051737	52	-1.17	0.2441
ETI	1.20	1.36	76	8.60*	3.40	52	16.27	**0.0001**
BMI (kg/m^2)	27.42	5.16	76	30.76	5.30	52	-3.53	**0.0006**
PSS Score	11.18	6.39	76	13.37	6.77	52	-1.84	0.0690
HADS Anxiety	3.97	3.33	76	5.33	3.55	52	-2.17	**0.0322**
HADS Depression	1.82	2.00	76	2.29	2.69	52	-1.08	0.2845

TABLE 5.1: Clinical Characteristics Associated with Early Life Adversity
N=128 total, Low ETI group N=76, High ETI group N=52
Means and standard deviations are reported for normally distributed data. ETI threshold = 4 (Low ETI: ETI-SR total ≤ 4, High ETI: ETI-SR total > 4). ETI: early traumatic inventory; BMI: body mass index, PSS: Perceived Stress Scale, HADS: Hospital Anxiety and Depression Scale.
p-significant <.05
***** Previous reports for mean ETI in healthy adults are 7.5 (sd 5.4)[41]

VIP metabolites	Super Pathway	Sub Pathway	beta	se	t	p-value	q-value
glutamate, gamma-methyl ester	Amino Acid	Glutamate Metabolism	-0.407	0.175	-2.322	**0.022**	**0.044**
5-oxoproline	Amino Acid	Glutathione Metabolism	-0.425	0.180	-2.356	**0.020**	**0.044**
formiminoglutamate	Amino Acid	Histidine Metabolism	-0.424	0.184	-2.308	**0.023**	0.219
N6-formyllysine	Amino Acid	Lysine Metabolism	0.423	0.188	2.254	**0.026**	0.219
N,N,N-trimethyl-5-aminovalerate	Amino Acid	Lysine Metabolism	-0.462	0.185	-2.501	**0.014**	0.219
N,N-dimethyl-5-aminovalerate	Amino Acid	Lysine Metabolism	-0.519	0.184	-2.822	**0.006**	0.219
N6,N6-dimethyllysine	Amino Acid	Lysine Metabolism	0.413	0.189	2.190	**0.030**	0.219
N1,N12-diacetylspermine	Amino Acid	Polyamine Metabolism	0.419	0.184	2.278	**0.024**	0.219
(N(1) + N(8))-acetylspermidine	Amino Acid	Polyamine Metabolism	0.402	0.185	2.177	**0.031**	0.219
diacetylspermidine*	Amino Acid	Polyamine Metabolism	0.468	0.186	2.513	**0.013**	0.219
lactate	Carbohydrate	Glycolysis, Gluconeogenesis, and Pyruvate Metabolism	-0.390	0.185	-2.102	**0.038**	0.401
xanthopterin	Cofactors and Vitamins	Pterin Metabolism	-0.410	0.186	-2.204	**0.029**	0.250
malate	Energy	TCA Cycle	-0.550	0.182	-3.016	**0.003**	**0.018**
tricarballylate	Energy	TCA Cycle	-0.378	0.188	-2.016	**0.046**	0.138
N-behenoyl-sphingadienine (d18:2/22:0)*	Lipid	Ceramides	-0.420	0.188	-2.232	**0.027**	0.282
LAHSA (18:2/OH-18:0)*	Lipid	Fatty Acid Hydroxyl Fatty Acid	-0.405	0.184	-2.198	**0.029**	0.282
dihydroorotate	Lipid	Fatty Acid Metabolism(Acyl Carnitine)	-0.485	0.187	-2.598	**0.011**	0.234
azelate (nonanedioate; C9)	Lipid	Fatty Acid, Dicarboxylate	-0.396	0.188	-2.102	**0.038**	0.282
maleate	Lipid	Fatty Acid, Dicarboxylate	-0.499	0.187	-2.671	**0.009**	0.234
mevalonate	Lipid	Mevalonate Metabolism	0.406	0.183	2.223	**0.028**	0.282
1-palmitoylglycerol (16:0)	Lipid	Monoacylglycerol	0.405	0.185	2.186	**0.031**	0.282

pregnen-diol disulfate*	Lipid	Pregnenolone Steroids	0.542	0.187	2.902	**0.004**	0.235
lithocholic acid sulfate (2)	Lipid	Secondary Bile Acid Metabolism	0.367	0.182	2.017	**0.045**	0.282
sphinganine	Lipid	Sphingolipid Synthesis	-0.384	0.188	-2.042	**0.043**	0.282
allantoin	Nucleotide	Purine Metabolism, (Hypo)Xanthine/Inosine containing	-0.423	0.185	-2.290	**0.024**	0.148
urate	Nucleotide	Purine Metabolism, (Hypo)Xanthine/Inosine containing	-0.569	0.182	-3.122	**0.002**	**0.036**
pseudouridine	Nucleotide	Pyrimidine Metabolism, Uracil containing	-0.376	0.185	-2.028	**0.045**	0.148
3-(3-hydroxyphenyl)propionate	Xenobiotics	Benzoate Metabolism	0.467	0.182	2.560	**0.012**	0.107
3-(4-hydroxyphenyl)propionate	Xenobiotics	Benzoate Metabolism	0.389	0.188	2.071	**0.040**	0.141
3,4-dihydroxybenzoate	Xenobiotics	Benzoate Metabolism	-0.395	0.179	-2.212	**0.029**	0.121
piperidine	Xenobiotics	Food Component/Plant	-0.459	0.187	-2.459	**0.015**	0.107
sitostanol	Xenobiotics	Food Component/Plant	-0.489	0.186	-2.630	**0.009**	0.107
sucralose	Xenobiotics	Food Component/Plant	-0.416	0.188	-2.218	**0.028**	0.121

TABLE 5.2: Gut Metabolites Associated with Early Life Adversity
N=128 total, Low ETI group N=76, High ETI group N=52
p-value significant <.05
Q-values derived from FDR correction, q-value significant <.05

Network A	Region A	Network B	Region B	LOADINGS Comp 1	LOADINGS Comp 2	VIP Comp 1	VIP Comp 2	t	p-value	q-value	Interpretation
Brain Signature 1											
SMN	R_SupFG (SMA)	SAL	R_SupCirInS (aINS)	-0.778		236.196	164.545	-4.271	**3.80E-05**	**2.99E-04**	high ETI ↑
SMN	R_PosCG (SI)	CEN	L_IntPS_TrPS (IPL)	-0.467		141.889	98.846	-4.149	**6.10E-05**	**2.99E-04**	high ETI ↑
DMN	R_InfTG (LTC)	SAL	R_SupCirInS (aINS)	-0.395		119.872	83.508	-4.120	**6.80E-05**	**2.99E-04**	high ETI ↑
DMN	R_SupTGLp (LTC)	SMN	R_SupFS (SMA)	-0.145		44.041	30.681	-4.023	**9.83E-05**	**2.99E-04**	high ETI ↑
DMN	R_PrCun	OCC	L_MOcG (OCC)	0.011		3.181	78.003	3.971	**1.19E-04**	**2.99E-04**	low ETI ↑
Brain Signature 2											
SMN	L_PaCL_S	SMN	R_Thal		-0.660		143.839	-3.353	**0.001**	**0.002**	high ETI ↑
DMN	L_MTG (LTC)	CAN	L_MedOrS (OFC)		-0.434		94.628	-2.525	**0.013**	**0.019**	high ETI ↑
DMN	R_ATrCoS (LTC)	CAN	R_RG (OFC)		-0.168		36.603	-2.674	**0.009**	**0.014**	high ETI ↑
DMN	R_PrCun	SAL	R_SupCirInS (aINS)		0.199		43.528	1.562	0.121	0.121	low ETI ↑
DMN	R_PrCun	SMN	L_PRCG (M1)		0.251		54.791	2.046	**0.043**	0.054	low ETI ↑
DMN	R_PrCun	SMN	R_PosCG (S1)		0.162		35.258	1.649	0.102	0.117	low ETI ↑
DMN	R_PrCun	SMN	L_PRCG (M1)		0.096		20.959	1.567	0.120	0.121	low ETI ↑
DMN	R_PrCun	OCC	L_MOcG (OCC)		0.358	3.181	78.003	3.971	**1.19E-04**	**2.99E-04**	low ETI ↑
ERN	L_ACgG_S (pACC)	SMN	L_InfCirInS (aINS)		0.277		60.415	3.583	**4.84E-04**	**1.04E-04**	low ETI ↑
OCC	R_CoS_LinS (OCC)	ERN	L_ACgG_S (pACC)		0.062		13.483	2.329	**0.021**	**0.029**	low ETI ↑

TABLE 5.3: Brain Connectivity Associated with Early Life Adversity
N=128 total, Low ETI group N=76, High ETI group N=52
p-value significant <.05
Q-values derived from FDR correction, q-value significant <.05

Comp: Components; VIP: variable importance projection

Networks:

SMN: sensorimotor, DMN: default mode, SAL: salience, CEN: central executive, CAN: central autonomic, ERN: emotion regulation, OCC: occipital.

Brain Regions:

SupFG: superior frontal gyrus, SMA: supplementary motor area, SupCirInS: superior segment of the circular sulcus of the insula, aINS: anterior insula, PosCG: postcentral gyrus, S1: primary somatosensory cortex, IntPS_TrPS: intraparietal sulcus (interparietal sulcus) and transverse parietal sulci, IPL: inferior parietal lobule, InfTG: inferior temporal gyrus, LTC: lateral temporal cortex, SupTGLp: lateral aspect of the superior temporal gyrus, SupFS: superior frontal sulcus, MOcG: middle occipital gyrus, OCC: occipital lobe, PaCL/S: paracentral lobule and sulcus, Thal: thalamus, MTG: middle temporal gyrus, MedOrS: medial orbital sulcus (temporal sulcus), OFC: orbitofrontal cortex, ATrCoS: anterior transverse collateral sulcus, RG: straight gyrus (gyrus rectus), PrCun: precuneus, PRCG: precentral gyrus, ACgG_S: anterior part of the cingulate gyrus and sulcus, pACC: pregenual anterior cingulate cortex,, InfCirInS: inferior segment of the circular sulcus of the insula, CoS_LinS: medial occipito-temporal sulcus (collateral sulcus) and lingual sulcus.

HIGH ETI (ETI-SR total > 4)					
			correlation coefficient	**p-value**	**q-value**
Brain x Metabolites					
R_InfTG - R_SupCirinS	DMN-SAL	malate	-0.292	0.003	**0.003**
R_ ATrCoS (LTC) - R_RG (OFC)	DMN-CAN	glutamate, gamma-methyl ester	-0.399	0.001	**0.003**
R_CoS_LinS - L_ACgG_S	OCC-ERN	malate	-0.279	0.001	**0.003**
Brain x Clinical Variables					
R_SupTGLp - R_SupFS	DMN-SMN	PSS Score	0.348	0.001	**0.002**
L_PaCL_S - R_Tha	SMN-SMN	BMI	-0.283	0.004	**0.002**
R_ATrCoS - R_RG	DMN-CAN	BMI	0.329	0.001	**0.004**
Metabolites x Clinical Variables					
HADS Anxiety		glutamate, gamma-methyl ester	-0.311	0.002	**0.005**
HADS Depression		glutamate, gamma-methyl ester	-0.299	0.003	**0.005**
HADS Depression		5-oxoproline	-0.322	0.020	**0.005**
HADS Anxiety		5-oxoproline	-0.289	0.003	**0.020**
HADS Depression		urate	-0.353	0.010	**0.013**
LOW ETI (ETI-SR total <= 4)					
			correlation coefficient	**p-value**	**q-value**
Brain x Metabolites					
L_PaCL_S - R_Tha	SMN-SMN	glutamate, gamma-methyl ester	-0.228	0.004	**0.004**
L_PaCL_S - R_Tha	SMN-SMN	5-oxoproline	-0.229	0.004	**0.004**
L_ACgG_S - L_InfCirIns	ERN-SMN	urate	-0.229	0.004	**0.004**
Brain x Clinical Variables					
R_PosCG - L_IntPS_TrPS	SMN-CEN	PSS Score	0.254	0.002	**0.003**
R_PosCG - L_IntPS_TrPS	SMN-CEN	HADS Anxiety	0.264	0.002	**0.003**
R_PosCG - L_IntPS_TrPS	SMN-CEN	HADS Depression	0.333	0.003	**0.003**
Metabolites x Clinical Variables					
BMI		glutamate, gamma-methyl ester	-0.291	0.011	**0.022**
ETI Total Score		5-oxoproline	0.253	0.023	**0.023**

BMI		5-oxoproline	-0.266	0.021	**0.023**
ETI Total Score		urate	0.276	0.001	**0.004**

TABLE 5.4: Early Life Adversity Interacts with Clinical Variables, Gut Metabolites and Brain Connectivity

N=128 total, Low ETI group N=76, High ETI group N=52

p-value significant <.05

Q-values derived from FDR correction, q-value significant <.05

Networks:

SMN: sensorimotor, DMN: default mode, SAL: salience, CEN: central executive, CAN: central autonomic, ERN: emotion regulation, OCC: occipital.

Brain Regions:

SupFG: superior frontal gyrus, SupCirInS: superior segment of the circular sulcus of the insula, PosCG: postcentral gyrus, IntPS_TrPS: intraparietal sulcus (interparietal sulcus) and transverse parietal sulci, InfTG: inferior temporal gyrus, SupTGLp: lateral aspect of the superior temporal gyrus, SupFS: superior frontal sulcus, PaCL/S: paracentral lobule and sulcus, Thal: thalamus, ATrCoS: anterior transverse collateral sulcus, RG: straight gyrus (gyrus rectus), ACgG_S: anterior part of the cingulate gyrus and sulcus, InfCirInS: inferior segment of the circular sulcus of the insula; CoS_LinS: medial occipito-temporal sulcus (collateral sulcus) and lingual sulcus.

Clinical Variables:

ETI: early traumatic inventory; BMI: body mass index, PSS: Perceived Stress Scale, HADS: Hospital Anxiety and Depression Scale.

References

1 Tomalski, P. & Johnson, M. H. The effects of early adversity on the adult and developing brain. *Curr Opin Psychiatry* **23**, 233-238, doi:10.1097/YCO.0b013e3283387a8c (2010).

2 Shonkoff, J. P. *et al.* The lifelong effects of early childhood adversity and toxic stress. *Pediatrics* **129**, e232-246, doi:10.1542/peds.2011-2663 (2012).

3 Romens, S. E., McDonald, J., Svaren, J. & Pollak, S. D. Associations between early life stress and gene methylation in children. *Child Dev* **86**, 303-309, doi:10.1111/cdev.12270 (2015).

4 Carpenter, L. L. *et al.* Association between plasma IL-6 response to acute stress and early-life adversity in healthy adults. *Neuropsychopharmacology* **35**, 2617-2623, doi:10.1038/npp.2010.159 (2010).

5 Joung, K. E. *et al.* Early life adversity is associated with elevated levels of circulating leptin, irisin, and decreased levels of adiponectin in midlife adults. *J Clin Endocrinol Metab* **99**, E1055-1060, doi:10.1210/jc.2013-3669 (2014).

6 Foster, J. A., Rinaman, L. & Cryan, J. F. Stress & the gut-brain axis: Regulation by the microbiome. *Neurobiol Stress* **7**, 124-136, doi:10.1016/j.ynstr.2017.03.001 (2017).

7 Mayer, E. A. Gut feelings: the emerging biology of gut–brain communication. *Nature Reviews Neuroscience* **12**, 453-466 (2011).

8 Martin, C. R., Osadchiy, V., Kalani, A. & Mayer, E. A. The Brain-Gut-Microbiome Axis. *Cell Mol Gastroenterol Hepatol* **6**, 133-148, doi:10.1016/j.jcmgh.2018.04.003 (2018).

9 Osadchiy, V., Martin, C. R. & Mayer, E. A. The Gut-Brain Axis and the Microbiome: Mechanisms and Clinical Implications. *Clin Gastroenterol Hepatol* **17**, 322-332, doi:10.1016/j.cgh.2018.10.002 (2019).

10 Osadchiy, V., Mayer, E.A., Bhatt, R., Labus, J.S., Gao, L., Kilpatrick, L.A., Liu, C., Tillisch, K., Naliboff, B., Chang, L., Gupta, A. History of early life adversity is associated with increased food addiction and sex-specific alterations in reward network connectivity in obesity. *Obesity Science & Practice* **5**, 416-436 (2019).

11 Bradford, K., Shih, W., Videlock, E.J., Presson, A.P., Naliboff, B.D., Mayer, E.A., Chang, L. Association between early adverse life events and irritable bowel syndrome. *Clinical Gastroenterology and Hepatology* **10**, 385-390 (2012).

12 Labus, J. S. *et al.* Differences in gut microbial composition correlate with regional brain volumes in irritable bowel syndrome. *Microbiome* **5**, 49, doi:10.1186/s40168-017-0260-z (2017).

13 Levine, M. E., Cole, S.W., Weir, D.R., Crimmins, E.M. Childhood and later life stressors and increased inflammatory gene expression at older ages. *Social Science & Medicine* **130**, 16-22 (2015).

14 Gupta, A. *et al.* Gene expression profiles in peripheral blood mononuclear cells correlate with salience network activity in chronic visceral pain: A pilot study. *Neurogastroenterol Motil* **29**, doi:10.1111/nmo.13027 (2017).

15 Teicher, M. H., Samson, J.A., Anderson, C.M., Ohashi, K. The effects of childhood maltreatment on brain structure, function and connectivity. *Nature Reviews* **17**, 652-666 (2016).

16 Gupta, A. *et al.* Early adverse life events are associated with altered brain network architecture in a sex- dependent manner. *Neurobiol Stress* **7**, 16-26, doi:10.1016/j.ynstr.2017.02.003 (2017).

17 Etkin, A., Egner, T., Peraza, D.M., Kandel, E.R., Hirsch, J. Resolving Emotional Conflict: A Role for the Rostral Anterior Cingulate Cortex in Modulating Activity in the Amygdala. *Neuron* **51**, 871-882 (2006).

18 Cisler, J. M., James, G.A., Tripathi, S., Mletzko, T., Heim, C., Hu, X.P., Mayberg, H.S., Nemeroff, C.B., Kilts, C.D. Differential functional connectivity within an emotion regulation neural network among individuals resilient and susceptible to the depressogenic effects of early life stress. *Psychological Medicine* **43**, 507-518 (2013).

19 Stein, M. B., Simmons, A.N., Feinstein, J.S., Paulus, M.P. Increased amygdala and insula activation during emotion processing in anxiety-prone subjects. *The American Journal of Psychiatry* **164**, 318-327 (2007).

20 Hodel, A. S. *et al.* Duration of early adversity and structural brain development in post-institutionalized adolescents. *Neuroimage* **105**, 112-119, doi:10.1016/j.neuroimage.2014.10.020 (2015).

21 Miskovic, V., Schmidt, L. A., Georgiades, K., Boyle, M. & Macmillan, H. L. Adolescent females exposed to child maltreatment exhibit atypical EEG coherence and psychiatric impairment: linking early adversity, the brain, and psychopathology. *Dev Psychopathol* **22**, 419-432, doi:10.1017/S0954579410000155 (2010).

22 Honeycutt, J. A. *et al.* Altered corticolimbic connectivity reveals sex-specific adolescent outcomes in a rat model of early life adversity. *Elife* **9**, doi:10.7554/eLife.52651 (2020).

23 Dong, T. S. & Gupta, A. Influence of Early Life, Diet, and the Environment on the Microbiome. *Clin Gastroenterol Hepatol* **17**, 231-242, doi:10.1016/j.cgh.2018.08.067 (2019).

24 Zijlmans, M. A., Korpela, K., Riksen-Walraven, J. M., de Vos, W. M. & de Weerth, C. Maternal prenatal stress is associated with the infant intestinal microbiota. *Psychoneuroendocrinology* **53**, 233-245, doi:10.1016/j.psyneuen.2015.01.006 (2015).

25 Yassour, M. *et al.* Natural history of the infant gut microbiome and impact of antibiotic treatment on bacterial strain diversity and stability. *Sci Transl Med* **8**, 343ra381, doi:10.1126/scitranslmed.aad0917 (2016).

26 Backhed, F. *et al.* Dynamics and Stabilization of the Human Gut Microbiome during the First Year of Life. *Cell Host Microbe* **17**, 852, doi:10.1016/j.chom.2015.05.012 (2015).

27 Bergstrom, A. *et al.* Establishment of intestinal microbiota during early life: a longitudinal, explorative study of a large cohort of Danish infants. *Appl Environ Microbiol* **80**, 2889-2900, doi:10.1128/AEM.00342-14 (2014).

28 Callaghan, B. L. *et al.* Mind and gut: Associations between mood and gastrointestinal distress in children exposed to adversity. *Dev Psychopathol* **32**, 309-328, doi:10.1017/S0954579419000087 (2020).

29 Hantsoo, L. *et al.* Childhood adversity impact on gut microbiota and inflammatory response to stress during pregnancy. *Brain Behav Immun* **75**, 240-250, doi:10.1016/j.bbi.2018.11.005 (2019).

30 Wall, R. *et al.* Bacterial neuroactive compounds produced by psychobiotics. *Adv Exp Med Biol* **817**, 221-239, doi:10.1007/978-1-4939-0897-4_10 (2014).

31 Zheng, P. *et al.* Gut microbiome remodeling induces depressive-like behaviors through a pathway mediated by the host's metabolism. *Mol Psychiatry* **21**, 786-796, doi:10.1038/mp.2016.44 (2016).

32 Dalile, B., Vervliet, B., Bergonzelli, G., Verbeke, K., Van Oudenhove, L. Colon-delivered short-chain fatty acids attenuate the cortisol response to psychosocial stress in healthy men: a randomized, placebo-controlled trial. *Neuropsychopharmacology* **0**, 1-10 (2020).

33 Van de Wouw, M., Boehme, M., Lyte, J.M., Wiley, N., Strain, C., O'Sullivan, O., Clarke, G., Stanton, C., Dinan, T.G., Cryan, J.F. Short-chain fatty acids: microbial metabolites that alleviate stress-induced brain-gut axis alterations. *The Journal of Physiology* **596**, 4923-4944 (2018).

34 Lyte, M., Vulchanova, L. & Brown, D. R. Stress at the intestinal surface: catecholamines and mucosa-bacteria interactions. *Cell Tissue Res* **343**, 23-32, doi:10.1007/s00441-010-1050-0 (2011).

35 De Palma, G. *et al.* Microbiota and host determinants of behavioural phenotype in maternally separated mice. *Nat Commun* **6**, 7735, doi:10.1038/ncomms8735 (2015).

36 Moussaoui, N., Jacobs, J.P., Larauche, M., Biraud, M., Million, M., Mayer, E., Tache, Y. Chronic Early-life Stress in Rat Pups Alters Basal Corticosterone, Intestinal Permeability, and Fecal Microbiota at Weaning: Influence of Sex. *Journal of Neurogastroenterology and Motility* **23**, 135-143 (2017).

37 Sheehan, D. V. *et al.* The Mini-International Neuropsychiatric Interview (M.I.N.I.): the development and validation of a structured diagnostic psychiatric interview for DSM-IV and ICD-10. *The Journal of clinical psychiatry* **59 Suppl 20**, 22-33;quiz 34-57 (1998).

38 Bremner, J. D., Bolus, R. & Mayer, E. A. The early trauma inventory self report (ETI-SR). *Gastroenterology* **128**, A340-A340 (2005).

39 Bremner, J. D., Bolus, R. & Mayer, E. A. Psychometric properties of the Early Trauma Inventory-Self Report. *J Nerv Ment Dis* **195**, 211-218, doi:10.1097/01.nmd.0000243824.84651.6c (2007).

40 Horberg, N. *et al.* Early Trauma Inventory Self-Report Short Form (ETISR-SF): validation of the Swedish translation in clinical and non-clinical samples. *Nord J Psychiatry* **73**, 81-89, doi:10.1080/08039488.2018.1498127 (2019).

41 Cohen, S., Kamarck, T. & Mermelstein, R. A global measure of perceived stress. *J Health Soc Behav* **24**, 385-396 (1983).

42 Zigmond, A. S. & Snaith, R. P. The hospital anxiety and depression scale. *Acta Psychiatr Scand* **67**, 361-370, doi:10.1111/j.1600-0447.1983.tb09716.x (1983).

43 Dong, T. S. *et al.* Improvement in Uncontrolled Eating Behavior after Laparoscopic Sleeve Gastrectomy Is Associated with Alterations in the Brain-Gut-Microbiome Axis in Obese Women. *Nutrients* **12**, doi:10.3390/nu12102924 (2020).

44 Dong, T. S. *et al.* A Distinct Brain-Gut-Microbiome Profile Exists for Females with Obesity and Food Addiction. *Obesity (Silver Spring)* **28**, 1477-1486, doi:10.1002/oby.22870 (2020).

45 Osadchiy, V. *et al.* Analysis of brain networks and fecal metabolites reveals brain-gut alterations in premenopausal females with irritable bowel syndrome. *Transl Psychiatry* **10**, 367, doi:10.1038/s41398-020-01071-2 (2020).

46 Tong, M., Jacobs, J. P., McHardy, I. H. & Braun, J. Sampling of intestinal microbiota and targeted amplification of bacterial 16S rRNA genes for microbial ecologic analysis. *Curr Protoc Immunol* **107**, 7 41 41-47 41 11, doi:10.1002/0471142735.im0741s107 (2014).

47 Caporaso, J. G. *et al.* QIIME allows analysis of high-throughput community sequencing data. *Nat Methods* **7**, 335-336, doi:10.1038/nmeth.f.303 (2010).

48 Lozupone, C. & Knight, R. UniFrac: a new phylogenetic method for comparing microbial communities. *Appl Environ Microbiol* **71**, 8228-8235, doi:10.1128/AEM.71.12.8228-8235.2005 (2005).

49 Anderson, M. J. A new method for non-parametric multivariate analysis of variance. *Austral Ecology* **26**, 32-46 (2001).

50 Love, M. I., Huber, W. & Anders, S. Moderated estimation of fold change and dispersion for RNA-seq data with DESeq2. *Genome Biol* **15**, 550, doi:10.1186/s13059-014-0550-8 (2014).

51 Evans, A. M., DeHaven, C. D., Barrett, T., Mitchell, M. & Milgram, E. Integrated, nontargeted ultrahigh performance liquid chromatography/electrospray ionization tandem mass spectrometry platform for the identification and relative quantification of the small-molecule complement of biological systems. *Anal Chem* **81**, 6656-6667, doi:10.1021/ac901536h (2009).

52 Melander, A. *et al.* 35th Annual Meeting of the European Association for the Study of Diabetes : Brussels, Belgium, 28 September-2 October 1999. *Diabetologia* **42**, A1-A330, doi:10.1007/BF03375458 (1999).

53 Schaefer, A., Kong, R., Gordon, E.M., Laumann, T.O., Zuo, X., Holmes, A.J., Eickhoff, S.B., Yeo, B.T.T. Local-Global Parcellation of the Human Cerebral Cortex from Intrinsic Functional Connectivity MRI. *Cerebral Cortex* **28**, 3095-3114 (2018).

54 Destrieux, C., Fischl, B., Dale, A. & Halgren, E. Automatic parcellation of human cortical gyri and sulci using standard anatomical nomenclature. *Neuroimage* **53**, 1-15, doi:10.1016/j.neuroimage.2010.06.010 (2010).

55 Edlow, B. L., Takahashi, E., Wu, O., Benner, T., Dai, G., Bu, L., Grant, P.E., Greer, D.M., Greenberg, S.M., Kinney, H.C., Folkerth, R.D. . Neuroanatomic connectivity of the human ascending arousal system critical to consciousness and its disorders. *J Neuropathol Exp Neurol* **71**, 531-546 (2012).

56 Benjamini, Y. & Hochberg, Y. Controlling the false discovery rate: a practical and powerful approach to multiple testing. *Journal of the Royal Statistical Society. Series B (Methodological)* **57**, 289-300 (1995).

57 Ilievski, V. *et al.* Experimental Periodontitis Results in Prediabetes and Metabolic Alterations in Brain, Liver and Heart: Global Untargeted Metabolomic Analyses. *J Oral Biol (Northborough)* **3**, doi:10.13188/2377-987X.1000020 (2016).

58 Donohoe, D. R. *et al.* The microbiome and butyrate regulate energy metabolism and autophagy in the mammalian colon. *Cell Metab* **13**, 517-526, doi:10.1016/j.cmet.2011.02.018 (2011).

59 Scheperjans, F., Pekkonen, E., Kaakkola, S. & Auvinen, P. Linking Smoking, Coffee, Urate, and Parkinson's Disease - A Role for Gut Microbiota? *J Parkinsons Dis* **5**, 255-262, doi:10.3233/JPD-150557 (2015).

60 Weisskopf, M. G., O'Reilly, E., Chen, H., Schwarzschild, M. A. & Ascherio, A. Plasma urate and risk of Parkinson's disease. *Am J Epidemiol* **166**, 561-567, doi:10.1093/aje/kwm127 (2007).

61 Li, B. *et al.* Metabolite identification in fecal microbiota transplantation mouse livers and combined proteomics with chronic unpredictive mild stress mouse livers. *Transl Psychiatry* **8**, 34, doi:10.1038/s41398-017-0078-2 (2018).

62 Behr, C. *et al.* Gut microbiome-related metabolic changes in plasma of antibiotic-treated rats. *Arch Toxicol* **91**, 3439-3454, doi:10.1007/s00204-017-1949-2 (2017).

63 Schiavone, S., Colaianna, M. & Curtis, L. Impact of early life stress on the pathogenesis of mental disorders: relation to brain oxidative stress. *Curr Pharm Des* **21**, 1404-1412, doi:10.2174/1381612821666150105143358 (2015).

64 Epel, E. S. *et al.* Accelerated telomere shortening in response to life stress. *Proc Natl Acad Sci U S A* **101**, 17312-17315, doi:10.1073/pnas.0407162101 (2004).

65 Tyrka, A. R. *et al.* Alterations of Mitochondrial DNA Copy Number and Telomere Length With Early Adversity and Psychopathology. *Biol Psychiatry* **79**, 78-86, doi:10.1016/j.biopsych.2014.12.025 (2016).

66 Wu, J. L. *et al.* L-malate reverses oxidative stress and antioxidative defenses in liver and heart of aged rats. *Physiol Res* **57**, 261-268 (2008).

67 Randhawa, M., Sangar, V., Tucker-Samaras, S. & Southall, M. Metabolic signature of sun exposed skin suggests catabolic pathway overweighs anabolic pathway. *PLoS One* **9**, e90367, doi:10.1371/journal.pone.0090367 (2014).

68 Kumar, A. B., A.K. Pyroglutamic acid: throwing light on a lightly studied metabolite. *Current Science* **102**, 288-297 (2012).

69 Hor, Y. Y. *et al.* Lactobacillus sp. improved microbiota and metabolite profiles of aging rats. *Pharmacol Res* **146**, 104312, doi:10.1016/j.phrs.2019.104312 (2019).

70 Tsuge, Y. K., A. . in *Production of Platform Chemicals from Sustainable Resources Biofuels and Biorefineries* (ed Z. Fang, Smith, Jr. R., Qi, X.) 437-455 (Springer, Singapore, 2017).

71 Hawkins, R. A., Simpson, I.A., Mokashi, A., Vina, J.R. Pyroglutamate stimulates Na+-dependent glutamate transport across the blood brain barrier. *FEBS Letters* **580**, 4382-4386 (2006).

72 Dong, X., Wang, Y., Qin, Z. Molecular mechanisms of excitoxocitiy and their relevance to pathogenesis of neurodegenerative diseases. *Acta Pharmacologica Sinica* **30**, 379-387 (2009).

73 Du, Y., Chen, C.P., Tseng, C., Eisenberg, Y., Firestein, B.L. Astroglia-mediated effects of uric acid to protect spinal cord neurons from glutamate toxicity. *Glia* **55**, 463-472 (2007).

74 Gee, D. G. *et al.* Early developmental emergence of human amygdala-prefrontal connectivity after maternal deprivation. *Proc Natl Acad Sci U S A* **110**, 15638-15643, doi:10.1073/pnas.1307893110 (2013).

75 Li, W., Mai, X., Liu, C. The default mode network and social understanding of others: what do brain connectivity studies tell us. *Frontiers in Human Neuroscience* **8** (2014).

76 Cavanna, A. E. & Trimble, M. R. The precuneus: a review of its functional anatomy and behavioural correlates. *Brain* **129**, 564-583, doi:10.1093/brain/awl004 (2006).

77 Tao, Y., Liu, B., Zhang, X., Li, J., Qin, W., Yu, C., Jiang, T. The structural connectivity pattern of the default mode network and its association with memory and anxiety. *Frontiers in Neuronatomy* **9** (2015).

78 Brakowski, J., Spinelli, S., Dorig, N., Bosch, O.G., Manoliu, A., Holtforth, M.G., Seifritz, E. Resting state brain network function in major depression – Depression symptomatology, antidepressant treatment effects, future research. *Journal of Psychiatric Research* **92**, 147-159 (2017).

79 Kerns, J. G. *et al.* Anterior cingulate conflict monitoring and adjustments in control. *Science* **303**, 1023-1026, doi:10.1126/science.1089910 (2004).

80 Bush, G., Luu, P. & Posner, M. I. Cognitive and emotional influences in anterior cingulate cortex. *Trends in cognitive sciences* **4**, 215-222 (2000).

81 Menon, V. & Uddin, L. Q. Saliency, switching, attention and control: a network model of insula function. *Brain Struct Funct* **214**, 655-667, doi:10.1007/s00429-010-0262-0 (2010).

82 Xu, J., Van Dam, N.T., Feng, C., Luo, Y., Ai, H., Gu, R., Xu, P. . Anxious brain networks: A coordinate-based activation likelihood estimation meta-analysis of resting-state functional connectivity studies in anxiety. *Neuroscience & Biobehavioral Reviews* **96**, 21-30 (2019).

83 Pechtel, P., Pizzagalli, D.A. Effects of early life stress on cognitive and affective function: an integrated review of human literature. *Psychopharmacology* **214**, 55-70 (2011).

84 Qiao, J., Li, A., Cao, C., Wang, Z., Sun, J., Xu, G. Aberrant Functional Network Connectivity as a Biomarker of Generalized Anxiety Disorder. *Frontiers in Human Neuroscience* **11** (2017).

85 Tillisch, K., Labus, J., Kilpatrick, L., Jiang, Z., Stains, J., Ebrat, B., Guyonnet, D., Legrain-Raspaud, S., Trotin, B., Naliboff, B., Mayer, E.A. Consumption of fermented milk product with probiotic modulates brain activity. *Gastroenterology* **144**, 1394-1401 (2013).

86 Allen, A. P., Hutch, W., Borre, Y.E., Kennedy, P.J., Temko, A., Boylan, G., Murphy, E., Cryan, J.F., Dinan, T.G., Clarke, G. Bifidobacterium longum 1714 as a translational psychobiotic: modulation of stress, electrophysiology and neurocognition in healthy volunteers. *Translational Psychiatry* **6** (2016).

87 Osadchiy, V. *et al.* Correlation of tryptophan metabolites with connectivity of extended central reward network in healthy subjects. *PLoS One* **13**, e0201772, doi:10.1371/journal.pone.0201772 (2018).

88 Gao, W., Salzwedel, A.P., Carlson, A.L., Xia, K., Azcarate-Peril, M.A., Styner, M.A., Thompson, A.L., Geng, X., Goldman, B.D., Gilmore, J.H., Knickmeyer, R.C. Gut microbiome and brain functional connectivity in infants - a preliminary study focusing on the amygdala. *Psychopharmacology* **236**, 1641-1651 (2019).

89 Hawkins, R. A., O'Kane, R.L., Simpson, I.A., Vina, J.R. Structure of the blood-brain barrier and its role in the transport of amino acids. *The Journal of Nutrition* **136**, 218S-226S (2006).

90 Shao, X., Lu, W., Gao, F., Li, D., Hu, J., Li, Y., Zuo, Z., Jie, H., Zhao, Y., Cen, X. Uric acid induces cognitive dysfunction through hippocampal inflammation in rodents and humans. *Journal of Neuroscience* **36**, 10990-11005 (2016).

91 Bartolomei, F., Bonini, F., Vidal, E., Trebuchon, A., Lagarde, S., Lambert, I., McGonigal, A., Scavarda, D., Carron, R., Benar, C.G. How does vagal nerve stimulation (VNS) change EEG brain functional connectivity? *Epilepsy Research* **126**, 141-146 (2016).

92 Cao, J., Lu, K., Powley, T.L., Liu, Z. Vagal nerve stimulation triggers widespread responses and alters large-scale functional connectivity in the rat brain. *PLoS One* **12**, e0189518 (2017).

93 Bechara, A., Damasio, H. & Damasio, A. R. Emotion, decision making and the orbitofrontal cortex. *Cereb Cortex* **10**, 295-307, doi:10.1093/cercor/10.3.295 (2000).

94 Chen, A. C. & Etkin, A. Hippocampal network connectivity and activation differentiates post-traumatic stress disorder from generalized anxiety disorder. *Neuropsychopharmacology* **38**, 1889-1898, doi:10.1038/npp.2013.122 (2013).

95 Rabinak, C. A. *et al.* Altered amygdala resting-state functional connectivity in post-traumatic stress disorder. *Front Psychiatry* **2**, 62, doi:10.3389/fpsyt.2011.00062 (2011).

96 Geracioti, T. D., Jr. *et al.* Effect of traumatic imagery on cerebrospinal fluid dopamine and serotonin metabolites in posttraumatic stress disorder. *J Psychiatr Res* **47**, 995-998, doi:10.1016/j.jpsychires.2013.01.023 (2013).

97 Lozupone, C., Stombaugh, J.I., Gordon, J.I., Jansson, J.K., Knight, R. Diversity, stability and resilience of the human gut microbiota. *Nature* **489**, 220-230 (2012).

98 Yousri, N. A. *et al.* Long term conservation of human metabolic phenotypes and link to heritability. *Metabolomics* **10**, 1005-1017, doi:10.1007/s11306-014-0629-y (2014).

99 Osadchiy, V., Martin, C. R. & Mayer, E. A. Gut Microbiome and Modulation of CNS Function. *Compr Physiol* **10**, 57-72, doi:10.1002/cphy.c180031 (2019).

100 Wu, G. D. *et al.* Linking long-term dietary patterns with gut microbial enterotypes. *Science* **334**, 105-108, doi:10.1126/science.1208344 (2011).

101 Tanes, C. *et al.* Role of dietary fiber in the recovery of the human gut microbiome and its metabolome. *Cell Host Microbe* **29**, 394-407 e395, doi:10.1016/j.chom.2020.12.012 (2021).

102 Fuemmeler, B. F., Dedert, E., McClernon, F. J. & Beckham, J. C. Adverse childhood events are associated with obesity and disordered eating: results from a U.S. population-based survey of young adults. *J Trauma Stress* **22**, 329-333, doi:10.1002/jts.20421 (2009).

103 Osadchiy, V. *et al.* History of early life adversity is associated with increased food addiction and sex-specific alterations in reward network connectivity in obesity. *Obes Sci Pract* **5**, 416-436, doi:10.1002/osp4.362 (2019).

104 Gupta, A., Osadchiy, V. & Mayer, E. A. Brain-gut-microbiome interactions in obesity and food addiction. *Nat Rev Gastroenterol Hepatol* **17**, 655-672, doi:10.1038/s41575-020-0341-5 (2020).

Appendix: Supporting information related to Chapter 3

Appendix 1 contains supporting information related to **Chapter 3**, in which I report that gestational protein restriction (PR) alters fetal brain signatures and long-term behavioral outcomes in offspring, which are modulated by the maternal microbiome and can be ameliorated by select microbially-informed interventions. In order to further examine neural signatures of gestational malnutrition in the fetal brain, and how these may lead to observed behavioral impairment in adulthood, I have investigated multiple avenues of inquiry. I start by investigating fetal and placental disruption at a mid-gestational timepoint, and identify late gestation as the period where fetal disruption becomes grossly apparent. I then clarify that the anxiety-like and cognitive behavioral impairment reported in **Chapter 3** is specific, because we do not see impairment in other behavioral domains. Next, I use targeted metabolomics, histology, and quantitative polymerase chain reaction (qPCR) to investigate possible mechanisms of fetal brain disruption in response to both gestational PR and maternal microbial depletion, including short chain fatty acids (SCFA), hypothalamic-pituitary-adrenal (HPA) axis targets, serotonergic axons, neuronal proliferation, and microglia. I then take a look at splenic and placental insufficiency in response to gestational PR, as well as to microbial depletion or targeted interventions. And finally, I test a probiotic supplementation during gestation to try to combat persistent behavioral phenotypes of PR-exposed offspring.

Placental insufficiency precedes fetal growth restriction in gestational PR

In **Chapter 3**, we profile various fetal and maternal phenotypes at embryonic day (E) 18.5 in response to gestational PR. Prior to honing in on this late gestational timepoint, I first investigated a mid-gestational timepoint, E14.5, where we have previously found disruptions in response to maternal perturbations (**Chapter 4**;[1,2]). When investigating gross weight changes, I observed a lack of apparent fetal growth restriction at this timepoint, but did observe placental insufficiency **(Fig. A.1a-b)**. Placental disruptions preceding fetal have been previously reported in dietary models, and may suggest impaired support of the fetus via disruptions in nutrient, oxygen,

or waste transfer[3]. As observed at E18.5 (**Chapter 3**), maternal post-transection weight was significantly less in PR-fed dams compared to those fed control diet (CD) at E14.5, which was not explained by a difference in diet consumed **(Fig. A.1c-d)**. PR dams also displayed smaller spleen weight as a percentage of total body weight **(Fig. A.1e)**, suggesting potential immune disruption on the maternal side. Immune function has been highlighted previously in malnourished children[4] and is appreciated as an essential function during neurodevelopment[5]. Furthermore, maternal immune activation during pregnancy is a risk factor for neurodevelopmental disorders in offspring[6].

Although I did not observe differences in fetal size at this timepoint, I were curious about alterations in brain size, or in brain to body ratio. Using micro-computed tomography (uCT), we found no significant differences in total fetal volume or surface area, fetal brain or ventricular volume, or fetal brain to body ratio between CD and PR **(Fig. A.1e-j)**. This is in contrast to previous reports which suggest altered brain size and structure following PR, both in postnatal humans[7] and in prenatal animal models[3].

Due to the observed decrease in placental size in PR litters, I were curious about placental function, and whether this may partially underly the observed fetal growth restriction at late-gestation **(Chapter 3)**. Using immunostaining and confocal imaging, we saw no significant differences in integrated density of laminin in the placental labyrinth (the fetal compartment) between CD and PR placentas **(Fig. A.1k)**. Laminin is a component of placental endothelial cells, and therefore provides insight into feto-placental vasculature, which did not appear to be disrupted in this case. However, past work has described abnormalities in placental blood vessels and perfusion following gestational PR[8,9]. Overall, the E14.5 experiments suggest that in the context of gestational PR, placental and maternal weight changes precede fetal growth restriction. However, it is unclear from our investigation the degree to which placental size implies impaired function, and whether the placental phenotype might contribute to later fetal growth restriction.

Offspring behavioral impairment following gestational PR is domain-specific

In **Chapter 3** we investigate anxiety-like behavior and cognitive impairment in adult offspring subject to gestational PR and associated rearing. To confirm whether this behavior was specific, or if there was a more general behavioral impairment phenotype, I ran a full battery of behavioral tests on adult offspring, cross-fostered within or across maternal diet condition, and fed control diet from birth. The battery included assays for exploratory/risk-taking, social, sensorimotor gating, and tactile sensation behaviors.

I ran the elevated plus maze test to measure anxiety-like behavior[10]. I found a significant reduction in the ratio of entries to closed versus open arms in PR→PR offspring compared to PR→CD by litter average **(Fig. A.2e)**, which seems to be driven by male offspring specifically **(Fig. A.2f)**. This may suggest increased exploratory or risk-taking behavior or decreased anxiety-like behavior, although this effect was not replicated in the ratios for time spent or distance traveled in the closed arm, either by litter average or in either sex **(Fig. A.2a-d)**.

I ran the three-chamber social preference test to measure motivation for social interaction[11]. I found a significant increase in the ratio of entries to social versus empty zone in PR→PR offspring compared to both PR→CD and CD→PR, although this effect was only apparent in female offspring, not by litter average **(Fig. A.2k-l)**. This may suggest a female-specific preference for social interaction, however this was not replicated in the ratios for time spent or distance traveled in the social zone, either by litter average or in either sex **(Fig. A.2g-j)**.

I ran acoustic startle and pre-pulse inhibition testing to measure sensorimotor gating[12]. There were no significant differences in amount of pre-pulse inhibition or in magnitude of startle response, either by litter average or in either sex **(Fig. A.2m-p)**, suggesting intact sensorimotor gating.

I ran adhesive removal test and Von Frey filament test to measure tactile sensitivity and sensorimotor function in front and back paws, respectively[13,14]. In adhesive removal test, there was no significant difference in latency to contact or removal of the tape from the front paws by

litter average **(Fig. A.2q)**, although there was a trending increase in latency to removal in female PR→PR offspring compared to PR→CD **(Fig. A.2r)**. Similarly, there was no significant difference in back paw withdrawal threshold by litter average **(Fig. A.2s)**, although there was a significant decrease in withdrawal threshold in CD→PR males, and a trending decrease in CD→PR females, compared to CD→CD controls **(Fig. A.2t)**. These findings are modest, but may suggest impaired fine motor response in females subjected to PR gestation and associated rearing, but increased tactile sensitivity in both sexes subjected to PR associated rearing alone.

Overall, behavioral results from these additional assays provide less consistent and convincing evidence for impairment compared to the assays presented in **Chapter 3**, suggesting a primary effect of PR on anxiety-like and cognitive behaviors.

Serotonergic axons are disrupted by gestational protein restriction and maternal microbial depletion

Following observations of behavioral impairment in anxiety-like and cognitive domains in adult offspring exposed to gestational PR and associated rearing **(Chapter 3)**, I was curious about effects of PR on fetal brain that may manifest as behavioral dysregulation in adulthood. My first hypothesis was that neuronal or microglial proliferation may play a role, as impaired neuronal proliferation[15] and altered microglial proteome[16] were previously reported in a gestational PR model. To this end, we used immunostaining and confocal imaging to investigate neural proliferation and microglia in the hippocampus **(Fig. A.3a)** and frontal cortex **(Fig. A.3b)** of CD and PR fetus at E18.5. However, we saw no significant differences in integrated density of nestin (a marker of neural stem cells and progenitors), or in the number of cells positive for Ki67 (a marker of proliferation) in either of the examined brain regions **(Fig. A.2b-c, A.3b-c)**. Additionally, we saw no significant differences in the number of cells positive for Iba1 (a marker of microglia) with or without Ki67, or in the integrated density of Iba1 per positive cell (a measure of microglial inflammation) in either of the examined brain regions **(Fig. A.2d-f, A.3d-f)**. These results provide

contrasting evidence to prior findings which reported that gestational PR decreased neural stem cells/progenitors and reduced proliferation in the ganglionic eminences in mid- and late-gestation[15].

In **Chapter 3** we also highlight the potential for HPA axis signaling to be disrupted by PR, as we saw elevated corticosterone in PR maternal serum and fetal brains at E18.5. Stress during critical periods can be neurotoxic, is known to interact with both maternal microbiome and fetal neurodevelopment[17,18], and to precipitate anxiety- and cognitive-related behavioral deficits in offspring[19]. For this reason, I wanted to further investigate HPA axis-related targets in the fetal brain using qPCR. I quantified *Hsd11b1* and *Hsd11b2*, which act to convert cortisol to and from its inactive form, cortisone, as well as *Fkbp5*, which is involved in regulation of glucocorticoid receptors. I quantified these genes in the fetal brains of SPF (specific pathogen-free; conventional microbiome) CD and PR dams, but also in those of dams treated with broad-spectrum antibiotics (ABX) to deplete the microbiota, to assess contributions of maternal microbiome. Interestingly, there were no significant differences in these genes between any of the groups **(Fig. A.5a-d)**.

In **Chapter 3**, we discussed transcriptomic and metabolomic signatures of PR in fetal brain. One significantly downregulated gene was *Slc6a4*, which encodes serotonin transporter (SERT). Furthermore, tryptophan and associated metabolic pathways were significantly downregulated in PR maternal serum but upregulated in fetal brain, and one of the metabolites in the 10M cocktail which ameliorated select PR phenotypes in offspring was 3-indoxyl sulfate, a tryptophan catabolite. Based on these findings, I wondered whether serotonergic signaling could be disrupted in the fetal brain following PR exposure. To investigate, we used immunostaining and confocal imaging to assess SERT+ axons in the hippocampus **(Fig. A.6a)** and frontal cortex **(Fig. A.7a)** at E18.5. We looked at SPF CD and PR fetuses, as well as ABX PR, to assess contributions of maternal microbiome. We found that fetuses subject to PR had significantly reduced SERT+ axons, measured by count and sum length, particularly in hippocampal CA3 **(Fig. A.6c-d)** and frontal cortex layers IZ, SZ, and CP **(Fig. A.7c-d)**. Furthermore, ABX PR fetal brains

had further reduced SERT+ axons in the VZ and IZ of the frontal cortex. Importantly, in all hippocampal and frontal cortex subregions the staining of NeuN was consistent between groups **(Fig. A.6b, A.7b)**, suggesting a serotonergic-specific depletion, rather than fewer neurons overall. Interestingly, the direction of this depletion is consistent with the behavioral impairments reported in **Chapter 3**, where PR offspring displayed worse learning and memory in Barnes maze testing compared to CD, and ABX PR offspring performance was further exacerbated compared to SPF PR. Although this experiment is by no means causal, it is intriguing to postulate about whether serotonergic circuits in the fetal brain could underly later behavioral disruption in response to gestational PR. Indeed, tryptophan and serotonin were altered by protein restriction during gestation and lactation in rats[20], serotonin regulates many neurodevelopmental processes including neurogenesis, proliferation, differentiation, and plasticity, and altered levels during gestation have been linked to behavioral impairments, including anxiety and cognitive, in offspring[21].

Gestational PR influences select SCFAs in fetal brain in late gestation

Based on previous findings from the lab in which the SCFA acetate, butyrate, and propionate were sufficient to rescue maternal microbiome depletion- and maternal protein restriction-induced placental insufficiency[2], I wondered about how gestational PR was affecting SCFA levels in maternal serum and fetal brain. Surprisingly, I found no significant effect of ABX treatment, and only moderate effects of gestational PR on SCFA levels in fetal brain. 2-Methylbutyric acid and Isobutyric acid were both significantly reduced in SPF PR fetal brain compared to SPF CD, and in ABX PR fetal brain compared to ABX CD, suggesting a microbiome-independent effect of diet on these metabolites **(Fig. A.8a, e)**. Isovaleric acid was reduced in SPF PR fetal brain compared to SPF CD, but this effect did not reach significance **(Fig. A.8f)**. Furthermore, acetic acid was significantly increased in ABX PR fetal brain compared to ABX CD, and the same trend was apparently in SPF PR compared to SPF CD, although the latter did not

reach significance **(Fig. A.8b)**. I found no significant effect of diet on SCFA levels in maternal serum. Isovaleric acid did show an ABX affect, whereby it was increased in SPF CD maternal serum compared to ABX CD maternal serum, but this did not reach significance **(Fig. A.8f).** Butyric acid, hexanoic acid, propionic acid, and valeric acid showed no significant effects of either diet or microbiome, in either tissue type **(Fig. A.8c-d, g-h).**

These results showing no ABX-driven changes in SCFA are surprising, as SCFA have been shown to be altered following microbial depletion[22,23]. Alterations in select SCFA in fetal brain may underly some of the neurodevelopmental impairments reported here and in **Chapter 3**, as SCFA are known to be neurodevelopmentally influential[24]. Interestingly, the SCFA butyrate has been reported to ameliorate cognitive and neurophysiological impairments following maternal low-fiber diet[25], however, the limited differences reported here are consistent with the lack of behavioral amelioration following SCFA supplementation discussed in **Chapter 3.**

Gestational PR induces placental and splenic insufficiency in late-gestation

Based on the findings of placental and splenic insufficiency at E14.5 detailed above **(Fig. A.1)**, I was curious whether these phenotypes would persist to E18.5. I found that indeed, in E18.5 litters SPF PR dams had significantly smaller spleens **(Fig. A.9a)** and placentas **(Fig. A.9e)** compared to SPF CD. Additionally, ABX PR placentas and spleens were significantly smaller than ABX CD, and ABX CD spleens were also significantly smaller than SPF CD, suggesting the maternal microbiota may support spleen growth during pregnancy, but that depletion does not remove the diet-induced difference in either spleen or placenta size. Because select maternal microbiota-informed interventions were effective at ameliorating select PR phenotypes **(Chapter 3)**, I was curious if the same would be the case here. However, supplementation with short-chain fatty acids or the 10M microbially-modulated metabolite cocktail failed to ameliorate maternal spleen **(Fig. A.9b-c)** or placental size **(Fig. A.9f-g)**. Supplementation with a consortia of seven bacteria found to be depleted in PR dams also had no significant effect on placental size **(Fig.**

A.9h) but significantly exacerbated spleen size **(Fig. A.9d)**. To further explore the placental phenotype in particular, we used uCT, and found that SPF PR placentas had significantly smaller volume and surface area compared to SPF CD **(Fig. A.9i-j)**. In conclusions, the placental and splenic insufficiency induced by gestational PR were persistent, did not appear to be microbiome-dependent, and were not ameliorated by any microbially-informed interventions.

Bacterial supplementation has mild and mixed effects on PR phenotypes

In **Chapter 3**, we showed that a microbially-modulated metabolite cocktail (10M) was sufficient to ameliorate select phenotypes of gestational PR, including maternal corticosterone, offspring survival, and adult behavioral impairment in a sex-dependent manner. We further showed that PR dams had diet-driven taxonomic differences throughout pregnancy. I was curious whether supplementing the microbes themselves, rather than microbe-dependent products, would have a similar result to 10M. Indeed, probiotic supplementation has been effective in ameliorating gastrointestinal consequences of malnutrition in children[26]. To this end, we identified seven bacterial genera that were significantly reduced in PR dams **(Fig. A.10a)**, cultured representative strains of each, and supplemented them (7B), or a PBS vehicle, throughout gestation via daily oral gavage to PR-fed dams **(Fig. A.10b)**. I found a nonsignificant increase in fetal size at E18.5 **(Fig. A.10c)** and no significant differences in maternal weight or diet consumed **(Fig. A.10d-e)**, maternal corticosterone **(Fig. A.10f),** litter size **(Fig. A.10g)**, or offspring weight in the first two weeks or life or in adulthood **(Fig. A.10i-j)**. There was a small increase in litter survival **(Fig. A.10h)**.

Adult offspring supplemented with 7B showed no significant behavioral amelioration compared to PBS-supplemented controls by litter average **(Fig. A.11a-e)**, although they did have a near-significant increase in latency to escape **(Fig. A11b)** and errors **(Fig. A11e)** during the acquisition and probe phases of Barnes Maze, respectively. When separating by sex, however, adult offspring of 7B-supplemented and PR-fed dams displayed significantly different behavioral

responses, compared to PBS-supplemented offspring. Namely, male offspring supplemented with 7B during gestation displayed reduced anxiety-like behavior, spending significantly more time, and traveling near-significantly greater distance in the center of the open field, whereas female offspring showed the opposite effect, displaying greater anxiety-like behavior **(Fig. A.12a-b)**. Additionally, male offspring supplemented with 7B during gestation spent significantly less time in the target zone during the probe trial of Barnes Maze **(Fig. A.12e)**, while neither males nor females had a significant difference in errors made during the probe phase **(Fig. A.12f)**, nor in latency to escape or to target zone during the acquisition phase of Barnes Maze **(Fig. A.12c-d)**.

Together, these results suggest that 7B supplementation fails to ameliorate prenatal fetal or maternal PR phenotypes, and has a bidirectional, sex- and domain-specific impact on behavioral outcomes following PR. It is unclear why some of the behavioral phenotypes were exacerbated particularly in female offspring, but it is possible that the probiotic cocktail had unforeseen pathogenic or dysbiotic potential, or that the microbes interacted with host to induce detrimental metabolomic outputs that manifested in a sex-specific manner. More investigation would be required to confirm this; however these results make apparent that the 10M intervention reported in **Chapter 3** is a more promising potential therapeutic for PR-induced phenotypes.

Methods

Mice

8-week old male and female C57Bl/6J mice were purchased from Jackson Laboratories and maintained on 12-h light-dark cycle in temperature- and humidity-controlled environment. All mice were kept under sterile conditions (autoclaved cages, bedding, water bottles, and water). All experiments were performed in accordance with the NIH Guide for the Care and Use of Laboratory Animals using protocols approved by the Institutional Animal Care and Use Committee at UCLA.

Protein restriction

Mice were first subjected to a microbiota normalization, where two scoops of bedding were removed from each cage, mixed together, and deposited back in each cage to normalize microbiota between all mice in each testing cohort. At least 5 days after normalization, male and female mice were given either 6% protein diet (Teklad Envigo; TD.90016) or 20% control diet (Teklad Envigo; TD.91352) *ad libitum* for at least 2 weeks. Following this habituation period, mice were paired and time-mated. At E0.5, determined by observation of copulation plug, pregnant dams were individually housed and continued to be fed the same diet through gestation. Weights and fecal samples were collected from each dam at E0.5 and 18.5, with a subset collected at E0.5, 7.5, 10.5, 14.5, 18.5.

Antibiotic treatment

For "ABX" treatment groups, SPF male and female mice were gavaged twice daily for one week with neomycin (100 mg/kg), metronidazole (100 mg/kg) and vancomycin (50 mg/kg), as previously described[2,27]. During this time, ampicillin (1 mg/mL) was provided *ad libitum* in drinking water. Mice were then time-mated as described above. Following gavage, mice were maintained on ampicillin (1 mg/mL), neomycin (1 mg/mL) and vancomycin (0.5 mg/mL) *ad libitum* in drinking water for the duration of the experiment.

Tissue collections

For E14.5 measures, dams were sacrificed by cervical dislocation at E14.5. The entire uterine horn, including all conceptuses, was removed and placed in ice cold 1x PBS. Dams were weighed to record post-transection weight. Maternal spleen was removed and weighed. Each fetus and placenta was dissected from the amniotic sac and weighed. At random, whole fetuses were collected for uCT and serially diluted in EtOH, and whole placentas were fixed in 4%

paraformaldehyde (PFA) for 24 hours, cryoprotected in 30% sucrose until saturated, and then frozen in OCT (TissueTek) in cryo-molds and stored at -80°C for subsequent histology.

In a separate cohort, dams were sacrificed by cervical dislocation at E18.5. Blood was collected by cardiac puncture into vacutainer SST tubes (Becton Dickinson) and allowed to clot for 1 hour at room temperature, before centrifuging at 1500xg, 4°C for 10 minutes. Serum supernatant was collected and stored at -20°C for subsequent metabolomics. The entire uterine horn, including all conceptuses, was removed and placed in ice cold 1x PBS. Dams were weighed to record post-transection weight. Maternal spleen was removed and weighed. Each fetus was dissected from the amniotic sac and weighed. At random, whole placentas were collected for uCT and serially diluted in EtOH, and fetal brains were dissected and either placed into RNAlater (Invitrogen) for subsequent qPCR, snap-frozen in liquid nitrogen for subsequent metabolomics, or fixed in 4% PFA for 48 hours, cryoprotected in 30% sucrose until saturated, and then frozen in OCT (TissueTek) in cryo-molds for subsequent histology. All brain samples were stored at -80°C.

Targeted Metabolomics

Fetal brains stored at -80°C and maternal serum stored at -20°C were sent to *Metabolon* for targeted metabolomic quantification. For brain samples, 1.5-2 fetal brains were pooled. Mouse serum and mouse brain samples are analyzed for eight short chain fatty acids: acetic acid (C2), propionic acid (C3), isobutyric acid (C4), butyric acid (C4), 2-methyl-butyric acid (C5), isovaleric acid (C5), valeric acid (C5) and caproic acid (hexanoic acid, C6) by liquid chromatography with tandem mass spectrometry (LC-MS/MS). Mouse serum and mouse brain samples were spiked with stable labelled internal standards, homogenized, and subjected to protein precipitation with an organic solvent. After centrifugation, an aliquot of the supernatant was derivatized. The reaction mixture was injected onto an Agilent 1290/AB Sciex QTrap 5500 LC MS/MS system equipped with a C18 reversed phase UHPLC column. The mass spectrometer was operated in

negative mode using electrospray ionization (ESI). The peak area of the individual analyte product ions was measured against the peak area of the product ions of the corresponding internal standards. Quantitation was performed using a weighted linear least squares regression analysis generated from fortified calibration standards prepared immediately prior to each run. LC-MS/MS raw data were collected using AB SCIEX software Analyst 1.6.3 and processed using SCIEX OS-MQ software v1.7. Data reduction was performed using Microsoft Excel for Office 365 v.16

Quantitative RT-PCR

Fetal brains stored at -80°C in RNAlater (Invitrogen) were thawed and homogenized with a bead-beater. RNA was extracted using the PureLink RNA Mini Kit (Invitrogen) and cDNA was synthesized using the qScript cDNA Synthesis Kit (Quantabio), all according to manufacturer instructions. qPCR with reverse transcription was performed on a QuantStudio 5 thermocycler (ThermoFisher Scientific) using SYBR green master mix with Rox passive reference dye and validated primer sets obtained from Primerbank (Harvard). Genes of interest were analyzed by fold change compared to the housekeeping gene *Gapdh*.

Immunofluorescence

Placental tissue staining

E14.5 placental staining was performed as previously described[2]. Briefly, placentas were fixed in 4% PFA for 24 hours at 4°C, cryoprotected in 30% sucrose in PBS 4°C until saturated, embedded in OCT (TissueTek), and sectioned at 12 µm using a Leica CM1950 cryostat. Slices were placed directly onto coated slides and stored at -20°C until staining. Antigen retrieval was performed using !0% citrate buffer (DAKO) at 95°C for 20 minutes then at room temperature for 15 minutes. Sections were blocked with 10% goat serum for 1 hour at room temperature, then incubated for 16 hours at 4°C with laminin rabbit anti-mouse antibody (1:250, Sigma-Aldrich). Sections were then incubated for 1 hour at room temperature in their corresponding goat anti-

rabbit antibodies conjugated to Alexa Fluor 568 (1:1000, ThermoFisher Scientific) and DAPI (1:500, Invitrogen). Slides were cover-slipped and allowed to dry before imaging.

Fetal brain tissue staining

E18.5 fetal brains were fixed in 4% PFA for 48 hours at 4°C, cryoprotected in 30% sucrose in PBS 4°C until saturated, embedded in OCT (TissueTek), and serially sectioned at 15 µm, using a Leica CM1950 cryostat. Slices were placed directly onto coated slides and stored at -20°C until staining. Antigen retrieval was performed using 10% citrate buffer (DAKO) at 95°C for 20 minutes then at room temperature for 15 minutes. Sections were blocked with 10% goat serum for 1 hour at room temperature, then incubated with either staining panel #1 - Ki67 (1:150, ThermoFisher Scientific), Iba1 (1:500, Fijufilm), and Nestin (1:250, Novus) for 16 hours at 4°C; or with staining panel #2 - SERT (1:500, Abcam) and NeuN (1:1000, Millipore Sigma) for 16 hours at 4°C. Sections were then incubated for 1 hour at room temperature with either anti-chicken, anti-rat, and anti-rabbit secondary antibodies (1:1000, Abcam) and DAPI (1:500, Invitrogen) for staining panel #1; or with anti-rabbit and anti-guinea pig secondaries (1:1000, Abcam & ThermoFisher Scientific) and DAPI (1:500, Invitrogen) for staining panel #2. Slides were cover-slipped and allowed to dry before imaging.

Image acquisition

All images were acquired using a Zeiss Axio Examiner LSM 780 confocal microscope with a 20x objective. For placental stains, 5 Z-stack images at 1um intervals were acquired. For brain staining panel #1, 10 Z-stack images at 0.65um intervals were acquired. For brain staining panel #2, 8 Z-stack images at .97um intervals were acquired. For all tissue types, two sections per sample were imaged using Zen Black 2012 software *(*Zeiss). Images were stitched with a 10% overlap, and the complete range of *z* series was compressed using Zen Blue 2021 software (Zeiss).

Image analysis

All image analysis was done using ImageJ (NIH). For laminin analysis[2], each image was thresholded to exclude background and autofluorescence, by a researcher blinded to condition. ROIs were drawn to include the full area of the placental labyrinth. Laminin integrated density was measured and normalized to full tissue coverage area.

For fetal brain analysis, ROIs for hippocampal and frontal cortex subregions were drawn manually using the Allen Brain Atlas and confirmed by a second researcher. For staining panel #1, proliferating cells were quantified by counting colocalization of Ki67 and DAPI, or Ki67, DAPI, and Iba1. Non-proliferating microglia were quantified by counting colocalization of Iba1 and DAPI. Neural progenitors and stem cells were quantified by measuring Nestin integrated density. All measures were normalized to DAPI tissue coverage area. For staining panel #2, serotonergic axons were quantified by tracing SERT-positive axons using the NeuronJ plugin (NIH). Serotonergic axon count and total visible axon length were recorded for each ROI. Neurons were quantified by NeuN integrated density. All measures were normalized to DAPI tissue coverage area.

Micro–computed tomography

Placental and fetal tissue were prepped and scanned as previously described[1,2,27] **(Chapter 4)**. Briefly, whole E14.5 fetuses and E18.5 placentas were serially dehydrated, from 30 to 50 to 70% ethanol and incubated in 4% (w/v) phosphotungstic acid diluted in 70% ethanol for 4 days at 4°C. Tissues were scanned at 60 kVp/150 μA with a 1-mm Al filter at 8 μm resolution using a benchtop μCT scanner (SkyScan 1275, Bruker). Reconstructions of two-dimensional images were generated using dynamic range adjustment and gaussian smoothing, a ring artifact reduction of 10, and a defect pixel mask of 8%. Whole placental and fetal volumes and surface area were reconstructed and measured using CTAn and CTVol software (Bruker Corporation),

using a threshold range of 88 (minimum) to 255 (maximum). ROIs were drawn manually to obtain whole brain and ventricle volume. Brain to body ratio was calculated.

Behavioral testing

For behavioral cohorts, dams were allowed to give birth, with birth date denoted as P0. At E17.5, dams were given shepherd shacks to reduce stress ahead of birth. At P0, dams and diet were weighed, pups were counted, and all diet groups were switched to CD. Complete litters were cross-fostered. Subsequently, litters were checked daily for pup survival. Litters were denoted as not survived if <4 remained at weaning. Pups were weighed on P3, 5, 7, 9. 11, 13, and toe-tattooed P4-P6, for identification purposes. Pups were weaned P24-P26, and separated into cages with same-sex litter mates. Adult behaviors were run beginning when mice were ~90 days old. All mice were habituated in the testing room 30 minutes prior to test start. Whenever possible, behavioral tests were run before 12:00pm. Tests were run in order of least to most stressful, in the order described below, with at least 3 days separating each test. All equipment was cleaned with 70% ethanol and allowed to dry in between mice.

Open field test – 7B cohort only

Open field test was employed to assess locomotion and thigmotaxis as a proxy for anxiety-like behavior[35,36]. Mice were placed into open field arenas (27.5 cm^2) for 10 minutes under bright light. Videos were recorded using an overhead camera, and the first 5 minutes of each test were analyzed using AnyMaze 7.1 for time spent in center zone, distance traveled in center zone/total distance traveled, total distance traveled, and mean speed.

Elevated plus maze – SPF cohort only

Elevated plus maze was employed to assess exploratory and risk-taking behaviors as a proxy for anxiety-like behavior[10]. The apparatus consisted of four arms (30x5cm each) in a “plus”

formation, two of which are enclosed with walls and two of which are not. The maze was set up on a tripod to elevate it above the ground. Mice were placed into the center and allowed to freely explore all arms for 5 minutes. Videos were recorded with an overhead camera and analyzed using AnyMaze7.1. If a mouse fell off the apparatus, it was re-run again at the end of the testing period. Direction of open versus closed arms was counterbalanced across sex and condition. The time, distance/ total distance traveled, and entries to the closed versus open arms was calculated using the following method: (closed - open) / (closed + empty).

Three-chamber social preference – SPF cohort only

The three-chamber social preference test was run to assess sociability[11]. The apparatus was made up of three chambers (20x40.5cm) separated by clear walls but with holes enabling mice to freely enter each end chamber from the center. Sex-matched conspecific mice were habituated to the cup and testing chamber for 10 minutes prior to testing. Test mice were placed in the empty apparatus and allowed to explore freely for 10 minutes. An inverted wire cup was then placed in each end chamber, one empty and one containing the con-specific. Location of social cup was counterbalanced across sex and condition. Test mice were then allowed to freely explore for another 10 minutes. Videos were recorded with an overhead camera and analyzed using AnyMaze7.1. The time, distance/total distance traveled, and entries to the social versus empty zone in the second phase of testing were calculated using the following method: (social - empty) / (social + empty).

Adhesive removal test – SPF cohort only

Adhesive removal test was run as previously described[27] to assess tactile sensitivity[14]. Mice were placed into an empty cage for 1 minute to acclimate. Each mouse was then scruffed, and a small (0.35cm^2) square of medical tape (North) was gently applied to each front paw with curved forceps (AESCULAP). The mouse was replaced into the empty cage, and the latency to

notice and remove tape from each paw was recorded, with a cut-off of 5 minutes. The values for left and right paw were averaged for analysis.

Von Frey filament test – SPF cohort only

Von Frey filament test was run as previously described[27] to assess tactile sensitivity[13]. Mice were placed onto a wire mesh surface elevated within a testing chamber and acclimated to the surface for 10 minutes. Von Frey filaments were then applied to the bottom of each hind paw, increasing in filament force until a paw withdrawal reflex was observed. Filaments were then toggled between the withdrawal-inducing stimulus and one below, to confirm response force.

Barnes maze – 7B cohort only

Barnes maze was employed to assess spatial learning and memory[38]. The Barnes maze apparatus has an elevated round surface (90cm diameter) with 20 holes evenly spaced around the perimeter. One hole was denoted as the “escape” hole, and an escape box was attached below the hole. The position of the escape hole was kept consistent within mice, but counterbalanced between mice. Spatial cues (black and white geometric shapes printed on 9x11in paper) were placed around the maze, and kept consistent throughout training and testing. On day 1 of the testing protocol, each mouse was allowed to freely explore the Barnes maze apparatus for 5 minutes with no white noise under mild light, with no escape box present. Immediately following, each mouse was placed under a wire cup in the center of the apparatus, with white noise and bright light for 1 minute. Finally, each mouse was gently guided to the escape hole and into the escape box, and white noise and bright light were removed, for 1 minute. On days 2-5, each mouse was subject to three training trials, with an inter-trial latency of 20-45 minutes. The training trials consisted of 15s habituation, where mice were placed under a wire cup in the center of the apparatus with bright light and white noise. The cup was then lifted, and mice were given 180s to escape into the escape hole, thereby ending the test. If the mouse did not escape by 180s, they

were gently guided into the escape hole. At the end of each trial, mice were left for 1 minute in the escape hole, with no white noise. On day 6, a probe test was run to assess long-term memory. Each mouse was subject to one probe trial, consisting of a 15s habituation, and then a 180s test without the escape box. Videos were recorded using an overhead camera and analyzed in AnyMaze 7.1. For the training trials, latency to find the escape hole and latency to enter the escape box were analyzed. For the probe trial, time spent in the escape hole vicinity, and errors, defined as non-escape hole vicinities a mouse entered *before* entering the escape hole vicinity, were analyzed.

Pre-pulse inhibition and acoustic startle – SPF cohort only

Acoustic startle was run to assess sensorimotor gating and anxiety-like behavior[12]. Mice were placed into Plexiglass cylinders (3.2cm internal diameter) mounted onto a sensor platform inside a recording chamber. Mice were habituated for 5 minutes with white noise, before being subjected to a presentation of acoustic startle stimuli and pre-pulse stimuli via a high frequency speaker 15cm from testing cylinder. Maximal response occurring 100 milliseconds after presentation of stimulus was taken as startle amplitude. For acoustic startle, the first 6, middle 10, and last 6 responses to 120db were averaged to get three trials. For pre-pulse inhibition, each trial type (70db, 75db, 80db) were averaged, and then divided by the middle trial of acoustic startle. The results were then multiplied by 100 and subtracted from 100 to get the percent inhibition produced by that prepulse value.

<u>In vivo bacterial supplementation</u>

Taxonomic selection for bacterial treatment

Data from 16S rRNA gene sequencing **(Chapter 3)** were assessed to identify ASVs that were significantly decreased in PR dams compared to CD controls. Each ASV found to be decreased in PR dams was then analyzed with a two-way repeated measures ANOVA. All ANOVA results

were filtered with a post-hoc two-stage step-up method of Benjamini, Krieger, and Yekutieli, FDR = 8%. ASV sequences that showed a significant main effect of condition that survived correction were then queried in NCBI BLAST to identify the closest related species. When no species matched 100%, a close match was selected based on its presence in the gut microbiome and any relation to protein metabolism based on existing literature. Seven species were identified from this selection process, with following % matches to original sequences: *Lactococcus lactis* (100%), *Sporobacter termitidis* (94.8%), *Parasuterella excrementihominis* (100%), *Clostridium disporicum* (99.2%), *Emergencia timonensis* (97.6%), *Lachnospiraceae bacterium* (100%), and *Lactobacillus johnsonii* (98%).

Bacterial culture

The following strains were obtained from DSMZ collection and propagated as instructed: *Lachnospiraceae bacterium* DSM 111138, *Emergencia timonensis* DSM 101844, *Parasutterella excrementihominis* DSM 21040, *Lactococcus lactis* DSM 20481, *Lactobacillus johnsonii* DSM 10533, *Sporobacter termitidis* DSM 10068*, Clostridium disporicum* DSM 5521. The cultures were routinely grown anaerobically in their respective media and temperature (**Table A.S1**). The grown cells were combined to reach to 10^9 cells/mL. The 16S rRNA gene from colonies of each culture was PCR-amplified using 8F (5'-AGAGTTTGATCCTGGCTCAG-3' and 1492R (5'-GGTTACCTTGTTACGACTT- 3') primers and sent for Sanger sequencing (Laragen). To confirm viability and cell counts, the gram-positive bacteria were stained with crystal violet and counted under a microscope using a hemocytometer. Gram negative bacteria were counted without a

stain. Between $8.9X10^8$ to $4.6X10^9$ cells/mL of each bacterium were mixed in equal amounts and aliquoted in glycerol and frozen at -80°C. On each gavage day, the mixtures were thawed, spun down at 12000 x g for 10 minutes, glycerol supernatant was removed, and the bacterial pellet was resuspended in sterile PBS under anaerobic conditions.

Bacterial supplementation

All mice were habituated on PR diet, and bred as described above. Once copulation plugs were observed, bacterial mixture (7B) in 200uL sterile PBS was orally gavaged once per day from E0.5-E17.5. Control dams were orally gavaged with 200uL sterile PBS as a vehicle control. 7B and PBS litters were then used for E18.5 tissue collections, or for postnatal cross-fostering and behavioral testing, as described above.

Statistical Methods and Sample Sizes

Statistical analyses were performed using Prism 9.0 (Graphpad). Assays with two groups were assessed for normality and subsequently analyzed by either an unpaired two-tailed t-test with Welch's correction, or by a Mann-Whitney test. Tests on three or more groups were assessed by a one-way ANOVA, and when there were two factors, with a two-way ANOVA. Data over time were assessed with a repeated measures ANOVA or mixed measures analysis. Tukey or Sidak post-hoc tests were used, based on Prism recommendations. All prenatal weight measures and postnatal behavioral measures were run using litter as a biological replicate, with all fetuses or offspring averaged within each litter. For prenatal weights and maternal metrics, at least 9 litters per group were analyzed. For behavioral experiments, 6 litters per group were tested. To assess sex differences in the behavioral results, and in adult weights, individual male and female offspring were treated as biological replicates. For qPCR, 5 fetal brains each from different litters were run per group. For uCT, 4-8 placentas or brains were analyzed per group, with 2-3 averaged per litter. For histology, 5-10 placentas or brains were analyzed per group, with 2 slices averaged per tissue.

For targeted metabolomics, 6 litters were analyzed, with 1.5-2 fetal brains pooled per litter. Whole litters were excluded from all analyses if they had fewer than 4 fetuses or pups (as done previously[2]). For prenatal measures, no viable fetuses within any litters were excluded from reported analyses. For behavioral measures, individual offspring were occasionally excluded from all tests due to health reasons (i.e. developing malocclusion) or from a specific test or trial due to a test-related event (i.e. escaping the testing chamber). These occasions were rare, and not associated with a particular group or condition. All data are plotted as mean +/- SEM. Significant differences are denoted as follows: *$p < 0.05$, **$p < 0.01$, ***$p < 0.001$, ****$p < 0.0001$, n.s. not significant.

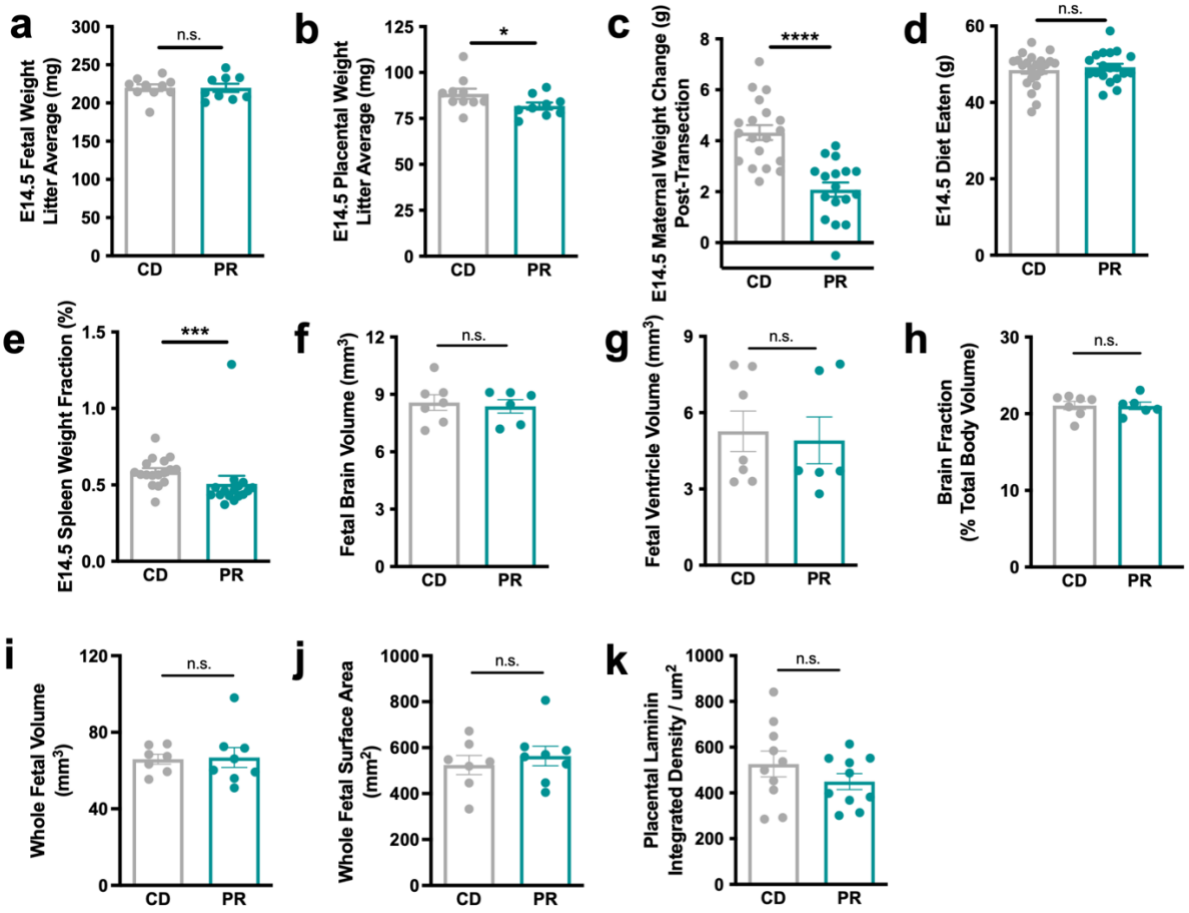

Figure A.1: Gestational protein restriction induces placental and splenic insufficiency but not fetal growth restriction at mid-gestation. a, Fetal weight at E14.5 from SPF CD and SPF PR dams, all fetuses averaged within each litter (Mann Whitney test, n = 10, 9, from left to right). **b,** Placental weight at E14.5 from SPF CD and SPF PR dams, all fetuses averaged within each litter (Mann Whitney test, n = 10, 9, from left to right). **c,** Maternal weight change, from E0.5 to E14.5, in SPF CD and SPF PR dams (unpaired Welch's t-test, n = 19, 17, from left to right). **d,** Maternal diet eaten, from E0.5 to E14.5 in SPF CD and SPF PR dams (Mann Whitney test, n = 26, 21, from left to right). **e,** Maternal spleen weight fraction at E14.5 from SPF CD and SPF PR dams (Mann Whitney test, n = 17, 16, from left to right). **f,** Fetal brain volume measured by uCT at E14.5 from SPF CD and SPF PR dams, 2-3 fetuses averaged per litter (unpaired Welch's t-test, n = 7, 6 litters from left to right). **g,** Fetal brain ventricle volume measured by uCT at E14.5 from SPF CD and SPF PR dams, 2-3 fetuses averaged per litter (Mann Whitney test, n = 7, 6 litters from left to right). **h,** Fetal brain to body volume ratio measured by uCT at E14.5 from SPF CD and SPF PR dams, 2-3 fetuses averaged per litter (unpaired Welch's t-test, n = 7, 6 litters from left to right). **i,** Whole fetal volume measured by uCT at E14.5 from SPF CD and SPF PR dams, 2-3 fetuses averaged per litter (Mann Whitney test, n = 7, 8 litters from left to right). **j,** Whole fetal surface area measured by uCT at E14.5 from SPF CD and SPF PR dams, 2-3 fetuses averaged per litter (unpaired Welch's t-test, n = 7, 6 litters from left to right). **k,** Placental labyrinth laminin integrated density at E14.5 from SPF CD and SPF PR dams, 2 placentas averaged per litter (unpaired Welch's t-test, n = 10 litters per group). Mean +/- SEM, *p < 0.05, **p < 0.01, ***p < 0.001, ****p < 0.0001, n.s. not significant.

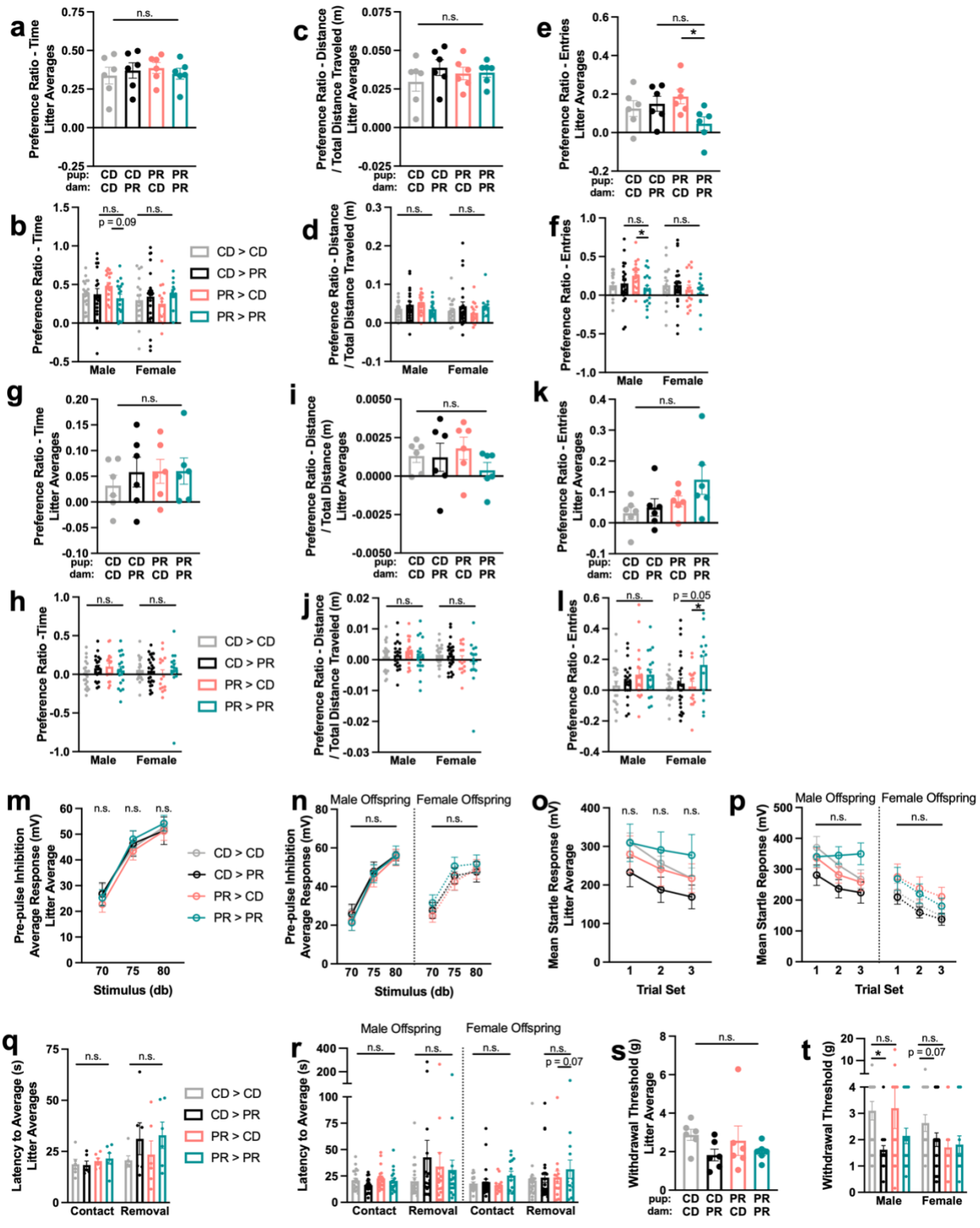
a
Preference Ratio - Time Litter Averages
n.s.
pup: CD CD PR PR
dam: CD PR CD PR
c
Preference Ratio - Distance / Total Distance Traveled (m) Litter Averages
n.s.
e
Preference Ratio - Entries Litter Averages
n.s.
*
b
Preference Ratio - Time
n.s.
p = 0.09
n.s.
CD > CD
CD > PR
PR > CD
PR > PR
Male
Female
d
Preference Ratio - Distance / Total Distance Traveled (m)
f
Preference Ratio - Entries
g
Preference Ratio - Time Litter Averages
i
Preference Ratio - Distance / Total Distance (m) Litter Averages
k
Preference Ratio - Entries Litter Averages
h
Preference Ratio -Time
j
Preference Ratio - Distance / Total Distance Traveled (m)
l
Preference Ratio - Entries
p = 0.05
m
Pre-pulse Inhibition Average Response (mV) Litter Average
Stimulus (db)
n
Male Offspring
Female Offspring
Pre-pulse Inhibition Average Response (mV)
o
Mean Startle Response (mV) Litter Average
Trial Set
p
Mean Startle Reponse (mV)
q
Latency to Average (s) Litter Averages
Contact
Removal
r
Latency to Average (s)
p = 0.07
s
Withdrawal Threshold (g) Litter Average
t
Withdrawal Threshold (g)

Figure A.2: Gestational protein restriction and associated rearing does not alter all behaviors in adult offspring. a, Time preference ratio in elevated plus maze, all offspring averaged within each litter (two-way ANOVA with Sidak, n = 6 litters per group). Top row refers to pup condition, bottom row refers to dam condition. **b,** Time preference ratio in elevated plus maze, individual offspring stratified by sex (two-way ANOVA with Sidak for each sex, n = 20, 20, 19, 18, 18, 25, 15, 14, from left to right). **c,** Distance preference ratio in elevated plus maze, controlled by total distance traveled, all offspring averaged within each litter (two-way ANOVA with Sidak, n = 6 litters per group). Top row refers to pup condition, bottom row refers to dam condition. **d,** Distance preference ratio in elevated plus maze, controlled by total distance traveled, individual offspring stratified by sex (two-way ANOVA with Sidak for each sex, n = 20, 20, 19, 18, 18, 25, 15, 14, from left to right). **e,** Entries preference ratio in elevated plus maze, all offspring averaged within each litter (two-way ANOVA with Sidak, n = 6 litters per group). Top row refers to pup condition, bottom row refers to dam condition. **f,** Entries preference ratio in elevated plus maze, individual offspring stratified by sex (two-way ANOVA with Sidak for each sex, n = 20, 20, 19, 18, 18, 25, 15, 14, from left to right). **g,** Time preference ratio in 3-chamber social preference test, all offspring averaged within each litter (two-way ANOVA with Sidak, n = 6 litters per group). Top row refers to pup condition, bottom row refers to dam condition. **h,** Time preference ratio in 3-chamber social preference test, individual offspring stratified by sex (two-way ANOVA with Sidak for each sex, n = 22, 20, 19, 18, 19, 25, 15, 14, from left to right). **i,** Distance preference ratio in 3-chamber social preference test, controlled by total distance traveled, all offspring averaged within each litter (two-way ANOVA with Sidak, n = 6 litters per group). Top row refers to pup condition, bottom row refers to dam condition. **j,** Distance preference ratio in 3-chamber social preference test, controlled by total distance traveled, individual offspring stratified by sex (two-way ANOVA with Sidak for each sex, n = 22, 20, 19, 18, 19, 25, 15, 14, from left to right). **k,** Entries preference ratio in 3-chamber social preference test, all offspring averaged within each litter (two-way ANOVA with Sidak, n = 6 litters per group). Top row refers to pup condition, bottom row refers to dam condition. **l,** Entries preference ratio in 3-chamber social preference test, individual offspring stratified by sex (two-way ANOVA with Sidak for each sex, n = 22, 20, 19, 18, 19, 25, 15, 14, from left to right). **m,** Average startle response in pre-pulse inhibition test, all offspring averaged within each litter (three-way repeated-measures ANOVA with Sidak, n = 6 litters per group). **n,** Average startle response in pre-pulse inhibition test, individual offspring stratified by sex (three-way repeated measures ANOVA with Sidak for each sex, n = 22, 19, 20, 25, 19, 15, 18, 14, from top to bottom). **o,** Average startle response in acoustic startle test, all offspring averaged within each litter (three-way repeated-measures ANOVA with Sidak, n = 6 litters per group). **p,** Average startle response in acoustic startle test, individual offspring stratified by sex (three-way repeated measures ANOVA with Sidak for each sex, n = 22, 19, 20, 25, 19, 15, 18, 14, from top to bottom). **q,** Latency to contact and removal in adhesive removal test, right and left paws averaged, all offspring averaged within each litter (two-way ANOVAs with Sidak (one each for contact and removal), n = 6 litters per group). **r,** Latency to contact and removal in adhesive removal test, right and left paws averaged, individual offspring stratified by sex (two-way ANOVAs with Sidak (one each for contact and removal for each sex), n = 22, 19, 20, 25, 19, 15, 18, 14, from top to bottom). **s,** Withdrawal threshold in Von Frey filament test, all offspring averaged within each litter (two-way ANOVA with Sidak, n = 6 litters per group). Top row refers to pup condition, bottom row refers to dam condition. **t,** Withdrawal threshold in Von Frey filament test, individual offspring stratified by sex (two-way ANOVA with Sidak for each sex, n = 22, 20, 19, 18, 19, 25, 15, 14, from left to right). Mean +/- SEM, *$p < 0.05$, n.s. not significant.

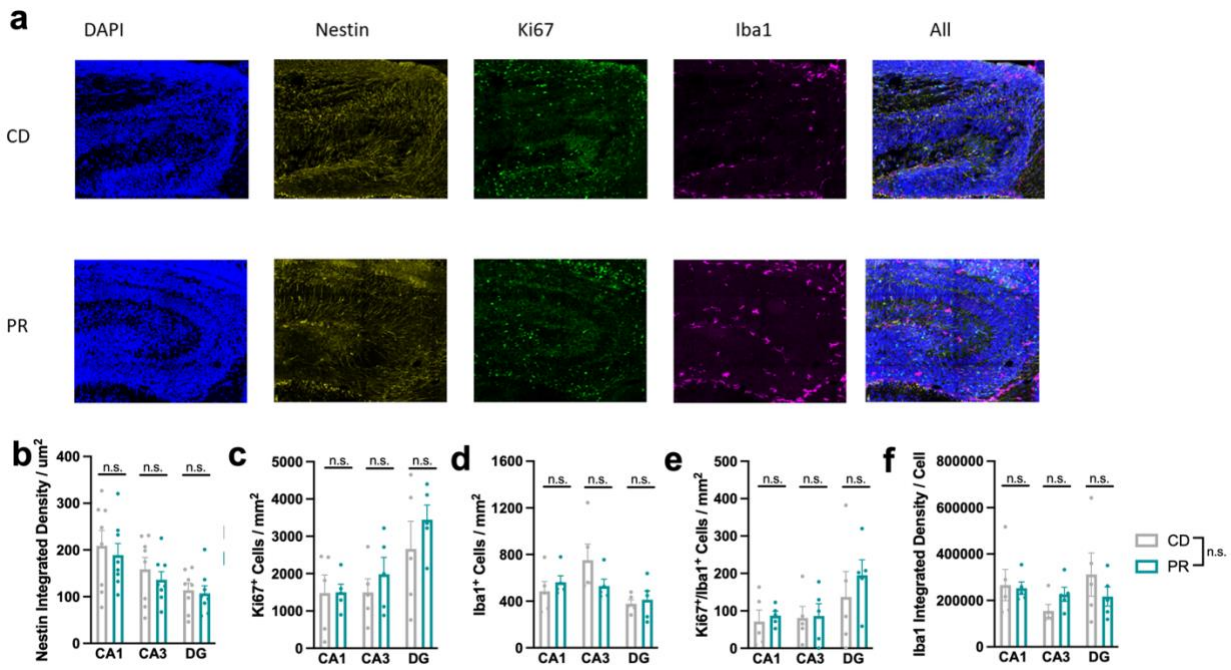

Figure A.3: Gestational protein restriction does not alter proliferation or microglia in the developing hippocampus. a, Representative images of cells stained for DAPI, Iba1, Ki67, Nestin, and merged in the hippocampus. **b,** Expression of total Nestin integrated density in the hippocampus subregions of E18.5 PR and CD mice (two-way repeated measures ANOVA with Sidak, n=8 brains per group, 2 slices per brain). **c,** Expression of Ki67+ cells in the hippocampus subregions of E18.5 PR and CD mice (two-way repeated measures ANOVA with Sidak, n=5 brains per group, 2 slices per brain). **d,** Expression of Iba1+ cells in the hippocampus subregions of E18.5 PR and CD mice (two-way repeated measures ANOVA with Sidak, n=5 brains per group, 2 slices per brain). **e,** Expression of Ki67+/Iba1+ cells in the hippocampus subregions of E18.5 PR and CD mice (two-way repeated measures ANOVA with Sidak, n=5 brains per group, 2 slices per brain). **f,** Expression of Iba1+ per cell in the hippocampus subregions of E18.5 PR and CD mice (two-way repeated measures ANOVA with Sidak, n=5 brains per group, 2 slices per brain). All plots show mean +/- SEM; n.s. = not significant. All data points are representative of two brain slices averaged together.

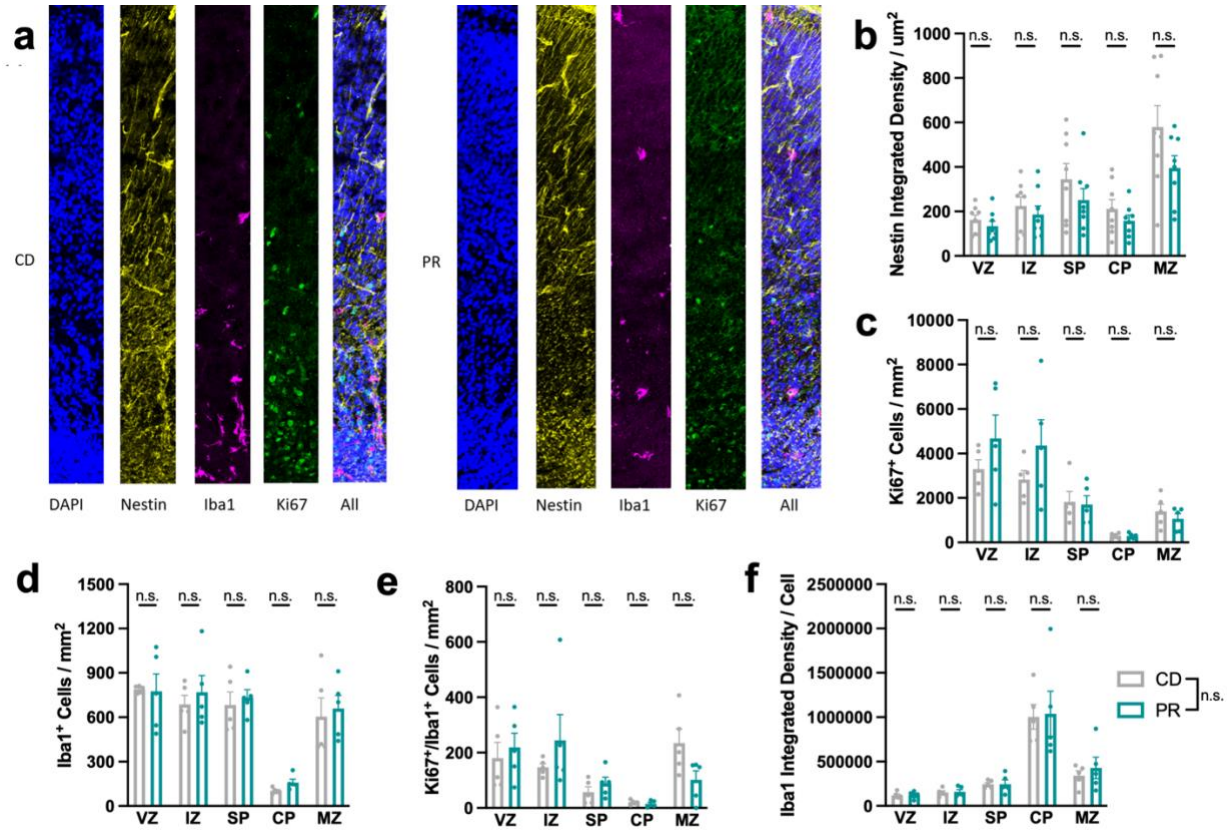

Figure A.4: Gestational protein restriction does not alter proliferation or microglia in the developing frontal cortex. a, Representative images of cells stained for DAPI, Iba1, Ki67, Nestin, and merged in the frontal cortex. **b,** Expression of total Nestin integrated density in the frontal cortex subregions of E18.5 PR and CD mice (two-way repeated measures ANOVA with Sidak, n=8 brains per group, 2 slices per brain). **c,** Expression of Ki67+ cells in the frontal cortex subregions of E18.5 PR and CD mice (two-way repeated measures ANOVA with Sidak, n=5 brains per group, 2 slices per brain). **d,** Expression of Iba1+ cells in the frontal cortex subregions of E18.5 PR and CD mice (two-way repeated measures ANOVA with Sidak, n=5 brains per group, 2 slices per brain). **e,** Expression of Ki67+/Iba1+ cells in the frontal cortex subregions of E18.5 PR and CD mice (two-way repeated measures ANOVA with Sidak, n=5 brains per group, 2 slices per brain). **f,** Expression of Iba1+ per cell in the frontal cortex subregions of E18.5 PR and CD mice (two-way repeated measures ANOVA with Sidak, n=5 brains per group, 2 slices per brain). All plots show mean +/- SEM; n.s. = not significant. All data points are representative of two brain slices averaged together.

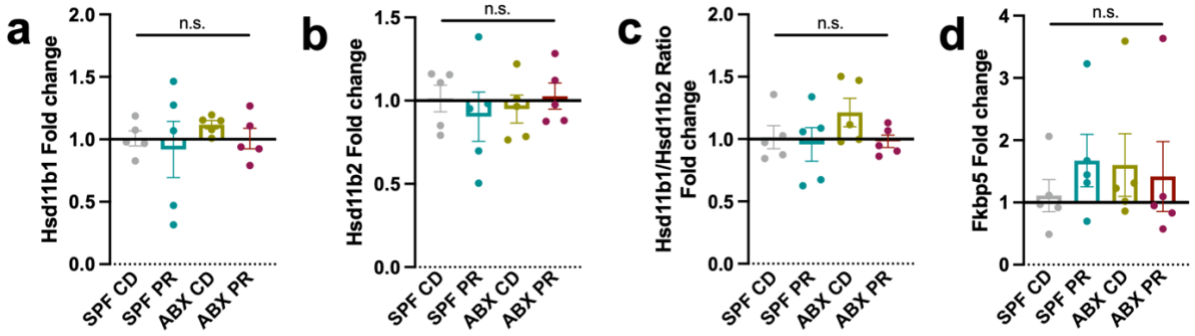

Figure A.5: Gestational protein restriction and maternal microbiota depletion does not influence HPA axis related genes in fetal brain. a, Hsd11b1 gene expression fold change at E18.5 from fetal brains of SPF CD, SPF PR, ABX CD, ABX PR dams (two-way ANOVA with Sidak, n = 5 per group). **b,** Hsd11b2 gene expression fold change at E18.5 from fetal brains of SPF CD, SPF PR, ABX CD, ABX PR dams (two-way ANOVA with Sidak, n = 5 per group). **c,** Hsd11b1/Hsd11b2 gene expression fold change ratio at E18.5 from fetal brains of SPF CD, SPF PR, ABX CD, ABX PR dams (two-way ANOVA with Sidak, n = 5 per group). **d,** Fkbp5 gene expression fold change at E18.5 from fetal brains of SPF CD, SPF PR, ABX CD, ABX PR dams (two-way ANOVA with Sidak, n = 5 per group).

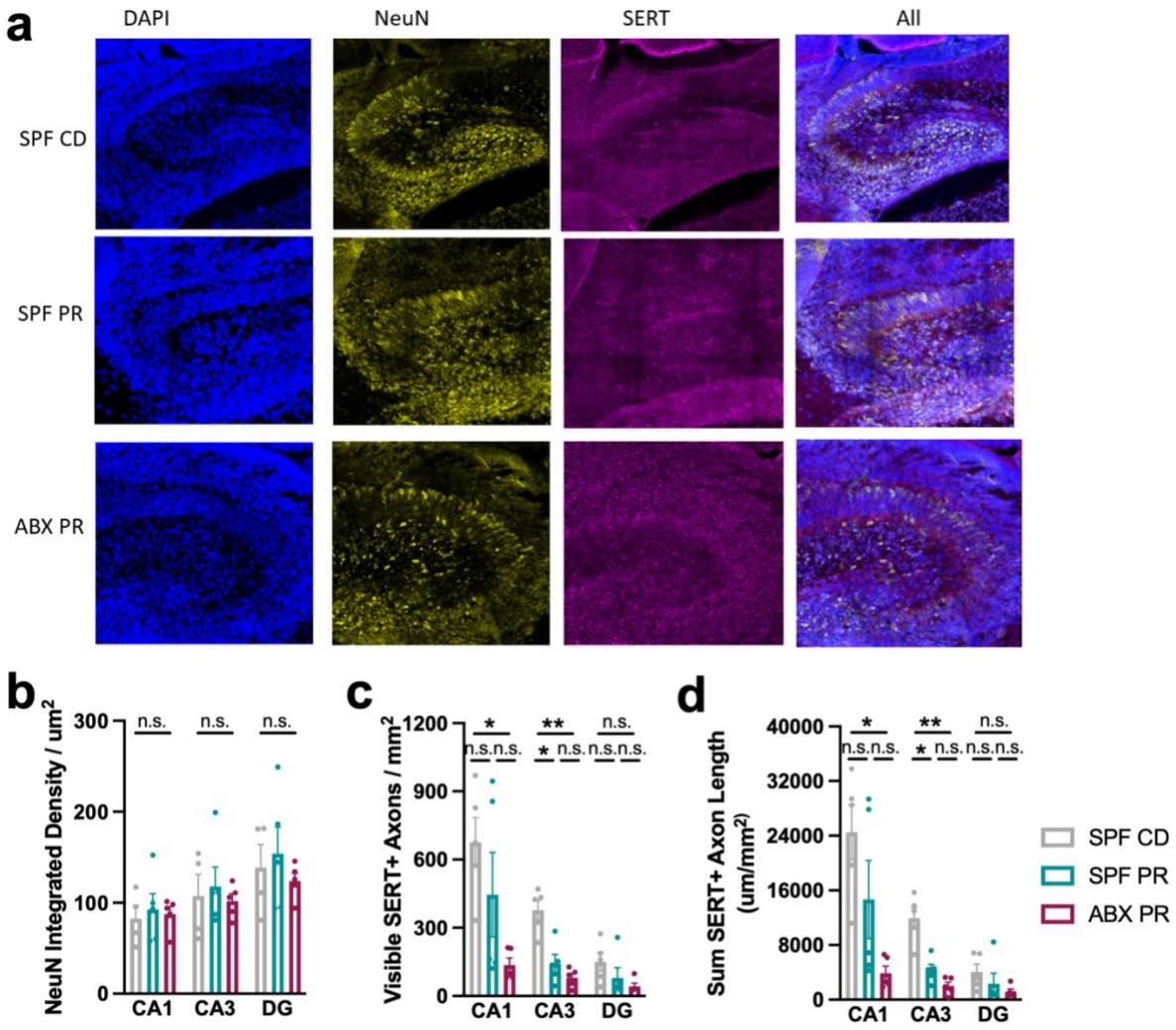

Figure A.6: Gestational protein restriction and maternal microbial depletion decrease SERT+ axons in the developing hippocampus. a, Representative images of cells stained for DAPI, NeuN, SERT, and merged in the hippocampus. **b,** Expression of total NeuN integrated density in the hippocampus subregions of E18.5 PR and CD mice (two-way repeated measures ANOVA with Tukey, n=4, 5, 5 brains per group, 2 slices per brain). **c,** Count of visible SERT+ axons in the hippocampus subregions of E18.5 PR and CD mice (two-way repeated measures ANOVA with Tukey, n=5 brains per group, 2 slices per brain). **d,** Sum length of visible SERT+ axons in the hippocampus subregions of E18.5 PR and CD mice (two-way repeated measures ANOVA with Tukey, n=5 brains per group, 2 slices per brain). All plots show mean +/- SEM; *p < 0.05, **p < 0.01, n.s. not significant. All data points are representative of two brain slices averaged together.

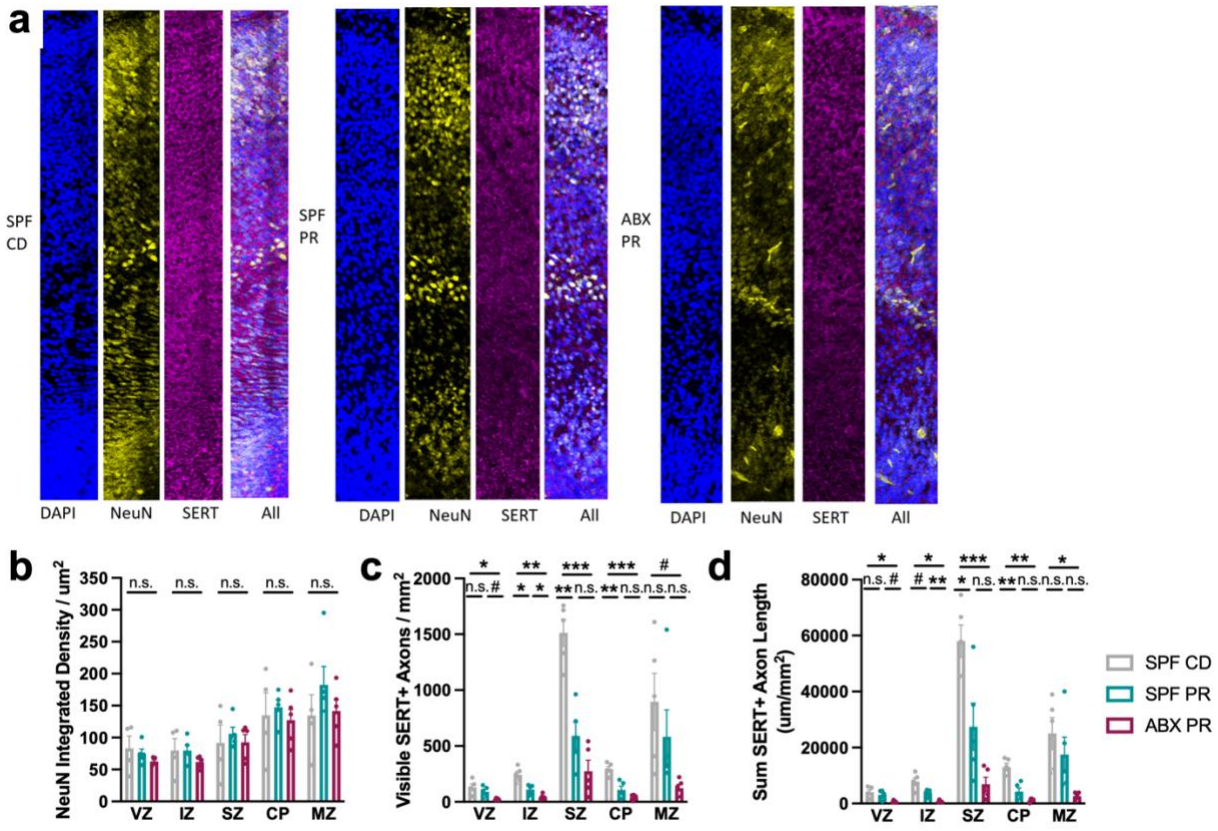

Figure A.7: Gestational protein restriction and maternal microbial depletion decrease SERT+ axons in the developing frontal cortex. a, Representative images of cells stained for DAPI, NeuN, SERT, and merged in the frontal cortex. **b,** Expression of total NeuN integrated density in the frontal cortex subregions of E18.5 PR and CD mice (two-way repeated measures ANOVA with Tukey, n=4, 5, 5 brains per group, 2 slices per brain). **c,** Count of visible SERT+ axons in the frontal cortex subregions of E18.5 PR and CD mice (two-way repeated measures ANOVA with Tukey, n=5 brains per group, 2 slices per brain). **d,** Sum length of visible SERT+ axons in the frontal cortex subregions of E18.5 PR and CD mice (two-way repeated measures ANOVA with Tukey, n=5 brains per group, 2 slices per brain). All plots show mean +/- SEM; #p < 0.1, *p < 0.05, **p < 0.01, ***p < 0.001, n.s. not significant. All data points are representative of two brain slices averaged together.

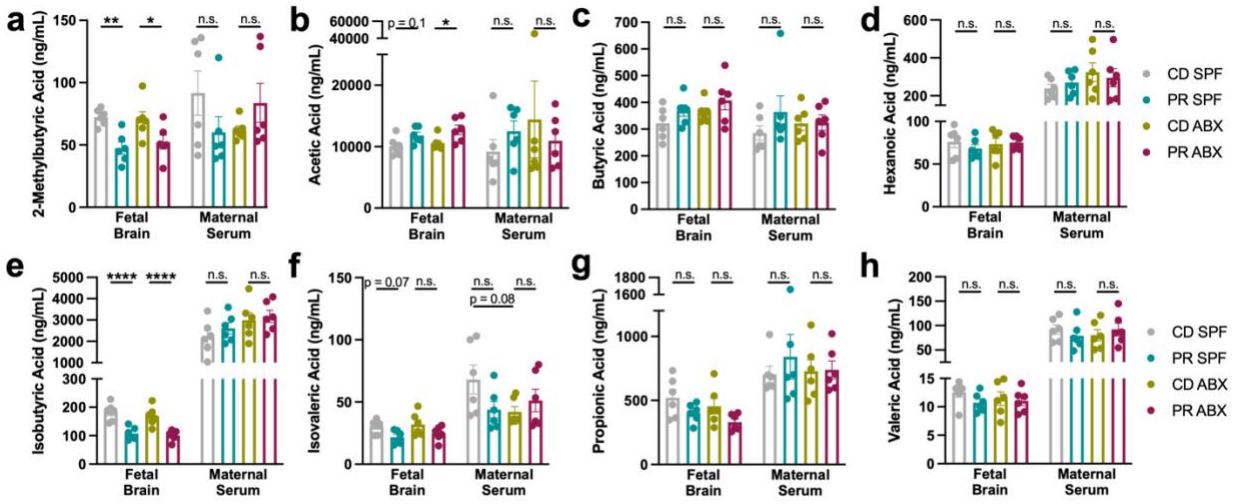

Figure A.8: Gestational protein restriction influences select short chain fatty acids in fetal brain but not maternal serum. a-h, Targeted metabolomic quantification of short chain fatty acids (two-way ANOVA with Sidak per tissue type, n = 6 litters per group, 1.5-2 brains pooled per litter). All plots show mean +/- SEM; *p < 0.05, **p < 0.01, ***p < 0.001, ****p < 0.0001, n.s. not significant.

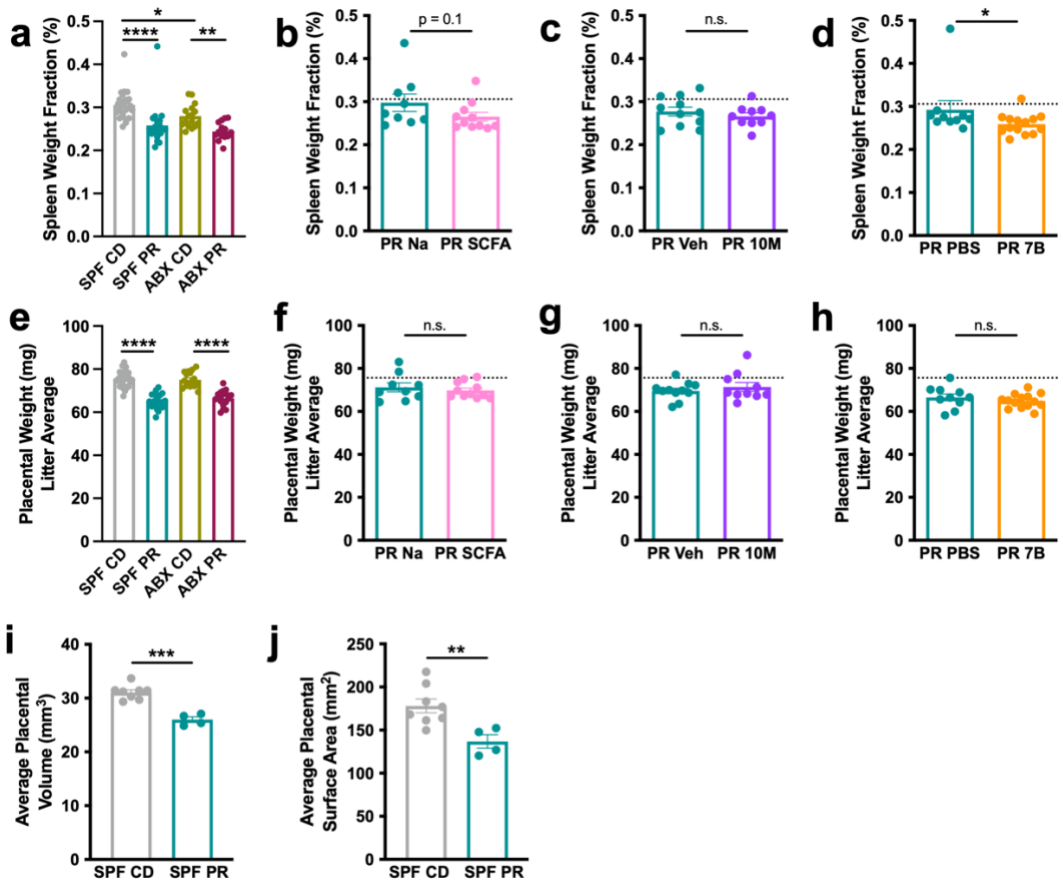

Figure A.9: Gestational protein restriction induces splenic and placental insufficiency at late-gestation, regardless of microbial interventions. a, Maternal spleen weight fraction at E18.5 from SPF CD, SPF PR, ABX CD, ABX PR dams (two-way ANOVA with Sidak, n = 25, 21, 16, 17, from left to right). **b,** Maternal spleen weight fraction at E18.5 from SPF PR + Na and SPF PR + SCFA dams (Mann Whitney test, n = 9, 11, from left to right). Dotted line indicates average value for SPF CD litters. **c,** Maternal spleen weight fraction at E18.5 from SPF PR + Veh and SPF PR + 10M dams (unpaired Welch's t-test, n = 11, 10, from left to right). Dotted line indicates average value for SPF CD litters. **d,** Maternal spleen weight fraction at E18.5 from SPF PR + PBS and SPF PR + 7B dams (Mann Whitney test, n = 10, 14, from left to right). Dotted line indicates average value for SPF CD litters. **e,** Placental weight at E18.5 from SPF CD, SPF PR, ABX CD, ABX PR dams, all placentas averaged within each litter (two-way ANOVA with Sidak, n = 28, 21, 16, 17, from left to right). **f,** Placental weight at E18.5 from SPF PR + PBS and SPF PR + 7B dams, all placentas averaged within each litter (unpaired Welch's t-test, n = 9, 11, from left to right). Dotted line indicates average value for SPF CD litters. **g,** Placental weight at E18.5 from SPF PR + Veh and SPF PR + 10M dams, all placentas averaged within each litter (Mann Whitney Welch's t-test, n = 11, 10, from left to right). Dotted line indicates average value for SPF CD litters. **h,** Placental weight at E18.5 from SPF PR + PBS and SPF PR + 7B dams, all placentas averaged within each litter (unpaired Welch's t-test, n = 10, 14, from left to right). Dotted line indicates average value for SPF CD litters. **i,** Placental volume measured by uCT at E18.5 from SPF CD and SPF PR dams, 2 placentas averaged per litter (unpaired Welch's t-test, n = 8, 4 litters from left to right). **j,** Placental surface area measured by uCT at E18.5 from SPF CD and SPF PR dams, 2 placentas averaged per litter (unpaired Welch's t-test, n = 8, 4 litters from left to right). Mean +/- SEM, *p < 0.05, **p < 0.01, ****p < 0.0001, n.s. not significant.

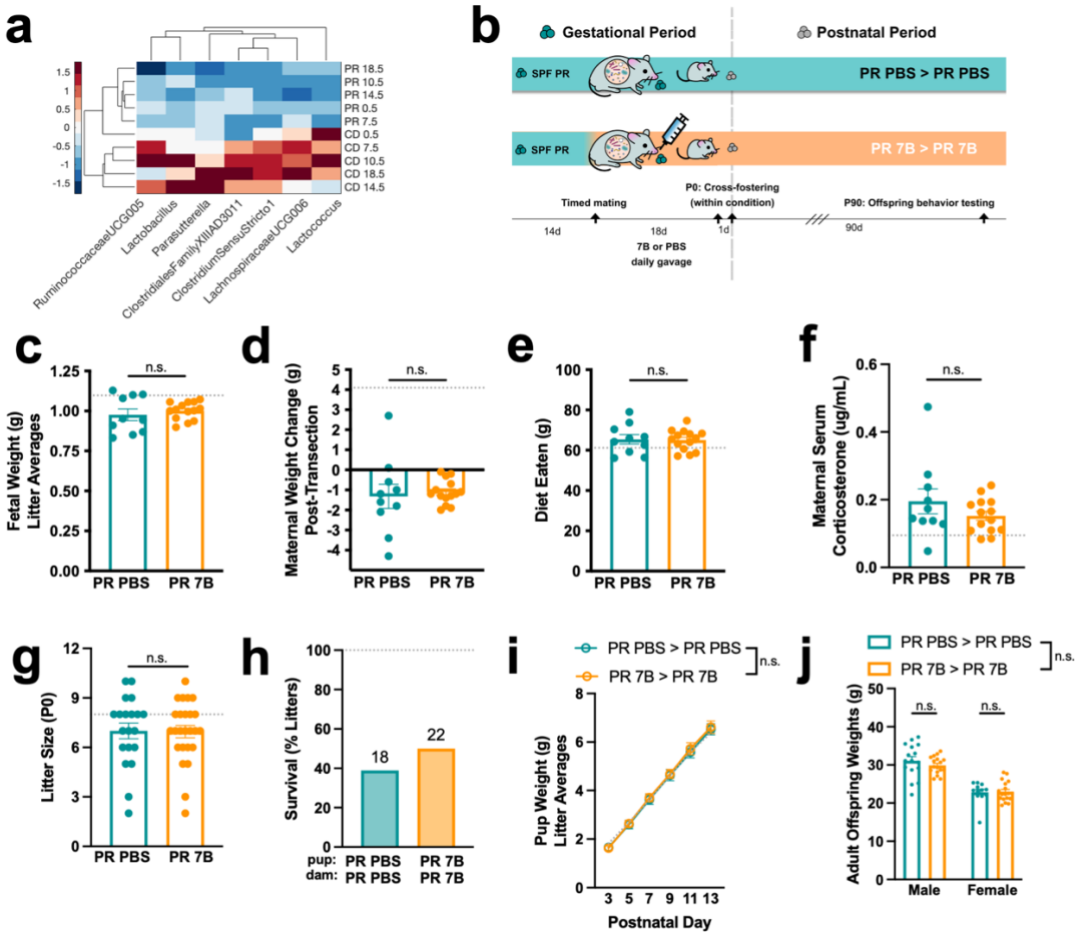

Figure A.10: Maternal 7B supplementation has no effect on gross measures of maternal and offspring health. a, Heatmap of genera used to BLAST for candidates for 7B supplementation, hierarchical clustering around 0, SD = 1 (n = 5 dams per group at each timepoint). **b,** Graphic of cross-fostering paradigm for 7B experiments. **c,** Fetal weight at E18.5 from SPF PR + PBS and SPF PR + 7B dams, all fetuses averaged within each litter (unpaired Welch's t-test, n = 10, 14, from left to right). Dotted line indicates average value for SPF CD fetuses. **d,** Maternal weight change, from E0.5 to E18.5 post-transection, in SPF PR + PBS and SPF PR + 7B dams (unpaired Welch's t-test, n = 10, 14, from left to right). Dotted line indicates average value for SPF CD dams. **e,** Diet eaten, from E0.5 to E18.5 in SPF PR + PBS and SPF PR + 7B dams (unpaired Welch's t-test, n = 10, 14, from left to right). Dotted line indicates average value for SPF CD dams. **f,** Corticosterone measured in serum in SPF PR + PBS and SPF PR + 7B dams at E18.5 (Mann Whitney test, n = 10, 14 from left to right). Dotted line indicates average value for SPF CD dams. **g,** Litter size, pups per litters, measured at P0, from SPF PR + PBS and SPF PR + 7B dams (Mann Whitney test, n = 20, 25, from left to right). Dotted line indicates average value for SPF CD litters. **h,** Litter survival (percentage of total litters), from SPF PR + PBS pups > SPF PR + PBS dams and SPF PR + 7B pups > SPF PR + 7B dams (n = 18, 22, from left to right). Dotted line indicates average value for SPF CD litters. Top row refers to pup condition, bottom row refers to dam condition. **i,** Pup weights, all offspring averaged within each litter (two-way repeated measures ANOVA with Sidak, n = 7, 11 litters per group, from top to bottom). Dotted line indicates average value for SPF CD litters. **j,** Adult weights, male and female offspring (two-way ANOVA with Sidak, n = 16, 17, 12, 18, from left to right). Mean +/- SEM, *p < 0.05, **p < 0.01, ***p < 0.001, ****p < 0.0001, n.s. not significant.

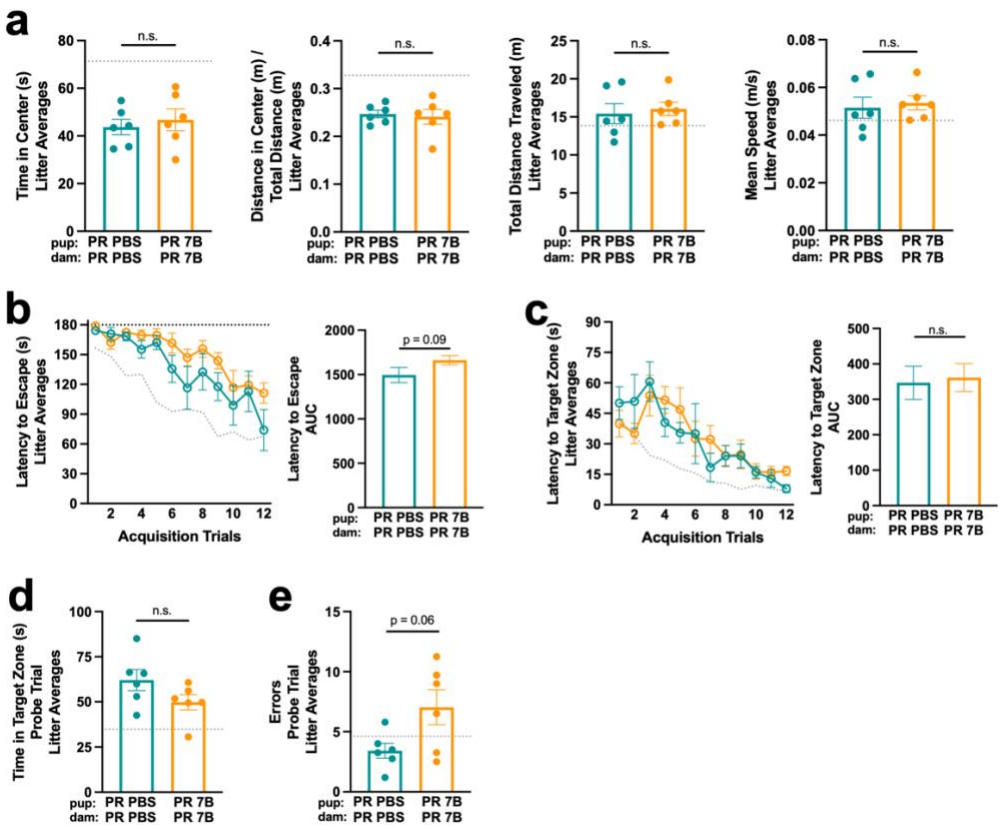

Figure A.11: Maternal 7B supplementation does not influence anxiety-like, locomotor, or cognitive behavioral measures in adult offspring exposed to gestational protein restriction. a, Left: Time in center in open field test, all offspring averaged within each litter (unpaired Welch's t-test, n = 6 litters per group). Top row refers to pup condition, bottom row refers to dam condition. Dotted line indicates average value for SPF CD litters. Left-middle: Distance in center in open field test, controlled by total distance traveled, all offspring averaged within each litter (unpaired Welch's t-test, n = 6 litters per group). Top row refers to pup condition, bottom row refers to dam condition. Dotted line indicates average value for SPF CD litters. Right-middle: Total distance traveled in open field test, all offspring averaged within each litter (unpaired Welch's t-test, n = 6 litters per group). Top row refers to pup condition, bottom row refers to dam condition. Dotted line indicates average value for SPF CD litters. Right: Mean speed in open field test, all offspring averaged within each litter (unpaired Welch's t-test, n = 6 litters per group). Top row refers to pup condition, bottom row refers to dam condition. Dotted line indicates average value for SPF CD litters. **b,** Left: Latency to escape in Barnes maze, all offspring averaged within each litter (n = 6 litters per group). Dotted line indicates average value for SPF CD litters. Right: AUC of latency to escape (unpaired Welch's t-test). Top row refers to pup condition, bottom row refers to dam condition. **c,** Left: Latency to target zone in Barnes maze, all offspring averaged within each litter (n = 6 litters per group). Dotted line indicates average value for SPF CD litters. Right: AUC of latency to target zone (unpaired Welch's t-test). Top row refers to pup condition, bottom row refers to dam condition. **d,** Time in target zone in Barnes maze probe trial, all offspring averaged within each litter (unpaired Welch's t-test, n = 6 litters per group). Dotted line indicates average values for SPF CD litters. **e,** Errors made in Barnes maze probe trial, all offspring averaged within each litter (unpaired Welch's t-test, n = 6 litters per group). Dotted line indicates average values for SPF CD litters. Mean +/- SEM, *p < 0.05, **p < 0.01, ***p < 0.001, ****p < 0.0001, n.s. not significant.

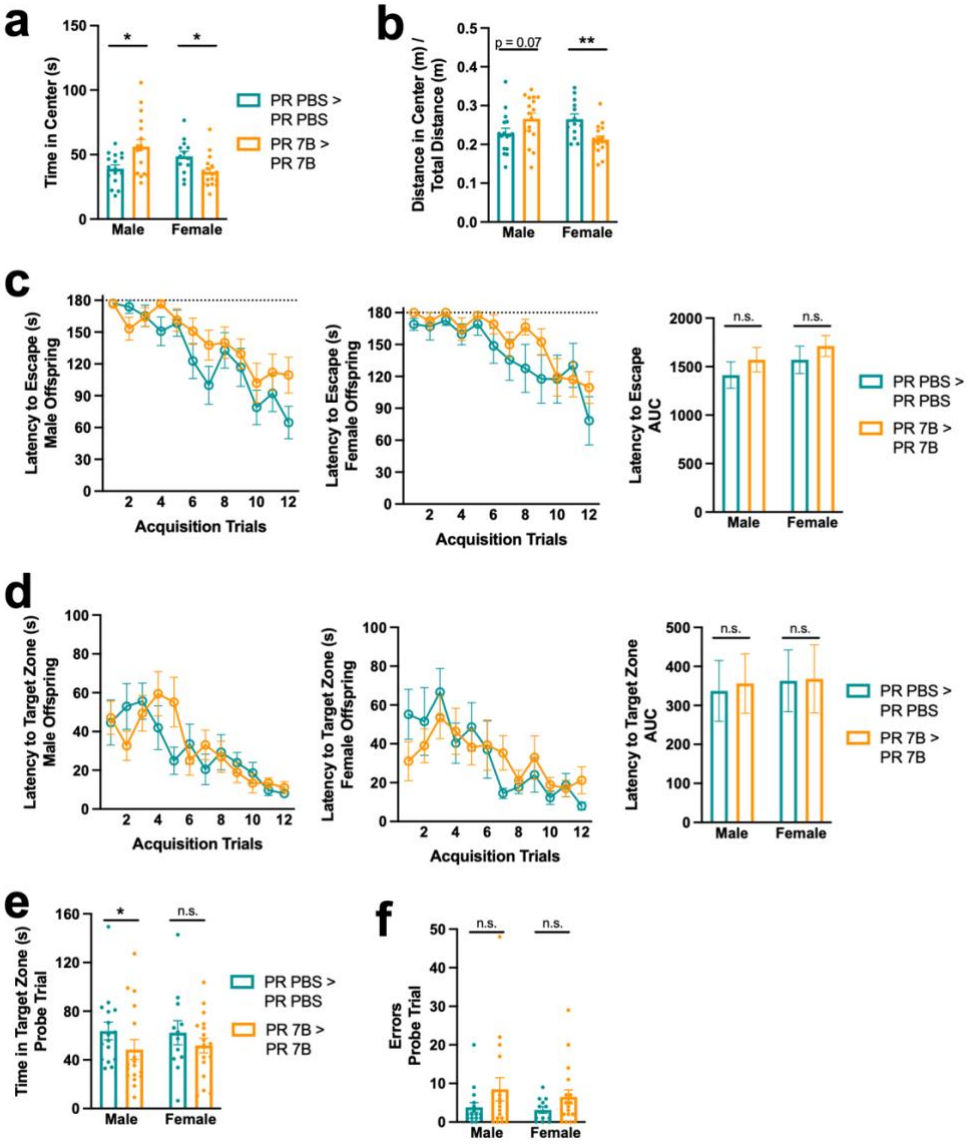

Figure A.12: Adult offspring exhibit select sexually dimorphic behavioral alterations in response to gestational protein restriction and 7B supplementation. a, Time in center in open field test, male and female offspring (unpaired Welch's t-test for each sex, n = 16, 17, 13, 17, from left to right). **b,** Distance in center in open field test, controlled by total distance traveled, male and female offspring (unpaired Welch's t-test for each sex, n = 16, 17, 13, 17, from left to right). **c,** Left: Latency to escape in Barnes maze acquisition phase, male offspring (n = 16, 17). Middle: Latency to escape in Barnes maze acquisition phase, female offspring (n = 12, 18). Right: AUC of latency to escape (unpaired Welch's t-test for each sex). **d,** Left: Latency to target zone in Barnes maze acquisition phase, male offspring (n = 16, 17). Middle: Latency to target zone in Barnes maze acquisition phase, female offspring (n = 12, 18). Right: AUC of latency to target zone (unpaired Welch's t-test for each sex). **e,** Time in target zone in Barnes maze probe trial, male and female offspring (Mann-Whitney test for each sex, n = 16, 12, 17, 18, from left to right). **f,** Errors in Barnes maze probe trial, male and female offspring (Mann-Whitney test for each sex, n = 16, 17, 12, 18, from left to right). Mean +/- SEM, *p < 0.05, **p < 0.01, ***p < 0.001, ****p < 0.0001, n.s. not significant.

Cultures	Culturing conditions
Lachnospiraceae bacterium DSM 111138	Brain, Heart Infusion medium+ 0.010 ml/ml Cystein-DTT (DL-Dithiothreitol)-solution
Emergencia timonensis DSM 101844	PYG Medoum, anaerobic, 37 °C
Parasutterella excrementihominis DSM 21040	Chopped meat medium with sterile filtered 5% formiate/fumarate, 5% sterile bovine solution
Lactococcus lactis DSM 20481	Corynebacterium medium, anaerobic, 30 °C
Lactobacillus johnsonii DSM 10533	Man de Rogosa, anaerobic, 37 °C
Sporobacter termitidis DSM 10068	Sporobacter medium, anaerobic, 35°C
Clostridium disporicum DSM 5521	Chopped Meat Medium with Carbohydrates, anaerobic, 37 °C

Table A.S1: Culture conditions for mixed bacterial supplementation

References

1. Vuong, et al., H. E. Interactions between maternal fluoxetine exposure, the maternal gut microbiome and fetal neurodevelopment in mice. *Behavioral Brain Research* **410**, 113353 (2021).
2. Pronovost, et al., G. N. The maternal microbiome promotes placental development in mice. *Science Advances* **9**, (2023).
3. Gonzalez, et al., P. N. Chronic Protein Restriction in Mice Impacts Placental Function and Maternal Body Weight before Fetal Growth. *PLOS ONE* **11**, e0152227 (2016).
4. Bourke, et al., C. D. Immune Dysfunction as a Cause and Consequence of Malnutrition. *Trends in Immunology* **37**, 386–398 (2016).
5. Pronovost, E. Y., G. N. &. Hsiao. PDF [2 MB] Figures Save Share Reprints Request Perinatal Interactions between the Microbiome, Immunity, and Neurodevelopment. *Immunity* **50**, 18–36 (2019).
6. Han, V.X., et al. Maternal immune activation and neuroinflammation in human neurodevelopmental disorders. *Nature Reviews Neurology* **17**, 564–579 (2021).
7. Odabas, et al., D. Cranial MRI findings in children with protein energy malnutrition. *International Journal of Neuroscience* **115**, 829–837 (2005).
8. Lo, J.O., et al. Impaired placental hemodynamics and function in a non-human primate model of gestational protein restriction. *Scientific Reports* **13**, 841 (2023).
9. Rutland, C.S., et al. Effect of gestational nutrition on vascular integrity in the murine placenta. *Placenta* **28**, 734–742 (2007).
10. Walf, A.A. & Frye, C.A. The use of the elevated plus maze as an assay of anxiety-related behavior in rodents. *Nature Protocols* **2**, 322–328 (2007).
11. Yang, M., et al. Automated Three-Chambered Social Approach Task for Mice. *Current Protocols in Neuroscience* **8**, 2011.

12. Graham, F.K. The more of less startling effects of weak prestimulation. *Psychophysiology* **12**, 238–248 (1975).
13. Chaplan, S.R., et al. Quantitative assessment of tactile allodynia in the rat paw. *Journal of Neuroscience Methods* **53**, 55–63 (1994).
14. Bouet, V., et al. The adhesive removal test: a sensitive method to assess sensorimotor deficits in mice. *Nature Protocols* **4**, 1560–1564 (2009).
15. Gould, et al., J. M. Mouse maternal protein restriction during preimplantation alone permanently alters brain neuron proportion and adult short-term memory. *PNAS* **115**, E7398–E7407 (2018).
16. Zinni, M., et al. Impact of Fetal Growth Restriction on the Neonatal Microglial Proteome in the Rat. *Nutrients* **13**, 3719 (2021).
17. Jasarevic, E. *et al.* Stress during pregnancy alters temporal and spatial dynamics of the maternal and offspring microbiome in a sex-specific manner. *Scientific Reports* **7**, 44182 (2017).
18. Jasarevic, et al., E. The maternal vaginal microbiome partially mediates the effects of prenatal stress on offspring gut and hypothalamus. *Nature Neuroscience* **21**, 1061–1071 (2018).
19. Weinstock, M. The long-term behavioural consequences of prenatal stress. *Neuroscience & Biobehavioral Reviews* **32**, 1073–1086 (2008).
20. Martimiano, et al., P. H. M. Maternal protein restriction during gestation and lactation in the rat results in increased brain levels of kynurenine and kynurenic acid in their adult offspring. *Journal of Neurochemistry* **140**, 68–81 (2017).
21. Kepser, J. R., L. J. &. Homberg. The neurodevelopmental effects of serotonin: A behavioural perspective. *Behavioral Brain Research* **277**, 3–13 (2015).
22. Thion, M.S., et al. Microbiome Influences Prenatal and Adult Microglia in a Sex-Specific Manner. *Cell* **172**, 500–516 (2018).

23. Erny, et al., D. Host microbiota constantly control maturation and function of microglia in the CNS. *Nature Neuroscience* **18**, 965–977 (2015).
24. O'Riordan, K.J., et al. Short chain fatty acids: Microbial metabolites for gut-brain axis signalling. *Molecular and Cellular Endocrinology* **546**, (2022).
25. Yu, et al., L. Butyrate, but not propionate, reverses maternal diet-induced neurocognitive deficits in offspring. *Pharmacological Research* **160**, (2020).
26. Castro-Mejia, J.L., et al. Restitution of gut microbiota in Ugandan children administered with probiotics (Lactobacillus rhamnosus GG and Bifidobacterium animalis subsp. lactis BB-12) during treatment for severe acute malnutrition. *Gut Microbes* **11**, 855–867 (2020).
27. Vuong, H. E. *et al.* The maternal microbiome modulates fetal neurodevelopment in mice. *Nature* **586**, 281–286 (2020).